A study of the toxicological properties of propolis samples from Europe and Saudi Arabia and of their biological activity against protozoa.

A thesis presented in fulfilment of the Degree of Doctor of Philosophy in Pharmacy and Biomedical Sciences at the University of Strathclyde

By

ABDULLAH HAMDAN ALOTAIBI

2020

DECLARATION

‘This thesis is the result of the author’s original research. It was authored by the author and it has not recently been submitted for the assessment which has led to the award of a degree.’

Signed: _____

Date: _____

DEDICATION

I dedicate this thesis to my beloved mum, my precious wife Amal, my lovely kids, Joud and Hamdan, and my dear brothers and sisters in appreciation of their support, motivation and sacrifice in this accomplishment.

ACKNOWLEDGMENTS

Firstly, and foremost, Praise is to Allah and thanks to him who gave me health and wellness to complete my studies to obtain a PhD.

I am grateful to my supervisor Dr David G Watson, who gave me the opportunity to conduct this PhD and thank him for his invaluable guidance and support during the period of my study.

I would like to thank my second supervisor, Dr Valerie Ferro, for her assistance, I would like to express my sincere thanks to Prof. John Igoli, for his help with NMR experiments.

I am grateful to all my colleagues for their support and valuable times as we shared experiences and information.

Finally, I would like to thank The Saudi Ministry of Interior in the Kingdom of Saudi Arabia for funding my PhD study.

Abbreviations:

^{1}H NMR: Proton nuclear magnetic resonance

^{13}C NMR: Carbon nuclear magnetic resonance

1D: One Dimensional

2D: Two Dimensional

$CDCl_3$: Deuterated chloroform

$CHCl_3$: Chloroform

DMSO-*d6*: Deuterated dimethyl sulfoxide

COSY: Correlation spectroscopy

DEPT: Distortionless enhancement by polarisation transfer

DI: Deionised water

DMSO-*d6*: Deuterated dimethyl sulfoxide

EtOH: Ethanol

MeOH: Methanol

HE: Hexane

EtOAc: Ethyl acetate

CH_2Cl_2: Dichloromethane

GC: Gas chromatography

GC-MS: Gas chromatography-mass spectroscopy

HDL: High-density lipoprotein

HMBC: Heteronuclear multiple bond correlation

HPLC: High-pressure liquid chromatography

HRESI-MS: High-resolution electrospray ionisation mass spectroscopy

HSQC – Heteronuclear single quantum coherence

LC: Liquid chromatography

LC-MS: Liquid chromatography-mass spectrometry

MHz: Megahertz

NMR: Nuclear magnetic resonance

TLC: Thin layer chromatography

UV: Ultraviolet light

WHO: World Health Organization

VLC: Vacuum liquid chromatography

EC50: 50% Effective Concentration

APCI: Atmospheric pressure chemical ionisation

API: Atmospheric pressure ionisation

C: Carbon

CI: Chemical ionisation

CID: Collision-induced dissociation

CC: Column chromatography

DESI: Desorption electrospray ionisation

EI: Electron impact

ESI: Electrospray ionisation

ELSD: Evaporative light scattering detector

GF: Gel filtration chromatography

HPLC: High-performance liquid chromatography

HRMS: High-resolution mass spectrometry

MS: Mass spectrometry

m/z: Mass to charge ratio

MPLC: Medium pressure liquid chromatography

MALDI: Matrix-assisted laser desorption/ionisation

MP: Mobile phase

SP: Stationary phase

PLS: Partial least squares

PTLC: Preparative thin layer chromatography

PCA: Principal component analysis

SEC: Size-exclusion chromatography

TMS: Tetramethylsilane

TLC: Thin layer chromatography

TOF: Time-of-flight

UV/VIS: Ultraviolet/visible

µM: Micromolar

EEP: Ethanolic extract of propolis

T. brucei: Trypanosoma brucei

S: Singlet

d: Doublet

dd: Doublet of a doublet

t: Triplet

DMSO: Dimethyl sulphoxide

L50: A measured used in Toxicology study

Abstract

Propolis is a natural product collected by bees from plants to seal their hives for defence against external contamination, and a range of microorganisms and parasites including the protozoal species *Crithidia*. Propolis has been used as a folk medicine due to its therapeutic properties; thus, it is more likely that active components would be found in propolis rather than from random screening of plants. Ethanolic extracts of four samples from the UK (S224, S225, D6, D7), one from Poland(P) and two from Saudi Arabia (SB, T2) were profiled by high-resolution LC-MS and tested against a wide range of microorganisms including *T. brucei, L. mexicana, C. fasiculata, S. aureus.* Additionally, cell-based assays for cytotoxicity activities were evaluated. Several compounds were isolated, which are related to the three groups: flavonoids, phenylpropanoids and triterpenes. In total fifteen isolated compounds were obtained as follows: twelve from the UK samples most of which were flavonoids including 3-Acetoxypinobanksin (**1**), 7-Methoxychrysin (**2**), Kaempferol (**3**), Pinocembrin (**4**), 4'-Methoxykaempferol (**5**), Galangin (**6**), Chrysin (**7**), Apigenin (**8**), Pinostrobin (**9**), Cinnamic acid (**10**), Coumaric acid cinnamyl ester (**11a**) and Coumaric acid benzyl ester (**11b**). Two compounds were isolated from Polish propolis namely 4',7-Dimethoxykaempferol (**12**) and Naringenin 4',7-dimethyl ether (**13**), and three compounds from a Saudi propolis sample: Hesperetin-7-methyl ether (**14a**), Sakuranetin (**14b**) and Lupeol (**15**). Both the crude extracts and isolated compounds displayed variable activity against the range of microorganisms which were tested against including *S. aureus, T. brucei, C. fasiculata, T. congolense and L. mexicana.*

Table of Contents

List of Figures

List of Tables

1 Chapter 1

1.1 Introduction

Propolis generally referred to as “bee glue”, is the generic name given to the natural, resin-like substance which is produced by bees. Propolis is made from a mixture of bee saliva, beeswax and exudate/plant secretions gathered from tree buds, sap flows, or other botanical sources collected by the bees during visits to various types of plants (Simone-Finstrom and Spivak, 2010). Propolis is a very versatile, multifunctional substance with several applications in the hive such as the sealing of holes and cracks to the general reconstruction of the beehive. It is used to coat the inner surface of the beehive, helping to regulate the hive's internal temperature keeping it around an average of 35°C (El Sohaimy et al., 2014). It also guards against weather damage and serves to prevent the invasion of the colony by predators. The antiseptic properties of propolis help provide an aseptic environment within the hive protecting their larva, honey stores etc. from bacterial infections (Anjum et al., 2019). Upon heating, propolis generally softens becoming sticky at temperatures between 60°C and 100°C and also gives off a pleasant smell (Shehu et al., 2016). The word “propolis” is derived from Greek, “pro” which roughly means “defence for” while “polis” is interpreted to mean “city or community” therefore propolis translates to defence for the beehive (Castaldo and Capasso, 2002). For centuries, propolis has been used as alternative cure in traditional/folk medical preparations and treatments in addition to its applications within the hive, for the treatment of a plethora of human and animal diseases. Its

medicinal value is attributed to the full range of pharmacological properties which have been attributed to propolis including antiseptic, anti-inflammatory, anti-oxidant, antibacterial, antimitotic, antifungal, antiulcer, anticancer, and immunomodulatory properties. The chemical composition of propolis samples determines their biological properties. Which in turn is dependent on several factors such as the season, geographic origin of the samples and plant resources within proximity of the hive. Identification of the compounds contained in propolis from different regions and their corresponding biological activity has been a hot research topic for several research groups from around the world over the last few years. Propolis is obtained commercially by extraction with suitable organic solvents such as ethanol, methanol, chloroform, acetone and ether with each hive yielding about 150-200 g per annum. Propolis is an ingredient in several consumer products, including medicines such as lozenges, cough syrups, tablets. Food items and confectionaries, including food supplements, wine, cakes, chewing gum, chocolate bars. Cosmetics and personal care products such as soaps, powders, mouthwash, toothpaste, skin creams, gels and potions (Anjum et al., 2019).

1.2 History of propolis

The Greek, Roman, and Egyptian civilisations were amongst the first to have been reported to have used propolis. The primary use was for the sterilisation of wounds and to promote healing as well as for mummification (Burdock and toxicology, 1998, Sforcin, 2007). In England, propolis was listed as a pharmaceutical material and used as an ointment between the seventeenth and twentieth centuries (Castaldo and Capasso,

2002). It gained its popularity due to its antibacterial activity (Kuropatnicki et al., 2013). Propolis is an invaluable natural product which has been utilised for the treatment of diseases such as inflammation and arthritis in folk medicine from ancient times (Simone-Finstrom and Spivak, 2010). Since then, propolis has been an exciting subject for research in the pharmacological, medical and chemical sciences which has led to a lot more understanding and knowledge about some of its constituents. The components of propolis are classified, according to its geographic location of origin, into two main groups:

1) Propolis which originates from tropical and subtropical zones, and
2) Propolis which originates from temperate zones which include Europe, North America, New Zealand and Western Asia(Alday et al., 2016).

The primary source of temperate propolis is poplar and birch trees (Bankova and medicine, 2005). Bees in tropical and subtropical regions such as Tunisia and Australia utilise other plant sources such as leaf exudates of some Cistus spp or the 'grass trees' instead of the poplar tree because poplar and birch trees do not grow in these regions (Bankova et al., 2000). Propolis samples from Africa have so far not been adequately investigated to determine the source of some compounds such as fatty acids, terpenes, and flavonoids. Kasote *et al*. analysed some propolis samples from South Africa, and they reported that there were similarities between the samples and propolis produced in the temperate regions due to their high content of phenolic acids and flavonols (Kasote et al., 2014). Studies on propolis from several areas in Brazil have revealed that the predominant and more common chemical compounds found in the samples

were flavonoids, terpenoids, phenolic acids and their esters. The types of compounds most often reported as being identified from propolis samples include the flavonoids, aliphatic acids and esters, aromatic acids and esters, chalcones, terpenes, lignans, stilbenes, prenylated stilbenes and benzophenones, benzofurans, coumarins, xanthones and sugars (Salomao et al., 2008).

1.3 Physical properties and Composition of Propolis

1.3.1 Physical Properties of Propolis

Propolis is obtained usually as a highly resinous, sticky gum whose consistency and shape changes, like other lipophilic substances, depending on the temperature of the sample. It is glutinous and pliable in warm conditions, but hard and fragile in cold conditions (Hausen et al., 1987). The colour of Propolis can vary ranging from a dark yellow to brown with an associated resinous smell depending on the plant buds or leaves such as oak, pine, chestnut, eucalyptus or poplar amongst others mixed with wax (Huang et al., 2014). In one study carried out in Argentina Propolis samples from three locations were analysed to determine their organoleptic characteristics such as smell, taste, colour and appearance by various methods. It concluded that the smells of the samples varied widely based on origin and was also dependent on a volatile mixture of compounds. Depending on the plants which were local to the places of origin of the samples, the colour of the sample could be brown, green, black, light yellow to dark brown (Sosa-López et al., 2017). Characteristics such as colour and smell of the samples were dependent on the geographical locations from where the samples

originate, age and the plant pigments collected by bees (Marcucci et al., 2001). The best solvent commonly reported for propolis sample preparation is ethanol. However, other solvents may be used for the identification of the compounds contained in the propolis sample such as hexane, ethyl ether, chloroform water and methanol (Martinotti et al., 2015).

1.3.2 Propolis composition

The compounds found in propolis, bee glue or resin, originate from three primary sources. These include plant exudates which are collected by bees, various botanical parts of plants (including substances exuded from wounds in plants such as leaf buds), gums, mucilage, resins, lattices and lipophilic materials from leaves which can all be used by bees for the "manufacture" of propolis (Martinotti et al., 2015). Bee metabolism may also significantly modify the original composition of the propolis as secreted substances are added to the plant exudates collected, as well as foreign materials, of a plant or animal origin, which are introduced during propolis preparation (Salomao et al., 2008). The same study also highlighted that their chemical composition had substantial differences depending on the sites of collection. Propolis is used by bees to protect their hives from external contamination and more importantly, to prevent the disintegration of animals or insects which have been killed by the bees after entering the hive. Propolis consists of wax 30%, resins 50%, and balsams while the remaining 20% comprises of pollens and organic matter. These proportions are dependent on the region as well as the time of collection (Sawaya et

al., 2011, Ghisalberti et al., 1978). It is acknowledged that propolis is a valuable natural product suitable for the treatment of diseases such as inflammation and arthritis and has been used for the same in folk medicine from ancient times (Simone-Finstrom and Spivak, 2010). About 241 compounds were reportedly isolated from propolis between 2000 and 2012 (Huang et al., 2014). The main classes of compounds isolated were terpenes 17-19 as shown in Figure 1-1, also considered to be volatile compounds, flavonoids 1, 2, 10-15, sugars, phenolic compounds 3-9, 16-23, hydrocarbons, coumarins, and fatty acids. Also, inorganic elements such as copper, manganese, iron, calcium, aluminium, vanadium and silicon have been obtained from propolis samples (Huang et al., 2014). Flavonoids, phenolic acids and terpenoids are the most abundant compounds in propolis.

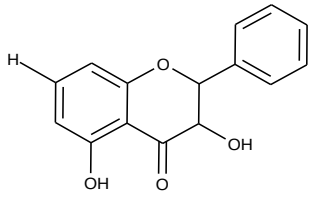

1 **Pinobanksin**

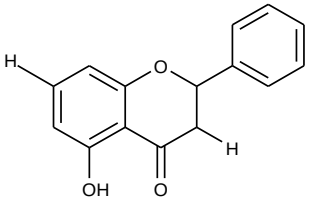

2 **Pinocembrin**

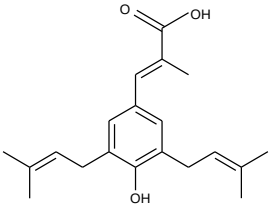

3 **Artepillin C**

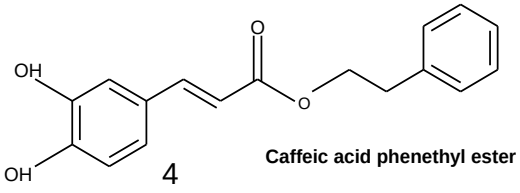

4 **Caffeic acid phenethyl ester**

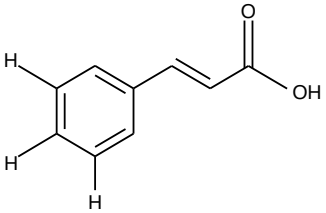

5 **Cinnamic acid**

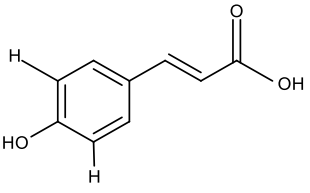

6 **p-coumaric acid**

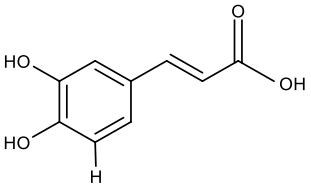

7 **Caffeic acid**

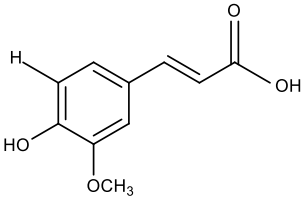

8 **Ferulic acid**

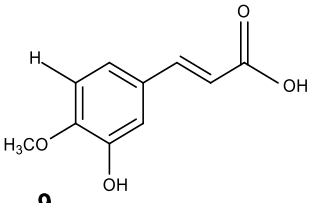

9 **Isoferulic acid**

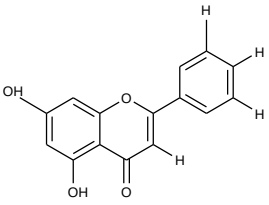

10 **Chrysin**

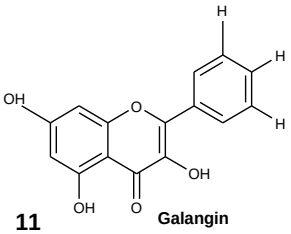

11 **Galangin**

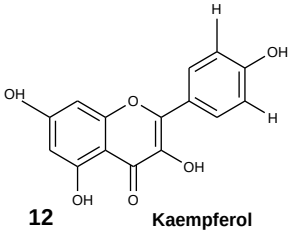

12 **Kaempferol**

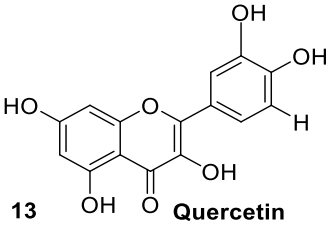

13 **Quercetin**

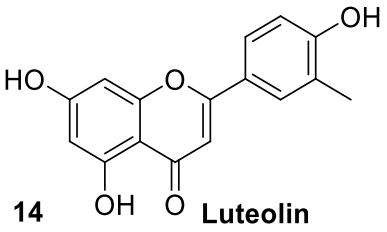

14 **Luteolin**

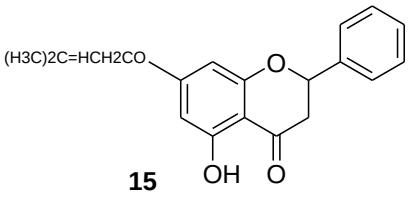

15 **7-O-prenylpinocembrin**

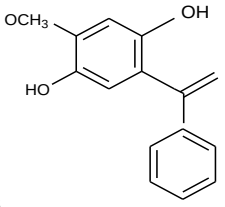

16 **Cearoin**

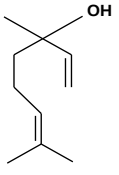

17 **LINALOOL**

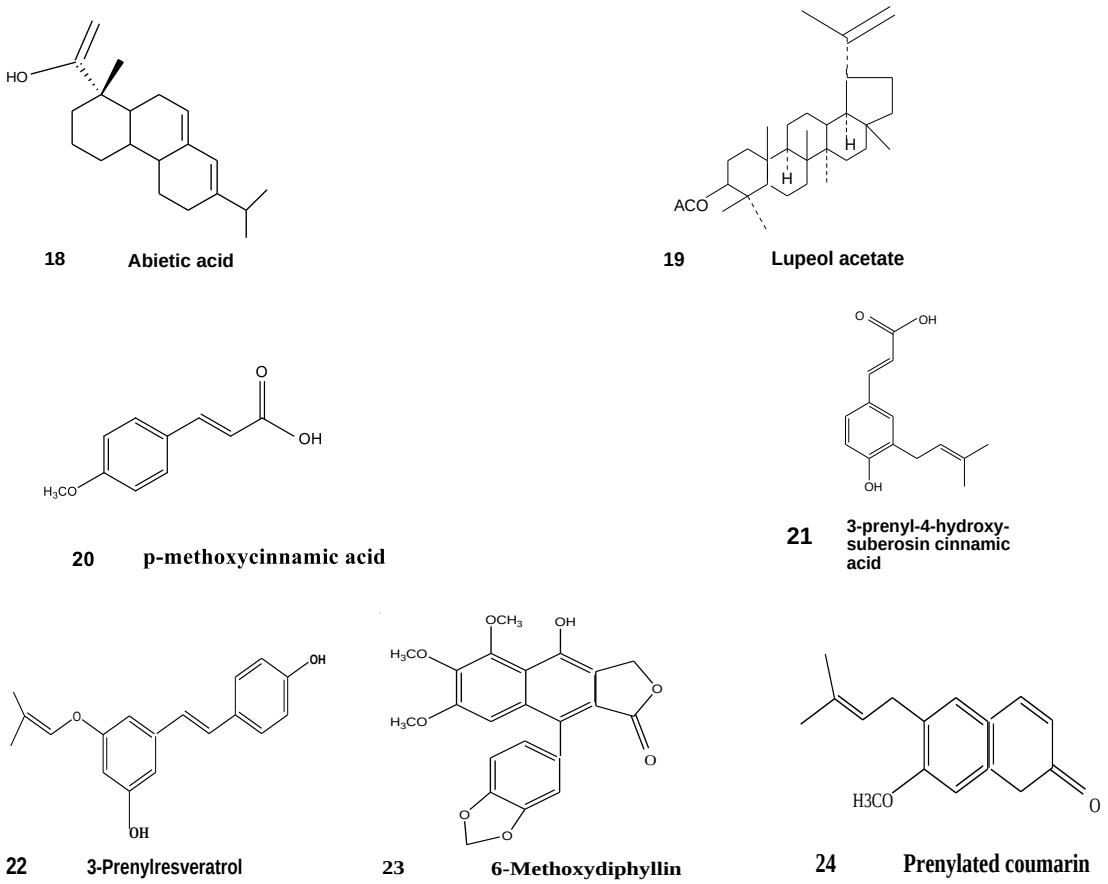

Figure 1-1: The structures of some flavonoids, other phenolics and terpenes identified in propolis.

1.3.2.1 Flavonoids

The word “flavonoid” comes from the Latin word “flavus,” which means yellow. Based on colour alone, only compounds with the flavone nucleus, which has a yellow colour, were considered to be flavonoids. This classification has now been widened to include all compounds with a flavan nucleus which encompasses both colourless (flavan-3-ol) and coloured (flavanone) cores and are understood to generally occur in plants (Das et al., 2019). Flavonoids contains phenolic compounds that are abundant in plants and contain pigments of different colours. Some essential functions of these

pigments include the protection of the plants from ultraviolet light and to offer a line of defence from bacterial and fungal phytopathogens. The chemical structure of flavonoids varies. However, they generally consist of the phenyl-benzo-γ-pyran (C6–C3–C6) characteristic skeleton which has 15 carbon atoms also known as the Flava nucleus comprising of two phenyl rings (A and B) and a ring heterocyclic pyran (C) which branches off from it as shown in Figure 1-2. Flavonoids include flavonols, flavones, flavanones, flavonoids, isoflavones, and anthocyanidins (Hernández-Rodríguez et al., 2019, Koœevar et al., 2007).

Flavonoids have been extensively studied because of their extensive biological properties which are essential for human health, Furthermore, due to the broad range of their medicinal properties, flavonoids are used as drugs and nutritional aids as well as for disease prevention as antioxidants, anti-inflammatory, antiallergic and anticancer therapies (Kumar and Pandey, 2013, Karuppagounder et al., 2015).

The biological properties of propolis are thought to be as a result of its flavonoids especially for the propolis samples from the temperate zone, from which a large number of flavonoid compounds such as Pinocembrin, Pinobanksin, Apigenin, Chrysin and Galangin amongst others have been identified (Burdock and toxicology, 1998, Havsteen, 1983). The assessments of flavonoids identified from Propolis samples to determine their biological activity tend to suggest that they contributed significantly to the biological activity of propolis(Bankova et al., 1983, Betances-Salcedo et al., 2017, Nunes et al., 2018).

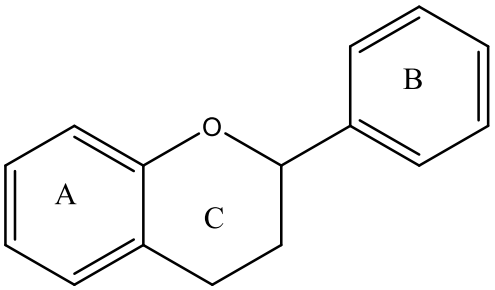

Figure 1-2: The skeleton of Flavan

1.3.2.2 Phenolic acids

The phenol structure, a hydroxyl group on an aromatic ring, is the core structural base of the phenolic compounds. Larger molecules are constructed around this core such as the coumarins, flavonoids, anthocyanins and phenolic acids. At least 300 compounds have been identified from Brazilian green propolis, the main ones being phenolic acids such as caffeic, ferulic, p-coumaric, and cinnamic acids (Marcucci et al., 2001). Seven phenolic acid compounds from Brazilian green propolis were also identified and characterised by a new study (Wildman, 2016).

Phenolic compounds play a variety of roles in plants which include the absorption of light, reduction of the growth of other competing plants, protecting the plant from being eaten by herbivores and pathogens, attracting pollinators, as well as encouraging the synergetic association with nitrogen-fixing bacteria (Wildman, 2016). Phenolic compounds are abundance in our nutrition. Thus, the reason for the increased interest from researcher's in phenolic compounds is due of their antioxidant properties and significant role in the prevention of many conditions related to oxidative stress, such

as cardiovascular disease, neurodegenerative inflammation and cancer. Phenolic acids are synthesised in plants from shikimic acid *via* the phenylpropanoid pathway and exist as glycosides or esters conjugated with hydroxyl-fatty acids, sterols, flavonoids and glucosides (Mandal et al., 2010). Generally, phenolic acids contain a phenolic ring and at least one organic carboxylic acid as a functional group.

Phenolic acids are usually categorised into three classes based on their structures; these are the C6-C3, C6-C2, and C6-C1 dependent on the number of carbon units in the side chain attached to the phenolic ring. They generally have the same basic skeleton; however, they differ based on the positioning as well as the number of hydroxyl groups on the aromatic ring of phenolic acids, as shown in Figure 1-1. Some of the most widely abundant phenolic acids are from the C6-C3 class, which are biosynthesised from hydroxycinnamic acid, and C6-C1 type compounds which have a general hydroxybenzoic structure. They are also some of the most important (Heleno et al., 2015). The hydroxybenzoic acids, of the C6-C1 class of compounds, including 4-hydroxybenzoic acid, are biosynthesised directly *via* the shikimate pathway (Ramawat and Mérillon, 2013). In medicine, phenols were traditionally used as antiseptics, while in propolis, these compounds are responsible for their antioxidant and anti-inflammatory properties (Huang et al., 2009).

1.3.2.3 Terpenoids

Terpenes are the generic name of a large class of compounds found in various parts of plants such as the flowers, leaves and roots. They are generally biosynthesised from isoprene and have a general formula, (C_5H_8) n, where n is the number of isoprene units.

Terpenes are often divided into classes based on the number of isoprene units (n) in the molecule. Examples of the types of terpenes include Hemiterpenes ($C_{20}H_{32}$, n=4), Triterpenes ($C_{30}H_{48}$, n=6), Tetraterpenes ($C_{40}H_{64}$, n=8), and Polyterpenes (C_5H_8)n[38]. The characteristic resinous smell of propolis is indicative of the presence of terpenes, and these compounds are often used to determine if a sample of propolis is real or a fake (Huang et al., 2014). Terpenes also play critical roles as antioxidants and antimicrobial agents in propolis (Oliveira et al., 2010).

1.4 Geographic variation of composition based on compounds present, which is dependent on plants visited.

Propolis contains a significant amount of secondary metabolites from plants; therefore, samples from around the world are not the same because of variations in the types of plants in the various regions. Thus, both the chemical composition and the biological activity of samples may vary based on their geographic origins and the local flora visited by the bees. In the temperate regions, the predominant plant sources are of the Populus spp. The bees, therefore, produce a Poplar-type propolis which is rich in flavones, flavanones as well as phenolic acids and their esters. On the other hand, in the tropical regions, the predominant plants are of the *Baccharis spp* and *Dalbergia spp*, which results in red or green propolis being produced. For example, Brazilian

green propolis is produced mostly from the alecrim plant (*Baccharis dracunculifolia*) (Heleno et al., 2015, Bankova, 2005). The categorisation of propolis samples reported between 2000 and 2012, based on their chemical composition was published in a recent review and is summarised in the table below Table **1-1** (Huang et al., 2014).

Table 1-1: The chemical categories reported in propolis between 2000 to 2012.

Chemical Category	**Example Compound**	**Geographical Origin**	**Plant Source**	**Bee Species**
Flavonoids	Luteolin	Australia, Brazil, Burma, Canada, Chinese, Cuba, Egypt, Greece, Japan, Kenya, Mexico, Nepal, Poland, Portugal, Solomon Island, Taiwan	*Populus, Macaranga, Dalbergia*	*Apis mellifera*
Prenylated flavanones	7-*O*-prenylpinocembrin	Greece, Japan		*Apis mellifera*
Neo-flavonoids	Cearoin	Nepal	*Dalbergia*	*Apis mellifera*

1.4.1 European Propolis

In Europe, the resinous exudate produced by the buds of poplar trees is the primary component of bee propolis. European propolis is rich in flavones and flavanones,

phenolic acids and their esters when compared with propolis samples from tropical regions which usually mainly contain terpenes (Bankova and medicine, 2005).

Several studies have reported on examples of European propolis. In one such report, 13 propolis samples from Serbia were studied to determine their antimicrobial activity, which concluded that propolis has significant antimicrobial activity against Gram-positive bacteria (Stepanovic et al.). Another study on samples of romanian propolis found that flavonoids and phenolic acids are the main biologically active compounds in romanian propolis. those propolis samples were tested against *E. coli* strains isolated from bovine mastitis, it highlighted similarly good antimicrobial activity based on its chemical composition (Niculae et al., 2015).

Several examples of propolis from Malta were analysed and reported to contain mono- and sesquiterpenyl esters of substituted benzoic acids which are postulated to originate from plants of the genus Ferula (Popova et al., 2011). Propolis samples from various locations in Greece were similarly reported to be especially rich in diterpenes while containing almost no phenolics. This was also the case with examples of propolis which originated from Croatia and Malta (Popova et al., 2011). The existence of diterpenes in propolis samples from Greece is attributable to the predominant plant resources, which are predominantly conifer species of the Cupressaceae family which are endemic to this region (Popova et al., 2010, Trusheva et al., 2003, Melliou and Chinou, 2004).

Propolis from Poland has been reported to contain compounds which have antibacterial and anti-proliferative properties (Popova et al., 2017, Przybyłek and Karpiński, 2019). The biological evaluation and characterisation of propolis from Poland revealed that it contained glycerol esters of phenolic acids along with remarkably high quantities of p-coumaric as well as ferulic acid and their benzyl esters (Popova et al., 2017, Krzek et al., 2006, Celińska-Janowicz et al., 2018). From the same country a study conducted on caffeic acid phenthyl ester (CAPE) and chrysin, which isolated as compounds of propolis and concluded that might prevent tumour cell progression and may be beneficial as potential chemotherapeutic or chemopreventive anticancer medicine (Sawicka et al., 2012). Studies into the chemical composition and biological activities have been reported for propolis samples from various geographic locations in Europe (Germany, Ireland, and the Czech Republic). The results revealed that the most abundant compounds in the samples were aromatic alcohols, aromatic acids, cinnamic acid and its esters, fatty acids, and flavanones (chrysin). The antimicrobial activities of these European propolis samples were assessed alone and in combination with known antibiotics. They revealed that all the propolis samples displayed moderate antibacterial activity against Gram-positive and Gram-negative bacteria with moderate antifungal activity as well. The propolis extracts were also found to have a synergistic boosting effect on the efficacy of the antibiotics against drug-resistant microorganisms, especially those antibiotics which act on cell wall syntheses such as vancomycin and oxacillin (AL-Ani et al., 2018). A study on UK propolis highlighted that propolis could be used with dressings to treat burns (Oliveira et al., 2016).

1.4.2 Saudi Propolis

Large quantities of propolis are produced in the southern and southwestern regions of the Kingdom of Saudi Arabia where a great variety of flowering plant species exists. A small number of studies have been conducted on propolis samples from Saudi Arabia mostly to determine their chemical compositions and biological activities as well as to compare of their features with those of other examples of propolis from different geographical regions. Propolis samples from Al-Bahah are rich in compounds such as sclerone, bergapten, 3,5,7-trimethoxyflavone and phloretin. A large number of aromatic acids, alcohols, phenol aldehydes, amongst other compounds (aliphatic acids, sugar derivatives, steroid derivatives and flavone derivatives) have been identified from samples of Baha propolis (Bakdash et al., 2018). Another study which reported on propolis from Baha examined the importance of propolis as anticancer drug candidates (Elnakady et al., 2017). Studies conducted on propolis samples from Saudi Arabia revealed that they contained flavonoids, phenolic acids, diterpenes and terpenes including p-coumaric acid, caffeic acid, apigenin, kaempferol, quercetin, rutin, ferruginol,3,4,-dihydro-2-(3,4-dihydroxyphenyl)-2H-chromene-3,7-diol and triterpene acetate (3'-acetoxy-19(29)-taraxasten-20a-ol) (Siheri et al., 2016, Jerz et al., 2014, Singh, 2014).

1.5 Biological activity of Propolis

1.5.1 Antibacterial, Antiviral, Antifungal, Antiparasitic Activities, and Antitrypanosomal:

The first studies into the antibacterial activity of propolis extracts were conducted in 1980 and found that *Streptococcus* species were sensitive to propolis extracts. It also noted that the alcoholic extract of propolis was effective against a *Bacillus* strain (Aminimoghadamfarouj and Nematollahi, 2017). A growth inhibition activity of 3 mg/mL was recorded against *Pseudomonas aeruginosa* and *Escherichia coli*. A synergistic antibacterial effect on *Staphylococcus aureus* and *Escherichia coli* was observed when alcoholic extracts were tested simultaneously in the medium with other antibiotics (Kuropatnicki et al., 2013). Sforcin *et al*. reported that propolis affected the formation of Flu viruses (A and B types) and also stated that the cell receptors at the viral adsorption step could be affected by propolis (Pobiega et al., 2017). Using (30 µg/mL) of propolis can dramatically reduce Herpes virus counts (Sforcin et al., 2000). Other reports also suggest that propolis strongly inhibits the proliferation of *Trypanosoma cruzi* at 15 µg/mL (Higashi and De Castro, 1994). Studies on alcoholic extracts of propolis samples have demonstrated that it can terminate the proliferation of protozoa, such as *Toxoplasma gondii* and *Trichomonas vaginalis*. Fatal effects were observed for three strains of *Trichomonas vaginalis* when exposed to extracts of propolis at a concentration of 150 µg/mL (Freitas et al., 2006). Ethanolic extract samples of argentinean propolis showed antifungal and anthelmintic activities (Salas

et al., 2016). The antifungal properties of diterpenoid propolis have been utilised in dental preparations to decrease the adhesion of fungi to surfaces (Ota et al., 2001).

Several *in vitro* studies on various samples of propolis extracts such as Chinese propolis, Brazilian propolis as well as propolis samples from Chile (Valenzuela-Barra et al., 2015) and Nepal (Funakoshi-Tago et al., 2015), all reported the observation of anti-inflammatory properties attributed to propolis (Wang et al., 2015). Although there are numerous beneficial applications of propolis, it has also been linked to some adverse effects such as toxicity and allergenic impacts (Banskota et al., 2001). To investigate the cytotoxic properties of Propolis, Awale *et al*., analysed red Propolis samples from Brazil against six different cancer cell lines resulting in the conclusion that propolis has significant cytotoxic activity (Li et al., 2008). Another *in vivo* study reported the cytotoxic effect of propolis on skin tumours in mice (Aminimoghadamfarouj and Nematollahi, 2017). The LD50 of the alcoholic propolis extract samples were reported at about 700 mg/kg, while a group of Russian researchers found an LD50 of 350 mg/kg (Burdock and toxicology, 1998). Flavonoids are well known for their antioxidant activity towards the oxidants in the cell membrane (Seven et al., 2010). Also, caffeic acid phenethyl ester is reported to block the production of reactive oxygen species (Ma et al., 2006). In general, propolis contains polyphenols (flavonoids, phenolic acids and their esters). Due to the flavonoids and antioxidant phenols concentrated in propolis which are considered powerful antioxidants, demonstrated to be capable of scavenging free radicals which cause significant interference with normal cell metabolism, propolis is considered to be a powerful

antioxidant (Anjum et al., 2019). Propolis has been reported to protect lipids and other compounds such as vitamin C from oxidation or the destruction caused by active free radicals. These free radicals along with other factors are responsible for cellular ageing and degradation in various conditions such as cardiovascular disease, which leads to heart attacks and strokes, arthritis, cancer, diabetes, as well as neurodegenerative diseases such as Alzheimer's disease (Kuropatnicki et al., 2013). Propolis is also used as an antioxidant in cosmetic products, such as face creams, ointments, lotions, and solutions (Huang et al., 2009). A thorough discussion of the properties of propolis is extensively covered in the following review papers (Kuropatnicki et al., 2013). From previous studies into the toxic properties of propolis, several reports on incidents of the allergenic effects of propolis highlight that the environment surrounding the hive location is one of the main factors responsible for the presence of some materials such as asphalt from road construction sites in propolis. This was also responsible for the presence of the metals reported in samples of Cuban propolis such as Iron (Fe), Zinc (Zn), Copper (Cu) and Magnesium (Mg), as well as the heavy metal lead (Pb) which was detected from samples of Brazilian propolis (Banskota et al., 2001).

A significant inverse association has been reported between the concentrations of the total quantities of phenolics in samples of propolis balsam and the MIC of the samples (Bankova, 2005). The higher the concentration, the lower the MIC ($P = 0.003$). Similarly, there is an observed relationship between the percentage of the total quantity of phenolics and the observed biological activity, which is helpful for the quantification of individual components. Propolis is a natural product widely used by people around

the world. It has generated a lot of attention over the last three decades due to its therapeutic activities which have produced diverse lines of research in several countries. Red propolis is found in several countries such as Brazil, Cuba, Mexico, China and Nigeria. Ten phenolic compounds were isolated from Nigerian red propolis (NRP) from Bonny, Rivers State, Nigeria (Omar et al., 2016). Also, the Cuban red propolis (CRP) was found to possess antibacterial, antiprotozoal and antifungal properties attributed to its chemical composition (Monzote et al., 2012). Samples of propolis from Libya were observed to have the following IC50 values: 1.56 µg/mL (*Trypanosoma brucei*) and 5.1–21.9 µg/mL (*Leishmania donovani*) (Siheri et al., 2014).

Samples of Nigerian red propolis and the compounds which it is reported to contain such as vestitol, calycosin, pinocembrin, macarangin, medicarpin, liquiritigenin, 8-prenylnaringenin, 6-prenylnaringenin, propolin D and riverinol, were assessed to determine their anti-trypanosomal activity against *Trypanosoma brucei*. The samples were found to have anti-trypanosomal activity with EC50 values ranging between 4.2 µg/mL for the crude extract to 16.6 µg/mL for riverinol (Rufatto et al., 2017). The anti-trypanosomal activity of nigerian propolis was found to be roughly similar to that of brazilian red propolis (Omar et al., 2016). A study was conducted on propolis from Chihuahua in Mexico found that it possesses hypoglycaemic and antioxidant activities (Rivera-Yañez et al., 2018).

Although not previously expected to be abundant in the composition of propolis, phenolics and flavonoids are now considered to be the main components responsible

for its biological activity which has led to the development of new techniques and uses for propolis. The chemical composition of propolis is very complex and depends largely on the geographical origin of the samples and the plants within proximity of the hive, in spite of this , it can potentially have significant applications for the development of new drugs, this will depend on further research and development, which would be important to ensure that these are safe to use.

The biological properties of each type of propolis will need to be associated with its chemical composition; therefore, it will be necessary to distinguish between propolis types. Ultimately, standardised products should be used in medical studies. There is, therefore, a need for more sophisticated techniques for the standardisation of propolis samples which has become apparent. Studies into the problem of standardisation of propolis by Bankova *et al*. concluded that the correct approach is to measure the concentrations of groups of active compounds rather than the concentrations of individual components (Bankova, 2005). This will enable scientists, through the use of standard protocols, to link specific types of the propolis to specific biological properties. This is particularly important when considering the reliability of the results obtained from studies on the biological properties of propolis and also help the general public to make better-informed choices when considering what propolis to use for their beneficial biological properties. Besides, the separation of organic compounds from propolis, studies into their mechanism of action on cells may play a significant role in the development of new products to add to the toolbox for the control of tumour growth and infection control and the treatment of several disease(Santos, 2012). Propolis can

be obtained in large quantities; therefore if it is possible to prove its efficacy in-vivo, it will be a potentially important natural resource for the treatment of protozoal infections (Omar et al., 2016).

1.6 Trypanosomiasis and Leishmaniasis

1.6.1 Trypanosomiasis

Trypanosomiasis is an infectious disease affecting vertebrates caused by infestations of parasitic protozoan trypanosomes of the genus Trypanosoma as a result of bites from the Tsetse fly found mainly in parts of Africa and South America. Protozoan trypanosomes are a genus of unicellular parasitic flagellate protozoa. In humans, it includes diseases like Chagas disease and African human Trypanosomiasis (African sleeping sickness/sleeping sickness). The name comes from the two Greek words, trypano- (borer) and soma (body). African human Trypanosomiasis has been listed as a neglected tropical disease by the World Health Organisation (WHO) (Barrett and Croft, 2012). This disease is transmitted to humans by Tsetse fly bites which cause infection by injection of the protozoal parasites leading to two types of human diseases which are sleeping sickness and Chagas' disease. For 40 years, there was no significant development in the treatment of these diseases which is currently managed by only by a limited number of antibiotics to which over time the parasites have become resistant (Bouteille et al., 2003). The deadly human disease sleeping sickness is caused by *Trypanosoma brucei*, while Chagas disease is caused by *Trypanosoma cruzi*. In sub-Saharan Africa, the primary vector-borne parasitic illness in humans is African

Trypanosomiasis or sleeping sickness carried by the Tsetse fly. In animals, it also causes animal trypanosomiasis called nagana in cattle and horses (Bouteille et al., 2003, Stich et al., 2003).

The *T. brucei* spp has traditionally been divided into three subspecies: *T. b. brucei*, *T. b. gambiense* and *T. b. rhodesiense*. Sleeping sickness which is caused by *T. brucei* in Africa, and Chagas disease which is caused by *T. cruzi* in Central or South America are both fatal if left untreated. In west Africa, a more chronic infection is caused by *T. b. gambiense*. Both of the African diseases can be transmitted through blood. Another species of trypanosomes, *T. congolense,* is responsible for the disease nagana in cattle and other animals in east and west Africa (Seebeck and Mäser, 2009, Steverding and vectors, 2008) . Studies have been conducted to investigate the effect of propolis from different parts of the world on different types of Trypanosomiasis which concluded that propolis had significant activity against these microorganisms (Dantas et al., 2006, Nweze et al., 2017, Siheri et al., 2019, Salomao et al., 2011).

1.6.2 Leishmaniasis

Leishmaniasis is a disease in humans caused by intracellular protozoan Leishmania parasites of the genus Leishmania which are responsible for both cutaneous and visceral (kala-azar) leishmaniasis (Torres-Guerrero et al.). Phlebotomine sand-flies transmit leishmaniasis to humans and animals by their bite, and it is endemic in Africa, Asia, the Americas and the Mediterranean areas with up to 2 million new infections each year (Torres-Guerrero et al.). Approximately 10 million people are affected by

cutaneous leishmaniasis. In comparison, about 400,000 people per year are affected by visceral leishmaniasis, which is caused *by L. donovani*, *L. infantum* and *L. chagasi*. Additionally, the sharing of drug injecting paraphernalia is a significant factor in the transmission of visceral leishmaniasis. Asia, primarily northeast India, Africa and Brazil account for 90% of cases with small numbers in Europe. Propolis has been demonstrated in *in vitro* tests to have significant positive effects against some types of Leishmania parasites. In one of these experiments, propolis from Brazil was reported to reduce the secondary chronic inflammatory reaction in the livers of mice caused by *L. amazonensis* (da Silva et al., 2016).

1.6.3 Treatment for Trypanosomiasis and Leishmaniasis

Both diseases progress in two stages, so the treatment options are dictated by the stage the disease is at in its life cycle. In Trypanosomiasis, the first stage is haemolymphatic, while the second stage is neurological (Barrett et al., 2007). Different drug therapies are thus used in the different stages of the disease. Similarly, different drugs are used to target the different stages in Leishmaniasis Table 1-2 (Davidson, 2005).

Table 1-2: Available of trypanocidal and Leishmaniasis drugs (Bouteille et al., 2003, Brown et al., 2005, Legros et al., 2002, Davidson, 2005).

Drug	**Activity of**	**Stage**	**Disease**	**Route First**	**Marketed**	**Comments**
Suramin	*T.b. rhodesiense* *T.b. gambiense*		Stage 1	IV.	1922	Not recommended for *T. b. gambiense*

Pentamidine		Stage 1	IM.	1937	Treatment failures
Diminazene aceturate	*T. b. gambiense*	Stage 1	IV.	1960	Veterinary use
Melarsoprol	*T. b. gambiense* *T.b. rhodesiense*	Stage 2	IV.	1949	2 to 12% mortality rates, reactive encephalopathy, treatment failures
Eflornithine	*T. b. gambiense*	Stage 2	IV.	1981	Difficult to administer Not effective against T.b. rhodesiense
Nifurtimox	*T. b. gambiense*	Stage 2	Per os (orally)	1960	Not approved for sleeping sickness Effects on T. b. rhodesiense unknown
Pentavalent antimonials	cutaneous leishmaniasis	first-line drug	20 mg/kg/day	1940	Patients should be hospitalised during systemic therapy.
Amphotericin B	cutaneous leishmaniasis	first-line drug	15 doses of 1 mg/kg	-	Unlicensed But a powerful antileishmanial agent

Miltaforcin	visceral leishmaniasis cutaneous leishmaniasis	first-line drug	Oral 2.5 mg/kg/day	-	It is teratogenic
Ketoconazole and itraconazole	cutaneous leishmaniasis	second-line drug	-	-	effective in cutaneous leishmaniasis caused by L. major or L. mexicana
Pentamidine	cutaneous leishmaniasis	second-line drug	Short course	-	effective in American cutaneous leishmaniasis

1.7 Instrumental methods

1.7.1 General introduction

Propolis is a complex mixture that consists of beeswax and secondary metabolites of plant origin. Lewis and Short defined it as “the third stage” in the process of making honey (Kuropatnicki et al., 2013). Traditional methods of phytochemistry such as chromatography and mass spectrometry, are utilised to isolate and detect compounds from propolis and NMR is used to characterise the compounds and in conjunction with other analytical methods, determine the structure of the isolated compounds. These methods have been applied with great success to the discovery of novel chemical compounds from propolis.

Advances in column chromatography and thin-layer chromatography in the 1970s were utilised to develop new chromatographic analytical techniques (Marston, 2007). As a result, it was possible to conduct more separations and extractions of propolis to identify its components. Gas chromatography (GC) and high-performance liquid chromatography (HPLC) applications were later developed and applied to propolis analysis in 1979 by Vanhaelen (Kuropatnicki et al., 2013). Vanhaelen-Fastre subsequently developed gas chromatography-mass spectrometry (GC-MS) applications which were used to to identify sugars in propolis (Kuropatnicki et al., 2013).

The separation techniques most commonly applied to isolate natural products are normal phase, reverse phase, and, to a lesser extent, gel permeation and ion-exchange chromatography (Salituro and Dufresne, 1998). Chromatographic methods are often applied to the separation of the complex mixture that is the propolis matrix into fractions of its components, in order to isolate, assist in the identification and quantification of the propolis component compounds.

Studies reported into the chemistry of propolis include large numbers which focus on European propolis which is composed of resins collected from Populus species because of the typical flavonoids found in the bud exudate of Populus species in temperate regions (Wollenweber and Buchmann, 1997). The use of High-Performance Liquid Chromatography (HPLC) is currently recommended for the analysis of propolis instead of Gas Chromatography-Mass Spectrometry (GCMS). This is due to problems with the lower reproducibility of the GCMS methods (Santos, 2012). An alternative method to

determine the patterns and content of the phenolic components of propolis utilising a high-resolution mass spectrometry method was recently applied with high accuracy (Kim et al., 2019). Also, one of the best analytical methods for propolis studies is Nuclear magnetic resonance (NMR), because it is capable of identifying components which may be either sensitive or insensitive to Ultraviolet Light (UL) (Santos, 2012).

1.7.2 Liquid Chromatography-Mass Spectrometry LC-MS

The Liquid Chromatography-Mass Spectrometry (LC-MS) system is considered to be one of the most popular techniques which are used for the separations and detection of a variety of compounds (Boyce et al., 2020). All chromatographic techniques are designed to separate compounds utilising several basic characteristics including, size, charge and the strength of interactions between compounds and the mobile phase or the stationary phase in which the polarity of compounds and their partitioning can play a significant role in the separation of compounds (Salituro and Dufresne, 1998).

LC-MS system is an integrated technique, which consists of a separation process by High-Performance Liquid Chromatography (HPLC) and a detection process by Mass Spectrometry (MS) as shown in the figure below (Figure 1-3).

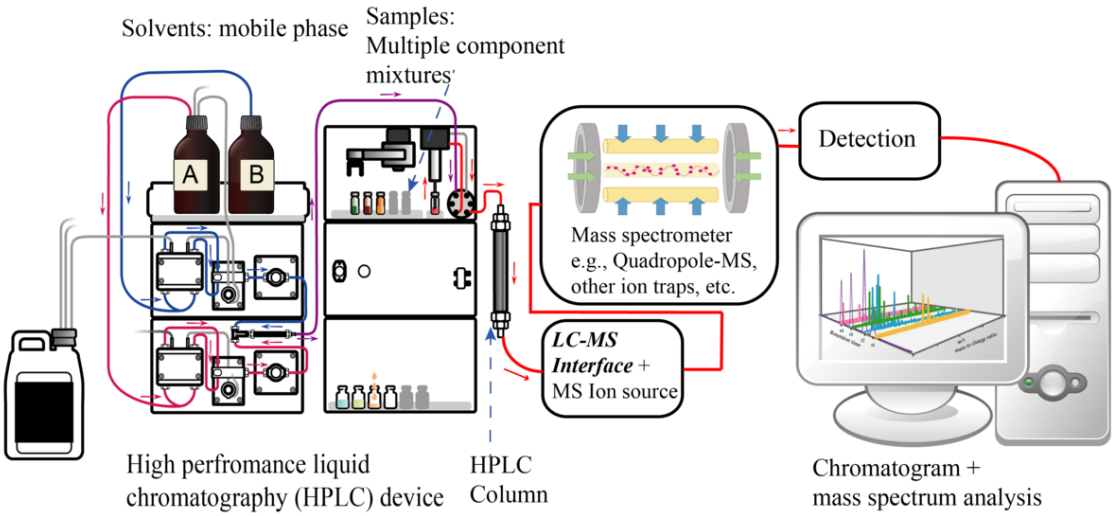

(https://www.microscopemaster.com/images/Liquid_chromatography_tandem_Mass_spectrometry_diagram.png)

Figure 1-3: The separation process in (LC) with the detection of (MS)

1.7.2.1 High-Performance Liquid Chromatography (HPLC)

In chromatographic separation in general, the analyte is introduced into a mobile phase which is in motion over a stationary phase. The stationary phase interacts with the molecules in the sample forming either strong or weak interactions which cause the various molecules to move at different rates in the mobile phase over the stationary phase releasing them separately at different times. The mobile phase varies depending on the technique, for example when the mobile phase is a gas, this type of chromatography is called gas chromatography (GC) which is also used in conjunction with mass spectrometry in GC-MS. GC is an outstanding technique for the identification of volatile substances. When the mobile phase is a liquid, it is called liquid chromatography (LC). High-pressure liquid chromatography (HPLC) is a potent tool for the separation of compounds and the detection of UV-absorbing compounds when connected to a UV detector. Non-UV-absorbing compounds can be detected with

the use of other methods of detection such as an evaporative light scattering detector (ELSD) to make an (HPLC-ELSD) system or Mass Spectroscopy (HPLC-MS).

The stationary phase for HPLC typically is packed into a column filled with a variety of very tiny particles of absorbent material, less than 5 μm in diameter, depending on the type of column. The liquid mobile phase (or eluent) is forced through the column by a pump at elevated pressure. Samples are injected onto the mobile-phase via a small volume at the head of the chromatographic column. A schematic diagram to illustrate the separation process appears below (

Figure 1-4). The blue and white circles represent two different molecular species with different polarities used to illustrate the process of separation on the column (Moldoveanu and David, 2013).

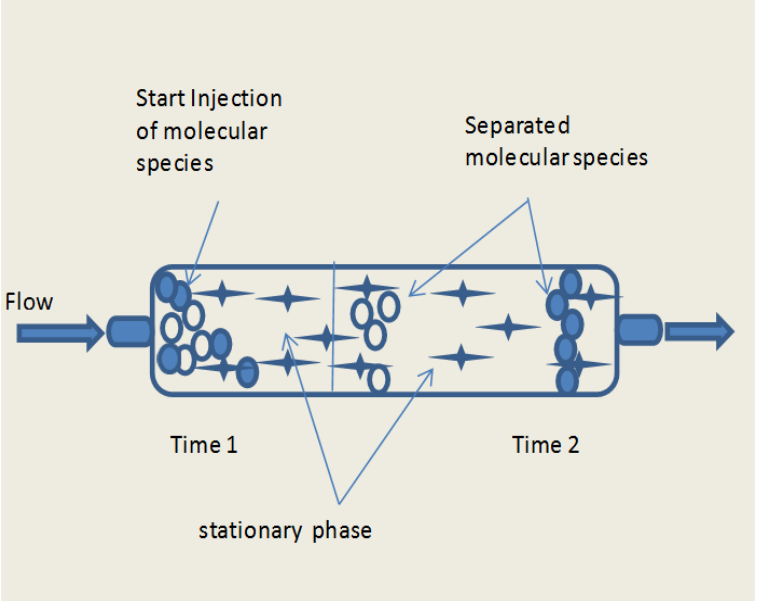

Figure 1-4: The separation process in the column

1.7.2.2 Column principle in chromatography

Moldoveanu et al. illustrated that there are two main combinations used as the stationary phase (SP) and the mobile phase (MP) commonly used for LC-MS (Moldoveanu and David, 2012). The first combination is for normal- phase chromatography in which the SP is polar and the MP is non-polar. The most common SPs for this kind of chromatography are silica or organic moieties with cyano and amino functional groups with MPs being non-polar organic solvents such as n-Hexane or Ethyl Acetate. The other combination is reversed-phase chromatography in which the SP is non-polar while the MP is polar. Octadecyl-C18 is the most popular material used as SP for this type of column because it consists of alkyl hydrocarbons, and these are a preferred stationary phase. Also, octyl-C8 and butyl-C4 are used in other applications. The chain lengths of the hydrocarbon chain in each of the different

materials is included in the title of the reversed-phase material. In normal-phase chromatography, the least polar compounds elute first from the MP followed by compounds with increasing polarity and the most polar compounds elute last using the same MP following the elution of each of the compounds respectively in order of increasing polarity. The mobile phase is typically made up of non-polar solvents such as hexane, ethyl acetate or chloroform. The amount of polar solvent in the MP is inversely proportional to the retention time. In reversed-phase chromatography, the most polar compounds elute first while the least polar compounds elute last. The MP is usually a mixture of water and a miscible polar organic solvent such as methanol, acetonitrile or THF. The amount of polar solvent in the MP is directly proportional to the retention time. The mechanism *via* which normal phase chromatography works is adsorptive and can thus be used for the analysis of solutes which are readily soluble in organic solvents, depending on their relative polarities such as amines, acids, metal complexes. In reversed-phase chromatography, its mechanism of action is *via* partition, which results in separations by non-polar differences.

1.7.2.3 Mass Spectrometry

A mass spectrometer (MS) is an analytical instrument designed to distinguish between compounds ions based to their mass to charge ratio (m/z) values (Salituro and Dufresne, 1998).

The sample is introduced into the MS in an eluent which comes from an LC column and enters the MS where it is ionised and separated with the aid of electrical and magnetic fields into different ions based on their m/z ratios after one of a variety of

ionisation methods produces the charged species. Standard ionisation techniques used in mass spectrometry include Electron Impact ionisation (EII), Fast Atom Bombardment (FAB), Electrospray Ionisation (EI), Atmospheric Pressure Chemical Ionisation (APCI) and Matrix-Assisted Laser Desorption Ionization (MALDI)**.** The mass spectrometer comprises a vacuum system, a detector and an atmospheric ionisation chamber.

The mass spectrometer consists of six parts; each with an essential unique function, as shown in the figure below Figure 1-5.

1- Ion source: it sprays the HPLC eluent into the atmospheric ionisation chamber.
2- Skimmer Cone: it has a sampling orifice to control the flow of sample gas-phase ions and reduces the gas load entering the vacuum system of the MS.
3- Quadrupole: the function of this is to separate ions according to their (m/z) by using electric fields.
4- Collision Cell: here ions are accelerated due to collision with neutral collision gas molecules causing the analyte to fragment.
5- Detector: after the ions are produced and separated, the ion detection system transforms the ions into a usable signal to detect them.
6- Vacuum system: it controls the high-level vacuum system enabling it to operate efficiently by preventing ions being destroyed by gases in the atmosphere.

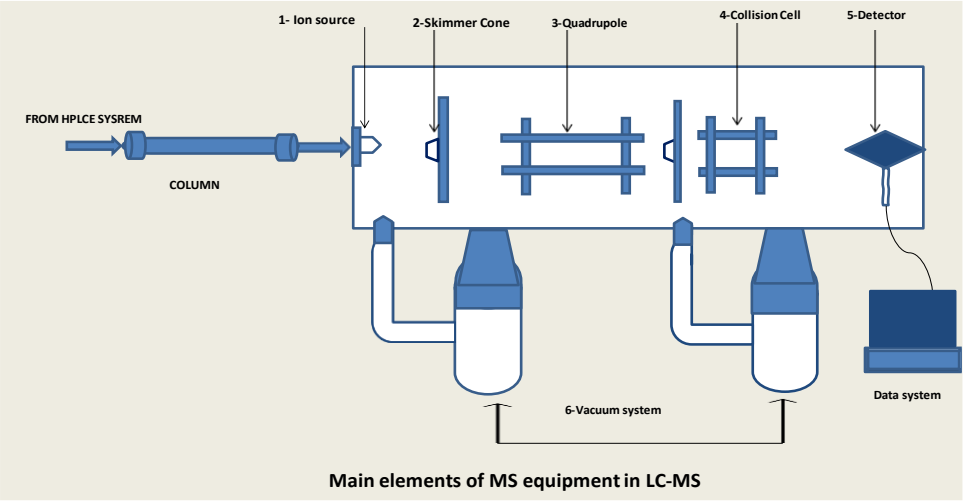

(https://www.chromacademy.com/)

Figure 1-5**:** Schematic diagram of a mass spectrometer (MS)

1.7.3 Evaporative Light Scattering Detector (ELSD)

A wide range of compounds with no or weak UV absorptions can be detected by Evaporative light scattering detection (ELSD) which is used as a semi-universal detector in high-performance liquid chromatography (HPLC) applications. Therefore, this technique is ideal for the detection of different types of natural products by using reversed phase-HPLC in conjunction with an ELSD detector. This technique is also commonly used as an analytical application for food and beverage analysis as well as pharmaceutical development (Dvořáčková et al., 2014).

The LC-ELSD technique functions by three main processes which include; mobile phase nebulisation to produce a narrow distribution of droplets, evaporation of the solvent and subsequent measurement of the light scattered from analyte particles depicted in the figure below (Figure 1-6).

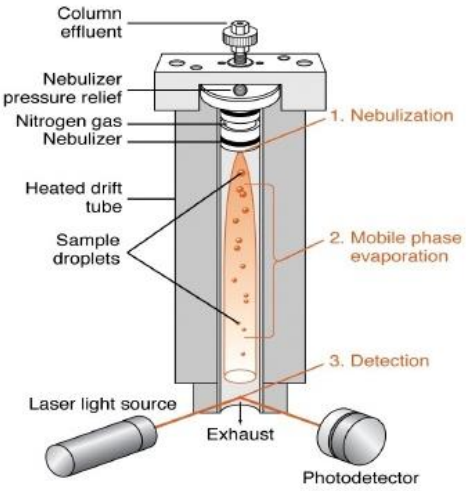

https://www.slideshare.net/bharathpharmacist/detectors-hplc-39635851

Figure 1-6: Evaporative Light Scattering Detector

A small portion of the mobile phase flow, diverted from the column to the detector, is nebulised using a gas which is usually either nitrogen or air to produce a plume of ultra-fine droplets containing the analyte in solution. These droplets then pass into a heated zone in which the solvent evaporates leaving the dry analyte particles which subsequently are irradiated with light. The amount of light scattered is detected and quantified by an internally mounted photodetector. The response of the ELSD can be tuned to optimise its performance by adjusting the gas flow, and temperature.

1.7.4 Medium-pressure liquid chromatography (MPLC)

Medium pressure liquid chromatography (MPLC) is used for the separation and purification of compounds and is capable of performing all types of chromatography processes. In this project, a Grace Reveleris® iES Chromatography System (Alltech, Carnforth, Lancs, UK) was utilised to purify crude extracts as well as fractions derived

from column chromatography. Samples for purification on the Reveleris system were dissolved in a minimum quantity of suitable solvent, typically (EtOAc) and combined with celite (1:2 w/w). The mixture was subsequently entirely dried in a fume-hood and then dry-loaded onto prepacked cartridges. Fractionation was conducted either under normal phase conditions, utilising a silica gel column (GraceResolv Silica 24 g/32 ml) or with a reverse-phase system, utilising a C18 (12 g) cartridge. For the latter situation, HPLC-ELSD-UV was employed for process optimisation utilising suitable isocratic conditions providing improved peak resolution for transfer to the Grace system. The Grace system included a detection System which provided two UV channels adjusted to (290 nm, 320 nm) for all experiments, and an ELSD capable of detecting both non-chromophoric and chromophoric substances within complex extracts over a single run, as shown in the figure below (Figure 1-7).

The resulting peaks were resolved either by slope or threshold detection using the integrated automatic fraction collector. Sensitivity levels of 'medium' were utilised for all runs, resulting in an acceptable compromise for the majority of cases leading to chromatograms with improved noise parameters. Data was collated and assessed *via* the Reveleris® Navigator™ Windows application and subsequently exported as a pdf file. Appropriately labelled test-tubes were used for fraction collection. The tubes containing the fractions from respective peaks were combined and concentrated under reduced pressure and individually weighed. HPLC-UV-ELSD was utilised to conducted fraction purity in each instance. Fractions with a purity above 80–90%, chemical purity were further assessed by NMR and by LC-MS.

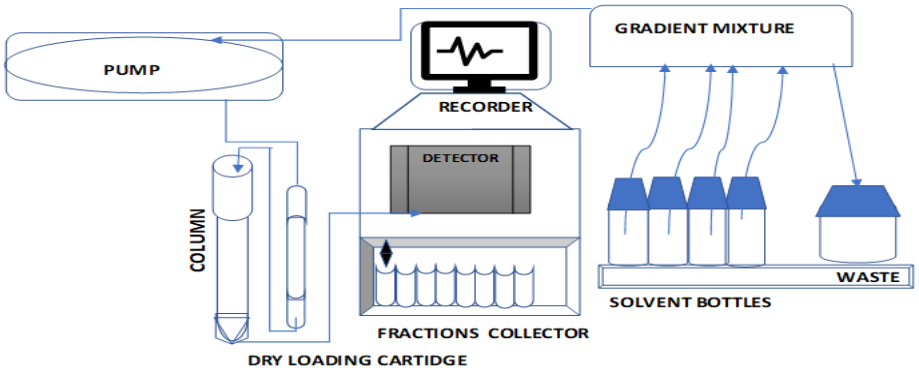

https://commons.wikimedia.org/wiki/File:Preparative_HPLC.svg

Figure 1-7: Schematic diagram of the basic components of MPLC

1.7.5 Nuclear Magnetic Resonance (NMR)

1.7.5.1 NMR Techniques: DEPT, COSY, HMBC, HMQC and NOESY.

Nuclear magnetic resonance (NMR) is widely acknowledged to be an analytical technique of primary importance for pharmaceutical analysis, especially for the determination of the structures of natural compounds, which facilitates the identification and verification of chemical compounds. Developed initially in 1946 by two discrete groups of physicists following the detection of radiofrequency signals emitted by proton nuclei in water and paraffin when placed in a magnetic field NMR has evolved into an invaluable analytical tool in science and medicine (Baianu and Prisecaru, 2011).

NMR is a physical phenomenon involving excitation of nuclei in a magnetic field with any electromagnetic radiation that is re-emitted being quantified. The resonance frequency of the energy released correlates with the strength of the applied magnetic

field as well as the magnetic characteristics of the atomic isotopes examined. All isotopes containing an odd number of protons and/or neutrons will exhibit an intrinsic magnetic moment, and angular momentum or a nonzero spin. In contrast, all nucleotides possessing even numbers of protons and neutrons have a total spin of zero. The most popular nuclei for examination are ^{1}H and ^{13}C (Wang and Bax, 1993). The components comprising an NMR spectrometer are depicted in the figure below Figure 1-8. NMR is considered to be the best technique for the simultaneous screening of multiple compounds from a variety of natural product classes such as waxes, terpenoids and phenolics which represent a variety of polarities, have no particular ionizability,

chromophore requirement or thermal stability, in comparison with the analytical techniques previously discussed. It can identify any substance comprising spin-active nuclei and is particularly appropriate for organic analysis. The primary constraints of NMR are its limits of resolution and sensitivity, but these can be overcome to some degree by applying a more energetic magnetic field.

In phytochemical analysis, NMR is predominantly used for the identification of structural morphologies used for the identification and verification of chemical compounds, by comparing NMR spectra obtained during analysis with standard spectra of reference samples, or spectral data previously made publicly available. Interpreting NMR data can be challenging, especially where complex impure propolis samples are considered (Connelly et al., 2002).

The present investigation attempted the identification of pure compounds from propolis *via* one-dimensional ^{1}H and ^{13}C NMR spectroscopy. It was possible to identify several known compounds by comparing the spectra resulting from the analysis of compounds obtained from the project with published spectral data. When required, 2D experiments were employed to aid the accurate assignment of proton and carbon chemical shifts for new or previously unknown substances (Stoyanova et al., 2001).

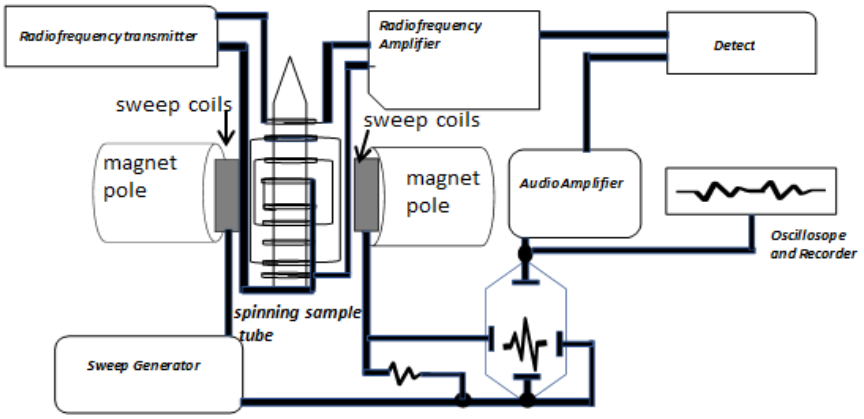

Figure 1-8: Schematic diagram of the basic components of an NMR spectrometer

^{1}H NMR provides the details of the protons existing within a molecule, including their chemical shifts, multiplicities (coupling information) and approximate numbers of protons from the integration. ^{1}H NMR was conducted for all substances identified in this study and was also employed even for crude extracts and fractions as an essential technique to facilitate structural identification. The resulting spectra aided the evaluation of the purity of any isolated substances (Elyashberg, 2015, Breitmaier and Sinnema, 1993).

^{13}C NMR provided details of the numbers and variety of carbon atoms existing in each isolated compound. The resulting spectra were either broad band-decoupled or J-modulated. For the broad band-decoupled spectra, the ^{1}H nuclei were irradiated. At the same time, the ^{13}C acquisition took place, to facilitate full decoupling of all protons from the ^{13}C nuclei, which then enabled each distinct ^{13}C environment within the molecule to produce a discrete singlet signal.

The *J*-modulated investigation assists in distinguishing carbon atoms relative to the level of their proton attachments (C, CH, CH_2 and CH_3). DEPT (Distortionless Enhancement by Polarization Transfer) spectrum constitutes a pulsed-sequence experiment which transforms details on the CH signal multiplicity and spin-spin coupling into a phase association. In a DEPT 135 spectrum, CH_3 and CH orient towards the positive spectral phase, while CH_2 protons orient towards the negative phase. The benefit of the DEPT 135 spectrum compared with a standard broad band-decoupled carbon spectrum is that this approach enables discrimination of C/CH_2 carbons from CH/CH_3 carbons in a single experiment (Dumas et al., 2002) An additional benefit is a high sensitivity with which the results can be obtained: four times greater than ^{1}H – ^{13}C polarisation transfer (Elyashberg, 2015, Breitmaier and Sinnema, 1993).

1.8 Aims and Objectives

The aims of this study are:

1- To isolate and characterise compounds from European propolis and samples from Saudi Arabia using chromatographic, mass spectrometric and NMR methods.

2- To test fractions and isolated compounds for anti-protozoal and anti-microbial activities.

3- To use the biological activity to target the active compounds in the fractions.

2 Chapter 2

2.1 MATERIALS AND GENERAL METHODS

2.1.1 Chemicals and laboratory materials

2.1.1.1 Solvents

HPLC grade solvents, including hexane, ethyl acetate, methanol, acetonitrile, and absolute ethanol were obtained from Fisher Scientific (Loughborough, UK). AnalaR grade formic acid (98%) from BDH-Merck (Dorset UK) and HPLC grade water was produced in house using a Milli Q system water purifier from Millipore, UK).

2.1.1.2 Chromatography

Silica gel of mesh size 200–425 μm, for column chromatography, Davisil grade 633 amorphous precipitated silica of pore size 60 A, and Celite filter agent for sample dry loading onto MPLC were purchased from Sigma-Aldrich (Dorset UK). Davisil grade 636 column grade silica gel, pore size 60A, mesh size 35–60 and TLC silica gel 60 F254 pre-coated aluminium sheets were obtained from Merck (Germany) and used for column chromatography and thin-layer chromatography respectively.

2.1.1.3 NMR

The NMR analyses were run in deuterated solvents including $CDCl_3$, DMSO-d_6 and Acetone-d_6, purchased from Sigma-Aldrich (Dorset UK).

Other materials were obtained as follows: 4 mL glass vials 45×14.75 mm (Kinesis Ltd, UK), ACE C18 column (3 mm x 150mm, 3µm) (Hichrom, UK), the syringes and Acrodisc filters, ultrasonic bath (Scientific Laboratory Supplies, Ltd) and rotary evaporator (Buchi, Switzerland) from Fisher Scientific (Loughborough, UK), Balance (Adventure, UK), Automatic pipettes (Gilson, Anachem, UK), LC-MS vails (Thermo, Germany), NMR tubes (5mm 300 MHz, 187 mm L, from (Norell USA), Glass columns for column chromatography were from (Rotaflo UK), Empty dry-loader cartridges for sample packing and loading onto the Grace Revelreis system, C18 (12 g) cartridge, and silica cartridge (24 g) from Alltech (Carnforth, Lancs, UK).

2.2 Collection of Propolis samples

European propolis samples D1-D20 were provided by Dr David Watson while Dr Khaled Saleh provided samples A21-A37 as in Table 2-1. All samples had a dark brown and slightly sticky appearance, except for the samples from Bulgaria, which were dark yellow and of slightly solid. The Polish sample P was purchased from a Polish Food company. In contrast, sample T2 was obtained from Saudi Arabia was obtained from a Saudi beekeeper Musa Alfuhaiqi and sample SB also from Saudi Arabia from Adel Alghamdi.

Table 2-1: Samples of European propolis used in the study.

code	Sample origin
D1	Gloucestershire, Wooton UK

D2	G29 Suffolk UK
D3	Pernik, West Bulgaria
D4	S22 Suffolk UK
D5	North Yorkshire UK
D6	Northamptonshire
D7	S170 Essex UK
D8	S225 Essex UK
D9	Starston, Norfolk, UK
D10	Devon, UK
D11	S206 Leicestershire, UK
D12	S205 Leicestershire, UK
D13	Derbyshire, UK
D14	G52 Lithuania
D15	G58 Lithuania
D16	G30 Suffolk UK
D17	S22 Suffolk UK
D18	S88 Bulgaria
D19	S89 Bulgaria
D20	S207 Cambridgeshire, UK
A21	Norfolk 2006 UK
A22	Northamptonshire UK
A23	S209 Northamptonshire UK
A24	AS207 Cambridgeshire UK
A25	S202 Yorkshire UK
A26	Northern Ireland UK
A27	Whitby H UK
A28	Whitby A UK
A29	Whitby Aa UK
A30	Whitby UK
A31	Essex UK
A32	S200 Berks UK
A33	S224 Midlands UK
A34	S203 Devon UK
A35	S230 Bucks UK
A36	Norfolk UK
A37	Norfolk A UK

2.3 Extraction of propolis samples

The propolis samples (500 mg) were extracted with 10 mL ethanol by sonication at 40 ^{o}C for 1h each. They were then spun on a centrifuge at 2500 rpm for 15 minutes. Each

sample was then filtered, and the filtrate collected. The filtered solids were re-extracted with ethanol (10 mL) and the extraction process repeated twice. The combined filtrates (EEP) were then dried using nitrogen gas. The weights of all the extracts were determined before storing them at -20 ^{o}C.

2.3.1 General profiling of crude samples of Propolis

The EEP of the propolis samples were dissolved in methanol (HPLC grade) to obtain a concentration of 1mg/mL, and the samples were filtered using a syringe filter (Acrodisc 0.45 µm). The sample solutions (10µL) were then injected into the LC-MS. The mobile phase composed of 0.1% formic acid in water as solvent A and 0.1% formic acid in acetonitrile as solvent B and set at a flow rate of 300µL/min Table 2-2. The high-resolution mass spectra were obtained using an LTQ Exactive Mass Analyser from Thermo Fisher Scientific (Hemel Hempstead, UK) with a needle voltage of -4.0 kV positive and negative mode. The liquid chromatography was performed on an ACE-C18 column (150×3 mm, 3 µm) from HiChrom UK. The MS detection range was from m/z 100 to 1500 with scanning performed under ESI polarity switching mode used permitting the acquisition of positive and negative ion data in a single experiment.

Table 2-2: Chromatography Methods for LC-MS analysis of European propolis extracts

S/N	Time min	%Solvent A	%Solvent B	Flow rate µL/min
0	0.00	70.0	30.0	300
1	30.0	0.00	100.0	300

2	40.0	0.00	100.0	300
3	41.0	70.0	30.0	300
4	50.0	70.0	30.0	300
5		100.0	0.00	300

A (0.1% v/v formic acid in H_2O) and B (0.1 % v/v formic acid in acetonitrile).

2.4 Purification of extracts

The nature of the Propolis samples and the class of compounds which are targeted for isolation is essential when choosing an appropriate protocol for the extraction of compounds from Propolis (Sarker et al., 2005). The first step for the extraction of Propolis is the screening of the samples under a microscope to remove any lingering impurities (e.g. wood, pollen, dead bees).. The most active extracts were selected to obtain fractions with active compounds. Four samples from the UK S224, S225, D6, D7, one from Poland (P) and two from Saudi Arabia T2 and SB, which showed high biological activity were subjected to further analytical techniques.

In this study, two methods A and B were used for the fractionation of the propolis samples. The methods were selected to optimise the detection and isolation of as wide a range of compounds from the samples as possible.

Method A, the ethanol extract of propolis (EEP) was subjected to column chromatography (CC) (General method 1)

Fractions were combined based on their LCMS profiling results. Fractions, with over 100 mg of material, were then subjected to fractionation and purification using Medium

Pressure Liquid Chromatography MPLC **(**General Method 4). The fractions from MPLC, based on their LCMS profiling, were combined and subjected to further purification using Sephadex column chromatography (General method 3).

Method B involved partitioning between dichloromethane and hexane**.** The ethanol extract of propolis (EEP) was dissolved in 200 mL of dichloromethane and filtered. Then 500 mL of hexane was added to the dichloromethane soluble portion, which resulted in immediate precipitation. The mixture was then filtered to obtain a clear filtrate and residue. The filtrate was allowed to dry in a fume hood. The residue and dried filtrate were subjected to column chromatography, elution beginning with hexane/ethyl acetate (80:20) (General method 1) or Vacuum Liquid Chromatography **(**General method 2**)** and gel filtration chromatography (General method 3).

2.4.1 General method 1: Column chromatography

A sample (2 g) of the ethanol extract of propolis (EEP) was dissolved in ethyl acetate. The solidified wax and residue were removed by filtration, and the filtrate was evaporated to dryness and mixed with 5 g of coarse silica in a beaker. The solvent was removed under a fume hood. Then silica gel 60 with a mesh size of 200–425 μm (50 g) was mixed with 200 mL of hexane and used to pack a glass column (55 x 3 cm). The sample mixed with silica was dry-loaded onto the top of the column, and elution was carried out as follows (collecting fractions in 50 mL flasks): 200 mL of hexane, F1; then 200 mL of hexane/ethyl acetate (80:20) F2; then 200 mL of hexane /ethyl acetate (60:40) F3; 200 mL of hexane/ethyl acetate (40:60) F4; 200 mL of hexane/ethyl acetate

(20:80) F5; 200 mL of ethyl acetate (100%)F6; and finally, 200 mL of ethyl acetate/methanol (70:30) F7 to produce 28 fractions which were dried and weighed. They were pooled according to their LC-MS profiling results and based on similarities in their abundance of compounds.

2.4.2 General method 2: Vacuum Liquid Chromatography (VLC)

Isolation and purification techniques are important for medicinal and aromatic plants as well as natural products. The chromatographic techniques were developed to be rapidly used for separation and also to find simple solutions to complex separation problems. VLC is an important and efficient method used in the separations of natural product mixtures which is widely used because of its simplicity of operation (Sticher, 2008). Dry Silica gel 60H was loaded in a glass Büchner funnel [13 cm (d) × 10 cm (h)] under vacuum. Propolis extracts (10 g) were dissolved in 25 ml of methanol and adsorbed onto a small amount of silica gel 60. The adsorbed sample was left to dry and thereafter loaded on the top of the column. The column was eluted starting with, n-hexane/EtOAc and EtOAc/MeOH mixtures as follows (collecting fractions in 500 mL round bottom flasks): 500 mL of hexane/ethyl acetate (70:30) F1; then 500 mL of hexane /ethyl acetate (50:50) F2; 500 mL of hexane/ethyl acetate (30:70) F3; 500 mL of hexane/ethyl acetate (10:90) F4; 500 mL of ethyl acetate (100%) F5; and finally, 500 mL of ethyl acetate / methanol (70:30) F6.The fractions were evaporated and weighed after drying. They were also examined by LC-MS to identify similar fractions.

2.4.3 General method 3: Gel filtration chromatography (GF)

This technique is known as filtration chromatography. It has the ability to separate molecules according to their size with a little or no interaction between the solute and the stationary phase. Larger molecules are eluted from the column first, and the lowest molecular weight compounds last because they tend to diffuse into the porous gel particles. A slurry of Sephadex LH-20 in methanol was loaded in a glass column [2 cm (id) × 100 cm (l)] and the bed was allowed to settle. The extract to be purified was dissolved in a minimum amount of methanol and then applied onto the column. The column was eluted isocratic with methanol after the extract was absorbed into the column bed. Fractions (3-5 mL) were collected, allowed to dry and after that examined by NMR.

2.4.4 General method 4: Medium pressure liquid chromatography (MPLC)

Medium pressure liquid chromatography (MPLC) has been used to separate and purify compounds, and it can perform all types of chromatography processes. This project utilised a Grace Reveleris® iES Chromatography System (Alltech, Carnforth, Lancs, UK) to purify crude extracts as well as fractions derived from column chromatography. EEP samples for purification on the Reveleris MPLC system were dissolved in a minimum quantity of ethyl acetate and combined with Celite (1:2 w/w). The mixture was allowed to dry and subsequently loaded into specified cartridges. Fractionation was carried out either under normal phase conditions using a silica gel column

(GraceResolv Silica 24 g/32 mL) or with reversed-phase conditions using a C18 (12 g) cartridge.

2.4.5 Thin Layer Chromatography (TLC)

Crude extracts and fractions from column chromatography, gel filtration chromatography and medium pressure liquid chromatography were examined by TLC to compare their profiles and identify similar ones for pooling. TLC was carried out on normal phase pre-coated aluminium backed silica gel plates. The extracts, fractions, and purified compounds were dissolved in an appropriate solvent and applied as a spot onto the plate approximately 2 cm above the base. Plates with samples were developed in suitable solvent systems. After development, the plates are dried, the solvent front marked and the spots were observed in daylight, UV light and by spraying with a colour developing reagent.

2.4.6 UV detection

Spots were observed under short UV (λ 254 nm) where they appeared as dark bands on a green background due to UV quenching and at long UV (λ 366 nm) where the fluorescent compounds show as coloured spots. Observed bands were circled or marked with a pencil.

2.4.7 Spray reagents

Developed TLC plates were also sprayed with p-anisaldehyde-sulphuric acid, vanillin-sulphuric acid. Sprayed plates were heated in a hot air heater to aid any colour

development. The Rf values were calculated, and fractions with similar TLC profiles were combined for NMR analysis.

2.5 Structure Elucidation

2.5.1 Nuclear Magnetic Resonance (NMR)

Proton NMR was the primary technique used for first-line evaluation and analysis of the extracts and fractions. Those with clean and discernible proton NMR were subjected to ^{13}C NMR. Where the results indicate a pure compound or identifiable mixtures, 2D NMR was run or acquired to tease out or elucidate the structures of the compounds or mixtures. The chemical shifts were and compare with literature reports to confirm the structures elucidated. NMR data were obtained either on a JEOL (JNM LA400) spectrophotometer (400 MHz) at SIPBS or a Bruker Avance III (400MHz) spectrophotometer at the Department of Pure and Applied Chemistry. For all NMR analysis, Tetramethylsilane (TMS) was used as an internal standard. Deuterated solvents such as $CDCl_3$, $(CD_3)_2CO$ and DMSO-d_6 were used for dissolving the samples Table 2-3. NMR experiments of samples with low quantities were carried out using Shigemi NMR tubes where samples were dissolved in 300 µl of $CDCl_3$ or DMSO-d_6 and placed into a Shigemi tube.

Table 2-3: Deuterated solvents used for NMR analysis

solvent	Chemical formula	^{1}H shift in ppm	^{13}C shift(s) in ppm
Deuterated DMSO	$(CD_3)_2SO$	2.50	39.5
Deuterated chloroform	$CDCl_3$	7.27	77.2

Deuterated Acetone	$(CD_3)_2CO$	2.05	29.8 and 206.2

2.5.2 Liquid chromatography coupled with High-resolution Mass Spectrometry (LC-HRMS).

2.5.2.1 Mass Spectrometry

Mass spectrometry in the form of liquid chromatography high-resolution mass spectrometry was used for mass profiling and mass analysis of the extracts and compounds. Part of the aim is to complement the results from NMR spectroscopy to confirm the structures elucidated and identify the compounds. High-resolution mass spectrometry provides an indication of the molecular formula, or elemental composition of the ions detected. The sample quantity required is usually small (about microgram quantities) and chromatographic separation unbundles the ions; thus, many more compounds are detected. Samples containing the purified compounds were dissolved in methanol (100 μg/mL). LC-MS experiments were conducted in both positive and negative ESI modes on either an UltiMate-3000 HPLC or an Accela HPLC system connected to an Exactive mass spectrometer. The sample solution (10-20 μL) was injected into an ACE 5 C18 column eluting with mobile phase A (0.1% (v/v) formic acid in water) and B (0.1% (v/v) formic acid in acetonitrile) (10% to 100% over 41 minutes) at a flow rate of 300 μL/ min. Some of the purified compounds were injected directly to the Exactive mass spectrometer to confirm their exact mass from the MS spectrum.

2.5.2.2 High-Resolution Mass spectrometry

HRMS was performed on an Accela 600 HPLC system combined with an Exactive (Orbitrap) mass spectrometer from Thermo Fisher Scientific (Hemel Hempstead, UK). The MS detection range was from m/z 100 to 1500 and scanning utilised ESI polarity positive and negative switching mode. The LC-MS system was controlled by Xcalibur version 2.2 (Thermo Fisher Corporation).

2.6 Antibacterial assay of propolis samples

Methicillin-resistant *Staphylococcus aureus* (MRSA) is considered to be responsible for an increasing number of serious nosocomial infections (Pujol et al., 1994).

The EEP of European propolis samples were assayed for antibacterial activity against *Staphylococcus aureus*. The assay was carried out at SIDR, University of Strathclyde.

Microorganisms.

Culti-Loops® of the following bacteria were purchased from Fisher Scientific (UK). Gram-positive bacteria, Staphylococcus *aureus* (ATTCC 29213)

Inoculum preparation.

Bacterial suspensions were prepared from loops primarily in nutrient broth (Sigma Aldrich, UK) by incubating at 37 °C for 24 hours. These were then transferred into nutrient agar and incubated for another 12 hours. The organisms were then sub-cultured onto fresh nutrient agar for two days. For inoculation, single colonies were transferred to (4–5 mL) Tryptone soya broth (Sigma Aldrich, UK) and incubated at 37 °C for 2 –

4 hours at 37 °C. The bacterial suspension was diluted to match a McFarland 0.5 standard by transferring colonies to saline (0.9% w/v NaCl) and 100 µL aliquots were transferred into cation-adjusted 10 mL Muleller-Hinton broth (Sensititre®, Trek-Diagnostic System, East Grinstead, UK). A 48 hours assay was carried out as flows:

Day 1 – of the required bacterial strains, a loopful of each was streaked on to individual Columbia with chocolated horse blood agar slopes and incubated at 37 °C overnight or for about 20 hours.

Day 2 – as done before, all bacterial strains were streaked, and a loopful of bacterial culture was transferred to a sterile universal container with sterile glass beads in 10 mL of 0.9% NaCl. The suspensions containing the bacteria were mixed thoroughly and then incubated on the bench to allow the beads to settle. Approximately ~1mL of the supernatant was then added to a fresh tube containing 10 mL sterile MHB type saline. Using the same saline as blank, the turbidity meter was zeroed, and sample turbidity was compared to that of a 0.5 McFarland standard (~1.5 x 108 CFUs/mL) and adjusted to achieve the same optical density (OD). A few drops of filter sterilised 0.02% Tween 80 was added to homogenise the suspension. The suspension was shaken to give a homogenous mixture, and the inoculum was diluted 1 in 1000 with Mueller Hinton Broth (MHB). The acquired results were transferred to Microsoft Excel for analysis and readings after 24 hours were deemed as optimal, and thus only these results are shown.

2.7 Anti-trypanosomal assay

Initial anti-trypanosomal tests against *Trypanosoma brucei* were carried out by Mr.Ibrahim Alfayes, Glasgow University using an AlamarBlueTM cell proliferation assay, according to a previously modified protocol (Räz et al., 1997). Using this assay, the half-maximal effective concentration (EC_{50}) values for compounds were determined. As controls, testing was carried out against a standard drug-sensitive *T. b. brucei* clone and two derived drug-resistant lines to help identify potential cross-resistance with existing drugs. The experiments were run in triplicate at each drug concentration serially diluted, and the EC_{50} values calculated. The assay was dependent on viable cells metabolising the blue non-fluorescent resazurin dye to the pink fluorescent resorufin. Using white opaque plastic 96-well plates (F Cell Star, Greiner Bio-one GmbH, Frickenhausen, Germany), serial dilutions of each compound or mixture were made in duplicate (i.e. 23 double dilutions and a no-drug control well) simplifying an optimally-defined EC_{50} value after scheming of the reading to a sigmoid curve with variable slope (GraphPad Prism 5.0). Two bloodstream clonal strains of *T. b. brucei* were utilised: first, the Lister strain 427 (s427) which was reported earlier by De Koning *et al*., 2000, and second, the B48 clone that was derived by in vitro adaptation to Pentamidine which belonged to the standard drug-sensitive control strain and the aqp2/aqp3 null strain from which the gene encoding the High-Affinity Pentamidine Transporter (HAPT1) has been deleted. The seeding density at the start of the experiment was 2×10^4 cells/well for each strain, and the cells were exposed to the test compounds for 48 hours at 37 °C/5% CO2. The Resazurin was then added to

the cells and incubated for a further 24 hours under the same conditions to allow the viable cells to metabolise the resazurin dye to the measurable pink fluorescent resorufin. At the end of the 24-hour incubation, Fluorescence was determined using a FLUOstar Optima (BMG Labtech, Aylesbury, UK) at wavelengths of 544 nm and 620 nm for excitation and emission, respectively (Omar et al., 2016).

2.7.1 Strains and cultures.

Bloodstream forms of *T. b. brucei* were grown in standard HMI-9 medium with 10% fetal bovine serum at 37 ºC/5% CO_2, in vented culture flasks, precisely as described (Gudin et al., 2006). The standard laboratory strain Lister 427WT (de Koning et al., 2000) was used as drug-sensitive standard, and the multi-drug resistant clone B48 (Bridges et al., 2007)was used to assess the potential for cross-resistance with the diamidine and melaminophenyl arsenical classes of trypanocides. *T. congolense* strain IL3000 (Savannah-type) was cultured as described previously in Minimal Essential Medium (MEM) base with 10% goat serum, supplemented with 14 µL/L β-mercaptoethanol, glutamine and antibiotics as described (Cerone et al., 2019).

Transgenic *Leishmania mexicana* promastigotes (5×10^6 cells.ml) of strain MYNC/BZ/62/M379 expressing the firefly luciferase gene and sensitive to the miltefosine APC12 with 12 alkyl carbon chain called APC12 (Hurrell et al., 2015) were designated WT; a related strain, C12Rx, resistant to 80 µg/mL APC12, was selected under controlled conditions by a stepwise progressive increase of APC12, with surviving stationary phase cells at each dose, used to inoculate subsequent cultures. Cells able to grow in the presence of the drug were cloned under drug pressure by

limiting dilution to 1 cell/mL in 20 ml of growth medium and plated out into 96-well plates. Both were cultured in complete Modified Eagle's Medium (M199 supplemented with 10% (v/v) heat-inactivated foetal calf serum) at 25 ºC. The transgenic line cultures were further supplemented with Hygromycin B in order to retain the luciferase gene.

A standard wild-type *C. fasciculata* (strain HS6, a kind gift from Professor Terry K. Smith, University of St-Andrews, UK) was grown at 27 °C in axenic serum-free defined media containing yeast extract (5 mg/mL), tryptone (4 mg/mL), sucrose (15 mg/mL), triethanolamine (4.4 mg/mL) and Tween 80 (0.5%) and supplemented with 10 μg/mL of haemin, precisely as described by Kipandula *et al* (Cerone et al., 2019)

2.7.2 Testing against *T. brucei, T. congolense and C. fasciculata*

The extracts were tested against *T. brucei* as described previously section 2.7, using our standard Alamar blue® (resazurin) method in white opaque 96 well plates (Greiner Bio-One, Frickenhausen, Germany), with 23 doubling dilutions and a no-drug control for each sample, using 2×10^4 *T. brucei* or 5×10^4 *T. congolense* per well and incubating 48 h with test compound prior to the addition of resazurin sodium salt (Sigma) and a further incubation of 24 h. The method is based on live cells metabolizing blue, non-fluorescent resazurin to pink, fluorescent resorufin, with fluorescence intensity being proportional to cell numbers (Gould et al., 2008). Stock solutions of each compound or mixture were prepared in DMSO for each concentration so that there was a constant percentage of DMSO per well (1% v/v).

Testing against *C. fasciculata* involved a very similar procedure, using 5×10^3 cells/well and incubations of 48 h and 24 h (27 ºC, 5% CO_2) before and after the addition of resazurin, respectively. Cell densities were determined using a haemocytometer after adding 1% v/v glycerol to the culture sample to immobilize the parasites. Cell density was then adjusted to 5×10^4 cells/mL with fresh medium, of which 100 µL was added to each well of a pre-prepared 96-well plate with the doubling dilution of test compound/sample.

Fluorescence was determined using a FLUOstar Optima (BMG Labtech, Durham, NC, USA) plate reader (λ_{ex} = 544 nm; λ_{em} = 590 nm) and the output was plotted to a sigmoid curve with variable slope (Prism 5.0, GraphPad software) to obtain 50% effective concentrations (EC_{50} values).

2.8 Testing against *L. mexicana*.

A *L.mexicana* WT and miltefosine APC12-resistant *L. mexicana* cell lines were screened with propolis samples at a starting concentration of 0.125 mg/mL, doubly diluted eleven times across a 96 well plate in triplicate and incubated for 72 h at 25 ºC. Wells with no propolis added were used in control experiments. After luciferin solution (1 µg/mL) was added, and the light emitted was measured using a luminometer (Biotek Synergy HT) at a wavelength of 440/40 nm. Viability was taken to be proportional to light emitted from each drug-treated well and was expressed as a fraction of emission from the 'no drug' control. IC_{50} values were determined using Prism 5.0, GraphPad software.

2.9 Cell viability assay of the propolis extracts

2.9.1 Cell Culture and Differentiation

This assay was carried out in Strathclyde Institute of Pharmacy and Biomedical Science as described in (Alqarni et al., 2018) , The THP-1 cell line was obtained from American Type Culture Collection-ATCC® (Porton Down, Salisbury, UK) and maintained at a 1×10^5 cell/mL seeding density in RPMI 1640 (Thermo Fisher Scientific, Loughborough, UK) containing 10% (v/v) foetal calf serum (FCS) (Life Tech, Paisley, UK), 2 mmol/L L-glutamine (LifeTech, Paisley, UK), and 100 IU/100 µg/mL penicillin/streptomycin (Life Tech, Paisley, UK). Cells were sub-cultured using fresh media every 2–4 days and maintained in an incubator (37 ˚C, 5%CO_2, 100%humidity). THP-1cells were differentiated using PMA (Sigma-Aldrich, Dorset, UK) at a final concentration of 60 µg g/mL and incubated for 48 h. THP-1cell differentiation was enhanced by removing the PMA-containing media and adding fresh media for a further 24 h. Cells were checked under a light microscope for the evidence of differentiation.

Cell viability was assessed by an Alamar® Blue (AB) cell viability reagent (Thermo Fisher Scientific, Loughborough, UK). The THP-1 cells were seeded at 1×10^4 cells/well in 96-well plates (Corning®, Sigma-Aldrich) and incubated at 37 °C and 5% CO_2 in a humid atmosphere for 24 h. After the 24-hour incubation period, the cells were treated with various concentrations of propolis ranging from 2 to 250 µg/mL in 100 µL of the medium. They were then re-incubated at 37 °C and 5% CO_2 for a further 24 h. cell culture media were used as positive and negative controls. After this, AB was added at a final concentration of 10% (v/v), and the resultant mixture incubated for a

further 4 h at 37 °C and 5% CO_2. Then, the plates were read at an excitation wavelength of 560 nm, and the emission at 590 nm was recorded on a SpectraMax M3 microplate reader (Molecular Devices, Sunnyvale, CA). Background-corrected fluorescence readings were converted to cell viability data for each test well by expressing them as percentages relative to the mean negative control value (n=3). Each sample was tested in triplicate, and the results are expressed as cell viability as a percentage of the cell only control. The equation (see Equation 1) used to determine the cell viability is shown below:

$$\textbf{\% Cell Viability} = \frac{\textbf{mean of samples (OD560-OD590)}}{\textbf{mean of control (OD560-OD590)}} \times \textbf{100}$$

Equation 1: Determination of cell viability.

Statistical analysis was carried out using GraphPad Prism for Windows (version 5.00, GraphPad Software, San Diego, CA, USA) to acquire dose–response curves and mean inhibitory concentration (IC50) values.

3 Chapter 3

3.1 Fractionation and testing of European propolis samples

3.1.1 Extraction of UK propolis samples

The propolis samples were extracted in ethanol (150 mL) followed by sonication with heating at 40 ºC for 1h. The extract was then filtered through filter paper. The filtrate was further filtered through filter paper three more times. The filtered solids were suspended in ethanol (100 mL), and the extraction process repeated 2 more times before being dried under a flow of air. The weights of all samples obtained were measured before storing at -20 ºC until used for further studies. The results of the extraction are summarised in Table **3-1**.

Table 3-1: Extracts from UK propolis samples

S/N	Sample code	Sample origin	Weight of sample (g)	Weight of ethanol extract (g)	% Yield
1	S224	Midlands- UK	26	11.5	44.8
2	S225	Essex- UK	33	15	47
3	D6	Northamptonshire -UK	13	7.5	57.7
4	D7	Essex -UK	18	10	55.5

3.1.2 The UK propolis purification procedures

Several instrumental methods were used to determine the constituents of the ethanol extracts and their chemical profile. These methods involved high-performance liquid chromatography in tandem with a variety of detectors, including high-resolution mass

spectrometry, evaporative light scattering detector (ELSD), ultraviolet detection (UV) and NMR. LC-MS profiling was obtained for the ethanolic extracts of all samples.

Fractions obtained from column chromatography and the purified fractions, as well as compounds obtained from MPLC and GF for all the EEP samples, were dissolved (1mg/mL) in methanol and sample solutions (10µL) were injected into the LC-MS system. The mobile phase was 0.1% formic acid in acetonitrile: 0.1% formic acid in water at a flow rate of 300µL/min. The high-resolution mass spectra were obtained in both ESI positive and negative modes on either an UltiMate-3000 HPLC instrument or an Accela HPLC system which were connected to an Exactive mass spectrometer. The separation of fractions and pure compounds were performed on an ACE-C18 column (150×3 mm, 3 µm) from HiChrom UK with 0.1% formic acid in water as mobile phase A and 0.1% formic acid in acetonitrile as B (25% to 100% in 41 minutes) at a flow rate of 300 µL/ min. The HPLC gradient used in this experiment is shown in Table 3-2.

Table 3-2: Chromatography methods for LC-MS of fractions and pure compounds from propolis

S/N	Time	%A	%B	Flow rate µL/min
0	0.00	75.0	25.0	300
1	30.0	0.00	100.0	300
2	35.00	0.00	100.0	300
3	36.00	75.0	25.0	300
4	41.00	75.0	25.0	300
5		100.0	0.00	300

A%(0.1% v/v formic acid in H_2O) and B% (0.1 % v/v formic acid in Acetonitrile)

3.1.3 Chemical profiling, purification, isolation and of Sample code S224

The EEP of sample S224 was subjected to chemical profiling using LC-HRMS as well as the fractions collected from column chromatography and the fractions collected from GF. The results of the analysis of sample S224 by LC-HRMS are summarised in Figure 3-1and Table 3-3.

Table 3-3: LC-MS profiling for S224 in negative and positive modes

Peak No **S224**	Rt (time)	{M-1}	{M+1}	Chemical Formula	RDB	Delta (ppm)	intensity
1	5.26	119.0503		C_8H_7O	5.5	0.519	1.80E7
2	5.26	179.03503		$C_9H_7O_3$	6.5	1.304	1.80E7
3	9.77	285.0771		$C_{16}H_{13}O_5$	11.5	0.644	2.44E7
4	10.72	269.0457		$C_{15}H_9O_5$	11.5	0.384	2.61E7
5	11.24	285.0407		$C_{15}H_9O_6$	11.5	0.767	2.75E7
6	11.67	271.07611		$C_{15}H_{11}O_5$	10.5	-0.246	6.56E7
7	11.92	299.0563		$C_{16}H_{11}O_6$	11.5	0.531	8.08E6
8	12.89	283.0613		$C_{16}H_{11}O_5$	11.5	0.506	6.51E6
9	13.60	315.0515		$C_{16}H_{11}O_7$	11.5	1.346	5.96E6
10	14.32	329.0671		$C_{17}H_{13}O_7$	11.5	1.410	6.62E6
11	14.50	287.0927		$C_{16}H_{15}O_5$	9.5	0.533	8.41E6
12	16.06	255.0663		$C_{15}H_{11}O_4$	10.5	0.188	1.32E7
13	16.42	313.0720		$C_{17}H_{13}O_6$	11.5	0.826	9.63E7
14	17.71	295.0978		$C_{18}H_{15}O_4$	11.5	0.873	4.44E7
15	18.43	327.0880		$C_{18}H_{15}O_6$	11.5	1.830	1.13E7
16	18.66	267.1031		$C_{17}H_{15}O_3$	10.5	1.469	2.26E7
17	19.94	279.1027		$C_{18}H_{15}O_3$	11.5	0.080	5.16E7
18	20.35	341.1032		$C_{19}H_{17}O_6$	11.5	0.435	1.03E7
19	20.74	375.0878		$C_{22}H_{15}O_6$	15.5	1.036	9.00E6
20	22.06	397.2021		$C_{24}H_{29}O_5$	10.5	0.259	2.28E7
21	22.58	403.1190		$C_{24}H_{19}O_6$	15.5	0.691	1.43E7
22	4.99		147.0440	$C_9H_7O_2$	6.5	-0.109	7.1E6
23	7.72		191.0702	$C_{11}H_{11}O_3$	6.5	-0.266	7.76E6
24	14.49		235.1695	$C_{15}H_{23}O_2$	4.5	1.206	8.07E6
25	17.13		161.0597	$C_{10}H_9O_2$	6.5	0.459	8.12E6
26	20.14		301.10696	$C_{17}H_{17}O_5$	9.5	-0.299	4.7E6
27	20.56		271.0962	$C_{16}H_{15}O_4$	9.5	-.869	2.93E7
28	20.86		269.08087	$C_{16}H_{13}O_4$	10.5	0.129	1.06E7
29	21.47		421.1995	$C_{26}H_{29}O_5$	12.5	-3.254	2.97E6
30	23.84		277.2161	$C_{18}H_{29}O_2$	4.5	-0.060	5.50E6

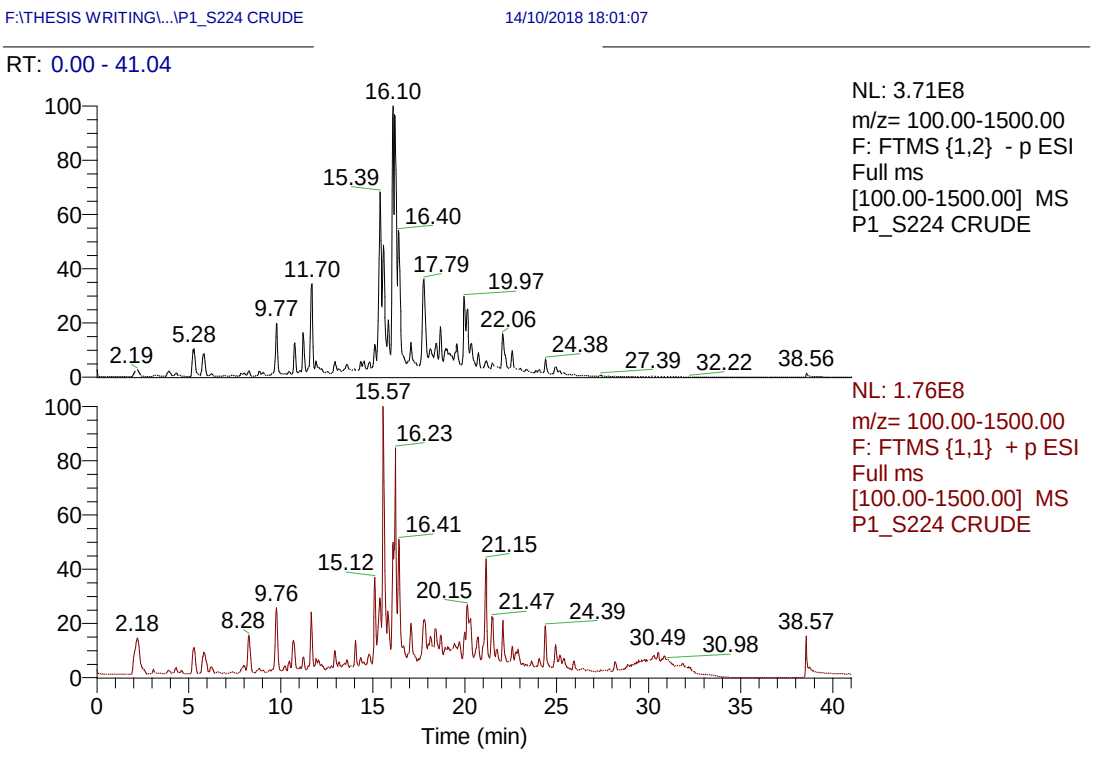

Figure 3-1: LC-MS chromatogram peaks of the ethanol extract of S224

The EEP of sample S224 was selected initially for further fractionation and purification using different chromatographic techniques. Using general method 1, the fractions and yields are presented in Table 3-4**.** Fractions from the method weighing more than 120 mg were further fractionated by medium pressure liquid chromatography (MPLC) on silica gel using a Grace Revelris® system with ELSD detection (General method 4). The fractions obtained were profiled by LC-MS and NMR.

Table 3-4: Mobile phase gradient and fractions obtained from column chromatography of S224.

Fraction No	Solvent system for CC S224	Fraction weight
1	Hexane 100% 50mL	12 mg
2	Hexane 100% 50mL	10 mg

3	Hexane 100% 50mL	12 mg
4	Hexane 100% 50mL	13 mg
5	Hexane 80% Ethyl acetate 20% 50mL	12 mg
6	Hexane 80% Ethyl acetate 20% 50mL	13 mg
7	Hexane 80% Ethyl acetate 20% 50mL	16 mg
8	Hexane 80% Ethyl acetate 20% 50mL	50 mg
9	Hexane 60% Ethyl acetate 40% 50mL	153 mg
10	Hexane 60% Ethyl acetate 40% 50mL	28 mg
11	Hexane 60% Ethyl acetate 40% 50mL	12 mg
12	Hexane 60% Ethyl acetate 40% 50mL	10 mg
13	Hexane 40% Ethyl acetate 60% 50mL(C1)	180 mg
14	Hexane 40% Ethyl acetate 60% 50mL(C2)	142 mg
15	Hexane 40% Ethyl acetate 60% 50mL (C3)	160 mg
16	Hexane 40% Ethyl acetate 60% 50mL(C4)	120 mg
17	Hexane 20% Ethyl acetate 80% 50mL	45mg
18	Hexane 20% Ethyl acetate 80% 50mL	52mg
19	Hexane 20% Ethyl acetate 80% 50mL	27mg
20	Hexane 20% Ethyl acetate 80% 50mL	32mg
21	Ethyl acetate 100% 50mL	50 mg
22	Ethyl acetate 100% 50mL	45 mg
23	Ethyl acetate 100% 50mL	55 mg
24	Ethyl acetate 100% 50mL	30 mg
25	Ethyl acetate 70% Methanol 30% 50mL	20 mg
26	Ethyl acetate 70% Methanol 30% 50mL	12 mg
27	Ethyl acetate 70% Methanol 30% 50mL	32 mg
28	4-Ethyl acetate 70% Methanol 30% 50mL	24 mg

3.1.3.1 Purification of column fractions from S224

Four fractions S224-C-H60-E40 (153 mg), S224-C1-H40-E60 (180 mg), S224-C3-H40-E60 (160 mg) and S224-C4-H40-E60 (120 mg) were selected for further

purification after TLC, LC-MS and NMR analysis. LC-MS profile indicated flavonoids and phenolic acids are the most abundant compounds in these fractions, and there was some similarity between S224-C3-H40-E60 (160 mg) and S224-C4-40-60 (120 mg); thus, they were combined for further fractionation.

Purification of fraction S224-C1-H40-E60 (yield 180mg) was carried out using Medium pressure liquid chromatography using a Grace (Revelris®) system in normal phase mode. The column used was a pre-packed silica column (12g), utilising hexane (A) and ethyl acetate (B) as solvents. The conditions for the gradient were from 100% hexane, up to 100% ethyl acetate over 141.6 minutes, at a flow rate of 20 ml/min and monitored by UV/ELSD as shown on the chromatogram in Figure 3-2. 103 fractions were collected in total with three fractions, F6 (13.7 mg), F7 (16.0 mg) and F8 (7.1 mg) as shown in Table 3-5, were analysed by NMR to characterize their constituent compounds. This resulted in the identification of F6 as 3-O- acetoxypinobanksin. At the same time, F7 and F8 were found to be identical with the same mixture of compounds and were subjected to fractionation by Sephadex LH20 using methanol as mobile phase. After separation, 12 fractions were collected and analysed with fraction F4 identified as 4'-Methoxykaempferol following analysis by LC-MS and NMR.

Table 3-5: The weights of some fractions of S224 C1-H40-E60 obtained from MPLC.

Fraction number	**Purified compound from MPLC**	**Yield (mg)**	**GF fraction**	**Purified compound from GF**	**Yield (mg)**
F3-5	-	3.5			

F6	3-O-acetoxypinobanksin	13.7			
F7	Similar	23.1	12	4'-Methoxykaempferol	2.5
F8					
F9	-	1.7			
F12	-	2.8			
F16	Chrysin	3.6			
F69	-	2.3			
F3+4 (2^{nd})	-	-			

* - a mixture of compounds.

Purification of the column fractions S224-C3+4-H40-E60 (yield 280mg) was carried out using Medium pressure liquid chromatography as previously described for fraction S224-C1-H40-E60. The gradient conditions were from 100% hexane to 100% of ethyl acetate over 75 minutes, at a flow rate of 30 ml/min and monitored by UV/ELSD as shown in the chromatogram in Figure 3-3, 70 fractions were collected after using the programme as described above. From the obtained fractions, F14, F15 and F16, had the highest yields as shown Table 3-6 and were analysed by LC-MS and NMR to determine if they were pure compounds. The results showed that F14 contained slightly different compounds and was therefore subjected to fractionation by Sephadex LH20 using methanol as mobile phase. After separation, nine fractions were collected, and each fraction was analysed by LC-MS and NMR, leading to F9 being identified as Kaempferol. Fractions F15 and F16 were similar and subjected to the same procedures

as previously done for fraction F14 and were subsequently identified as 4'-Methoxykaempferol. Fraction F19 was identified as Galangin.

Table 3-6: The weights of some fractions of S224C3+4- 40-60 obtained from MPLC.

Fraction number	**Purified compound from MPLC**	**Yield (mg)**	**GF Fraction**	**Purified compound from SEC**	**Yield (mg)**
F3	-	4.0	-	-	-
F7	-	8.3	-	-	--
F14	-	24.3	9	Kaempferol	5.0
F15	Identical	63.0	14	4'-	3.2
F16	mixtures of compounds			Methoxykaempferol	
F19	Galangin	3.0	-	-	-
F26	-	12.0	-	-	-
F45	-	19.0	-	-	-
F69	-	6.0	-	-	-

* - a mixture of compounds.

Fraction S224-C-60-40 (153mg) was also purified using Medium pressure liquid chromatography in normal phase mode as previously described for the purification of the column fraction S224-C3+4-H40-E60. From the 32 fractions obtained, the results of LC-MS analysis and NMR identified F3 and F4 as 7-Methoxychrysin. Fractions F8 to F15 (59 mg) were combined based on the results of LC-MS and NMR and subjected to fractionation by Sephadex LH20 column chromatography (GF) using methanol as mobile phase with a flow rate at 1.0 mL/min. After separation, 14 fractions were

collected, and LCMS and NMR analysis were carried out which identified fraction F4 as Pinocembrin as shown in Table 3-7.

Table 3-7: The yields of some fractions of S224C- 60-40 obtained from MPLC.

Fraction number	**Purified compound from MPLC**	**Yield (mg)**	**GF fractions**	**Purified compound from GF**	**Yield (mg)**
F3	7-Methoxychrysin	10.2			
F4					
F8	Identical mixture	59.0	14		6.5
F10				Pinocembrin	
F13					
F15					
F20	-	14.0	-	-	-
F25	-	17.0	-	-	-
F30	-	21.0	-	-	-

* - a mixture of compounds.

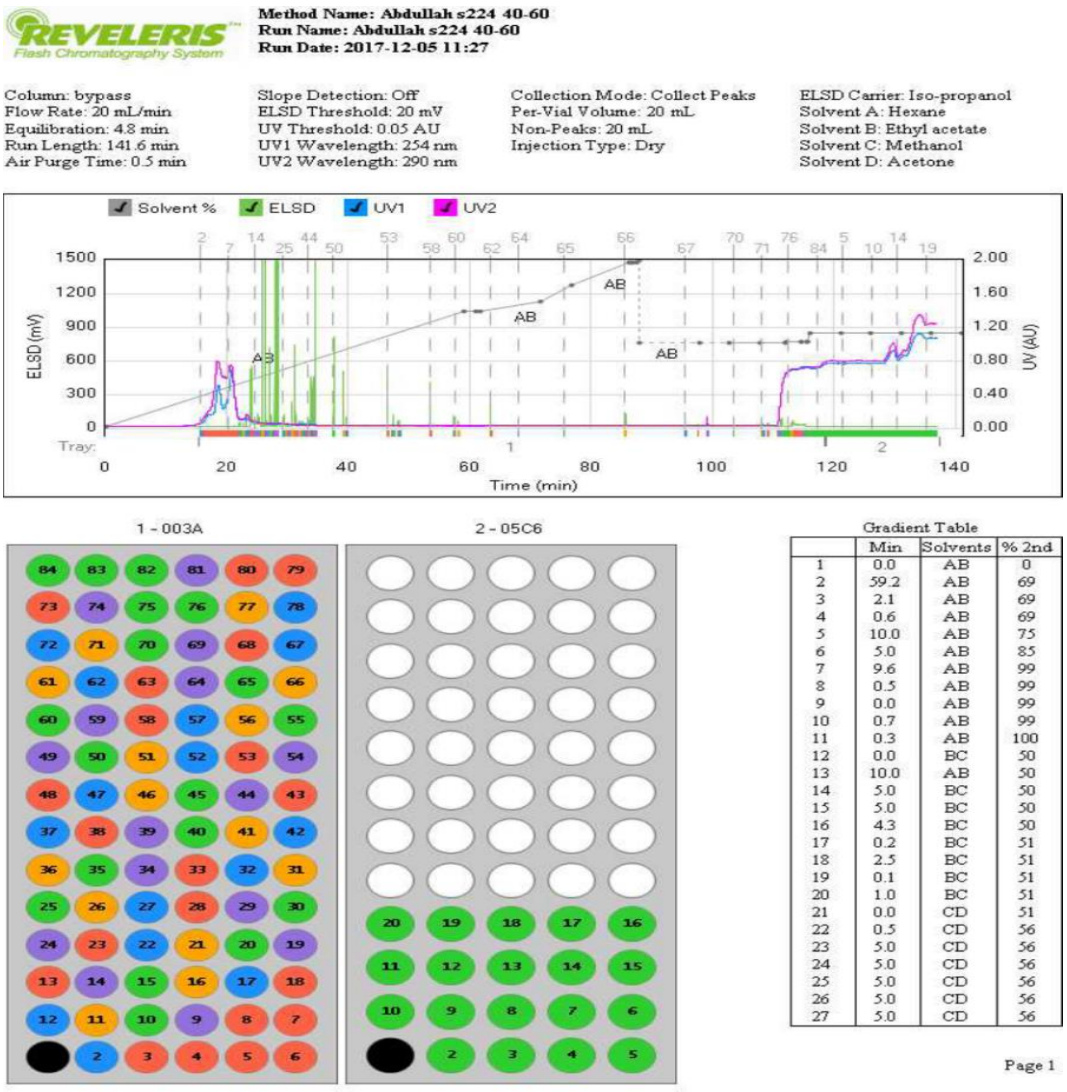

Figure 3-2: Chromatogram of column fraction S224C1-40-60 on MPLC.

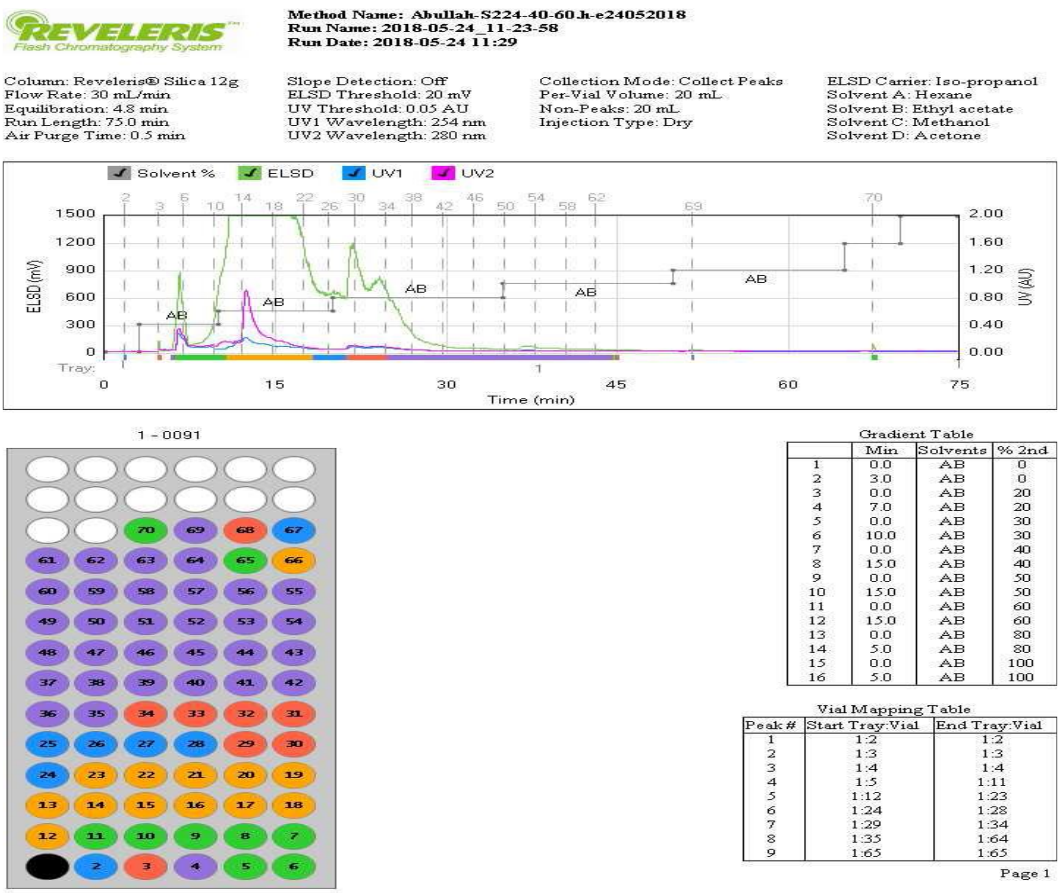

Figure 3-3: Chromatogram of column fraction S224C$_{3+4}$-40-60 on MPLC

3.1.3.2 Partitioning of S224 extracts

Approximately 23 g of the ethanol extract of S224 was dissolved in 200ml of dichloromethane and worked up as described in method B. 2g of the precipitate was then subjected to column chromatography. The fractions collected and their yield of components are given in Table 3-8. NMR and LC-MS analysis indicated the fractions that were most abundant in components, and these fractions C1 and C2 as (F1) and C3 and C4 as (F2) were combined and further purified using GF. The fractions collected from F1 were 16, while from F2, 20 fractions were collected. NMR and LC-MS

analysis of the fractions collected yielded 4'-Methoxykaempferol from F1 and Galangin from F2.

Table 3-8: Fractions and yields of components obtained from column chromatography of S224.

Fraction No	**Solvent system for CC S224**	**Fraction weight (mg)**	**GF fractions**	**Purified compound from GF**	**Weight (mg)**
1	Hexane 80% Ethyl acetate 20% 200ml	60			
2	Hexane 60% Ethyl acetate 40% 200ml	183			
3	Hexane 40% Ethyl acetate 60% 100ml F1(C1+C2)	221	16	4'-Methoxykaempferol	10.0
4	Hexane 40% Ethyl acetate 60% 100ml F2(C3+C4)	241	20	Galangin	12.2
5	Hexane 20% Ethyl acetate 80% 200ml	147			
6	Ethyl acetate 100% 200ml	162			
7	Ethyl acetate 70% Methanol 30% 50ml	86 -			

3.1.4 Purification and chemical profiling of sample D7

The EEP of sample D7 was subjected to chemical profiling using high-resolution mass spectrometry LC-HRMS using the fractions collected from column chromatography and gel filtration. The results of the analysis of sample D7 by LC-HRMS is given in the LC-MS chromatograms in positive ion mode Figure 3-4 and

Table 3-9.

Table 3-9: LC-MS profiling for D7 in positive ion mode.

Peak No D7	Rt(time)	{M+1}	Chemical Formula	RDB	Delta (ppm)	intensity
1	7.15	147.0439	$C_9H_7O_2$	6.5	-0.076	6.92E6
2	8.00	177.0545	$C_{10}H_9O_3$	6.5	-0.071	1.17E7
3	8.23	453.3432	$C_{23}H_{49}O_8$	-0.5	2.416	6.29E6
4	10.48	191.070	$C_{11}H_{11}O_3$	6.5	-0.061	1.75E7
5	12.79	161.0595	$C_{10}H_9O_2$	6.5	0.200	6.80E6
6	12.84	271.0597	$C_{15}H_{11}O_5$	10.5	-0.350	1.45E7
7	13.24	287.0548	$C_{15}H_{11}O_6$	10.5	-0.145	4.45E6
8	15.13	285.0754	$C_{16}H_{13}O_5$	10.5	-0.301	1.32E7
9	15.89	317.0654	$C_{16}H_{13}O_7$	10.5	-0.119	6.67E6
10	16.94	331.0810	$C_{17}H_{15}O_7$	10.5	-0.209	6.77E6
11	18.96	255.0647	$C_{15}H_{11}O_4$	10.5	-0.425	1.12E8
12	20.16	257.0805	$C_{15}H_{13}O_4$	9.5	-1.149	5.08E7
13	25.11	338.2663	$C_{17}H_{38}O_6$	-1.0	0.029	3.64E6
14	26.02	417.1330	$C_{25}H_{21}O_6$	15.5	-0.419	3.95E6
15	29.66	295.0963	$C_{18}H_{15}O_4$	11.5	-0.493	4.17E6
16	31.80	320.2558	$C_{17}H_{36}O_5$	0.0	0.360	1.10E7
17	31.99	269.0807	$C_{16}H_{13}O_4$	10.5	-0.317	1.17E7
18	34.09	318.2399	$C_{17}H_{34}O_5$	1.0	-0.363	1.09E7
19	37.04	277.2160	$C_{18}H_{29}O_2$	4.5	-0.529	1.19E7
20	38.13	383.3154	$C_{23}H_{43}O_4$	2.5	-0.486	3.49E6

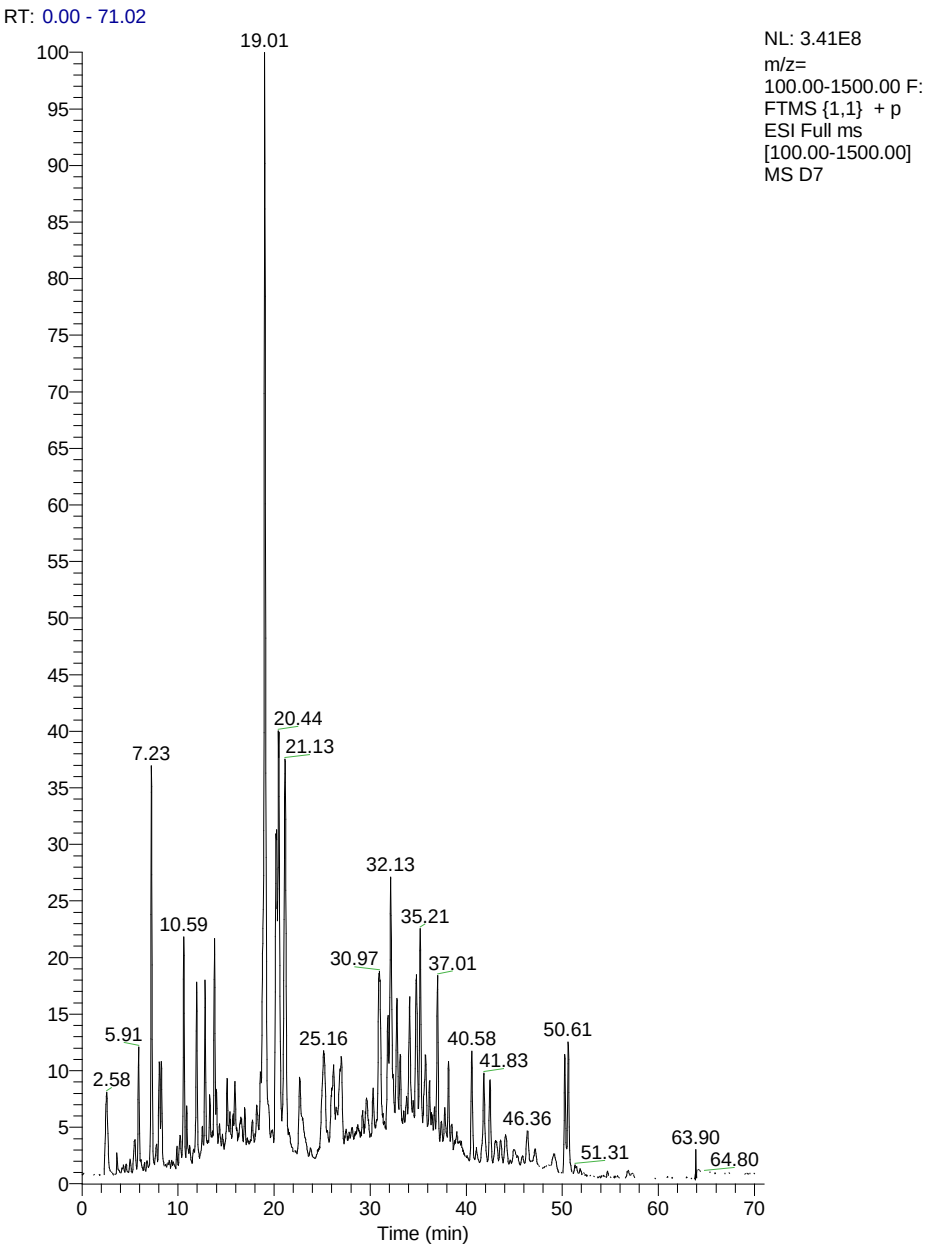

Figure 3-4: Chromatogram peaks of ethanol extract of D7 in LC-MS.

An amount of the EEP of D7 (18 g) was dissolved in 160 ml of dichloromethane and partitioned using the procedure of method B. Concurrently, another 2.0 g of D7 was subjected to column chromatography using the solvent system as in Table 3-10.

Twenty-eight (28) fractions (50 ml) were collected, and fractions which were found to be identical were combined based on TLC, LC-MS and NMR results giving 11 pooled fractions. Based on the above, four of the combined fractions were subjected to fractionation by the Sephadex LH20 process (GF) using methanol as mobile phase. Three compounds were obtained, as indicated in Table 3-10.

Table 3-10: Gradient solvent system and fractions from column chromatography of D7 and the compounds obtained from Sephadex LH20.

Fraction No D7	**Solvent System for CC**	**Fraction Weight (mg)**	**GF Fraction**	**Purified compound from GF**	**Weight (mg)**
1	Hexane 80% Ethyl acetate 20% 50ml	71	-	-	-
2	Hexane 60% Ethyl acetate 40% 50ml	98	8	Pinocembrin	4.5
3	Hexane 60% Ethyl acetate 40% 50ml	112	12	Galangin	5.8
4	Hexane 60% Ethyl acetate 40% 100ml (F3+F4)	150	-	-	-
5	Hexane 40% Ethyl acetate 60% 50ml	115	20	Chrysin	5.4

6	Hexane 40% Ethyl acetate 60% 50ml	122	-	-	-
7	Hexane 40% Ethyl acetate 60% 50ml	133	-	-	-
8	Hexane 40% Ethyl acetate 60% 50ml	94	-	-	-
9	Hexane 20% Ethyl acetate 80% 50ml	128	-	-	-
10	Ethyl acetate 100% 50ml	144	-	-	-
11	Ethyl acetate 70% Methanol 30% 50ml	91	-	-	-

* - a mixture of compounds.

3.1.5 Chemical profiling and purification of sample D6

Sample D6 was similarly profiled and subjected to chromatographic purification as previously described for other samples. The LC-MS profiling results of the EEP of sample D6 are presented in Figure 3-5 and

Table 3-11.

Peak No	Rt (minutes)	[M-1]	Chemical Formula	RDB	δ (ppm)	Intensity
1	1.88	179.05614	$C_6H_{11}O_6$	1.5	0.160	5.67E6
2	3.20	179.03503	$C_9H_7O_4$	6.5	0.380	1.06E7
3	3.20	179.03503	$C_9H_7O_4$	6.5	0.380	1.06E7
4	4.02	163.04010	$C_9H_7O_3$	6.5	0.200	6.80E6
5	5.38	363.07269	$C_{17}H_{15}O_9$	10.5	1.473	1.64E6
6	7.32	285.07706	$C_{16}H_{13}O_5$	10.5	0.748	2.21E7
7	8.12	269.04572	$C_{15}H_9O_5$	11.5	0.644	9.59E6
8	8.64	285.04068	$C_{15}H_9O_6$	11.5	0.767	1.06E7
9	9.16	271.06134	$C_{15}H_{11}O_5$	10.5	0.529	4.97E7
10	10.34	283.06137	$C_{16}H_{11}O_5$	11.5	0.612	8.69E6
11	10.89	299.05640	$C_{16}H_{11}O_6$	11.6	0.965	3.12E6
12	12.94	269.08206	$C_{16}H_{13}O_4$	10.5	0.475	1.03E8
13	13.08	253.05064	$C_{15}H_9O_4$	11.5	0.031	4.38E7
14	13.64	255.06638	$C_{15}H_{11}O_4$	10.5	0.384	9.48E7
15	13.99	313.07202	$C_{17}H_{13}O_6$	11.5	0.826	6.65E7
16	15.39	295.09760	$C_{18}H_{15}O_4$	11.5	0.060	4.78E7
17	16.15	327.08774	$C_{18}H_{15}O_4$	11.5	1.004	9.64E6
18	18.26	341.10327	$C_{19}H_{17}O_6$	11.5	0.611	1.38E7
19	20.30	355.11914	$C_{20}H_{19}O_6$	11.5	1.206	9.85E6
20	20.77	403.11893	$C_{27}H_{19}O_6$	15.5	0.542	5.42E6

Table 3-11: LC-MS profiling for D6 in negative mode

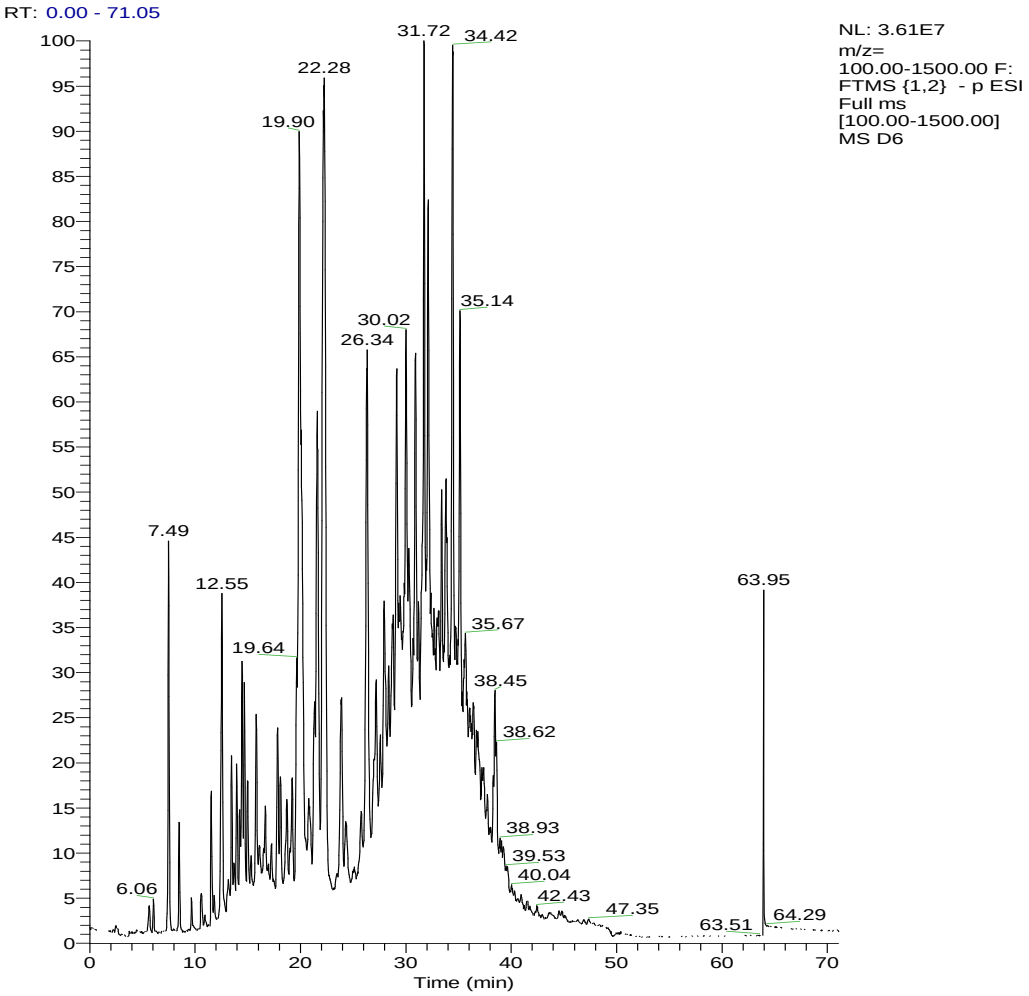

Figure 3-5: LC-MS peaks of the ethanol extract of D6

Sample D6 was subjected to the fractionation method B. A quantity of the EEP of D6 (7.5g) was dissolved in 65 ml of dichloromethane (DCM) and treated as described in method B. Another quantity of the EEP (2 g) was simultaneously subjected to column chromatography as described in general method 1. Fractions with high yield and interesting profiles were further subjected to GF chromatography as described in general method 3, leading to the isolation of four compounds, as shown in Table 3-12.

Table 3-12: Solvent system and fractions from column chromatography of D6 and the compounds obtained from Sephadex CC

S/No	Solvent system for CC	Fraction Weight (mg)	GF fractions	compound from GF	Weight of compound (mg)
1	Hexane 80% Ethyl acetate 20% 200ml	59	-	-	-
2	Hexane 60% Ethyl acetate 40% 100ml	162	14	Pinocembrin	3.2
3	Hexane 60% Ethyl acetate 40% 100ml	143	12	Galangin	3.1
4	Hexane 40% Ethyl acetate 60% 50ml	110	16	Kaempferol	4.9
5	Hexane 40% Ethyl acetate 60% 50ml	98	-	-	-
6	Hexane 40% Ethyl acetate 60% 50ml	113	14	Apigenin	6.5
7	Hexane 40% Ethyl acetate 60% 50ml	105	-	-	-

8	Hexane 20% Ethyl acetate 80% 200ml	164	-	-	-
9	Ethyl acetate 100% 50ml	185	-	-	-
10	Ethyl acetate 70% Methanol 30% 200ml	90	-	-	-

3.1.6 Chemical profiling and purification of sample S225

Sample S225 was similarly profiled and subjected to chromatographic purification as previously described for other samples. The LC-MS profiling results for EEP of sample S225 are presented in Figure 3-6 and

. The sample was also fractionated using method B, and Vacuum Liquid Chromatography as described in general method 2 section 2.4.2.

Table 3-13: LC-MS profiling of S225 in positive ion mode

Peak No	Rt (time)	[M+1]	Chemical Formula	RDB	δ (ppm)	Intensity
1	5.71	147.0439	$C_9H_7O_2$	6.5	-0.066	1.26E7
2	6.49	177.0548	$C_{10}H_9O_3$	6.5	0.219	5.55E6
3	9.12	191.0701	$C_{11}H_{11}O_3$	6.5	-0.081	1.32E7
4	10.51	317.0653	$C_{16}H_{13}O_7$	10.5	-0.269	3.55E6
5	10.56	241.0858	$C_{15}H_{13}O_3$	9.5	-0.031	2.44E7
6	10.61	287.0913	$C_{16}H_{15}O_5$	9.5	-0.060	2.61E7
7	10.65	309.0656	$C_{16}H_{13}O_5$	12.5	-2.720	2.75E7
8	11.67	271.07611	$C_{15}H_{11}O_5$	10.5	-0.160	8.56E6
9	12.12	145.0313	$C_9H_5O_2$	7.5	2.924	1.6E6
10	13.89	285.0755	$C_{16}H_{13}O_5$	10.5	-0.250	1.33E7
11	16.58	235.1691	$C_{15}H_{23}O_2$	4.5	-.0096	3.90E6
12	17.02	133.0298	$C_8H_5O_2$	6.5	1.414	2.24E6
13	17.28	255.0648	$C_{15}H_{11}O_4$	10.5	-0.365	5.71E7
14	18.29	257.0805	$C_{15}H_{13}O_4$	9.5	-0.325	3.03E7
15	18.54	301.0704	$C_{16}H_{13}O_6$	10.5	-0.195	3.19E7
16	19.00	315.0860	$C_{17}H_{15}O_6$	10.5	-0.255	1.01E7
17	22.23	161.0595	$C_{10}H_9O_2$	6.5	-0.116	5.55E6
18	29.25	301.10687	$C_{17}H_{17}O_5$	9.5	-0.118	6.9E6
19	29.82	271.0963	$C_{16}H_{15}O_4$	9.5	-0.175	6.30E6
20	30.20	269.0805	$C_{16}H_{13}O_4$	10.5	-0.265	8.21E6

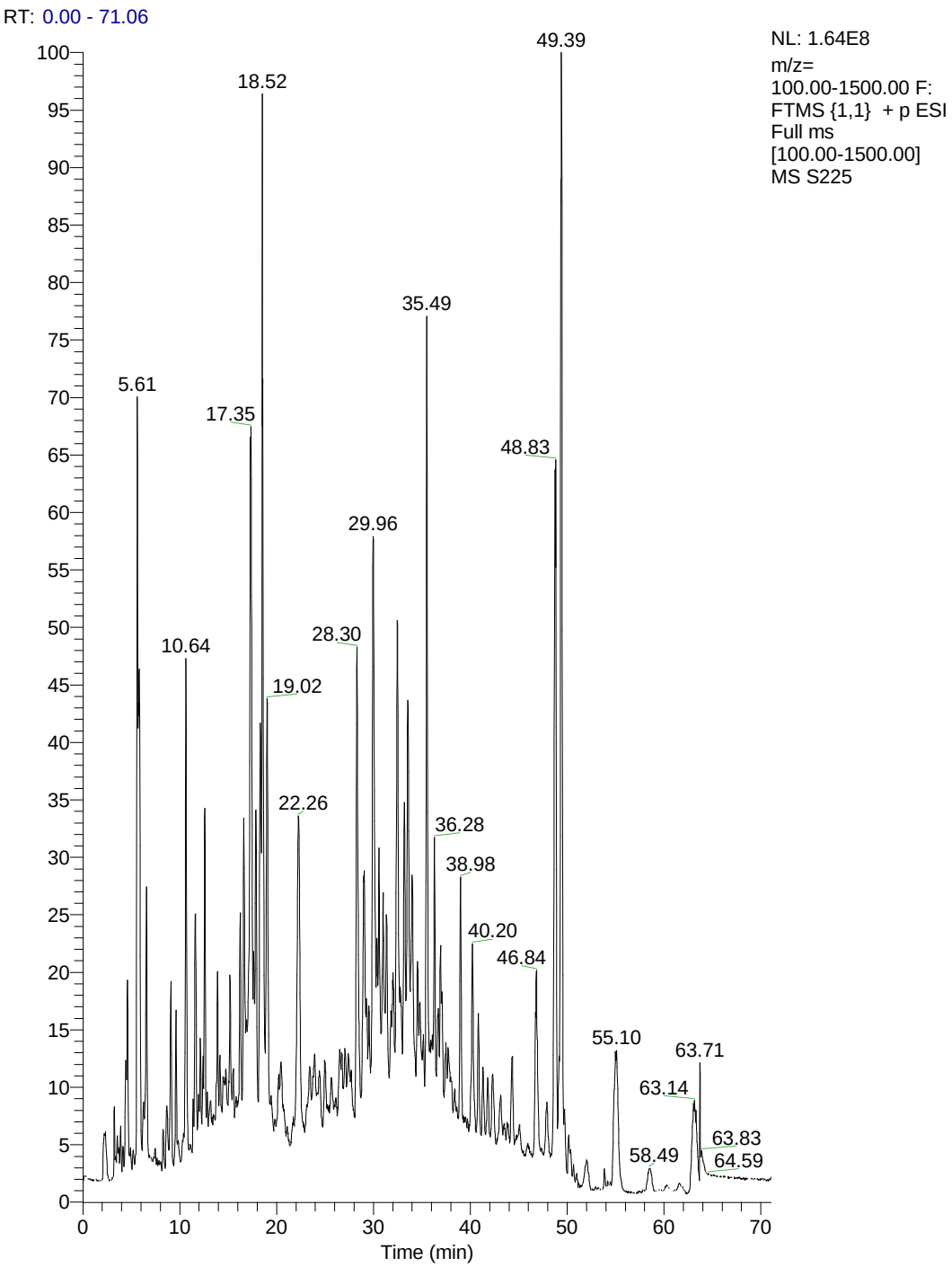

Figure 3-6: LC-MS chromatogram of ethanol extract of S225

3.1.7 Purification of S225 using Vacuum Liquid Chromatography

A quantity of the EEP of S225 (10 g) was subjected to Vacuum Liquid Chromatography as described in general method 2. Fraction F-1 from the VLC was further subjected to column chromatography as in general method 1. The mobile phase used, fractions weights and compounds obtained are summarised below in Table 3-14 and

Table 3-15.

Table 3-14: Solvent system and fractions from Vacuum Liquid Chromatography of S225.

Fraction No	**Solvent system for VLC**	**Fraction weight**
F1	Hexane 70% Ethyl acetate 30% 500ml	1.62 g
F2	Hexane 50% Ethyl acetate 50% 500ml	1.80 g
F3	Hexane 30% Ethyl acetate 70% 500ml	1.35 g
F4	Hexane 10% Ethyl acetate 90% 500ml	1.30 g
F5	Ethyl acetate 100% 500ml	1.10 g
F6	Ethyl acetate 70% Methanol 30% 500ml	0.82 g

Table 3-15: Solvent system and fractions from column chromatography of S225 VLC fraction F1.

Fraction No	Solvent system for CC S225-VLC-F1	Fraction	fraction weight (mg)	Purified compound	Compound weight (mg)
1	Hexane 80% Ethyl acetate 20% 200ml	F1-F25	52.0	-	-
2	Hexane 60% Ethyl acetate 40% 200ml	F1-F35	210.0	Pinostrobin	14.0
3	Hexane 40% Ethyl acetate 60% 200ml	F1-F30	453.0	Coumaric acid cinnamyl ester and Coumaric acid benzyl ester	26.2
4	Hexane 20% Ethyl acetate 80% 200ml	F1-F33	245.0	Cinnamic acid	24.0
5	Ethyl acetate 100% 200ml	F1-F20	139.0	-	-
6	Ethyl acetate 70% Methanol 30% 50ml	F1-F20	75.0	-	-

*- a mixture of compounds.

3.1.8 Compounds characterisation of the UK samples

3.1.8.1 Characterisation of fraction C1-H40-E60-MPLC-F6 as Pinobanksin 3-O- acetate (1)

The compound was obtained as a yellowish solid from a Grace Reveleris MPLC fraction. The compound showed up as a purple spot on TLC after spraying with anisaldehyde sulfuric acid reagent, as a dark spot under UV 254 and a yellow spot under UV 365 nm. The exact mass obtained by HRESILC-MS gave an $[M-H]^-$ ion at m/z = 313. 0728 (calculated for $C_{17}H_{13}O_6$; 313.0712) corresponding to a molecular formula $C_{17}H_{14}O_6$. Its proton NMR spectrum Figure 3-8 showed a chelated –OH signal at δ_H 11.51 (s) ppm and two coupled aliphatic doublets at δ_H 5.36 (1H, d, *J* = 11.7 Hz) and 5.85 (1H, d, *J* = 11.7 Hz) typical of a flavonol ring as structure Figure 3-7. Other sets of proton signals were for two meta coupled aromatic protons at δ_H 6.01 (1H, d, *J* = 2.2 Hz) and 6.06 (1H, d, *J* = 2.3 Hz), and a set of five coupled protons between δ_H 7.38 and 7.48 ppm indicating a monosubstituted aromatic ring. Also present was an acetoxymethyl proton at δ_H 2.06 ppm. The carbon spectrum showed a total of 17 carbon signals comprising of (DEPT) seven quaternary (including two carbonyl carbons at δ_C 191.7 and 169.7), two oxymethine (δ_C 81.4 and 72.6 ppm), one methyl at 20.47 and seven aromatic CH carbons. Using extensive 2D (^{1}H-^{1}H-COSY, ^{1}H-^{13}C HSQC and HMBC), the compound was identified as Pinobanksin 3-O-acetate **(1)**, as follows: Correlations in the HSQC (^1J) was used to identify the hydrogen bearing carbons. In comparison, ^3J correlations were used to identify the carbonyl carbons as well as the other quaternary carbons. Based on the 2D correlations, the chemical shifts for the

protons and carbon atoms in the compound were assigned, as summarised in Table **3-16**. The compound's identity was confirmed by comparison of its chemical shift data with literature reports (Tran et al., 2012). Pinobanksin-3-O-acetate was isolated from Jordanian propolis and tested in vitro for antibacterial activity exhibited antibacterial activity against methicillin-resistant *Staphylococcus aureus* (MRSA) and *E. coli* (Darwish et al., 2010)

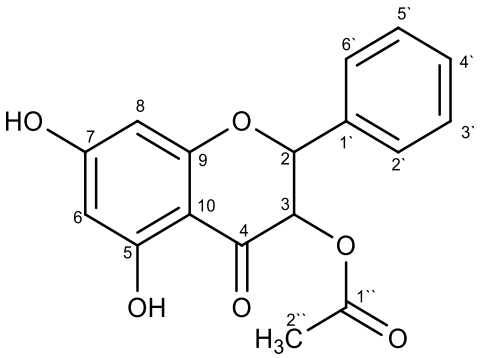

Figure 3-7: Chemical structure of Pinobanksin 3-O-acetate

Table 3-16: Chemical shifts for Pinobanksin 3-O-acetate

Position	Experimental		Literature*	
	^{1}H δ ppm (mult, J in Hz)	^{13}C δ ppm, (mult)	^{1}H δ ppm, (mult, J in Hz)	^{13}C δ ppm, (mult)
1	-	-	-	-
2	5.36 (1H, d, 11.7)	81.4 (CH)	5.36 (1H, d, *J* = 11.7)	81.3
3	5.85 (1H, d, 11.7)	72.6 (CH)	5.81 (1H, d, *J* = 11.7)	72.4
4	-	191.7 (C)	-	191.6
5	-	163.6 (C)	-	162.5
6	6.01 (1H, d, 2.2)	96.0 (CH)	6.00 (1H, d, *J* = 2.2)	95.9
7	-	166.9 (CH)	-	165.2

8	6.06 (1H, d, 2.2)	97.36 (C)	6.04 (1H, d, *J* = 2.2)	97.4
9	-	165.8 (C)	-	164.2
10	-	102.0 (C)	-	101.9
1`	-	135.9 (C)	-	135.1
2`	7.49(m)	127.4 (CH)		127.3
3`	7.44(m)	128.8 (CH)	7.44 (5H, m)	128.7
4`	7.45(m)	129.6 (CH)		129.6
5`	7.44(m)	128.8 (CH)		128.7
6`	7.49(m)	127.4 (CH)		127.3
1``	-	169.7 (C)	-	169.5
2``	2.06(m)	20.47 (CH_3)	2.02 (3H, s)	20.3
5-OH	11.51 (s)	-	11.47 (1H, s)	-

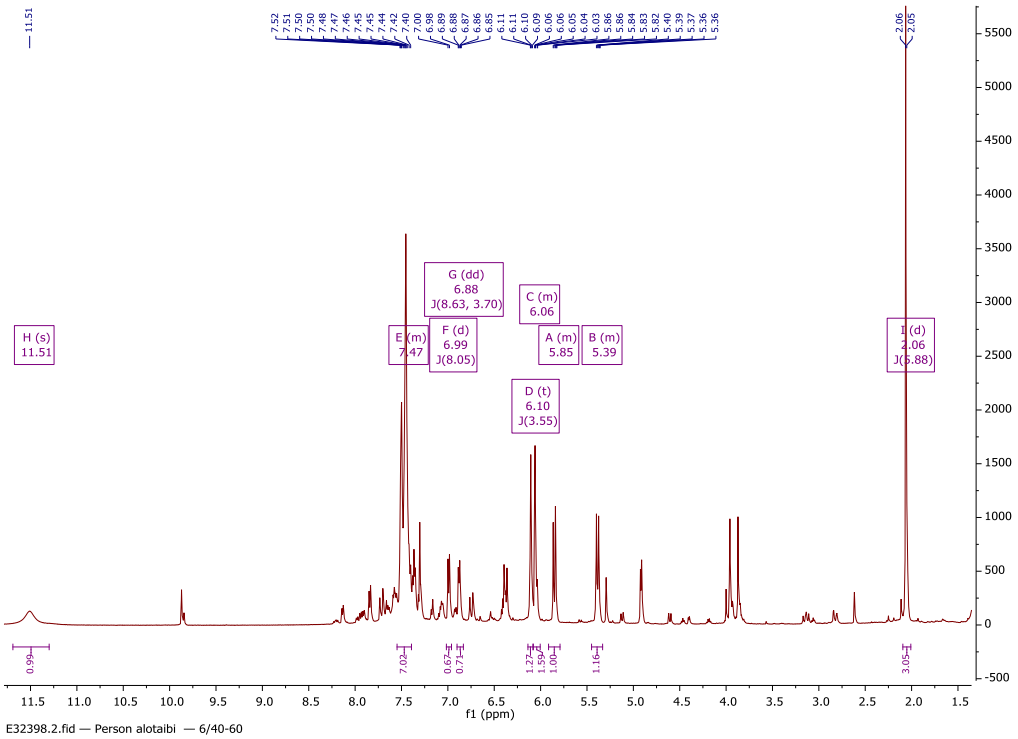

Figure 3-8: ^{1}H NMR (400 MHz) of Pinobanksin 3-O-acetate in CDCl3.

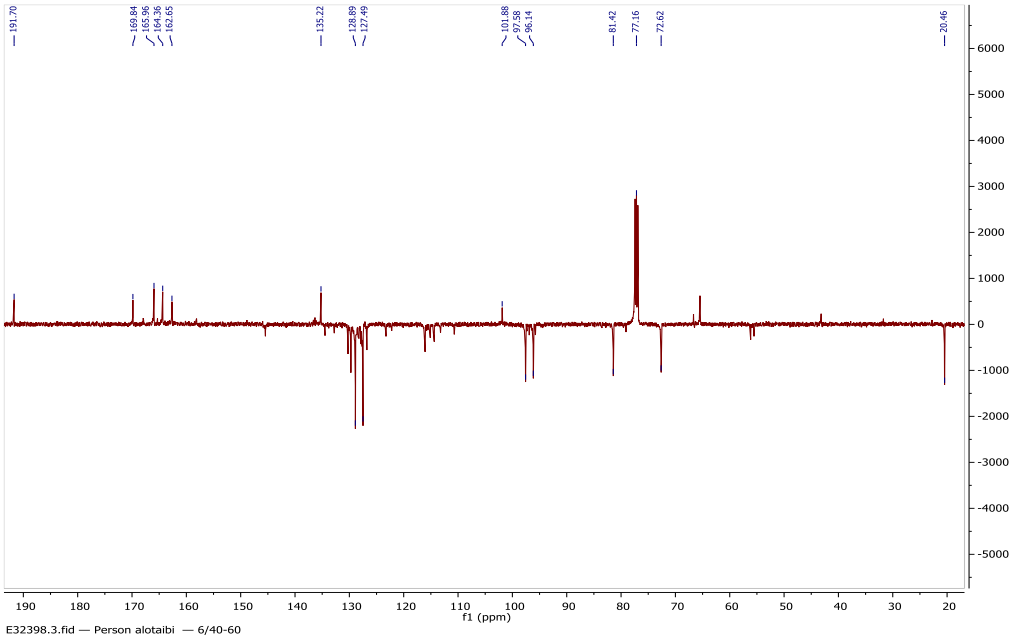

Figure 3-9: ^{13}C NMR (400 MHz) of Pinobanksin 3-O-acetate in $CDCl_3$.

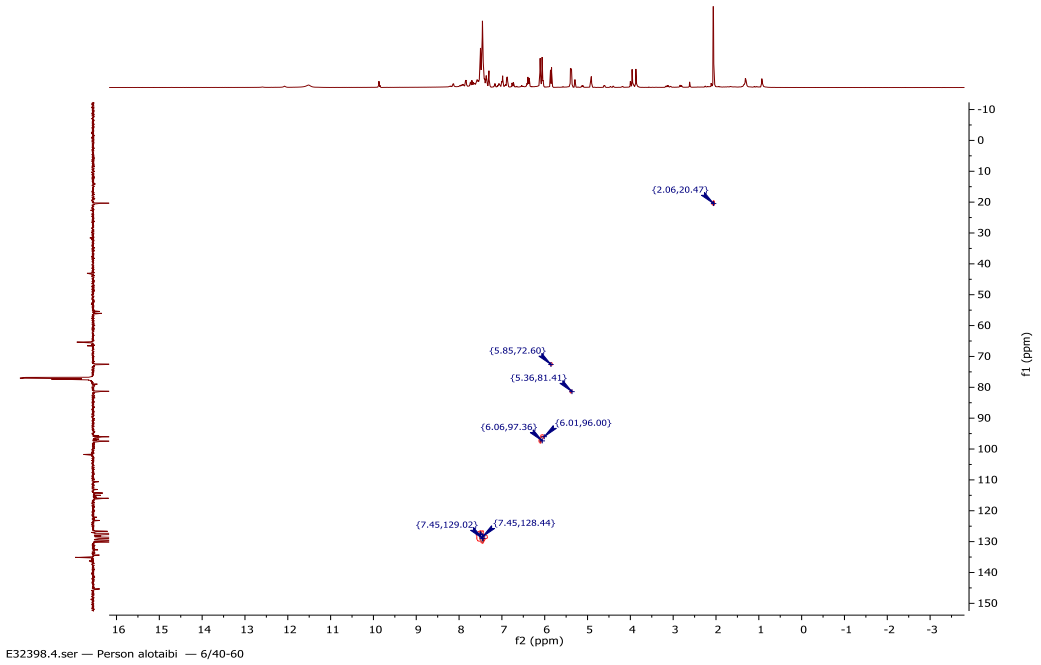

Figure 3-10: HSQC spectrum (400 MHz) of Pinobanksin 3-O-acetate in $CDCl_3$.

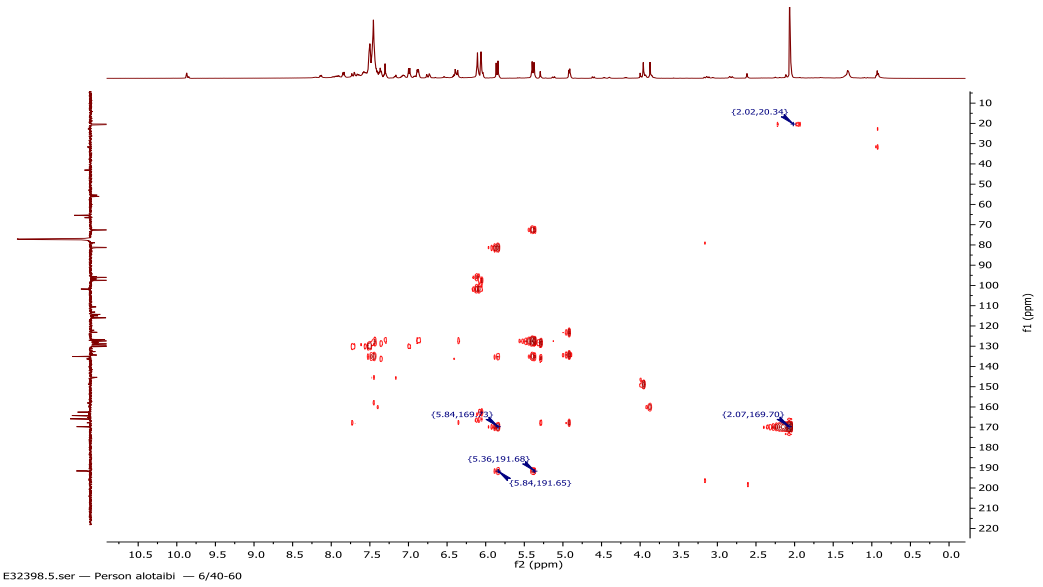

Figure 3-11: HMBC spectrum (400 MHz) of Pinobanksin 3-O-acetate in $CDCl_3$

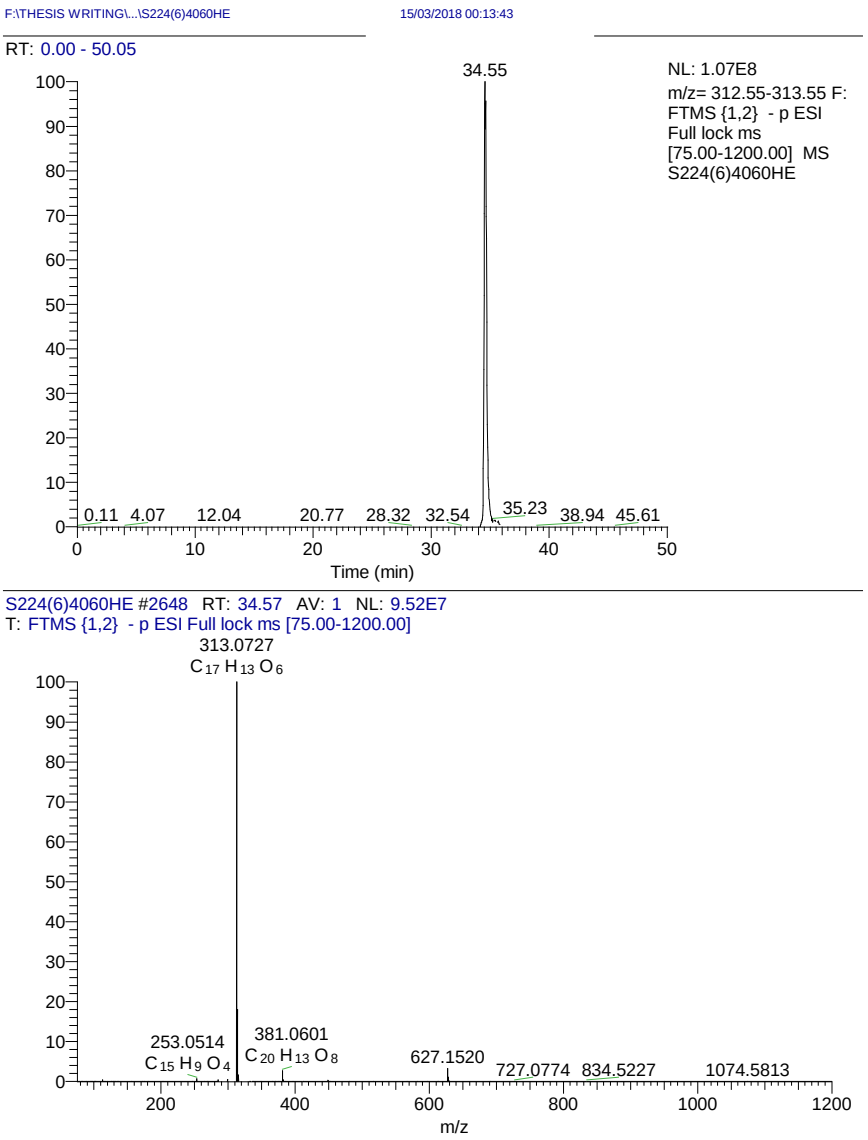

Figure 3-12: Extracted ion chromatogram and the mass spectrum in the negative ion mode (-ve ESI) indicated to Pinobanksin 3-O-acetate

3.1.8.2 Characterisation of fraction C1H40-E60-MPLC-F3+4 (2) as 7-methoxychrysin (2)

This compound was obtained as a white amorphous solid from a Grace Reveleris MPLC fraction. The positive mode HRESI-MS spectrum of the compound Figure 3-17 gave a molecular ion $[M+H]^+$ at m/z 269.0790 suggesting a molecular formula of

$C_{16}H_{12}O_4$ (Calc for ($C_{16}H_{13}O_4$), 269.0814). The ^{1}H NMR spectrum of the compound showed a chelated –OH proton at δ_H 12.72 (s) ppm and two meta coupled protons usually observed for ring A in flavones with H-6 resonating at δ_H 6.41(1H, *J* = 2.3 Hz) and H-8 at 6.54 (1H, *J* = 2.3 Hz). Two signals were observed for the five protons of a monosubstituted phenyl ring B at 7.54 (3H, m) and 7.90 (2H, m) and a singlet was also observed at 6.70 (1H, s). The methoxy protons were also observed as a singlet at 3.90 (3H,s) Figure 3-14. The signals in the ^{13}C spectrum though weak, showed the major carbon atoms in the compound: the carbonyl carbon at δ_C 175.2 ppm, the aromatic CH carbons at 132.0, 129.2, 126.5, 106.1, 98.4 and 92.9 while the methoxy carbon was at 56.0 ppm Figure 3-15. Using correlations in its 2D NMR, HSQC) Figure 3-16 the structure of the compound was confirmed as 7-methoxychrysin, and the chemical shifts for the protons and carbon atoms are given in Table 3-17 and literature reports (Talzhanov et al., 2005, Rosandy et al., 2013).

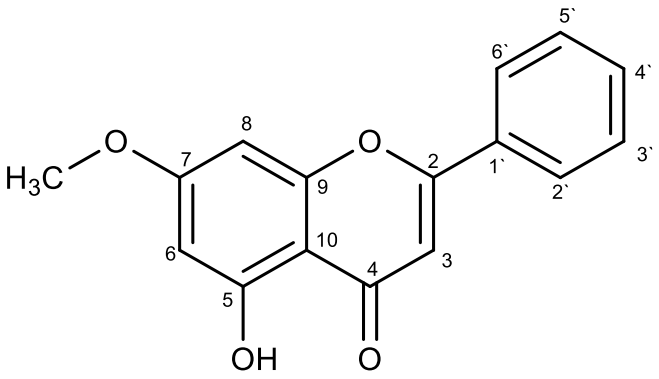

Figure 3-13: Chemical structure of 7-O-methoxychrysin

Table 3-17: Chemical shifts for 7-O-Methoxy Chrysin

Position	7-O-Methoxy Chrysin		Literature*	
	^{1}H δ ppm (mult, J in Hz)	^{13}C δ ppm, (mult)	^{1}H δ ppm, (mult, *J* in Hz)	^{13}C δ ppm, (mult)
1	-	-	-	-
2	-	164.6 (C)	-	164.0
3	6.70 (1H, s)	105.6 (CH)	6.67(s)	105.9
4	-	182.9(C)	-	182.5
5	-	162.8 (C)	-	162.2
6	6.41 (1H, d, 2.2)	98.1 (CH)	6.39(s)	98.2
7	-	165.8 (C)	-	165.6
8	6.54 (1H, d, 2.2)	92.6 (CH)	6.51(s)	92.7
9	-	156.0 (CH)	-	157.8
10	-	105.9	-	105
1`	-	132.6 (C)	-	131.9
2`	7.90 (1H, d)	126.4 (CH)	7.89(d,7.8)	126.3
3`	7.54 (1H, m)	129.0(CH)	7.54 (m)	129.1
4`	7.54 (1H, m)	131.0 (CH)	7.52 (m)	129.1
5`	7.54 (1H, m)	129.0 (CH)	7.54 (m)	129.1
6`	7.90 (1H, d)	126.4 (CH)	7.89(d,7.8)	126.3
7-OCH_3	3.90 (3H, s)	55.4 (CH)	3.89(s)	55.4
5-OH	12.72 (s)	-	12.73(s)	-

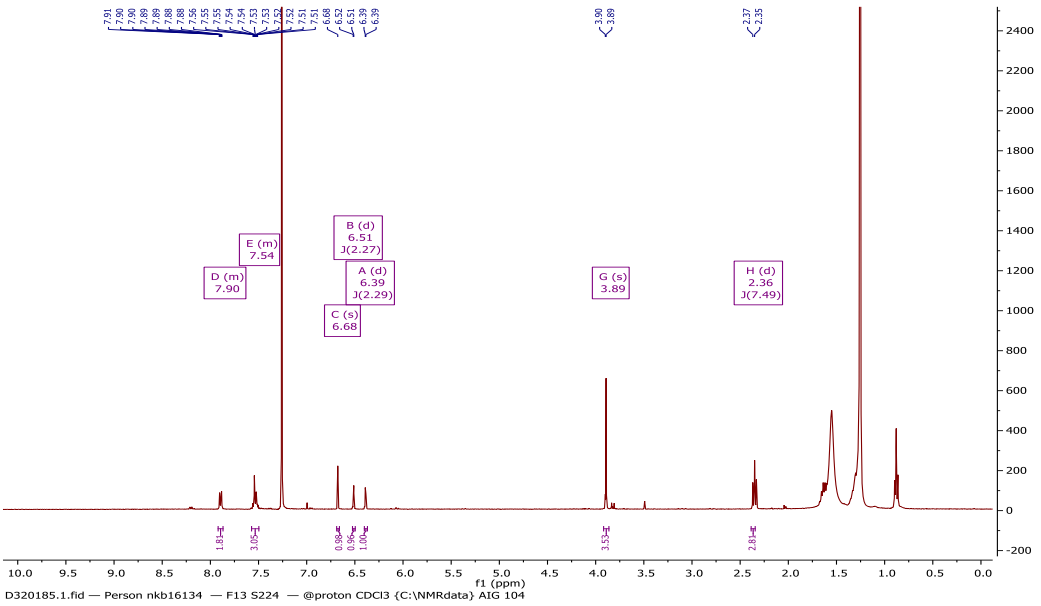

Figure 3-14:[1]H NMR (400 MHz) of 7-methoxychrysin in $CDCl_3$

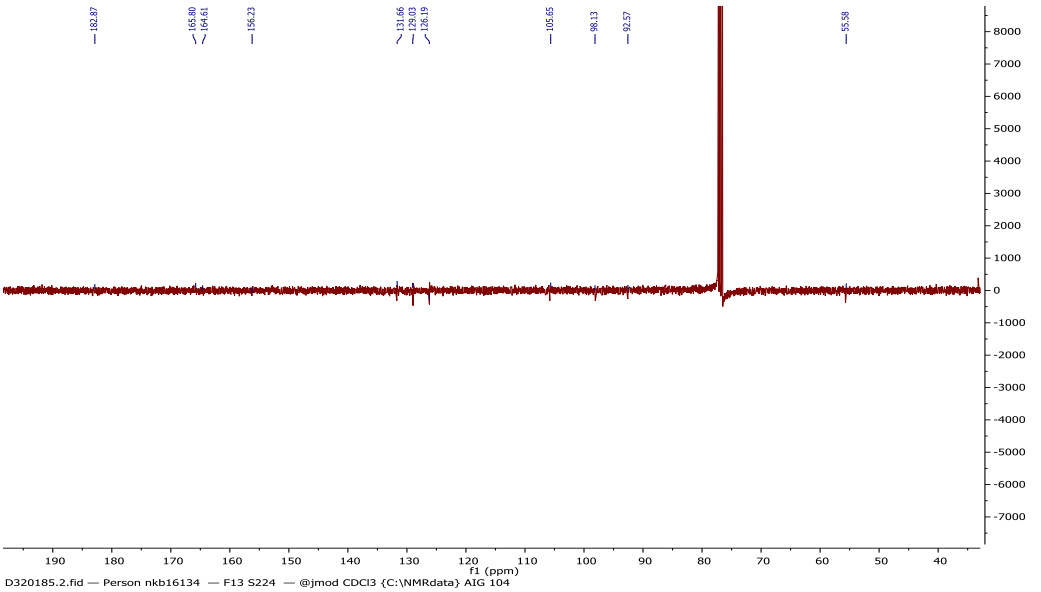

Figure 3-15: [13]C NMR (400 MHz) of 7-methoxychrysin in $CDCl_3$

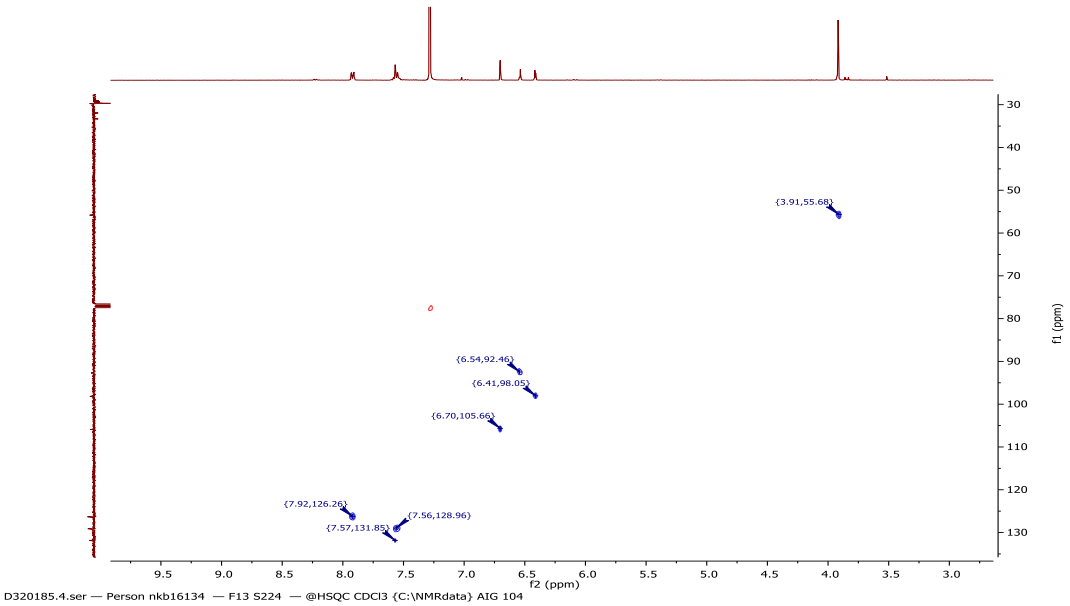

Figure 3-16: HSQC spectrum (400 MHz) for 7-methoxychrysin in $CDCl_3$

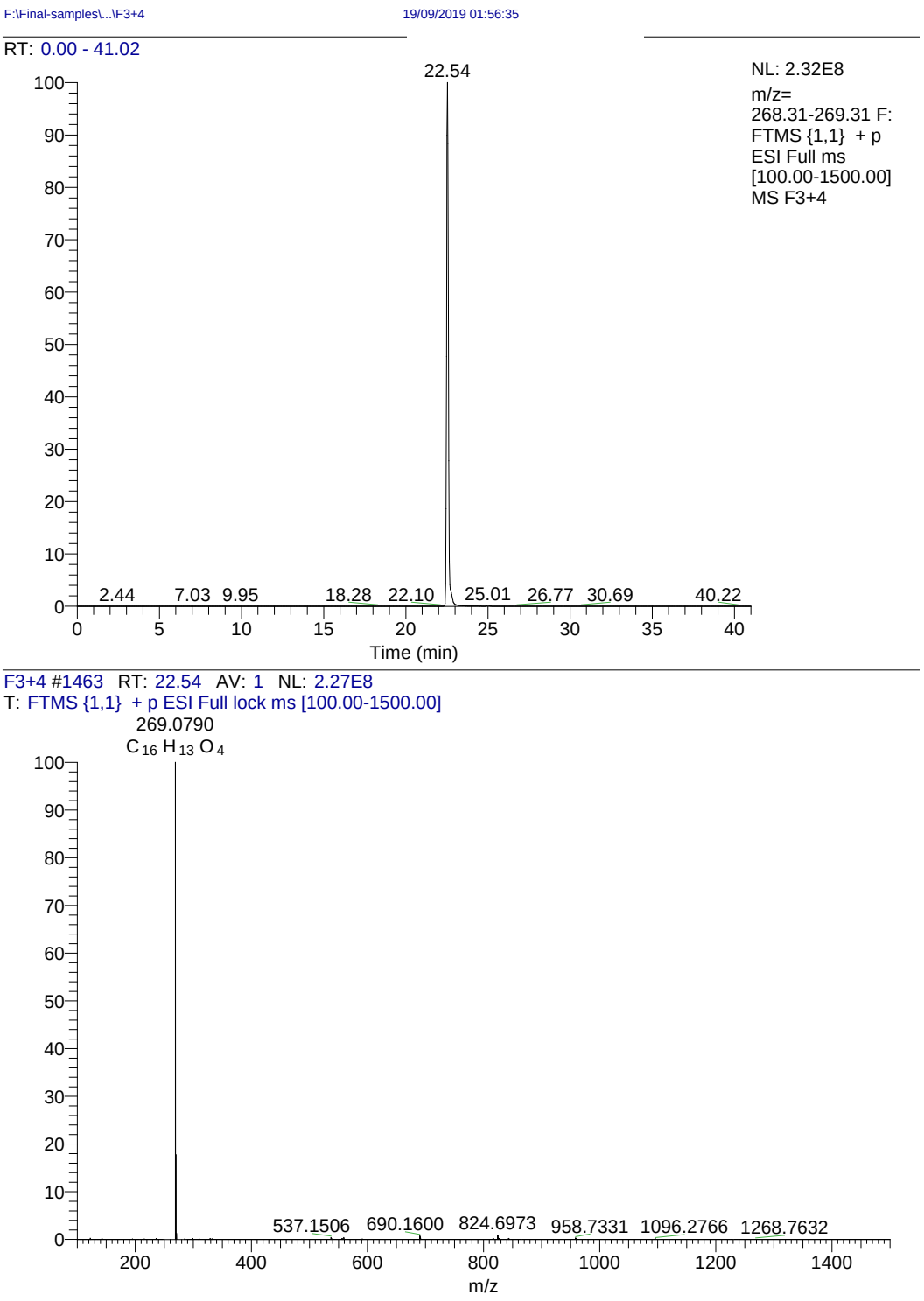

Figure 3-17: Extracted ion chromatogram and mass spectrum in the positive ion mode (+ve ESI) for 7-methoxychrysin

3.1.8.3 Characterisation of fraction C3+4-H40-E60-M14-S7 as Kaempferol (3)

The compound was obtained as a yellowish solid from a Grace Reveleris MPLC fraction and Sephadex. The negative mode HRESI-MS spectrum of the compound gave a molecular ion $[M-H]^-$ at m/z 285.0403, (Calcd 285.0399 for $C_{15}H_9O_6$) suggesting a molecular formula of $C_{15}H_{10}O_6$. H-6 and H-8 occurred as a doublet at δ 6.27 and 6.54 ppm, respectively. The signals of B ring were simply assigned by the reflection of symmetry. The H-2' and H-6' resonances happened as a sharp doublet at δ 8.16 ppm. The H-3' and H-5' resonances appeared as a doublet of doublets at δ 7.02 ppm Figure 3-19. The proton spectra were identical to compound (5) except for the absence of the methoxy group on ring B. The chemical shifts for the protons and carbon atoms are given in Table 3-18. It was thus identified as kaempferol and confirmed by literature reports (Bertelli et al., 2012).

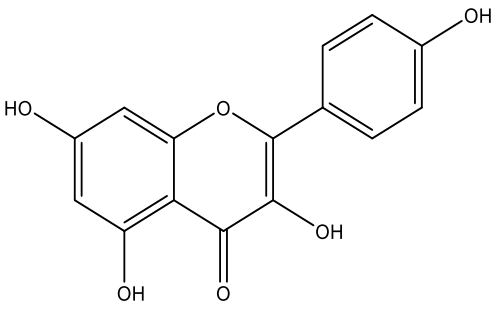

Figure 3-18: Chemical structure of Kaempferol

Table 3-18: Chemical shifts for Kaempferol

Position	**Kaempferol**		Literature*	
	^{1}H δ ppm (mult, *J* in Hz)	^{13}C δ ppm, (mult)	^{1}H δ ppm, (mult, *J* in Hz)	^{13}C δ ppm, (mult)
1	-	-	-	-

2	-	146.9 (C)	-	146.7
3	-	137.1	-	135.5
4	-	175.3 (C)	-	175.8
5	-	160.6 (C)	-	160.6
6	6.27 (1H, d, 2.2)	98.3 (C)	6.21 (1H, d,)	98.1
7	-	163.6 (C)	-	163.8
8	6.54 (1H, d, 2.2)	93.7 (CH)	6.46 (1H, d,)	93.4
9	-	156.6 (C)	-	156.1
10	-	103.5 (C)	-	103.0
1`	-	122.2(C)	-	121.6
2`	8.16 (1H, m)	129.7 (CH)	8.07 (1H, dd)	129.5
3`	7.02 (1H, m)	115.9 (CH)	6.94 (1H, dd)	115.4
4`	-	159.6 (C)		159.1
5`	7.02 (1H, m)	115.9 (CH)	6.94(dd)	115.4
6`	8.16 (1H, m)	129.7 (CH)	8.07(dd)	129.5
7-OH	-	-	10.78(s)	-
5-OH	12.16 (s)	-	12.50 (1H, s)	-
3-OH		-	9.35(s)	
4`-OH	-			

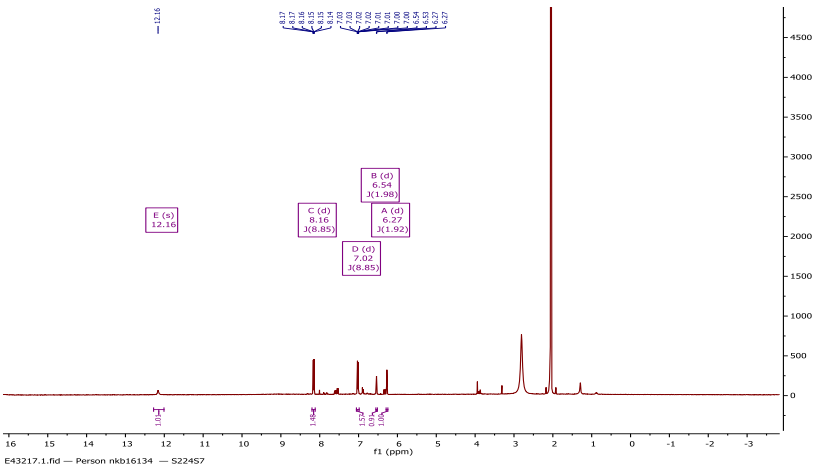

Figure 3-19: ^{1}H NMR (400 MHz) of Kaempferol in $CDCl_3$

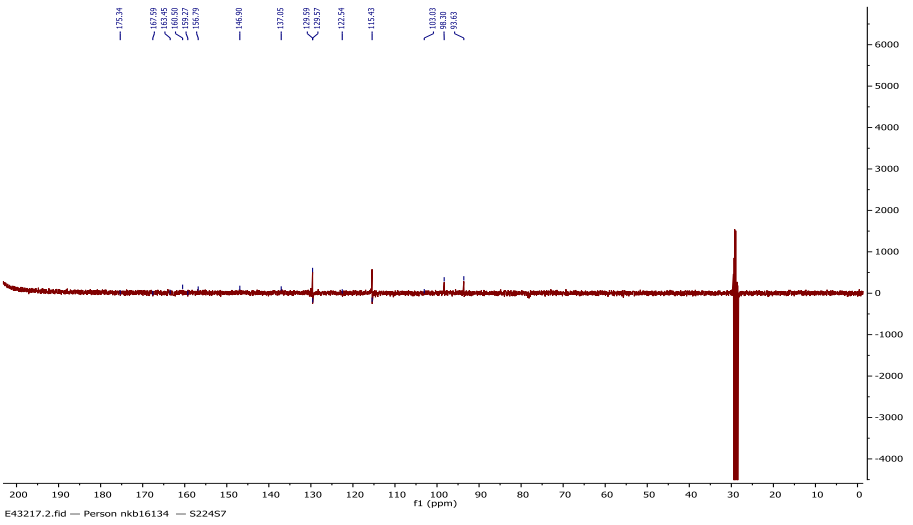

Figure 3-20: ^{13}C NMR (400 MHz) of Kaempferol in $CDCl_3$

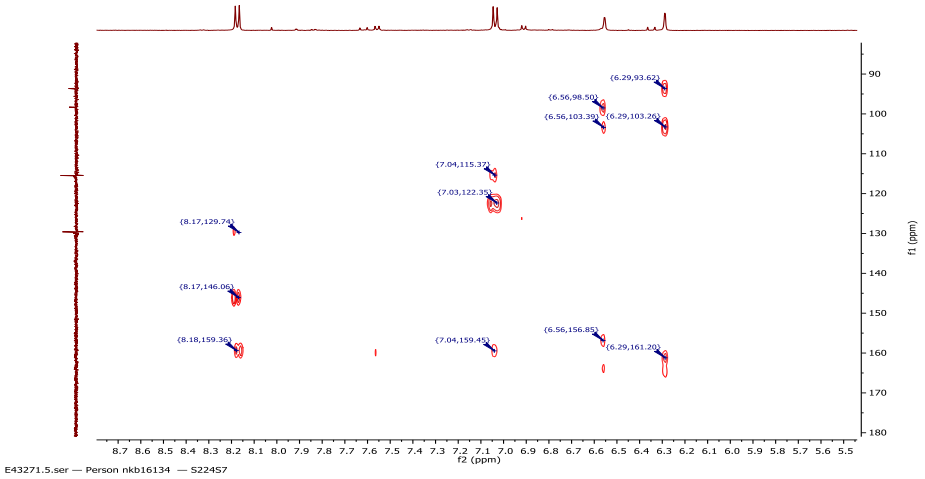

Figure 3-21: HMBC spectrum (400 MHz) of Kaempferol in $CDCl_3$

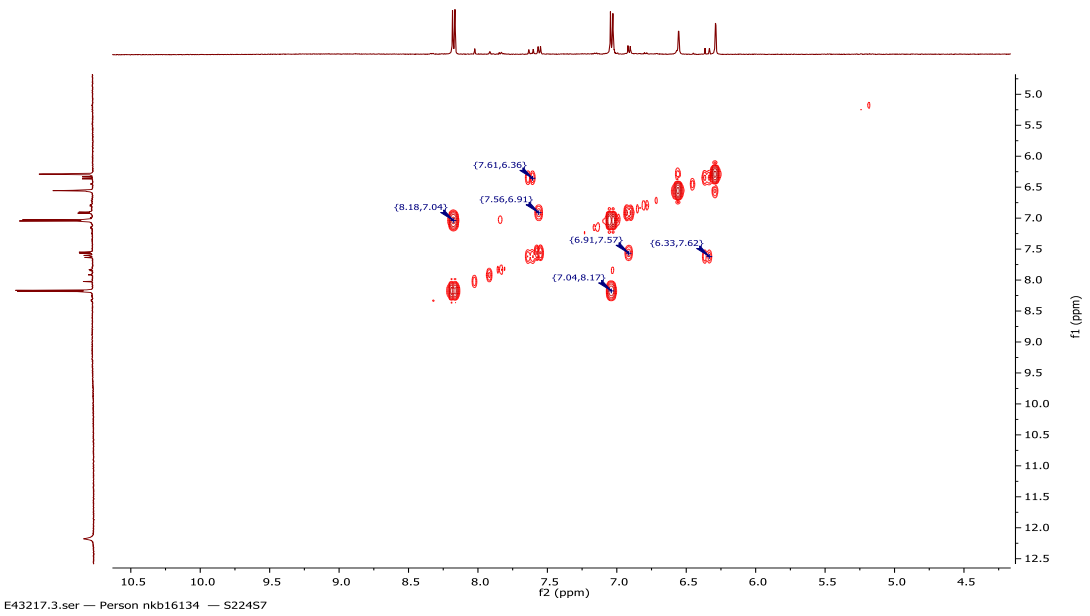

Figure 3-22: COSY spectrum (400 MHz) of Kaempferol in $CDCl_3$

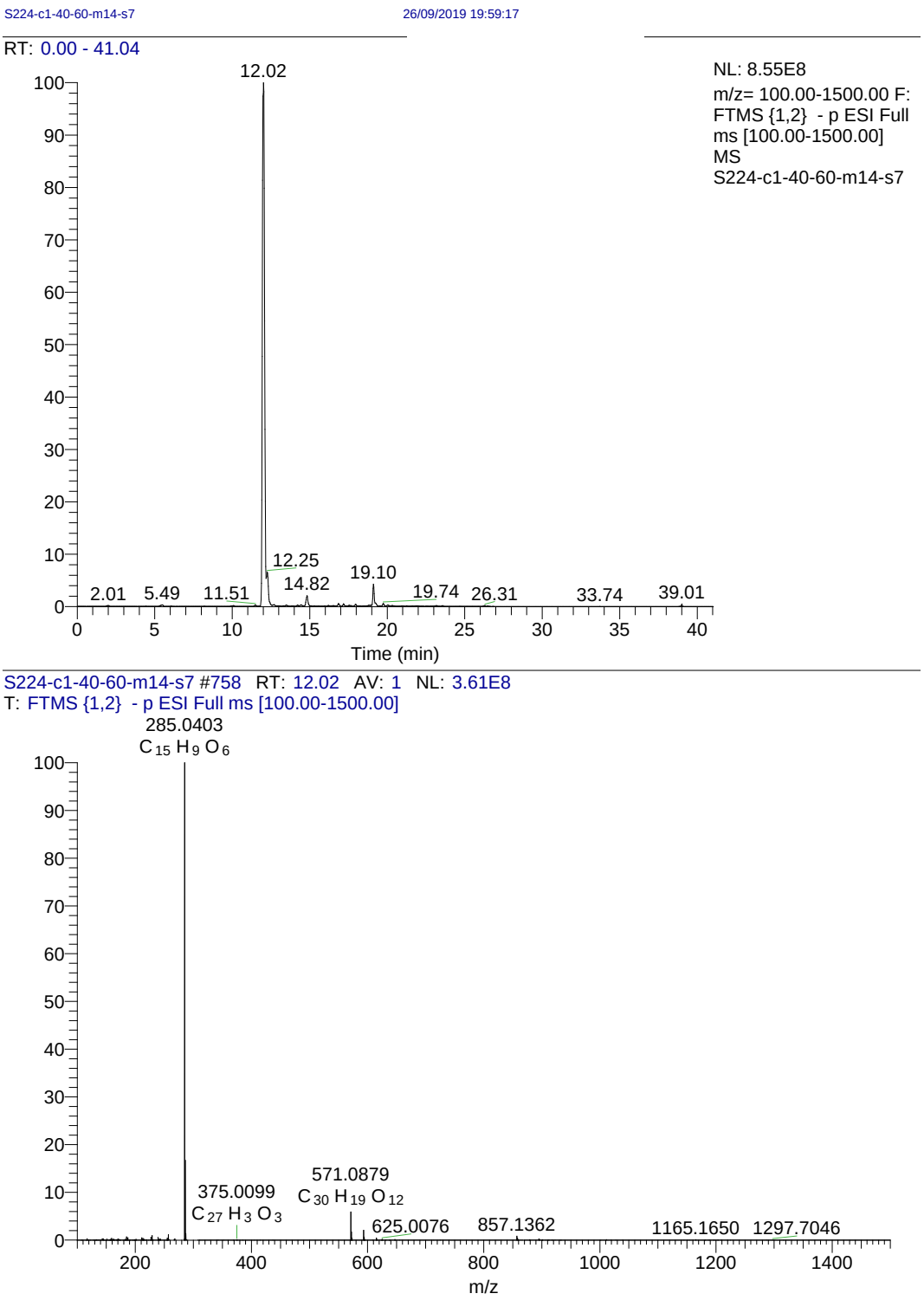

Figure 3-23: Extracted ion chromatogram and the mass spectrum in the negative ion mode (-ve ESI) for Kaempferol

Characterisation of fraction C H60-E40-mplc8-15-F4 as Pinocembrin (4)

The compound was obtained as yellow needle-shaped crystals from a Grace Reveleris MPLC fraction and Sephadex. The negative mode HRESI-MS spectrum of the compound gave a molecular ion $[M-H]^-$ at m/z 255.0665 ($C_{15}H_{11}O_4$), (Calc for 255.0657) suggesting a molecular formula of $C_{15}H_{12}O_4$. The proton spectrum showed three sets of aliphatic protons; hence the compound was predicted to be a flavanone. The ring b was also found to be unsubstituted due to the presence of a 5H multiplet Figure 3-25. The chemical shifts for the protons and carbon atoms are presented in Table 3-19.

Further examination of the spectra led to the identification of the compound as pinocembrin and was confirmed by literature reports (Bertelli et al., 2012). Pinocembrin is considered the most abundant compound in propolis from different plants, mainly from Populus and Pinus heartwood. Its biological activities were evaluated, including antioxidant, anti-inflammatory and antimicrobial and exhibits many pharmacological activities (Yang et al., 2013). It was isolated from Mexican Brown and red propolis (Granados-Pineda et al., 2018, Lotti et al., 2010). It was also isolated from South Africa propolis and tested against *T. brucei*, where it showed moderate activity (Omar et al., 2016).

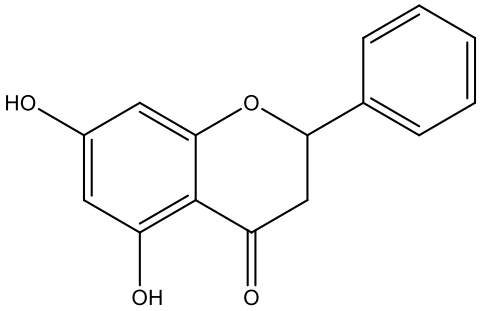

Figure 3-24: Chemical structure of Pinocembrin

Table 3-19: Chemical shifts for Pinocembrin

Position	**Pinocembrin**		Literature*	
	^{1}H δ ppm (mult, *J* in Hz)	^{13}C δ ppm, (mult)	^{1}H δ ppm, (mult, J in Hz)	^{13}C δ ppm, (mult)
1			-	-
2	5.58(1H, dd,12.8,3.2)	78.1(CH)	5.58 (1H, dd)	78.21
3a	3.17(1H, dd,17.1,12.8)	43.7 (CH_2)	3.23 (1H, dd)	42.77
3b	2.82(1H, dd)		2.79(1H, dd)	
4	-	196.8(C)		196.45
5	-	164.2(C)	-	164.10
6	5.97 (1H, d, 2.2)	96.0 (C)	5.87(dd)	96.50
7	-	166.2(C)	6.00 (1H, d, *J* = 2.2)	167.23
8	6.01 (1H, d, 2.1)	95.0 (CH)	5.87(dd)	95.62
9	-	162.9 (C)	-	163.65
10	-	102.2 (C)	-	102.30
1`	-	139.1(C)	-	139.64
2`	7.57 (1H, m)	127.3 (CH)	7.52(d)-	127.12
3`	7.45 (1H, m)	129.5 (CH)	7.34(5H, m)	129.13

4`	7.40 (1H, m)	129.4 (CH)	7.34(5H, m)	129.13
5`	7.45 (1H, m)	129.5 (CH)	7.34(5H, m)	129.13
6`	7.57 (1H, m)	127.3 (CH)	7.52 (5H, m)	127.12
7-OH	10.81 (1H, s)	-	10.79(s)	-
5-OH	12.16(s)	-	12.13(s)	-

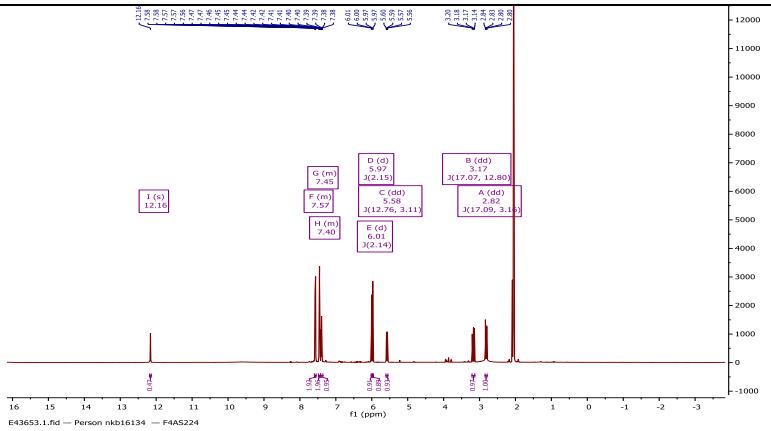

Figure 3-25: ^{1}H NMR (400 MHz) of Pinocembrin in Acetone-d_6

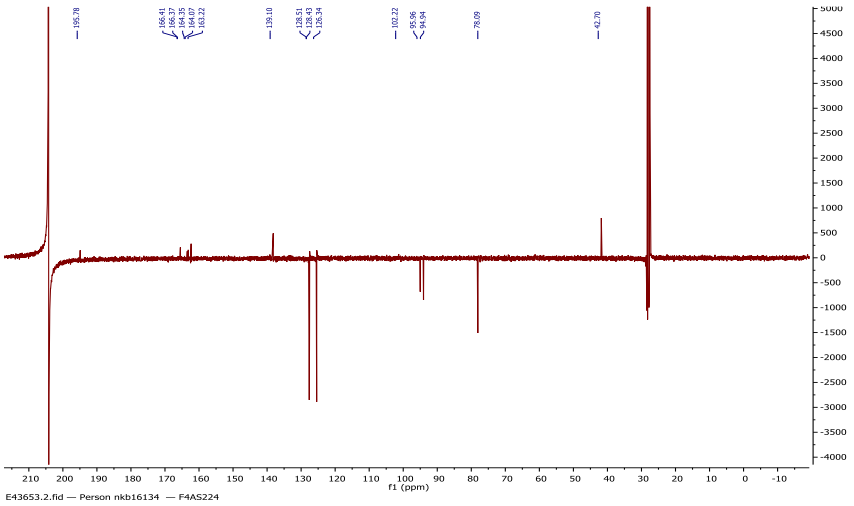

Figure 3-26: ^{13}C NMR (400 MHz) of Pinocembrin in Acetone-d_6

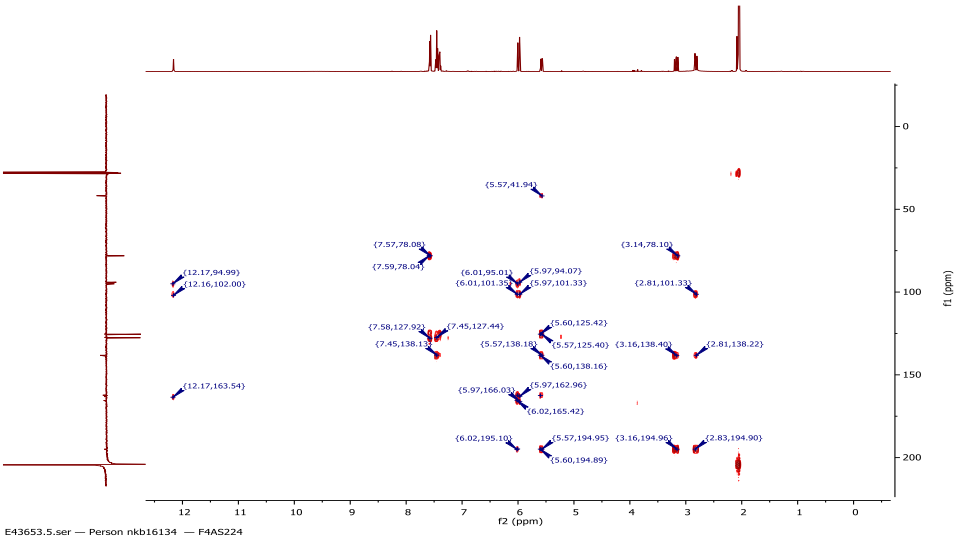

Figure 3-27: HMBC spectrum (400 MHz) of Pinocembrin in Acetone-d_6

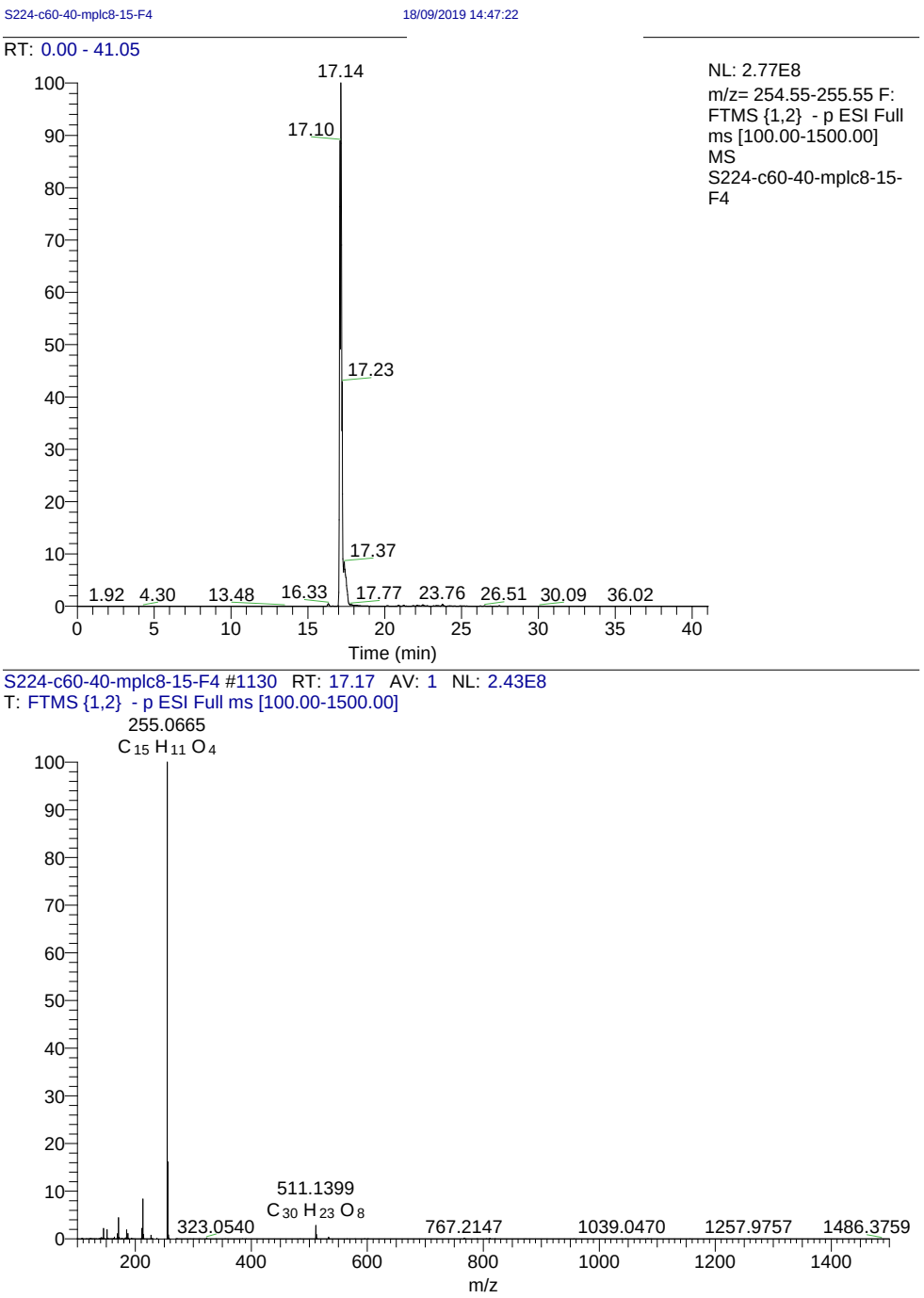

Figure 3-28: Extracted ion chromatogram and the mass spectrum in the negative ion mode (-ve ESI) for Pinocembrin

3.1.8.4 Characterisation of fraction C6S-C-H40-E60-S9 as 4'-Methoxykaempferol (5)

The compound was obtained as a light yellow solid following purification by column chromatography and Sephadex LH20. The positive mode HRESI-MS spectrum of the compound gave a molecular ion $[M+H]^+$ at m/z 301.0701 (Calc for ($C_{16}H_{13}O_6$), 301. 0712) suggesting a molecular formula of $C_{16}H_{12}O_6$. The ^{1}H-NMR Figure 3-30, ^{13}C-NMR Figure 3-31 and HMBC spectrum Figure 3-32, spectra of compound 5 showed H-6 and H-8 occurred as a doublet at δ 6.29 and 6.56 ppm, respectively. The signals of B ring were simply assigned by the reflection of symmetry. The H-2' and H-6' resonances happened as a sharp doublet at δ 8.23 ppm. The H-3' and H-5' resonances seemed as a doublet of doublets at δ 7.14 ppm, and H-4' occurred as a singlet at δ 3.98 ppm. The ^{13}C experimentations of compound 5 presented fourteen peaks. The most deshielded peak was 175.1 ppm which was assigned as the keto group (C-4), and the most shielded peak was at 54.9 ppm which was shown as ether group (4`-OCH_3). Further examination of its ^{13}C and 2D spectra identified the compound as 4'-Methoxykaempferol and was confirmed by literature reports (Lee et al., 2008). The chemical shifts for the protons and carbon atoms are given in Table 3-20.

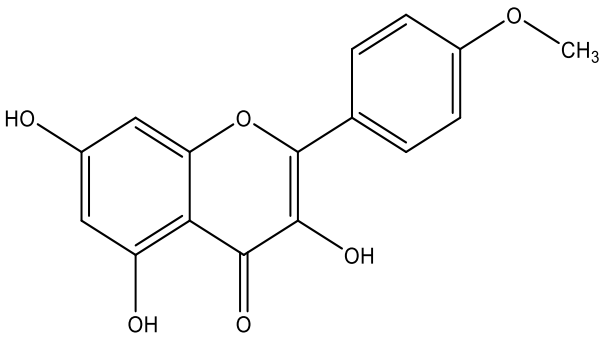

Figure 3-29: Chemical structure of 4'-Methoxykaempferol

Table 3-20: Chemical shifts for 4'-Methoxykaempferol

Position	**5,7-Dihydroxy-4'-methoxyflavonol** (4'-Methoxykaempferol)		Literature*	
	^{1}H δ ppm (mult, *J* in Hz)	^{13}C δ ppm, (mult)	^{1}H δ ppm, (mult, *J* in Hz)	^{13}C δ ppm, (mult)
1	-	-	-	-
2	-	146.0(C)	-	146.3
3	-	136.0 (C)	-	136.1
4	-	175.1(C)	-	176.1
5	-	161.5(C)	-	160.8
6	6.29 (1H, d, 2.2)	98.3 (C)	6.29 (1H, d)	98.3
7	-	164.4(C)	-	164.1
8	6.56 (1H, d, 2.2)	93.7 (CH)	6.45 (1H, d,)	93.6
9	-	157.2 (CH)	-	156.3
10	-	103.2(C)	-	103.7
1`	-	122.3(C)	-	123.3
2`	8.23(1 H, m)	129.5 (CH)	8.12(1H, d)	129.4
3`	7.14 (1H, m)	113.9 (CH)	7.09(1H, d)	114.1
4`	-	161.5 (C)	-	160.6
5`	7.14 (1H, m)	113.9 (CH)	7.09(1H, d)	114.1

6`	8.23(1 H, m)	129.5(CH)	8.12(IH, d)	129.4
7-OH	-	-	10.83 (1H, s)	-
5-OH	12.16(s)	-	12.43 (1H, s)	-
3-OH	-	-	9.47(1H, s)	
4'-OCH_3	3.90 (s)	54.9 (CH_3)	3.81(3H,s)	55.4

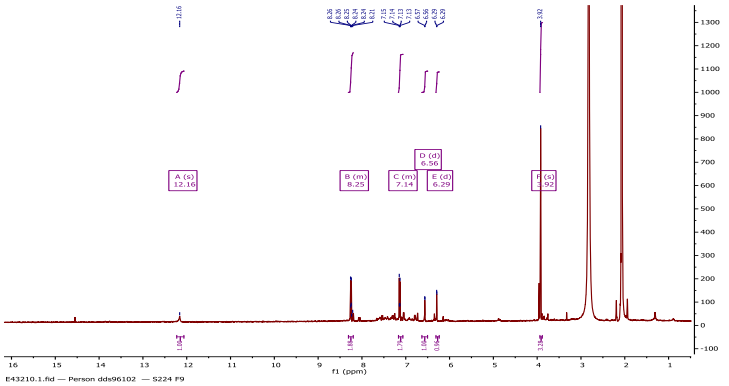

Figure 3-30: ^{1}H NMR (400 MHz) of 4'-Methoxykaempferol in Acetone-d_6

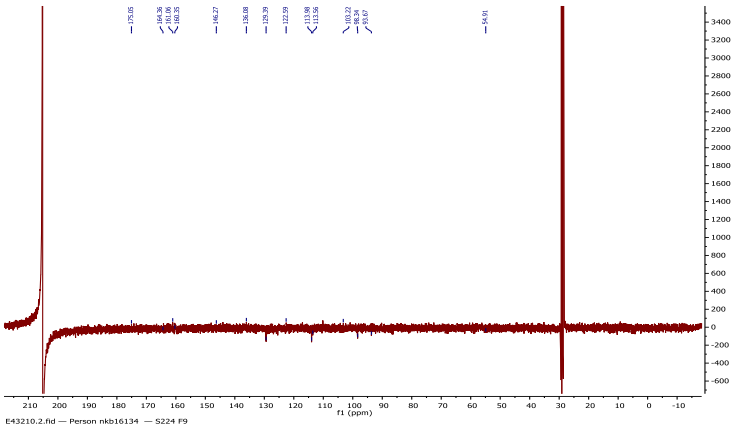

Figure 3-31: ^{13}C NMR (400 MHz) of 4'-Methoxykaempferol in Acetone-d_6

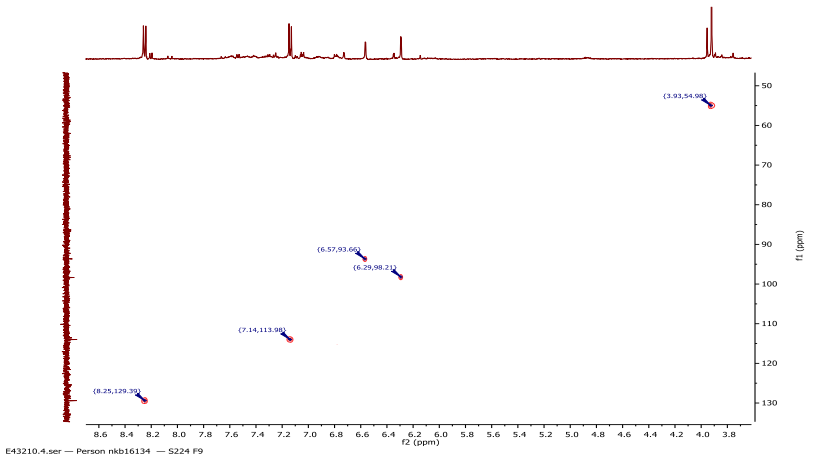

Figure 3-32: HSQC spectrum (400 MHz) of 4'-Methoxykaempferol in Acetone-d_6

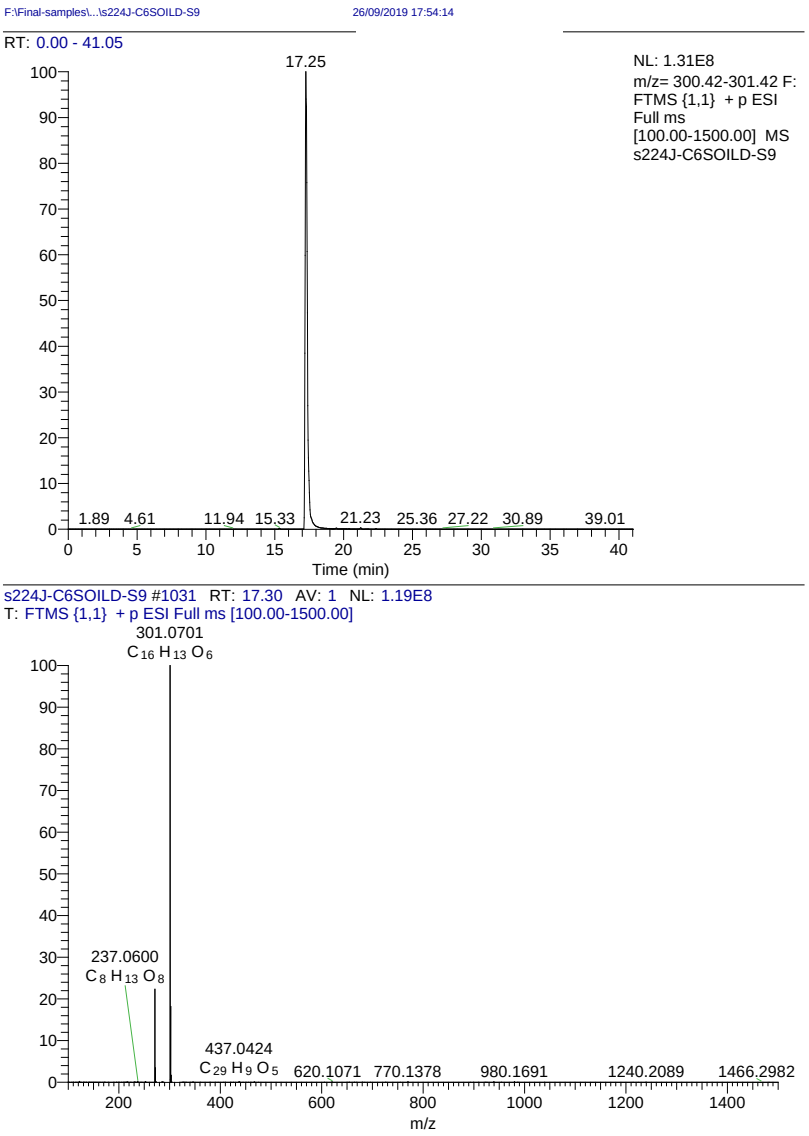

Figure 3-33: Extracted ion chromatogram and the mass spectrum in positive ion mode for 4'-Methoxykaempferol

3.1.8.5 Characterisation of fraction C6L-H40-E60-S8 as Galangin (6)

The compound was obtained as a yellow needle solid following purification by column chromatography and Sephadex LH20. The ^{1}H-NMR Figure 3-35, spectra of compound 6 showed H-6 and H-8 occurred as a doublet at δ 6.29 and 6.56 ppm, respectively. The

signals from the B ring were simply assigned by the reflection of symmetry. The H-2' and H-6' resonances happened as a sharp doublet at δ 8.26 ppm. The H-3' and H-5' resonances appeared as a doublet of doublets at δ 7.58 ppm and H-4' occurred as a multiplet at δ 7.52 ppm. The ^{13}C experiments for compound 6 presented thirteen peaks. The most deshielded peak was at 176.1 ppm, which was assigned as the keto group (C-4) Figure 3-37. The negative mode HRESI-MS spectrum of the compound gave a molecular ion $[M-H]^-$ at m/z 269.0428 (Calc for ($C_{15}H_9O_5$, 269.0450) suggesting a molecular formula $C_{15}H_{10}O_5$. The compound was identified as Galangin and confirmed by literature reports (Bertelli et al., 2012). The chemical shifts for the protons and carbon atoms are given in Table 3-21. Galangin was isolated from propolis from the north of Argentina (Sampietro et al., 2016).

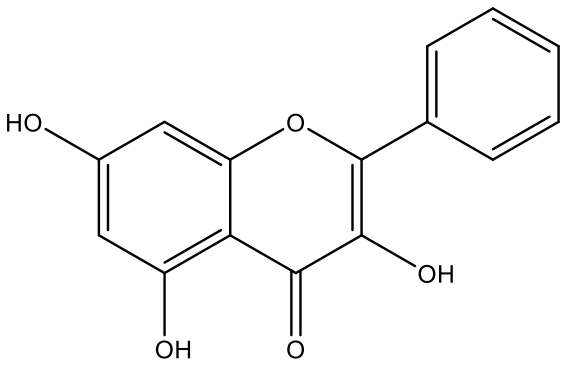

Figure 3-34: Chemical structure of Galangin

Table 3-21: Chemical shifts for Galangin

Position	**Galangin**		Literature*	
	^{1}H δ ppm (mult, J in Hz)	^{13}C δ ppm, (mult)	^{1}H δ ppm, (mult, J in Hz)	^{13}C δ ppm, (mult)
1	-	-	-	-
2	-	145.3 (C)	-	146.11
3	-	137.0 (C)	-	137.52
4	-	176.1(C)		176.68
5	-	161.5(C)	-	169.19
6	6.29 (1H, d, 2.2)	98.4 (C)	6.16(1H, d)	98.74
7	-	164.4(C)	-	164.65
8	6.56 (1H, d, 2.2)	93.7 (CH)	6.40(1H, d)	93.99
9	-	157.2 (CH)	6.04 (1H, d, *J* = 2.2)	156.83
10	-	103.4 (C)	-	103.65
1`	-	131.1(C)	-	131.38
2`	8.26 (1H, m)	127.6 (CH)	8.08 (1H, m)	127.94
3`	7.58 (1H, m)	128.5 (CH)	7.44(1H, m)	128.88
4`	7.52 (1H, m)	130.0 (CH)	7.44 (1H, m)	128.88
5`	7.58 (1H, m)	128.5 (CH)	7.44(1H, m)	128.88
6`	8.26 (1H, m)	127.6 (CH)	8.08 (1H, m)	127.94
7-OH	-	-	10.59(1H, s)	-
5-OH	12.08(s)	-	12.31(1H, s)	-
3-OH	-	-	9.59 (1H, s)	-

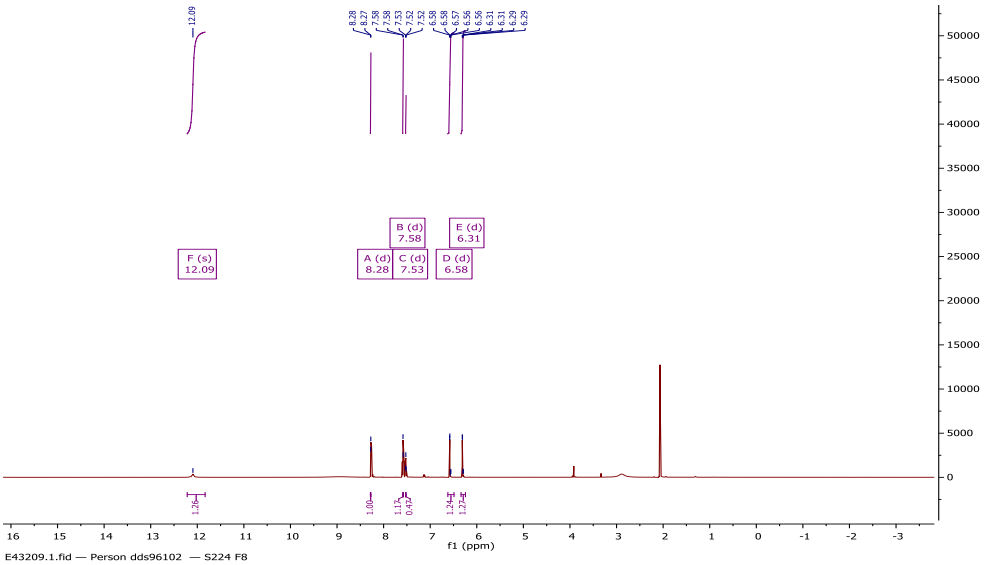

Figure 3-35: ^{1}H NMR (400 MHz) of Galangin in Acetone-d_6

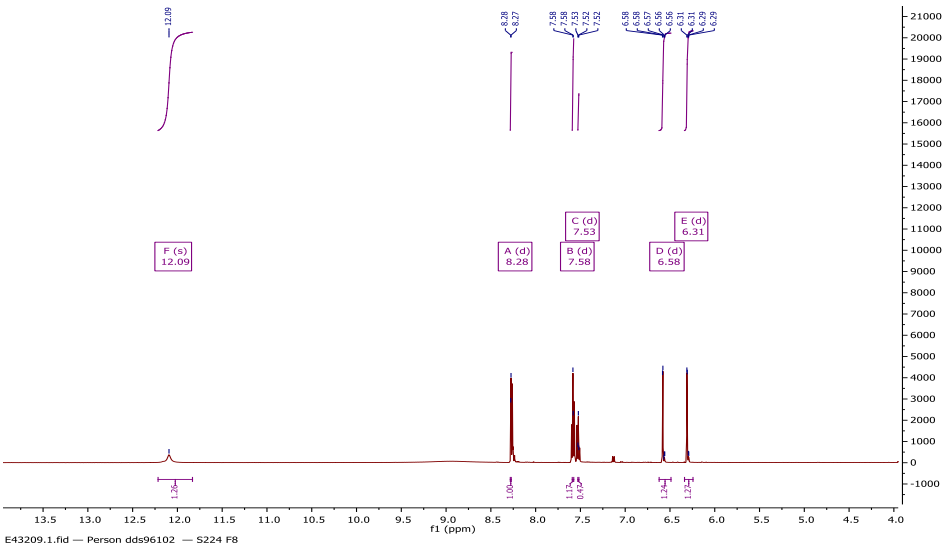

Figure 3-36: Expanded (4.00-13.50 ppm) ^{1}H NMR (400 MHz) spectrum of Galangin in Acetone-d_6

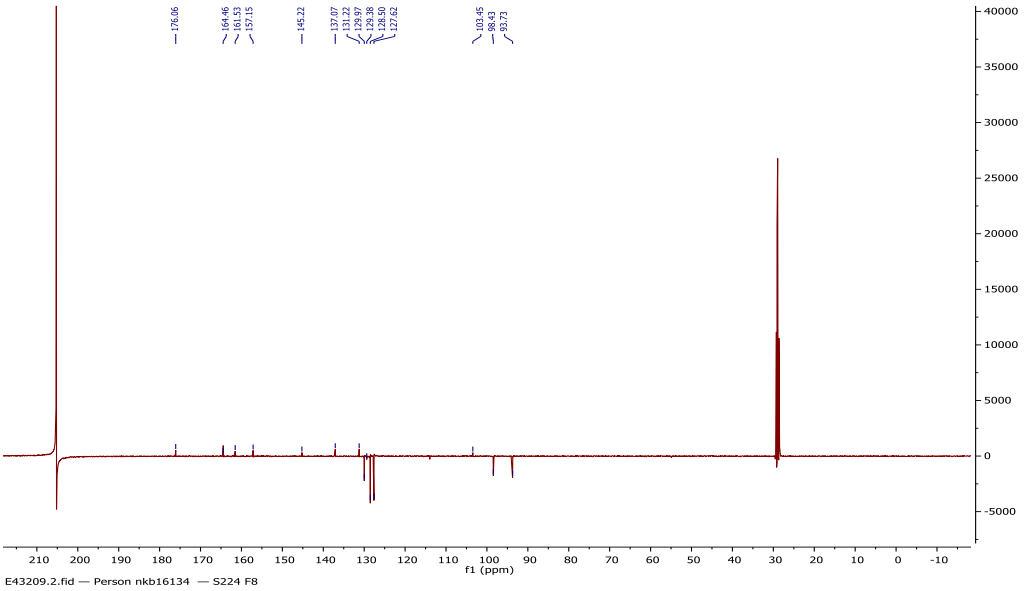

Figure 3-37: ^{13}C NMR (400 MHz) of Galangin in Acetone-d_6

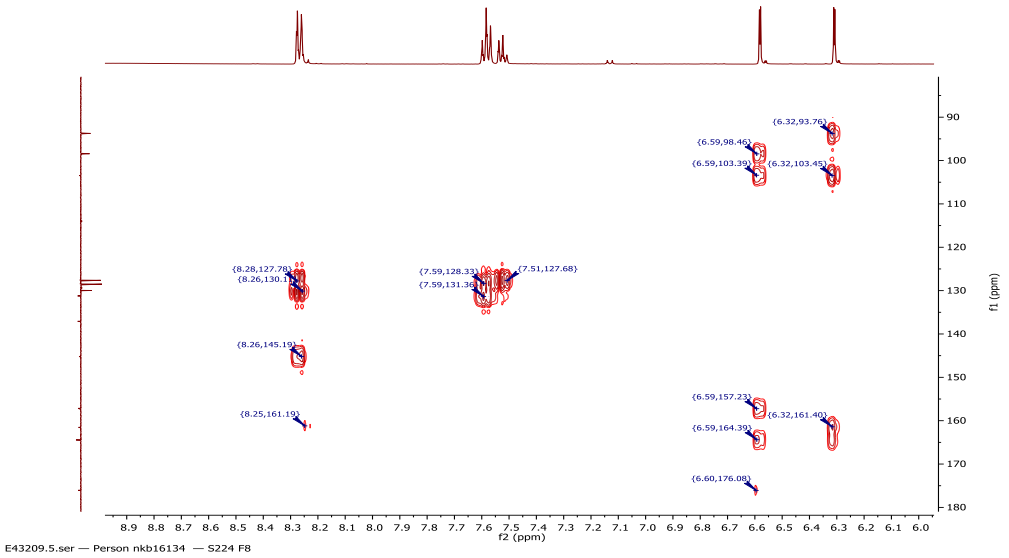

Figure 3-38: HMBC spectrum (400 MHz) of Galangin in Acetone-d_6

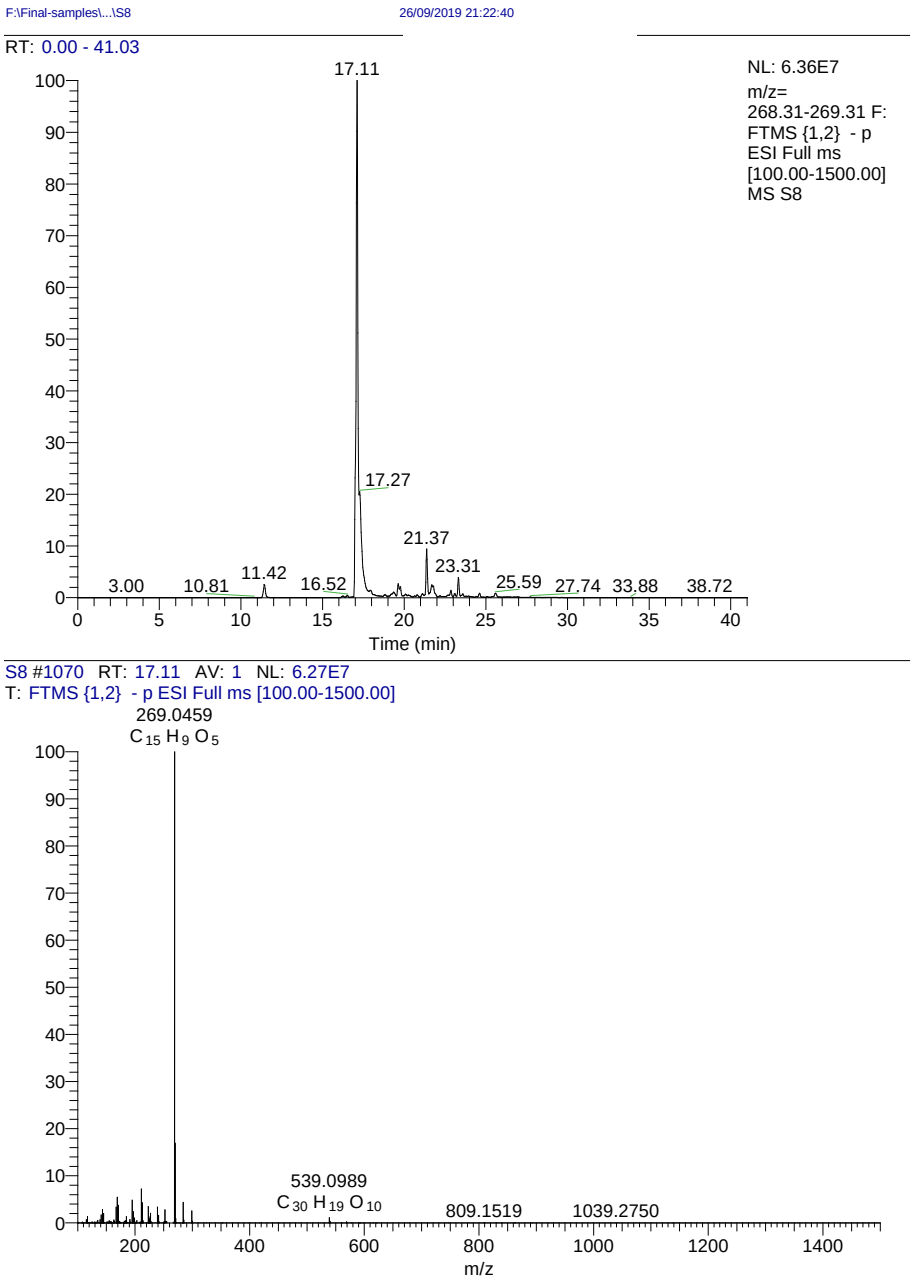

Figure 3-39: Extracted ion chromatogram and the mass spectrum in the negative ion mode for Galangin

3.1.8.6 Characterisation of fraction D7-C1-40-60-S17 as Chrysin (7)

The compound was obtained as a pale yellow solid from column chromatography and Sephadex LH20. The positive mode HRESI-MS spectrum of the compound gave a molecular ion $[M+H]^+$ at m/z 255.0632 (Calc for $C_{15}H_{11}O_4$, 255.0657) suggesting a molecular formula $C_{15}H_{10}O_4$. The compound in its proton spectrum showed a chelated hydroxyl proton at δ_H 12.80 ppm typical of a 5-OH substituted flavonoid. There were two meta coupled protons at δ_H 6.23 and 6.53 ppm as in ring A for 5, 7-dihydroxy substituted flavones. Three multiplets integrated for 5H between 7.55 and 8.07 indicated a mono-substituted benzene ring, and this must be ring B of the flavonoid. The proton singlet observed at δ_H 6.97 is the H-3 of the flavone

Figure 3-41. From all this data, the compound was identified to be chrysin and from its 2D (COSY, HSQC and HMBC) spectra the structure was confirmed as follows: Long range (HMBC) couplings (^3J and ^2J) from the 5-OH proton identified C-5, C-6 and C-10, while correlations from H-3 identified C-2, C-1' and confirmed C-10 Figure 3-43. Other correlations and couplings were as expected; thus, the compound was identified as 5, 7-dihydroxyflavone (Chrysin) and confirmed by comparison of its NMR chemical shift assignments with literature reports (Bertelli et al., 2012). The chemical shifts for the protons and carbon atoms are given in Table 3-22

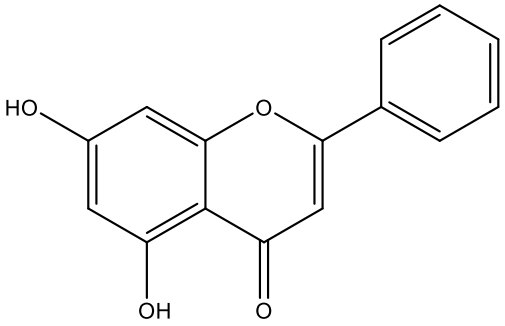

Figure 3-40: Chemical structure of Chrysin.

Table 3-22: Chemical shifts for Chrysin

Position	**Chrysin**		Literature*	
	^{1}H δ ppm (mult, J in Hz)	^{13}C δ ppm, (mult)	^{1}H δ ppm, (mult, J in Hz)	^{13}C δ ppm, (mult)
1			-	-
2	-	163.64 (C)	-	163.6
3a	6.97(1H, s)	105.66 (CH)	6.94 (1H, s)	105.63
4	-	182.34 (C)		182.30
5	-	161.94 (C)	-	161.94
6	6.23 (1H, d)	99.5 (CH)	6.22(d)	99.49
7	-	164.91 (C)		164.91
8	6.53(1H, d)	94.60 (CH)	6.51(1H, d)	94.58
9	-	157.94 (C)	-	157.91
10	-	104.45 (C)	-	104.44
1`	-	131.2 (C)	-	131.19
2`	8.07 (1H, m)	126.88 (CH)	8.04(1H, m)	126.84

3`	7.58(1H, m)	129.60 (CH)	7.58(1H, m)	129.56
4`	7.55(1H, m)	132.48 (CH)	7.58(5H, m)	132.42
5`	7.58(1H, m)	129.60 (CH)	7.58(1H, m)	129.56
6`	8.07 (1H, m)	126.88 (CH)	8.04(1H, m)	126.84
7-OH	10.90 (1H, s)	-	10.90(s)	-
5-OH	12.80 (s)	-	12.82(s)	-

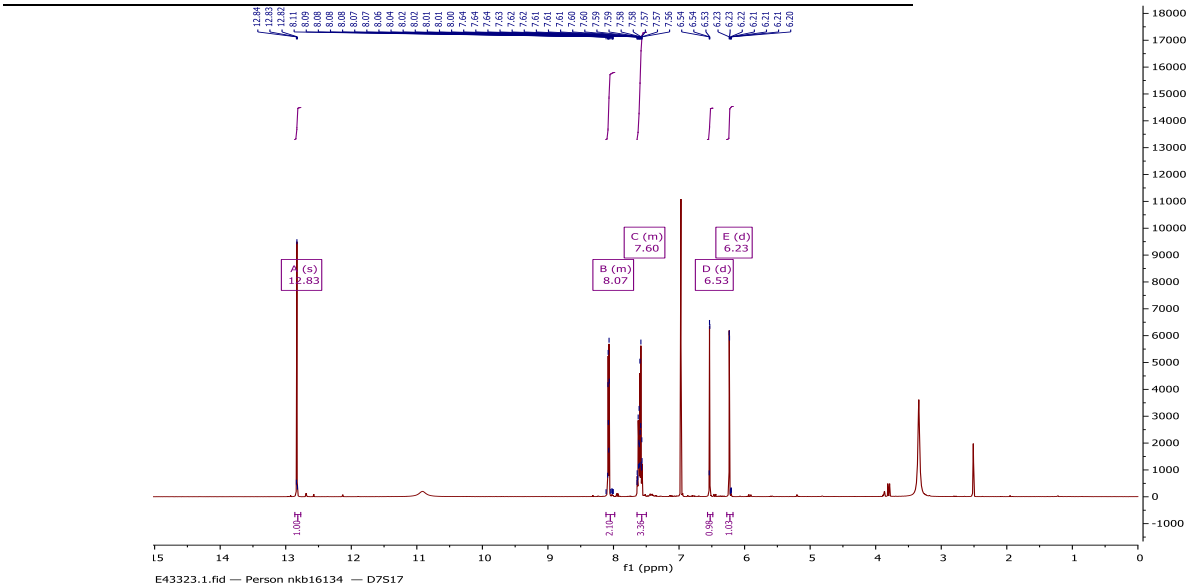

Figure 3-41: ^{1}H NMR (400 MHz) of Chrysin in DMSO-d_6

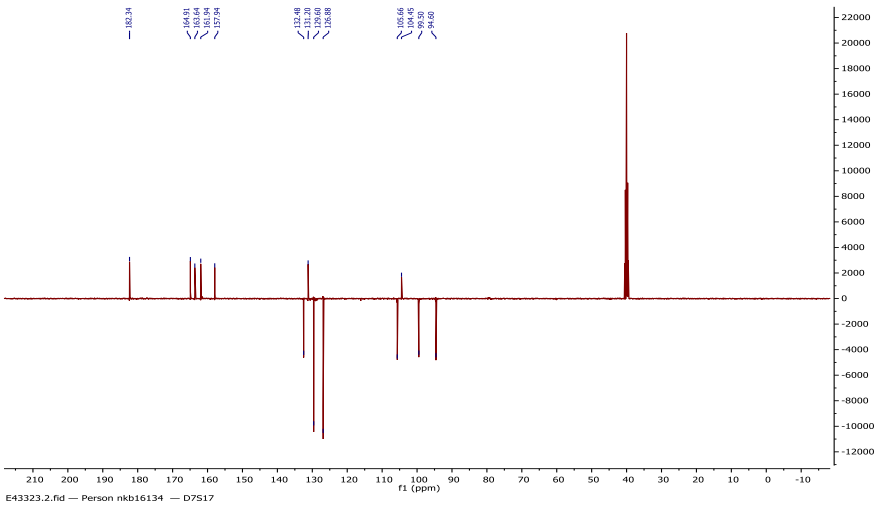

Figure 3-42: ^{13}C NMR (400 MHz) of Chrysin in DMSO-d_6

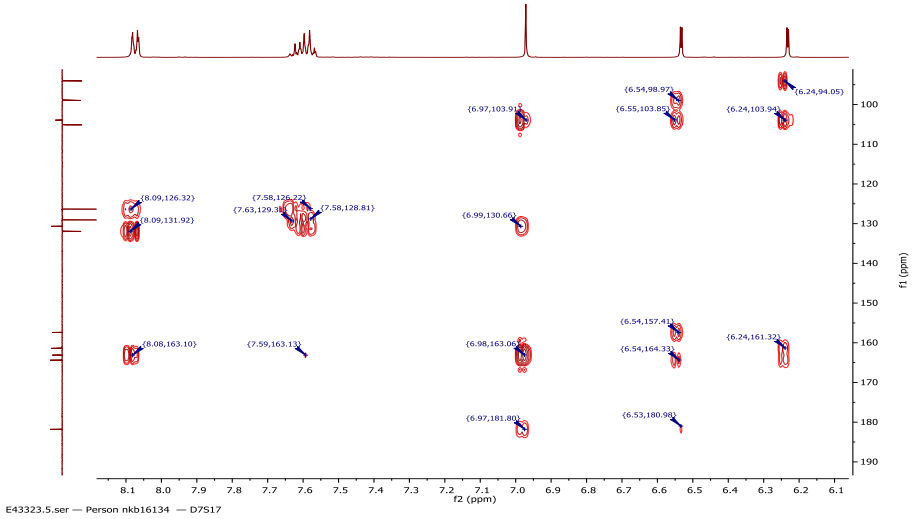

Figure 3-43: HMBC spectrum (400 MHz) of Chrysin in DMSO-d_6

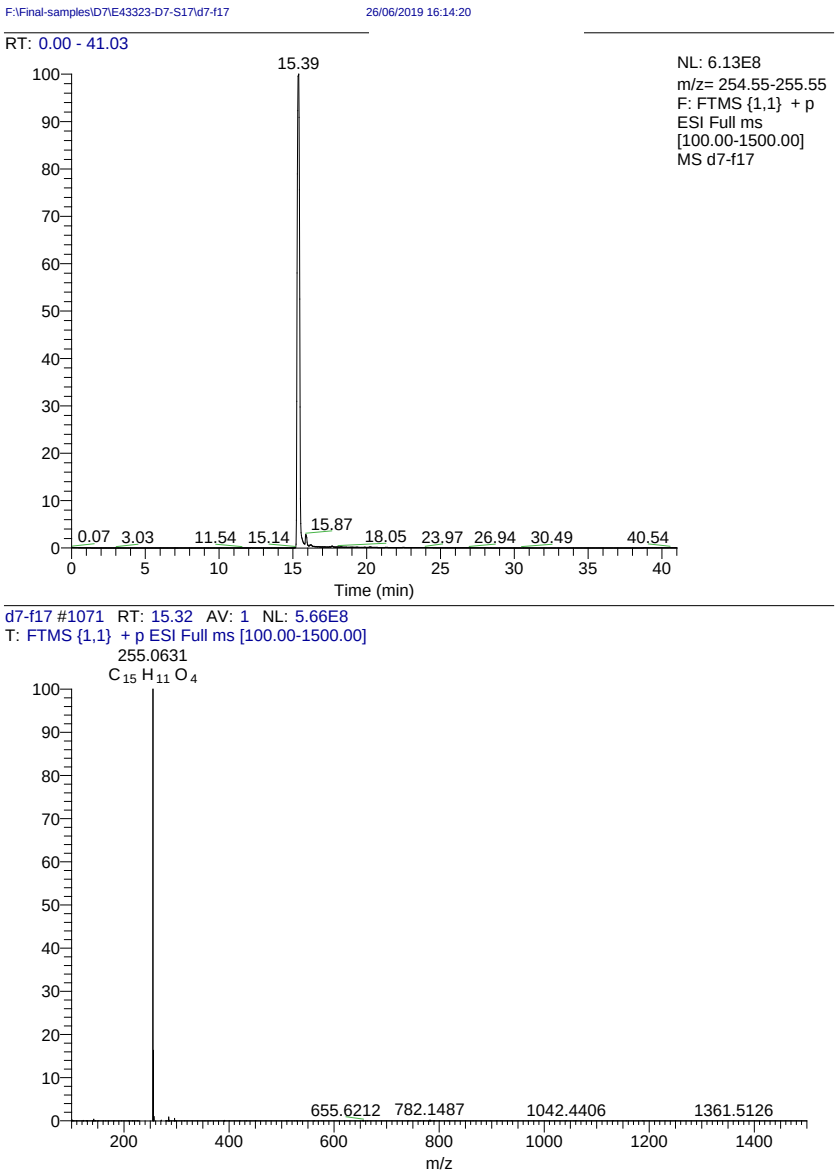

Figure 3-44: Extracted ion chromatogram and mass spectrum in positive ion mode for Chrysin

3.1.8.7 Characterisation of fraction D6-C1-H40-E60-SE-F8 as Apigenin (8)

The negative mode HRESI-MS spectrum of the compound gave a molecular ion $[M-H]^-$ at m/z 269.0454 (Calc for $C_{15}H_9O_5$, 269.0450) suggesting a molecular formula $C_{15}H_{10}O_5$. The compound in its proton spectrum showed a chelated hydroxyl proton at

δ_H 13.04 ppm typical of a 5-OH substituted flavonoid Figure 3-46. The presence of two meta coupled protons at δ_H 6.23, and 6.53 ppm completed the ring A substitution as in many 5, 7-dihydroxy substituted flavones. A pair of doublets at δ_H 7.05 and 7.97 ppm integrated for 2H each indicated a para-substituted benzene ring, and this must be on ring B of the flavonoid. The proton singlet observed at δ_H 6.66 is likely from the H-3 of the flavone. From all this data, the compound was inferred to be apigenin and from its 2D (COSY, HSQC and HMBC) spectra the structure was confirmed as follows: Long range (HMBC) couplings (^3J and ^2J) from the 5-OH proton identified C-5, C-6 and C-10, while correlations from H-3 identified C-2, C-1' and confirmed C-10 Figure 3-49. Other correlations and couplings were as expected; thus the compound was identified as 4', 5, 7-trihydroxyflavone (Apigenin) and confirmed by comparison of its NMR chemical shift assignments with literature reports (Bertelli et al., 2012). The chemical shifts for the protons and carbon atoms are given in Table 3-23. Apigenin was isolated from a crude chloroform extract of Moquinia kingie and was tested against *Trypanosoma cruzi* and was found to have activity against trypomastigotes in-vitro (Schinor et al., 2004).

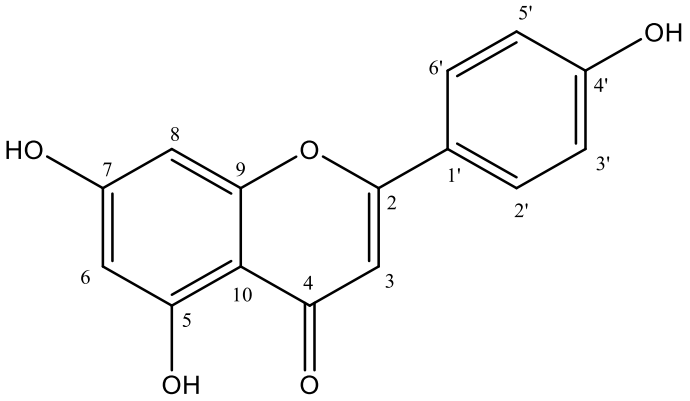

Figure 3-45: Chemical structure of Apigenin

Table 3-23: Chemical shifts for Apigenin

Position	**Apigenin**		Literature*	
	^{1}H δ ppm (mult, J in Hz)	^{13}C δ ppm, (mult)	^{1}H δ ppm, (mult, *J* in Hz)	^{13}C δ ppm, (mult)
1			-	-
2	-	163.7 (C)	-	164.59
3	6.66 (1H, s)	103.27 (CH)	6.75 (1H, s)	103.31
4	-	182.20 (C)		182.19
5	-	161.51 (C)	-	161.62
6	6.23 (1H, d)	99.4 (CH)	6.22 (d)	99.30
7	-	164.9 (C)		164.19
8	6.53 (1H, d)	94.57 (CH)	6.51(1H, d)	94.42
9	-	157.88 (C)	-	157.77
10	-	104.3 (C)	-	104.18
1`	-	131.2 (C)	-	121.66
2`	7.97 (1H, m)	128.43 (CH)	7.90 (1H, d)	128.90
3`	7.05 (1H, m)	115.96 (CH)	6.92 (1H, d)	116.41
4`	-	161.7 (C)	-	161.93

5`	7.05 (1H, m)	115.96 (CH)	6.92 (1H, m)	116.41
6`	7.97 (1H, m)	126.9 (CH)	7.90 (1H, m)	128.90
7-OH	10.90 (1H, s)	-	10.75 (s)	-
5-OH	13.04 (s)	-	12.96 (s)	-
4-OH			10.40 (s)	

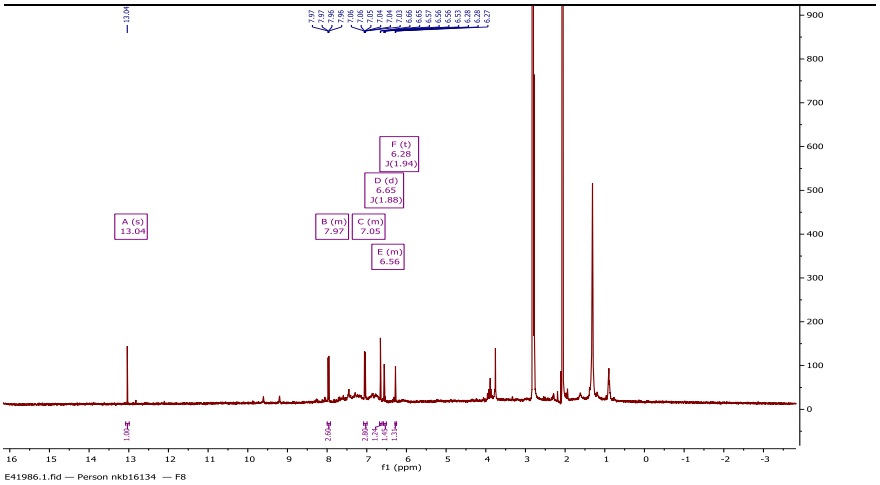

Figure 3-46: ^{1}H NMR (400 MHz) of Apigenin in Acetone d_6

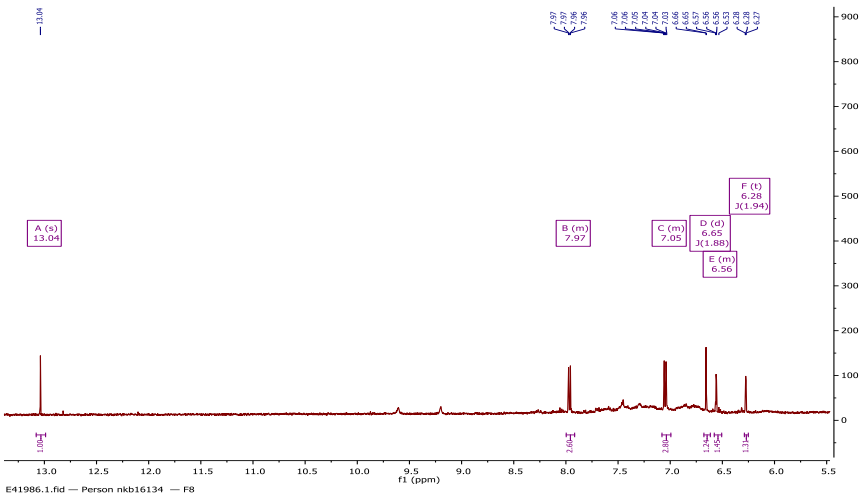

Figure 3-47: Selected ^{1}H NMR spectrum expansion of Apigenin in Acetone d_6

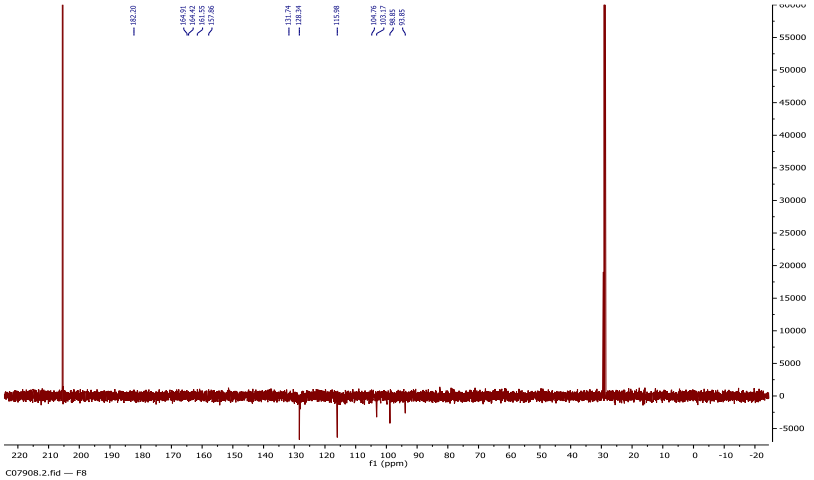

Figure 3-48: ^{13}C NMR (400 MHz) of Apigenin in Acetone d_6

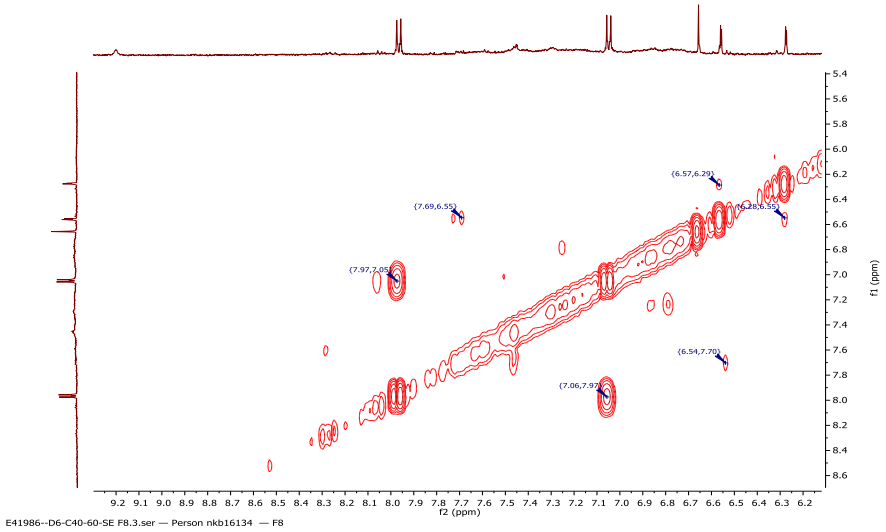

Figure 3-49: COSY spectrum (400 MHz) of Apigenin in Acetone d_6

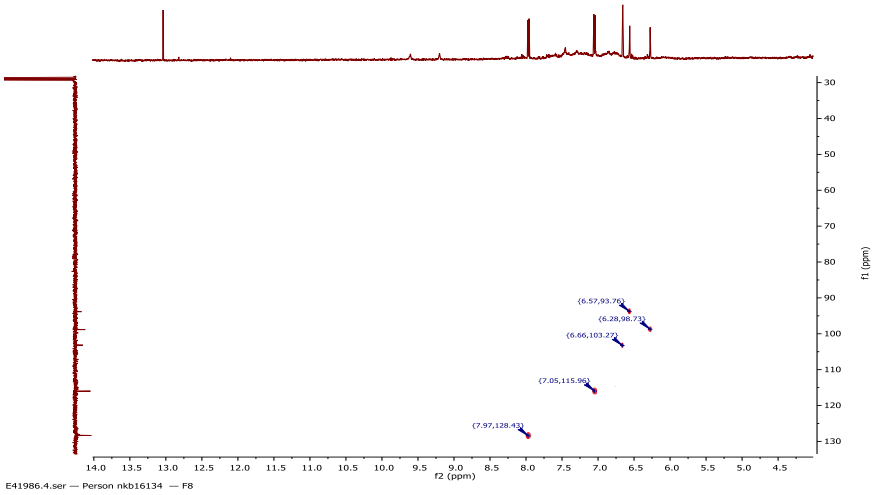

Figure 3-50: HSQC spectrum (400 MHz) of Apigenin in Acetone d_6

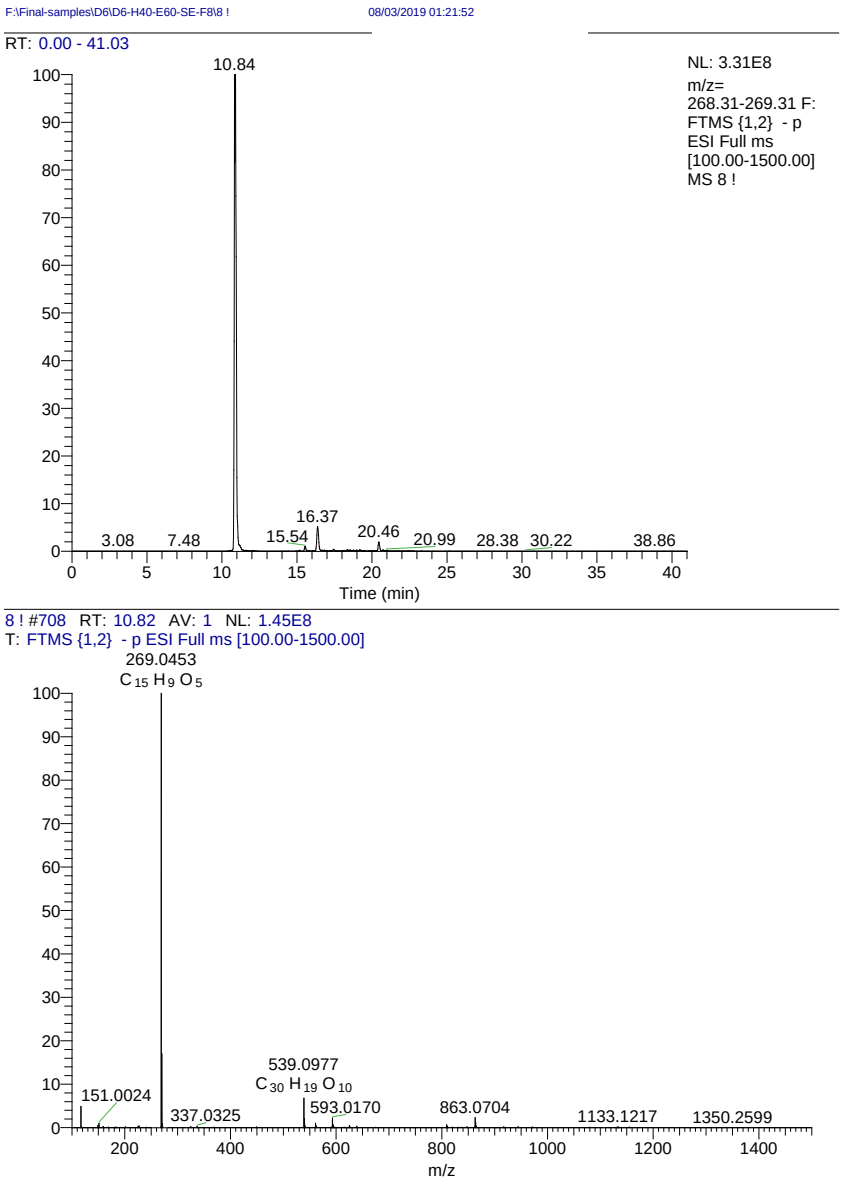

Figure 3-51: Extracted ion chromatogram and mass spectrum in negative ion mode for Apigenin.

3.1.8.8 Characterisation of fraction F1 VLC C60-40-C20-25 as Pinostrobin (9)

The compound was obtained as a dark yellow solid from column chromatography and Sephadex LH20. The positive mode HRESI-MS spectrum of the compound gave a molecular ion $[M+H]^+$ at m/z 271.0939 (Calc for $C_{16}H_{15}O_4$, 271. 0970) suggesting a

molecular formula of $C_{16}H_{14}O_4$. The proton spectrum of the compound showed signals for a deshielded and oxygenated methine doublet of doublets at δ_H 5.43 for H-2 and two other aliphatic protons at 2.83 and 3.09 ppm for H-3. Two meta coupled aromatic protons H-6 and H-8 appeared as doublets at δ 6.08 and 6.07 ppm. Five other aromatic proton signals for an unsubstituted benzene ring were observed at δ 7.41 (H-2',6'), 7.45 (H-3', H-5' and H-4') Figure 3-53. A set of methoxy protons was observed at 3.81 ppm. The ^{13}C-NMR spectrum showed signals for 16 carbons including one carbonyl at δ_C 196.5 (C-4), two aromatic CH at 95.4.0 (C-6) and 94.4 (C-8), two aliphatic carbons at 79.4 (C-2) and 43.8 (C-3) and one methoxy carbon at 55.8 ppm (7-OCH_3) Figure 3-54. The remaining carbons signals were attributed to an unsubstituted benzene ring and four quarternary aromatic carbons. Analysis of its 2D spectra identified the compound to be a substituted pinocembrin, and precisely Pinostrobin and the structure was confirmed using literature reports (Bertelli et al., 2012). The chemical shifts for the protons and carbon atoms are given in Table 3-24.

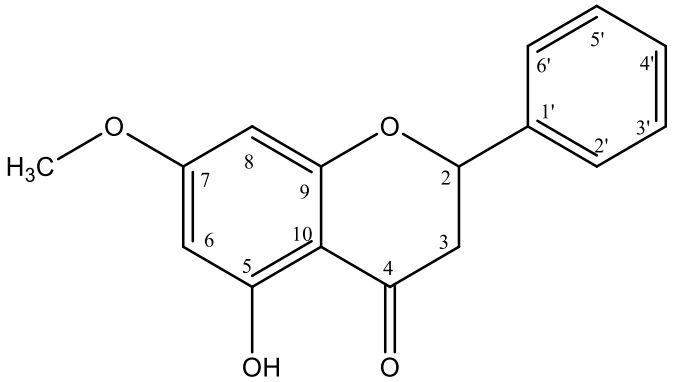

Figure 3-52: Chemical structure of Pinostrobin

Table 3-24: Chemical shifts for Pinostrobin

Position	**Pinostrobin**		Literature*	
	^{1}H δ ppm (mult, J in Hz)	^{13}C δ ppm, (mult)	^{1}H δ ppm, (mult, J in Hz)	^{13}C δ ppm, (mult)
1	-	-	-	-
2	5.43 (1H, dd, 13.0, 3.1)	79.4 (CH)	5.62(dd)	79.03
3a	2.83 (1H, dd, 17.2, 3.0)	43.8 (CH_2)	2.83 (dd)	42.63
3b	3.09 (1H, dd, 17.1, 3.1)		3.29(dd)	
4	-	196.5 (C)	-	196.92
5	-	161.4 (C)	-	163.71
6	6.08 (1H, d, 2.2)	95.4(CH)	6.00 (1H, d, *J* = 2.2)	95.24
7	-	168.3 (C)	-	167.94
8	6.07 (1H, d, 2.2)	94.4 (CH)	6.04 (1H, d, *J* = 2.2)	94.34
9	-	163.0 (C)	-	163.09
10	-	103.2(C)	-	103.10
1`	-	138.5 (C)	-	138.99
2`	7.45 (1H, m)	126.3 (CH)	-	127.06

3`	7.41 (1H, m)	129.0 (CH)	7.44 (5H, m)	129.06
4`	7.41 (1H, m)	129.0 (CH)		129.06
5`	7.41 (1H, m)	129.0 (CH)		129.06
6`	7.45 (1H, m)	126.3 (CH)		127.06
7-OCH_3	3.81 (3H, s)	55.8 (CH_3)	3.80(s)	56.33
5-OH	12.02 (s)	-	12.12 (1H, s)	-

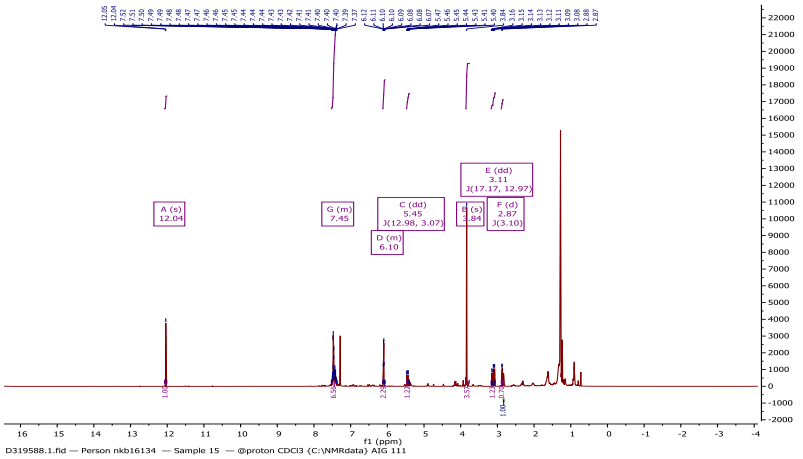

Figure 3-53: ^{1}H NMR (400 MHz) of Pinostrobin in $CDCl_3$

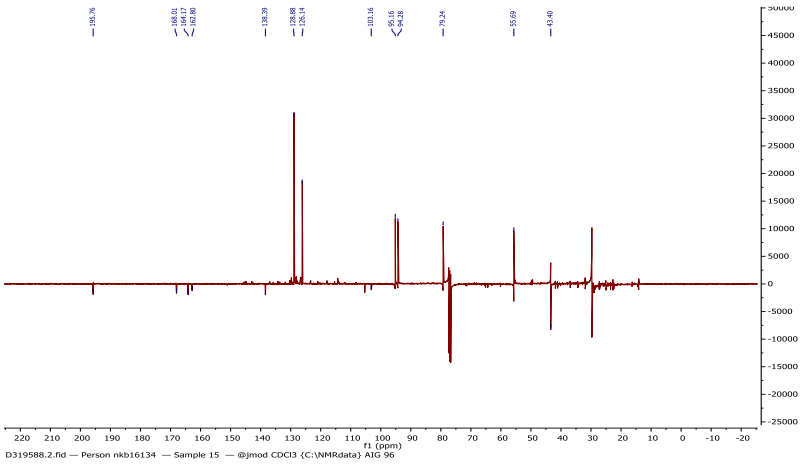

Figure 3-54: ^{13}C NMR (400 MHz) of Pinostrobin in $CDCl_3$

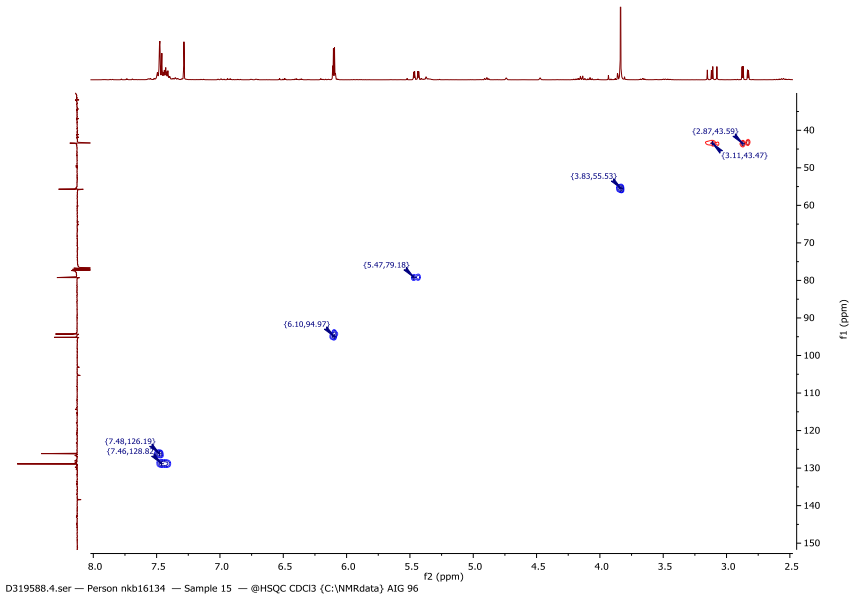

Figure 3-55: HSQC spectrum (400 MHz) of Pinostrobin in $CDCl_3$

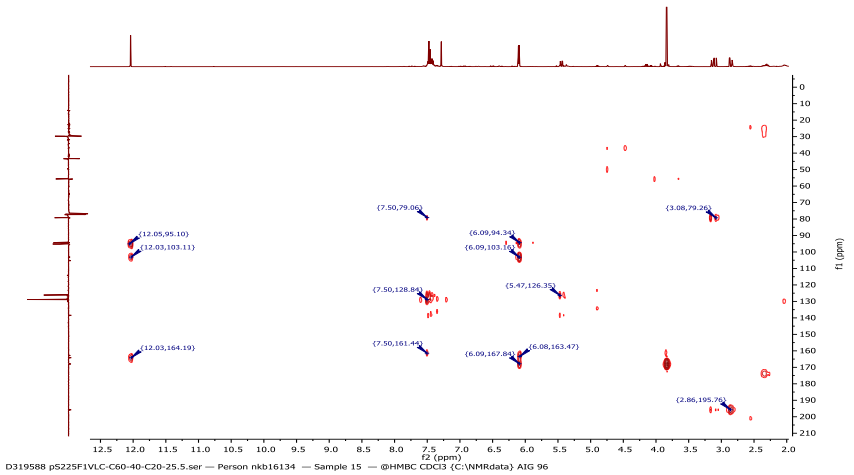

Figure 3-56: HMBC spectrum (400 MHz) of Pinostrobin in $CDCl_3$

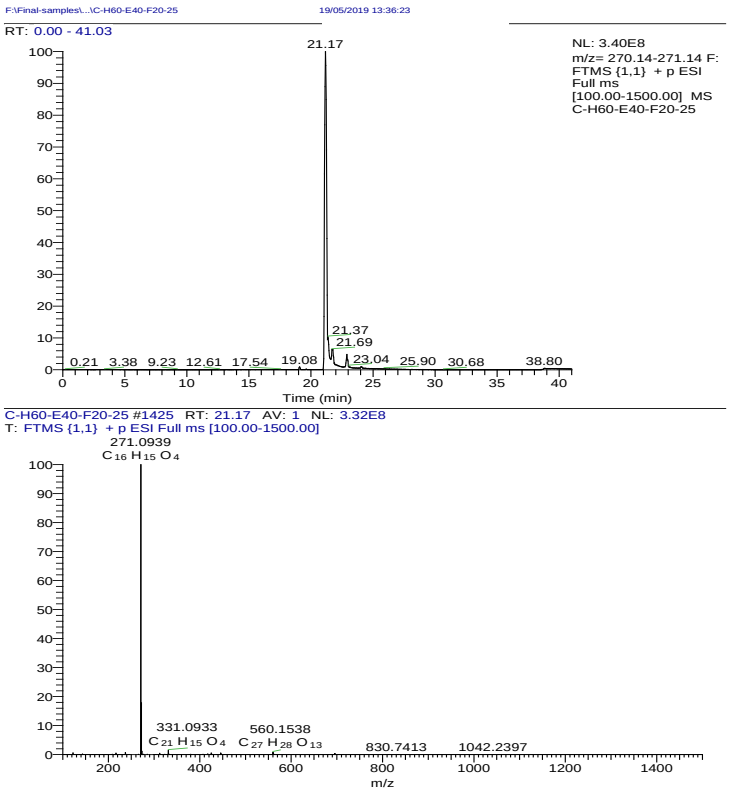

Figure 3-57: Extracted ion chromatogram and mass spectrum in positive ion mode for Pinostrobin

3.1.8.9 Characterisation of fraction F1 VLC C20-80-C30-33 as Cinnamic acid (10)

The compound was obtained as a dark yellow solid from column chromatography and Sephadex LH20. The positive mode HRESI-MS spectrum of the compound gave a molecular ion $[M+H]^+$ at m/z 149.0587 (Calc for ($C_9H_9O_2$), 149. 0602) suggesting a molecular formula of $C_9H_8O_2$. The proton spectrum showed the presence of two trans coupled olefinic protons and a 5H multiplet indicating an unsubstituted phenyl ring in the compound Figure 3-59. It was typical of a phenylpropanoid and was identified as cinnamic acid and confirmed by literature reports (Bertelli et al., 2012). The chemical shifts for the protons and carbon atoms are given in Table 3-25

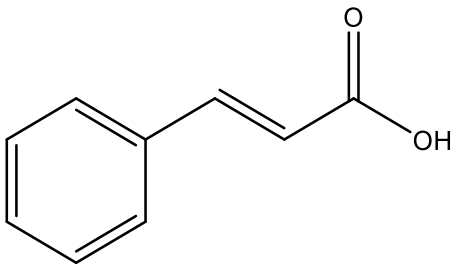

Figure 3-58: Chemical structure of Cinnamic acid.

Table 3-25: Chemical shifts for Cinnamic acid

Position	**Cinnamic acid**		Literature*	
	^1H δ ppm (mult, J in Hz)	^{13}C δ ppm, (mult)	^1H δ ppm, (mult, J in Hz)	^{13}C δ ppm, (mult)
1	-	171.8	-	168.00

2	6.46 (1H, d)	117.4 (CH)	6.53(d)	119.70
3	7.79 (1H, d)	147.2(CH)	7.59(d)	144.38
1’	-	134.2(C)	-	134.70
2’	7.58(1H, m)	128.4 (CH)	7.68(m)	128.65
3’	7.44 (1H, m)	129.0 (CH)	7.42(m)	129.36
4’	7.43(1H, m)	131.4(CH)	7.42(m)	130.67
5’	7.44 (1H, m)	129.0 (CH)	7.42(m)	129.36
6’	7.5(1H, m)	128.4 (CH)	7.68(m)	128.65
1-COOH	-	-	12.39(s)	-

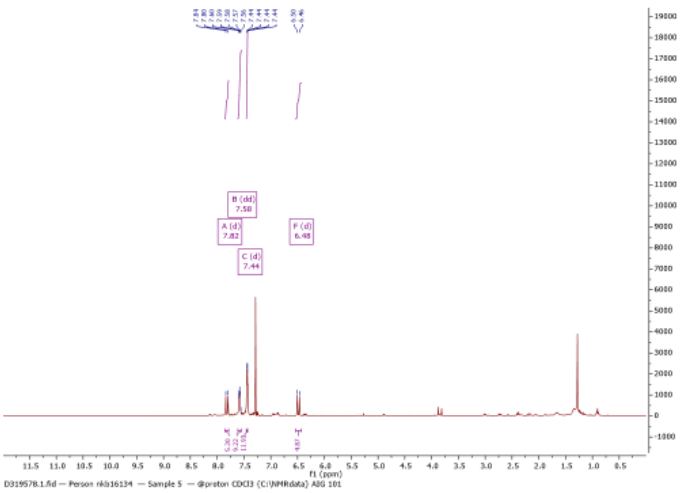

Figure 3-59: ^{1}H NMR (400 MHz) of Cinnamic acid in $CDCl_3$

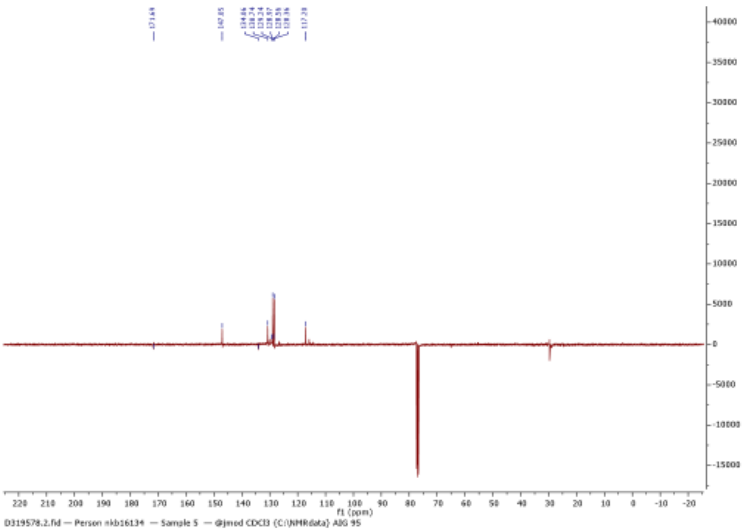

Figure 3-60: ^{13}C NMR (400 MHz) of Cinnamic acid in $CDCl_3$

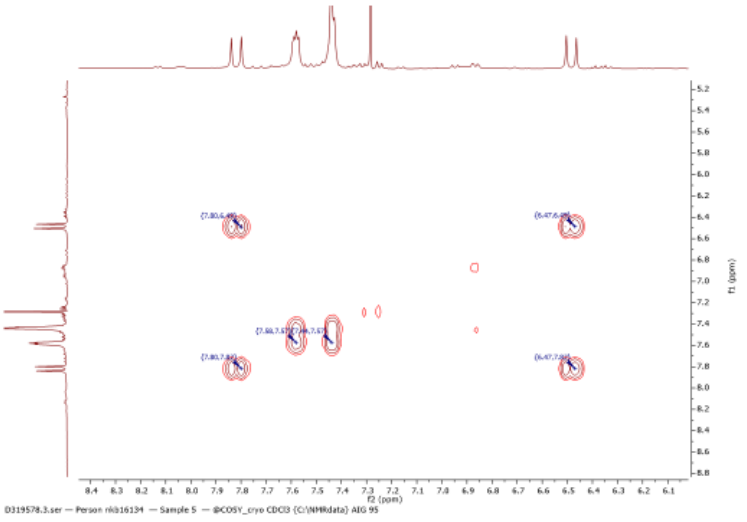

Figure 3-61: Selected HMBC spectrum expansion of Cinnamic acid in $CDCl_3$

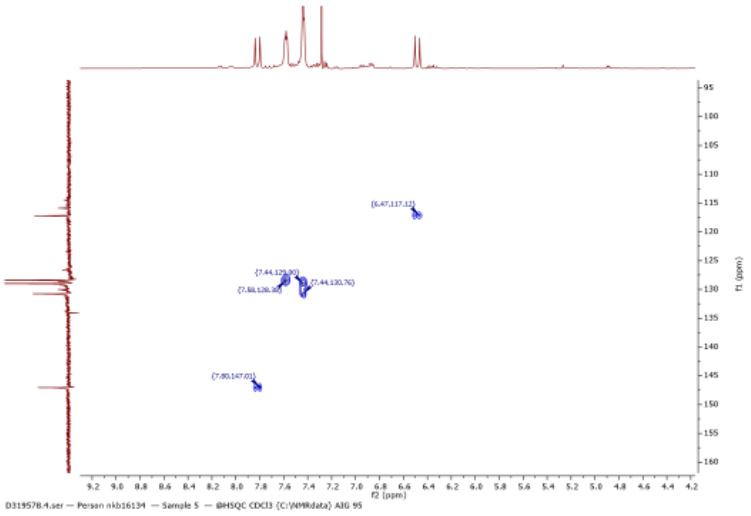

Figure 3-62: Selected HSQC spectrum expansion of Cinnamic acid in $CDCl_3$

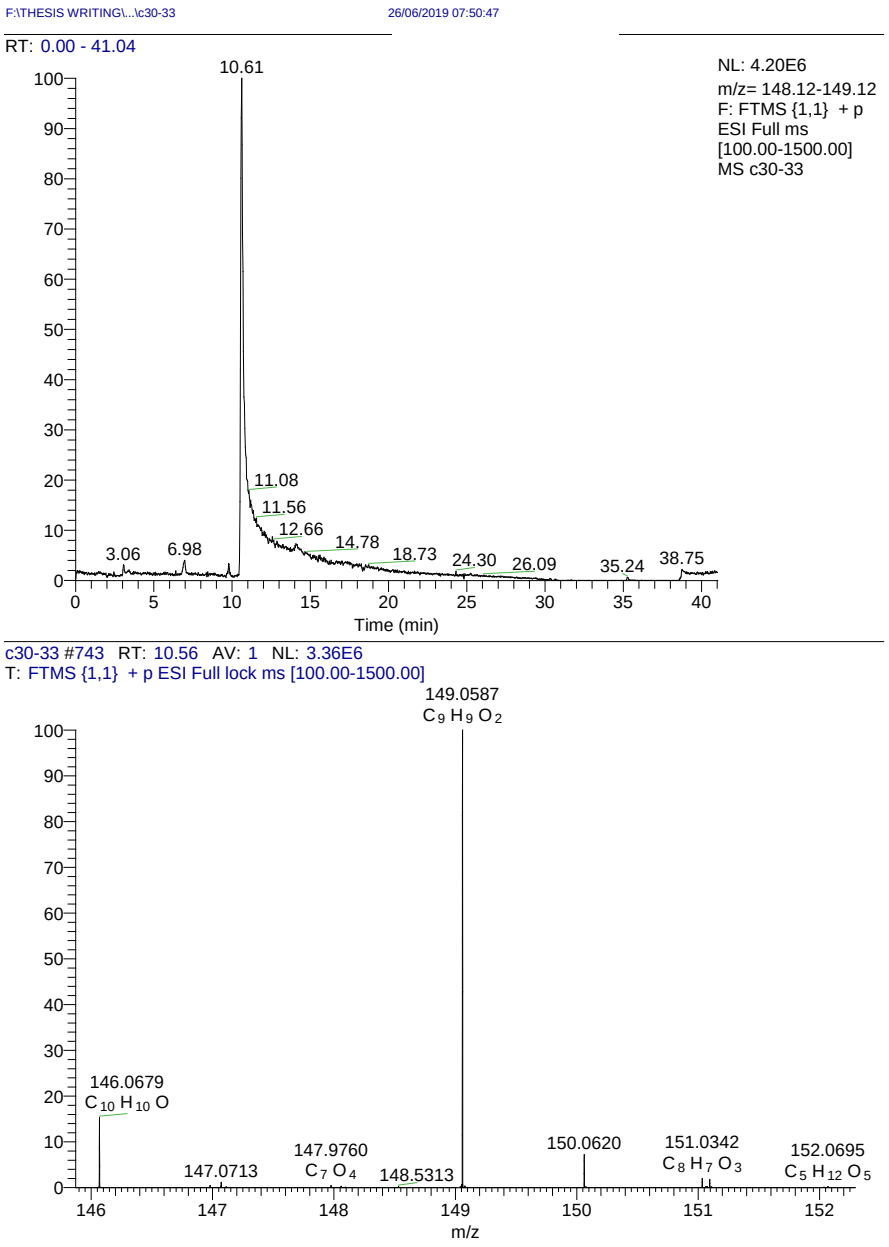

Figure 3-63: Extracted ion chromatogram and mass spectrum in positive ion mode for Cinnamic acid.

3.1.8.10 Characterisation of fraction F1 VLC C1H40-E60-C10-12 as Coumaric acid cinnamyl ester (11a)

The compound was obtained as a yellow solid following purification by column chromatography and Sephadex LH20. The negative mode HRESI-MS spectrum gave a molecular ion $[M-H]^-$ at m/z 279.0998 (Calc for $C_{18}H_{15}O_3$, 279.102120) suggested for a molecular formula of $C_{18}H_{16}O_3$. The compound's proton spectrum (400 MHz, $CDCl_3$) showed the presence of two aromatic doublets at δ_H 6.88 (2H, d, *J* = 8.6) and 7.44 ppm (2H, d, *J* = 8.6, H). Two trans ethylenic protons were observed at 6.35 (1H, d, *J* = 16.0) and 7.71 ppm (1H, d, *J* = 16.0) and at 6.72 (1H, d, *J* = 16.0) and 6.73 (1H, d, *J* = 16.0). There were two sets of aromatic protons (integrated for 5H) between 7.36 and 7.41 ppm for a mono-substituted phenyl ring Figure 3-65. The ^{13}C-NMR spectrum also showed an ester carbonyl signal at δ_C 167.7 ppm (C-1), four olefinic carbons and twelve aromatic carbon signals as well as an aliphatic oxygenated methylene carbon at 65.3 ppm (C-1′) Figure 3-66. The compound was identified as 4-hydroxycinnamic acid (p-coumaric acid) cinnamyl ester or coumaric acid cinnamyl ester, and its NMR spectral data were in agreement with literature reports (Lee et al., 2014). The chemical shifts for the protons and carbon atoms are given in Table 3-26.

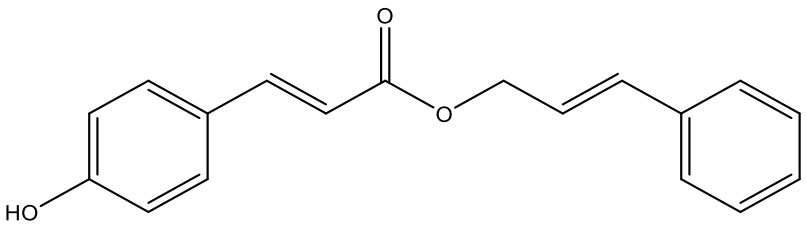

Figure: 3-64 Chemical structure of Coumaric acid cinnamyl ester.

Table 3-26: Chemical shifts for Coumaric acid cinnamyl ester

Position	**Coumaric acid cinnamyl ester**		Literature*	
	^{1}H δ ppm (mult, J in Hz)	^{13}C δ ppm, (mult)	^{1}H δ ppm, (mult, *J* in Hz)	^{13}C δ ppm, (mult)
1	-	167.7 (C)	-	167.3
2	6.35 (1H, d)	114.9 (CH)	6.33 (1H, d, *J* = 15.8)	115.5
3	7.71 (1H, d)	145.4 (CH)	7.67(1H, d, *J* = 15.8)	144.9
4	-	126.86 (C)	-	128.1
5	7.44 (1H, 2.3)	130.1 (CH)	7.44 (1H, d,8.2)	130.1
6	6.88 (1H, d)	116.0 (CH)	6.85 (1H, d, *J* = 8.2)	116.0
7	-	158.24 (C)	-	157.8
8	6.88 (1H, d)	116.0 (CH)	6.85 (1H, d, *J* = 8.2)	116.0
9	7.44 (1H, 2.3)-	130.1 (CH)	7.44 (1H, d, *J* = 8.2)	130.1
1`a 1`b	4.91 (2H, d)	65.3 (CH_2)	4.86 (2H, d, *J* = 6.2)	65.1
2`	6.37 (1H, d)	123.24 (C)	6.34 (1H, m)	123.5

3`	6.72 (1H, d)	134.38 (CH)	6.70 (1H, d, *J* = 15.8)	134.2
4`	-	136.2 (C)		136.4
5`	7.41 (1H, d)	126.66 (CH)	7.41 (1H, d, *J* = 7.6)	126.7
6`	7.36 (1H, d)	128.55 (CH)	7.34 (1H, d, *J* = 7.6)	128.7
7’	7.29 (1H, m,)	128.3 (CH)	7.25 (1H, m,)	128.7
8`	7.36 (1H, d)	128.55 (CH)	7.34(1H, d, *J* = 7.6)	128.7
9`	7.41 (1H, d)	126.66 (CH)	7.41(1H, d, *J* = 7.6)	126.7
7-OH	-	-	-	-

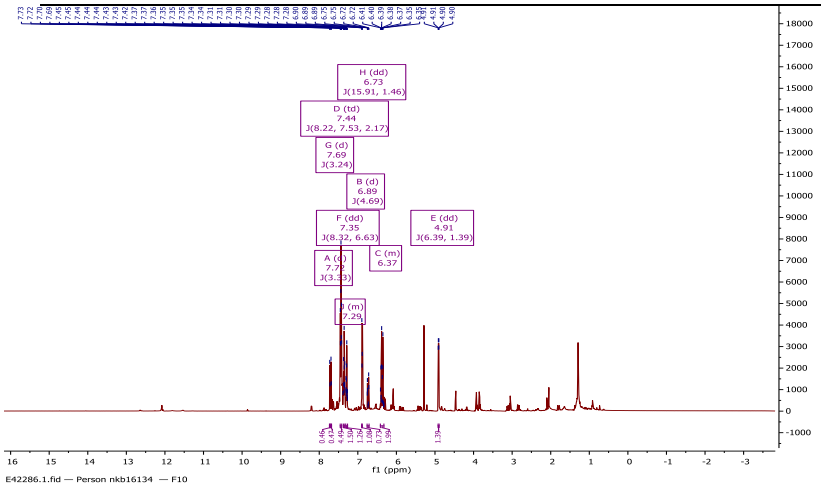

Figure 3-65: ^{1}H NMR (400 MHz) of Coumaric acid cinnamyl ester in $CDCl_3$

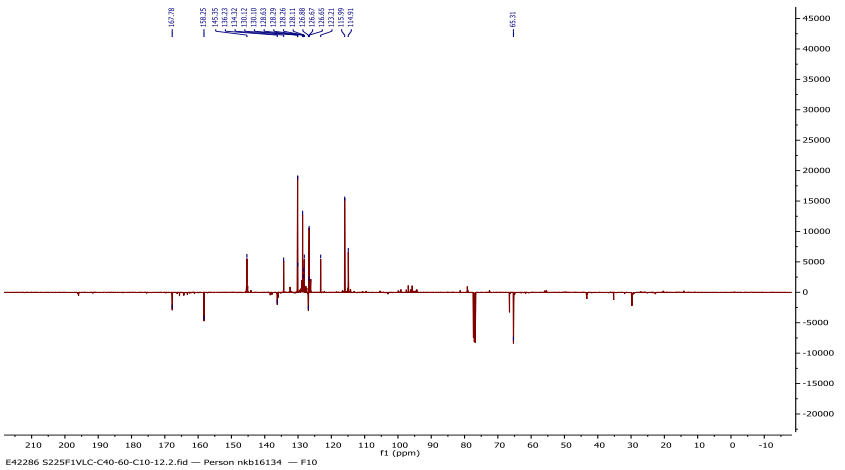

Figure 3-66: ^{13}C NMR (400 MHz) of Coumaric acid cinnamyl ester in $CDCl_3$

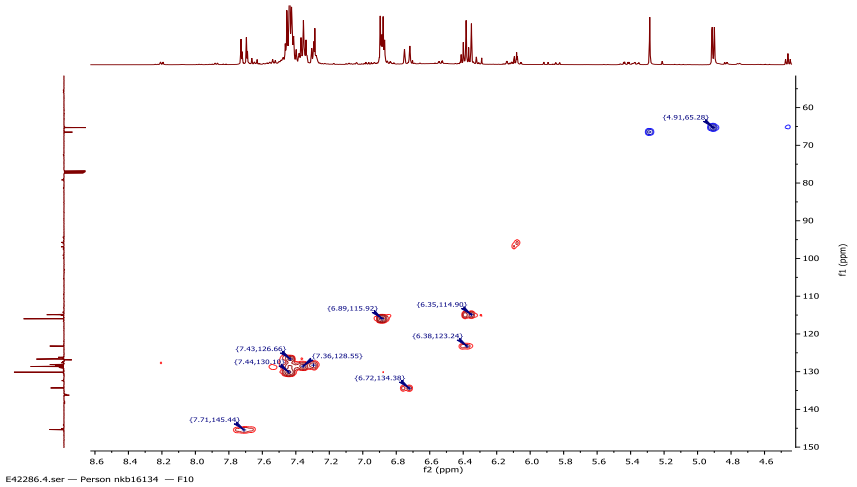

Figure 3-67: Selected HSQC spectrum expansion of Coumaric acid cinnamyl ester in $CDCl_3$

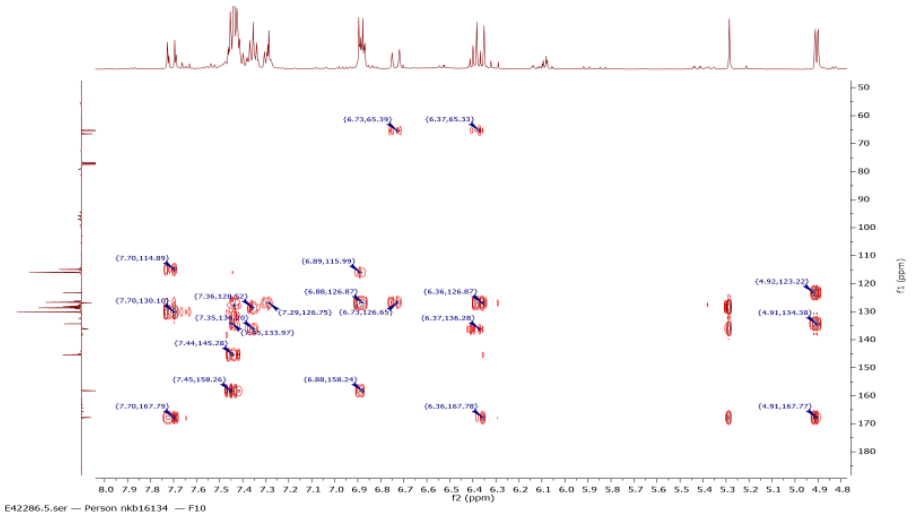

Figure 3-68: Selected HBMC spectrum expansion of Coumaric acid cinnamyl ester in $CDCl_3$

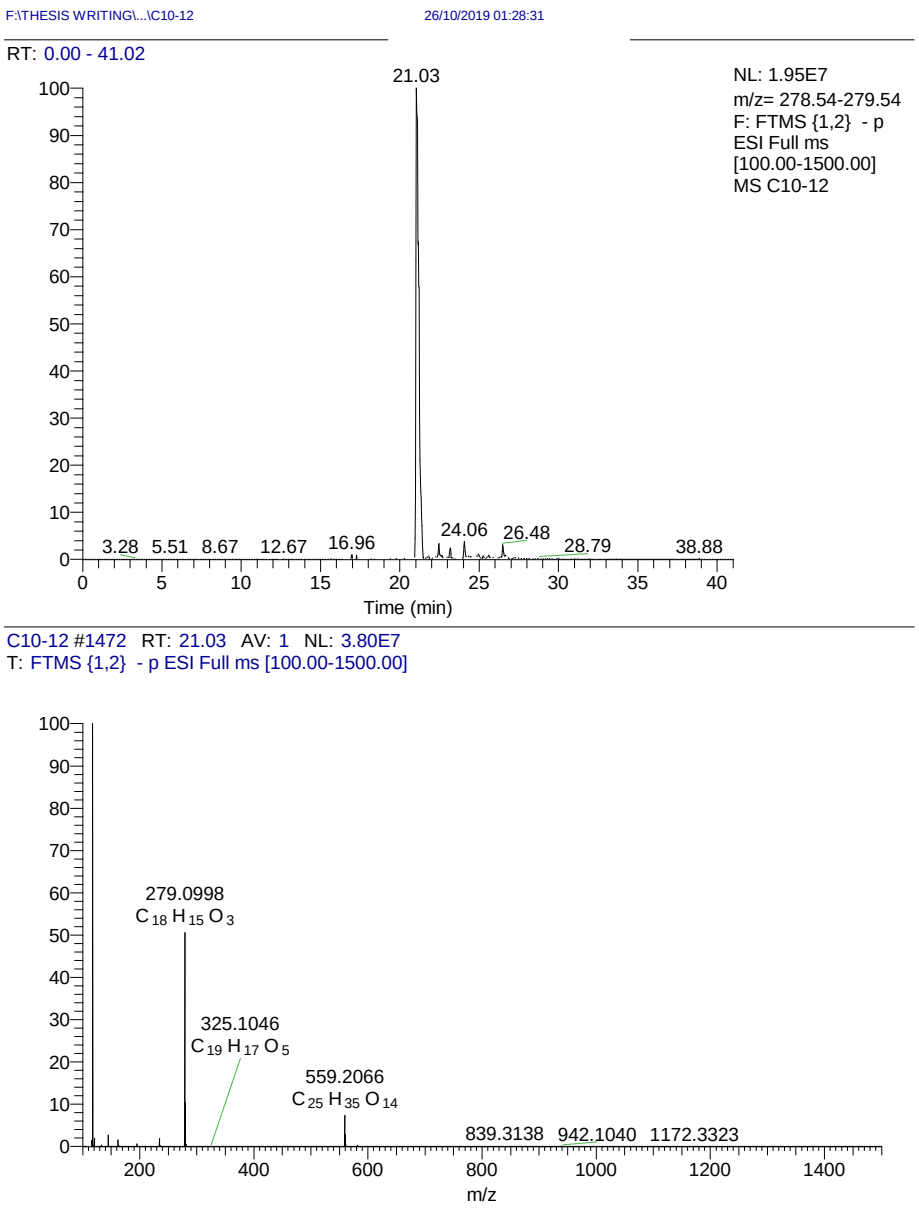

Figure 3-69: Extracted ion chromatogram and the mass spectrum in the negative ion mode for Coumaric acid cinnamyl ester

3.1.8.11 Characterisation of fraction F1 VLC C1H40-E60-C10-12 as Coumaric acid benzyl ester (11b)

The compound was obtained as a light-yellow powder after purification column chromatography and Sephadex LH20. The positive mode HRESI-MS spectrum of the compound gave a molecular ion $[M+H]^+$ at m/z 255.0996 (Calc for $C_{16}H_{15}O_3$, 255.

1021). suggesting a molecular formula of $C_{16}H_{14}O_3$. The compound's proton spectrum was similar to that of p-coumaric acid but with an extra mono-substituted phenyl ring and a set of methylene protons. The compound's proton (400 MHz, $CDCl_3$) spectrum had two aromatic doublets at δ_H 6.88 (2H, d, *J* = 8.6, H-6,8) and 7.44 ppm (2H, d, *J* = 8.6, H-5,9). Two trans coupled olefinic protons were observed at 6.34 (1H, d, *J* = 16.0, H-2) and 7.67 ppm (1H, d, *J* = 16.0, H-3). Also observed were multiplets for 5H aromatic protons between 7.29 and 7.43 ppm (indicating a mono-substituted phenyl ring) and a singlet for two methylene protons at 5.29 ppm Figure 3-71. The ^{13}C-NMR spectrum also showed an ester carbonyl signal at δ_C 167.7 ppm (C-1), two olefinic carbons at 114.9 and 145.4, two aromatic CH signals at 130.1 (C-5 and C-9), 116.0 (C-6 and C-8) and a phenolic quaternary aromatic carbon at 158.2 ppm. There were also signals for six other aromatic carbons and one oxygenated methylene carbon at 66.5 ppm Figure 3-72. The compound was identified as 4-hydroxycinnamic acid (p-coumaric acid) benzyl ester, and its NMR spectral data were in agreement with literature reports (Lee et al., 2014). The chemical shifts for the protons and carbon atoms are presented in Table 3-27.

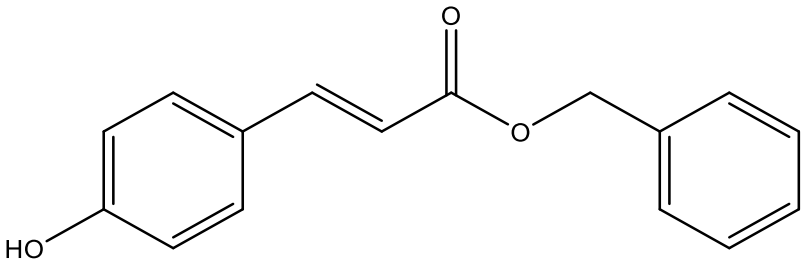

Figure 3-70: Chemical structure of Coumaric acid benzyl ester.

Table 3-27: Chemical shifts for Coumaric acid benzyl ester

Position	**Coumaric acid benzyl ester**		Literature*	
	^{1}H δ ppm (mult, J in Hz)	^{13}C δ ppm, (mult)	^{1}H δ ppm, (mult, *J* in Hz)	^{13}C δ ppm, (mult)
1	-	167.7 (C)	-	167.4
2	6.35 (1H, d)	114.9 (CH)	6.34 (1H, d, *J* = 15.8 Hz)	115.2
3	7.70 (1H, d)	145.4 (CH)	7.67(1H, d, J= 15.8Hz)	145.0
4	-	126.9 (C)	-	127.1
5	7.44 (1H, d)	130.1 (CH)	7.42 (1H, d,8.2Hz)	130.0
6	6.88 (1H, d)	116.0 (CH)	6.83 (1H, d, *J* = 8.2Hz)	115.9
7	-	158.2 (C)	-	157.8
8	6.88 (1H, d)	116.0 (CH)	6.83 (1H, d, *J* = 8.2Hz)	115.9
9	7.44 (1H, d)	130.1 (CH)	7.42 (1H, d,8.2Hz)	130.0
1`a 1`b	5.29 (2H, s)	66.5 (CH_2)	5.25 (2H, d,6.2Hz)	66.1
2`	-	136.0 (C)		136.1

3`	7.43 (1H, d)	126.7 (CH)	7.30 (1H, d, *J* =7.6Hz)	128.2
4`	7.36 (1H, d)	128.6 (CH)	7.34 (1H, d, *J* =7.6Hz)	128.7
5`	7.29 (1H, m,)	128.3 (CH)	7.28 (1H, m,)	128.7
6`	7.36 (1H, d)	128.55 (CH)	7.34 (1H, d, *J* =7.6Hz)	128.7
7’	7.43 (1H, d)	126.66 (CH)	7.40 (1H, d, *J* =7.6Hz)	128.6
7-OH	-	-	-	-

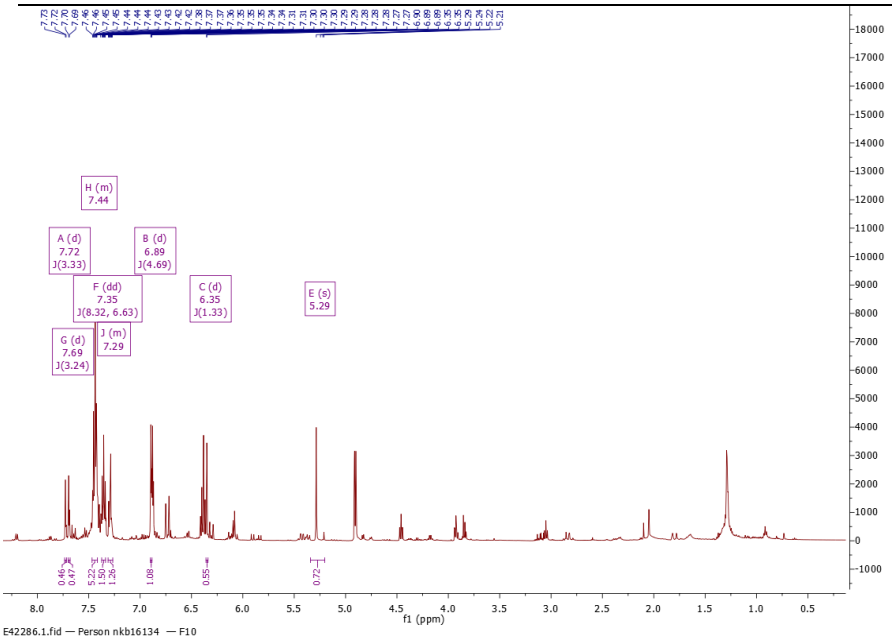

Figure 3-71: ^{1}H NMR (400 MHz) of Coumaric acid benzyl ester in $CDCl_3$

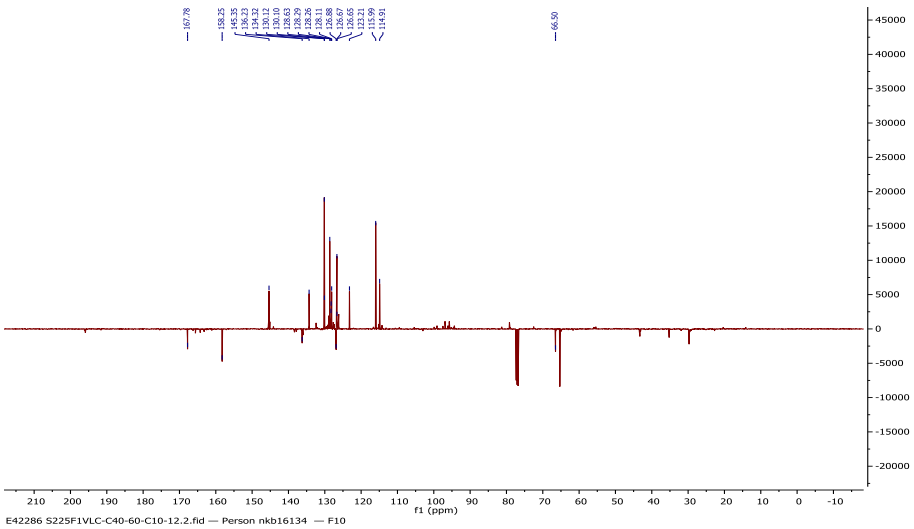

Figure 3-72: ^{13}C NMR (400 MHz) of Coumaric acid benzyl ester in $CDCl_3$

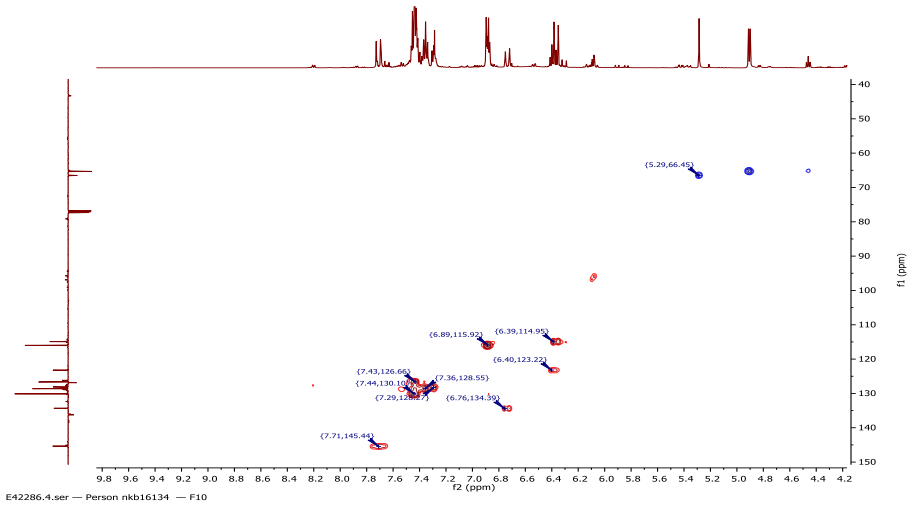

Figure 3-73: Selected HSQC spectrum expansion of Coumaric acid benzyl ester in $CDCl_3$

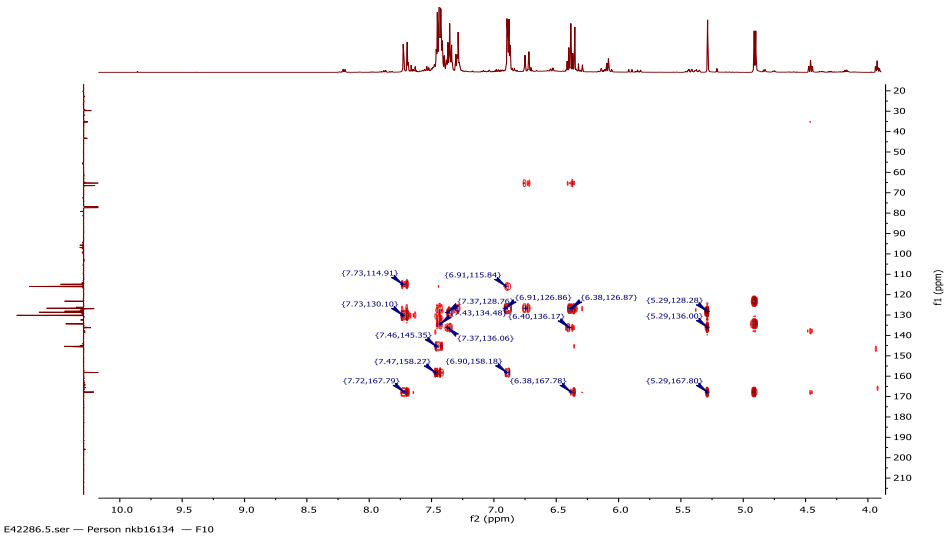

Figure 3-74: Selected HBMC spectrum expansion of Coumaric acid benzyl ester in $CDCl_3$

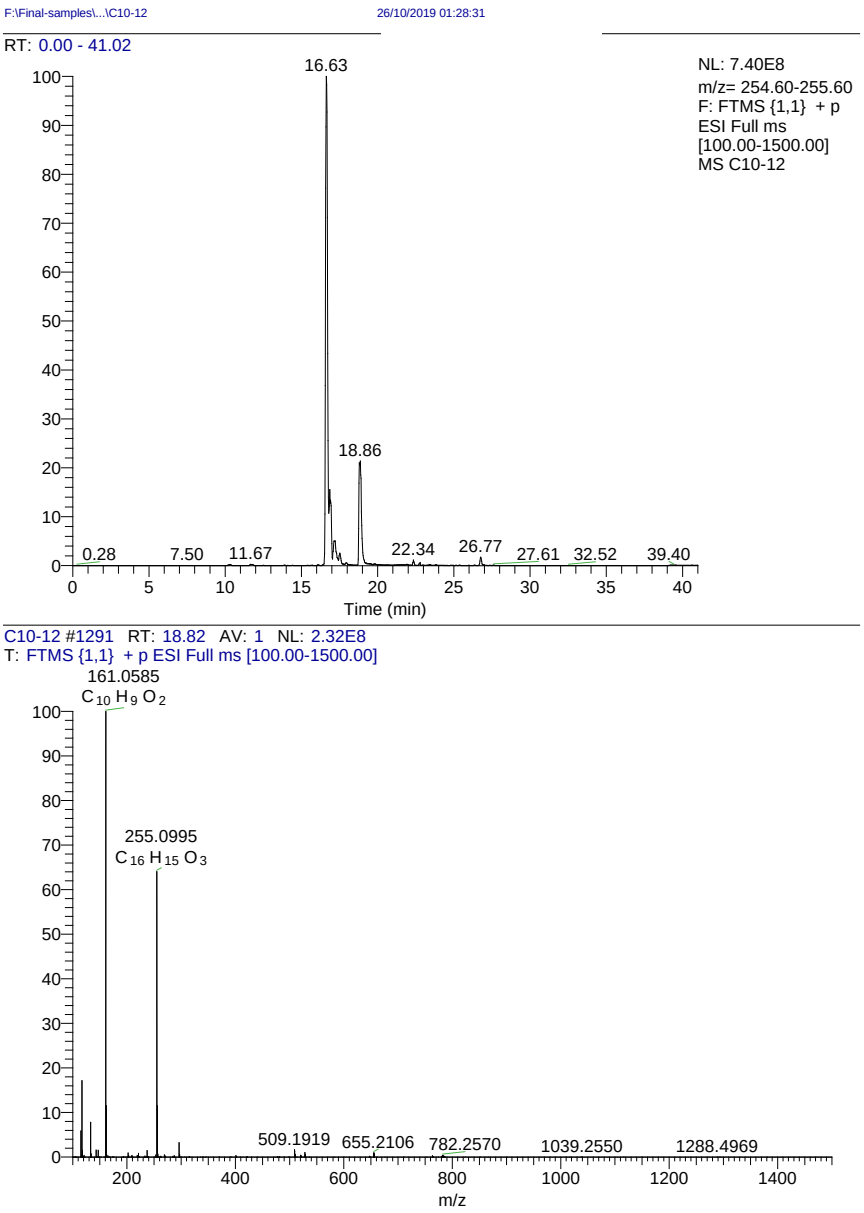

Figure 3-75: Extracted ion chromatogram and mass spectrum in positive ion mode for Benzyl p-coumarate

3.1.9 Biological activity for the UK propolis

3.1.9.1 Testing the biological activity of the crude propolis samples from the UK

Propolis samples S224, S225, D6 and D7, their fractions and the pure compounds isolated from them were subjected to biological screening. The results for these tests showed some significant activity against different parasites such as *Trypanosoma brucei*, *T. b. brucei ISMR1*, *T. congolense*, *Crithidia fasiculata*, *Leishmania mexicana* and *Mycobacterium marinum*. Additionally, the crude samples were tested against Staphylococcus aureus. Also, the cytotoxicity activity was assessed for all crude samples and pure compounds isolated against human cell lines.

3.1.9.1.1 Antibacterial determination of UK propolis samples against *S. aureus*

The antibacterial activity of ethanolic extract of the UK propolis samples against *S. aureus* was tested as described in section 2.6 and the results of screening of four samples S224, S225, D6 and D7 are shown in Table 3-28. As shown at two high concentrations 500 µg/mL and 250 µg/mL of ethanolic extract of the UK propolis samples all samples had some activity against *S. aureus* but did not display activity at 125µg/mL. Thus, the antibacterial potential of the propolis was relatively uninteresting.

Table 3-28: Antibacterial activity crude propolis sample extracts from UK against *S. aureus.*

Sample ID	Sample Conc		
	500 µg/mL	**250 µg/mL**	**125 µg/mL**
	Cell viability (% of control)		
S224	11.3	10.2	102.4
S225	14	8.4	107.8
D6	12.9	10.2	103.9
D7	10.5	8.9	103.6

3.1.9.2 In-vitro anti-trypanosomal activity of S224, S225, D6 and D7 against *T. brucei* (S427)

The assessment of the anti-trypanosomal activity of the crude extracts using an Alamar blue™ 96 well microplate assay as described in (Räz *et al*., 1997), was carried out by Mr.Ibrahim Alfayes, Glasgow University.

EEP of the UK propolis samples were tested against *T. brucei* (s427) in comparison with Pentamidine as drug control, and the EC_{50} values calculated. The results showed that the four-samples exhibited significant variable activity against *T. brucei* except for sample S225, which showed moderate activity against *T.brucei* with EC_{50} >10 µg/mL. The crude samples S224, D6 and D7, had significant variable activity against *T. brucei* with EC50 values of 5.28, 4.49, and 5.97µg/mL, respectively, as shown Table 3-29.

Table 3-29: EC_{50} (µg/mL) (n=3) of crude extracts of the UK propolis on Tb S427WT and B48

Exp code	Type of sample	Tb S427WT		B48			
		AVR	**SEM**	**AVR**	**SEM**	**RF**	**T-TEST**
S224	Extract crude	5.28	0.51	4.7	0.31	0.89	0.395
S225	Extract crude	14.04	0.13	10.6	1.64	0.75	0.102
D6	Extract crude	4.49	0.22	3.0	0.20	0.66	0.007
D7	Extract crude	5.97	0.17	4.6	0.26	0.78	0.013
Pentamidine(µM)		0.0027	3.90E-04	0.6	0.01	226.61	5.63E-07

* 1: **T.b. S427 WT** = *Trypanosoma brucei brucei* s427 wild type *Trypanosoma brucei brucei T.b*. S427 WT = *Trypanosoma brucei brucei* s427 wild type *Trypanosoma brucei brucei*

B48 = A resistant strain, which was derived from a *Trypanosoma brucei brucei* amino purine transporter-1 knockout (TbAT1-KO) strain after increased exposure to pentamidine and lacks both the TbAT1/P2 transporter and the high-affinity pentamidine transporter (HAPT), hence becomes highly resistant (>200 fold) to pentamidine.

Pentamidine is a standard veterinary drug used as a control in this assay.

P<0.005 = significant

EC_{50} values are found in µM for pentamidine, and as µg/mL for the propolis compounds, and calculate the average and SEM of 3 independent experiments. The unpaired t method tests. Statistical significance was determined comparing the EC_{50} value of the resistant strain with that of the same sample for the control strain s427. **RF**: resistance factor, being the EC_{50} value for the resistant strain divided by the EC_{50} value for the control (sensitive) strain.

3.1.9.3 In-vitro Cytotoxicity assay of S224, S225, D6 and D7 samples.

Toxic activity against the human cell line (THP cells) was assessed for the UK crude samples S224, S225, D6 and D7 to evaluate their cytotoxicity and to determine EC_{50} values(µg/mL). The recorded EC_{50} values are as shown in Table 3-30. The crude extracts of S224, D6 and D7, showed moderate cytotoxicity against the THP cells,

while the sample S225 had the highest cytotoxicity to THP cells exhibiting EC_{50}= 7.70 µg/mL.

Table 3-30: EC_{50} of Cytotoxicity of the UK samples against THP cells.

Exp code	Type of sample	EC50 (µg/mL)
S224	Extract crude	42.36
S225	Extract crude	7.70
D6	Extract crude	44.62
D7	Extract crude	44.20

3.1.9.4 In-vitro antitrypanosomal activity of S224, S225, D6 and D7 isolated pure compounds isolated against *T. brucei* (S427), *T. congolense,* B48 and *T. b. brucei* ISMR1

The anti-trypanosomal activity of the crude extracts using an Alamar blue™ 96 well microplate assay as described in (Räz *et al*., 1997), implemented by Ms.Ibrahem Alfyez, Glasgow University.

The pure compounds isolated from the UK samples were tested against *T. brucei* (s427), B48, *T. b. brucei* ISMR1 and *T. congolense* in comparison with Pentamidine as a drug control. When drug sensitivities were calculated, the results showed that all pure compounds isolated exhibited variable activity against *T. brucei*. The isolated compounds (1), (3), (5), (6), (7), (8) and (10), had significant variable activity against *T. brucei* (s427)WT with EC_{50} values of 6.07, 9.85, 4.56, 7.49, 4.56, 2.74 and 9.20µg/mL, respectively as shown in Table 3-31. The same pure compounds except

(1) showed variable activity against *T. b. brucei* ISMR1 and exhibited variable high activity with EC_{50} values of 11.41, 6.3, 8.2, 3.6, 2.5 and 9.5µg/mL, respectively. However, compound (1) previously tested previously against *T. congolense* exhibited high activity at 5.7µg/mL. Whereas, compound (2) showed EC_{50} value of 100 > µg/mL Table 3-31.

Table 3-31: EC50 values for anti-trypanosomal activity of isolated compounds from the UK samples against *T. brucei* (s427), *T. brucei* B4 and *T. b. brucei* ISMR1.

Exp code	**Isolated compound**	**Types of Trypanosoma**									
		Tb S427WT		**B48**				**ISMR1**			
		AVR	**SEM**	**AVR**	**SEM**	**RF**	**t-test**	**AVR**	**SEM**	**RF**	**t-test**
S224-C40-46-MPLC- F6	Pinobanksin 3-O-acetate **(1)**	6.07 (19.31 µM)	0.57	-	-	-	-	-	-	-	-
Pentamidine (µM)		0.0044	5.31 E-04								
S224-C40-46-MPLC- F6	Pinobanksin 3-O-acetate **(1)**	T. congolense									
		5.2(16.54 µM)	0.23								
Pentamidine (µM)		0.81	0.04	-	-	-	-	-	-	-	-
		Tb S427WT									
		AVR	**SEM**								
S224-C60-40-MPLC3+4	7-Methoxychrysin**(2)**	N/A	N/A	N/A	N/A	N/A	N/A	N/A	N/A	N/A	N/A
S224C3+4-MPLC14-S8	Kaempferol**(3)**	9.85 (34.43 µM)	0.42	14.23(49.75 µM)	0.02	1.45	0.00002	11.0 (41.03 µM)	0.43	1.12	0.066
S224-C60-40-MPLC8-15-F4	Pinocembrin**(4)**	16.36(63.89 µM)	0.70	21.4 (83.57 µM)	1.02	1.31	0.003	20.77(80.84 µM)	1.43	1.27	0.019
S224-c40-60-s9	4'-Methoxykaempferol**(5)**	4.56 (15.20 µM)	0.14	6.7(22.32 µM)	0.10	1.48	0.00001	6.3(20.9 µM)	0.20	1.39	0.00017
S224-c40-60-s8	Galangin**(6)**	7.49 (27.	0.16	8.6(31.8 µM)	0.27	1.14	0.007	8.2(30.3	0.53	1.09	0.190

		73 µM)						2 µM)			
D7C60-40-F17	Chrysin**(7)**	4.56 (17.95 µM)	0.32	6.2(24.40 µM)	0.53	1.35	0.024	3.6(14.17 µM)	0.76	0.80	0.247
D6-C3-H40-E60-SE-F8	Apigenin**(8)**	2.74 (10.14 µM)	0.40	2.6(9.7 µM)	0.13	0.95	0.716	2.5(9.32 µM)	0.18	0.93	0.611
S225F1VLC-60-40-C20-25	Pinostrobin**(9)**	14.28(52.87 µM)	0.12	15.2 (56.28 µM)	0.49	1.07	0.078	15.3 (59.64 µM)	0.48	1.07	0.054
S225F1VLC-C20-80-C30-33	Cinnamic acid**(10)**	9.20 (62.14 µM)	0.48	12.5 (84.42 µM)	0.24	1.36	0.0004	9.5(64.16 µM)	0.73	1.04	0.669
S225F1VLC-C40-60-C10-12	Coumaric acid cinnamyl ester **and** Coumaric acid benzyl ester**(11a and 11b)**	12.28	0.32	13.9	0.26	1.13	0.004	14.1	0.49	1.15	0.012
Pentamidine (µM		0.00241	0.000430	0.57	0.473	0.05	195.89	0.0.0527	0.0017	21.8	0.00000053

N/A: propolis numbers (2) inactive at 400 ug/mL

3.1.9.5 In-vitro Cytotoxicity assay of S224, S225, D6 and D7 pure compounds isolated.

Toxicity studies against human cell line (THP cells) were carried out for the UK pure compounds from the UK propolis samples (**1-11**) to evaluate their cytotoxicity and assesses EC50 values (µg/mL). All pure compounds showed moderate values against the THP cells, compound **(1)** showed the highest cytotoxicy to THP cells exhibiting an EC50 = 10.98 µg/mL (31.82 µM). In comparison, the least cytotoxic was **(9)** EC50> 100 µg/mL, as shown in Table 3-32.

Table 3-32: EC50 of Cytotoxicity of the UK pure compounds against THP cells.

Exp code	Isolated compound	EC50 (µg/mL)(µM)
S224-C40-46-MPLC- F6	Pinobanksin 3-O-acetate **(1)**	10.98 (31.82 µM)
S224-C60-40-MPLC3+4	7-Methoxychrysin**(2)**	20.82 (77.66 µM)
S224C3+4-MPLC14-S7	Kaempferol**(3)**	16.9 (59.1 µM)
S224-C60-40-MPLC8-15-F4	Pinocembrin**(4)**	44.88 (171.8 µM)
S224-c40-60-s9	4'-Methoxykaempferol**(5)**	21.59 (71.95 µM)
S224-c40-60-s8	Galangin**(6)**	11.36 (42.066 µM)
D7C60-40-F17	Chrysin**(7)**	11.42 (44.95 µM)
D6-C3-H40-E60-SE-F8	Apigenin**(8)**	20.99 (77.72 µM)
S225F1VLC-60-40-C20-25	Pinostrobin**(9)**	>100
S225F1VLC-C20-80-C30-33	Cinnamic acid**(10)**	22.2 (149.95 µM)
S225F1VLC-C40-60-C10-12	Coumaric acid Cinnamyl ester **and** Coumaric acid benzyl ester**(11a and 11b)**	39.42

3.1.10 Extraction of Polish propolis:

A sample of Polish propolis was extracted using the same protocol as used for the UK samples as in section 3.1, the results from which are shown below Table 3-33.

Table 3-33: The weight of Polish propolis sample before and after extractions

S/NO	Sample code	Sample Origin	Weight of raw sample (g)	Weight of ethanol extract (g)	% Yield
1	P	Poland	30.0	16.0	53

The EEP of the sample of Polish propolis was profiled as for the UK propolis samples. The LC-HRMS results for the sample are shown in Figure 3-76 and Table 3-34.

Table 3-34: LC-MS profiling for Poland Propolis Crude (P) in positive mode

Peak No	Rt (time)	{M+1}	Chemical Formula	RDB	δ (ppm)	intensity
1	5.64	195.0639	$C_{10}H_{11}O_4$	5.5	-6.172	6.57E6
2	9.77	287.0892	$C_{16}H_{15}O_5$	9.5	-7.559	1.81E7
3	10.77	271.0580	$C_{15}H_{11}O_5$	9.5	-7.710	2.35E7
4	11.22	287.0526	$C_{15}H_{11}O_6$	10.5	-8.168	6.80E6
5	11.96	301.0684	$C_{16}H_{13}O_6$	10.5	-7.233	9.14E6
6	12.99	285.0739	$C_{16}H_{13}O_5$	10.5	-6.349	1.04E7
7	13.24	287.0548	$C_{15}H_{11}O_6$	10.5	-0.145	4.45E6
8	13.63	317.0634	$C_{16}H_{13}O_7$	10.5	-6.810	6.32E6
9	14.81	263.0895	$C_{14}H_{15}O_5$	7.5	-7.184	2.08E7
10	14.86	427.1358	$C_{30}H_{19}O_3$	21.5	2.929	2.08E7
11	15.63	255.0632	$C_{15}H_{11}O_4$	10.5	-1.895	1.13E8
12	16.32	301.06815	$C_{16}H_{13}O_6$	10.5	-2.515	2.58E7
13	16.43	315.08350	$C_{17}H_{15}O_6$	10.5	-2.815	3.06E7
14	18.23	285.1101	$C_{17}H_{17}O_4$	9.5	-2.026	1.50E7
15	20.74	301.1051	$C_{17}H_{17}O_5$	9.5	-1.890	3.01E7
16	21.51	299.0886	$C_{17}H_{15}O_5$	10.5	-2.780	5.87E7
17	24.40	295.2244	$C_{18}H_{31}O_3$	3.5	-2.341	1.47E7

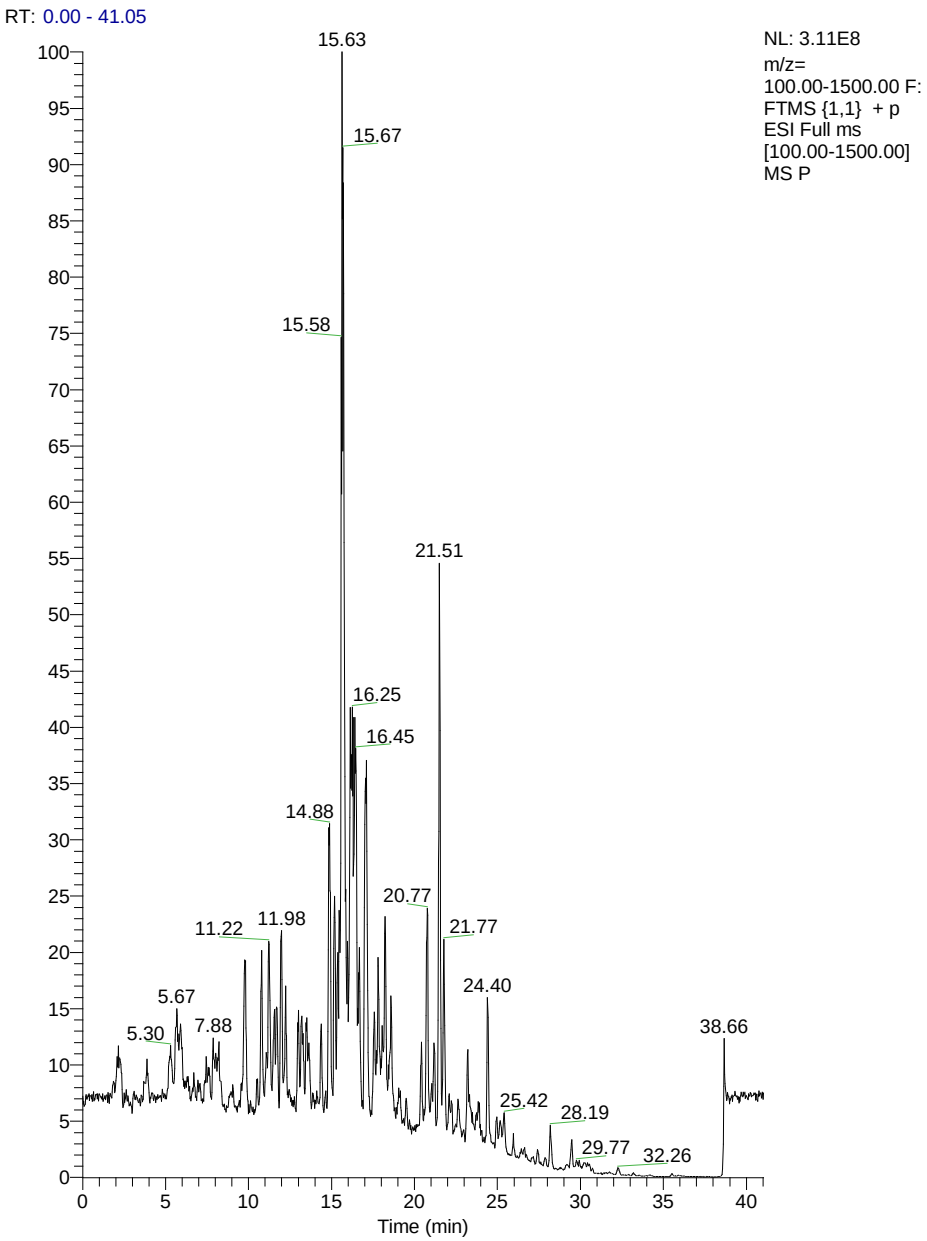

Figure 3-76: LC-MS chromatogram peaks of the ethanol extract of Poland propolis

3.1.11 Chemical profiling and purification of Sample P

A quantity of EEP from Poland P (30 g) was dissolved in 200 mL of dichloromethane and treated as in method B section 2.4. Additionally, another 600 mg of the extract was

subjected to fractionation by Sephadex LH20 according to general method 3. The fractions and yields obtained are presented in Table 3-35.

Table 3-35: Fractions from GF of Polish propolis (P) sample

Poland Fraction Code	Purified compound	Weight (mg)
P1	-	8.0
P2	-	13.0
P3	-	17.0
P4	-	12.0
P5	-	11.0
P6	-	14.0
P7	-	10.0
P8	-	13.0
P9	-	12.0
P10	-	9.0
P11	-	10.0
P12	-	11.0
P13	-	23.3
P14		
P15		
P16		
P17		
P18		
P19	-	12.0
P20	Naringenin 4',7-dimethyl ether	14.0
P21	-	13.0
P22	-	16.0
P23	-	14.0
P24	-	10.0
P25	-	12.0
P26	4’,7-dimethoxykaempferol	16.0
P27	-	11.0
P28	-	13.0
P29	-	12.0
P30	-	9.0
P31	-	6.0
P32	-	7.0

* - a mixture of compounds

3.1.12 Characterisation of fraction P-F26 of GF as 4',7-Dimethoxykaempferol (12)

The compound was obtained as a yellow powder after column chromatography and Sephadex column chromatography. The positive mode HRESI-MS spectrum of the compound gave a molecular ion $[M+H]^+$ at m/z 315.0838 (Calc for ($C_{17}H_{15}O_6$), 315.0869) suggesting a molecular formula $C_{17}H_{14}O_6$. The compound's proton spectrum was also that of a C-3 substituted flavone Figure 3-78. There were two methoxy groups and the presence of an AA'BB' splitting pattern indicated that ring B was monosubstituted and with a methoxy group owing to correlations from the methoxy group to the same carbon as the 2' and 6' protons to C-4'. A second methoxy signal was also observed at C-7 owing to correlations from H-6 and H-8 to the same carbon C-7 as the methoxy group. Therefore, C-3 must be –OH substituted, and the compound was identified as 4',7-dimethoxykaempferol and was confirmed by literature reports (Star et al., 1975, Inasaki, 2002). The chemical shifts for the protons and carbon atoms are given in Table 3-36.

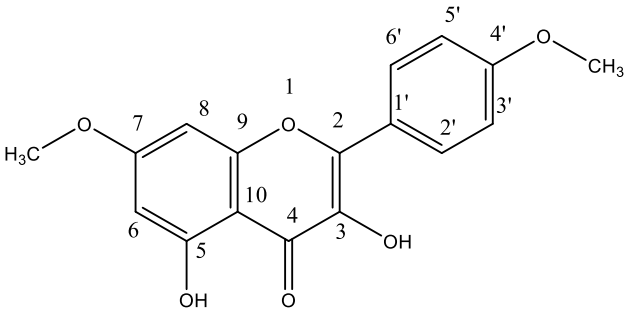

Figure 3-77: Chemical structure of 4',7-Dimethoxykaempferol

Table 3-36: Chemical shifts for 4',7-Dimethoxykaempferol

Position	**4',7-Dimethoxykaempferol**		Literature*	
	^{1}H δ ppm (mult, J in Hz)	^{13}C δ ppm, (mult)	^{1}H δ ppm, (mult, J in Hz)	^{13}C δ ppm, (mult)
1	-	-	-	-
2	-	145.7 (C)	-	147.89
3	-	135.6 (C)	-	137.99
4	-	175.1(C)	-	177.25
5	-	160.9 (C)	-	162.23
6	6.40 (1H, d, 2.2)	98.0 (CH)	6.43 (IH, d, *J* = l.5 Hz)	98.05
7	-	165.7 (C)	-	165.45
8	6.52 (1H, d, 2.2)	92.1 (CH)	6.55 (l H, d, *J*=1.5 Hz)	92.62
9	-	156.8 (C)	-	157.72
10	-	103.9 (C)	-	105.58
1`	-	123.2 (C)	-	123.60
2`	8.20 (1H, d)	129.4 (CH)	8.25 (1H, d, *J* = 9.0Hz)	128.05

3`	7.06 (1H, d)	114.0 (CH)	7.08 (1H, d, *J* = 9.0 Hz)	114.5
4`	-	161.1 (C)		162.61
5`	7.06 (1H, d)	114.0 (CH)	7.08 (1H, d, *J* = 9.0 Hz)	114.5
6`	8.20 (1H, d)	129.4 (CH)	8.25 (1H, d, *J* = 9.0Hz)	128.05
7-OCH_3	3.91 (s)	55.9 (CH_3)	3.92 (s)	55.79
5-OH	11.76 (s)	-	12.75 (s)-	-
3-OH	6.61	-	-	-
4`-OCH_3	3.92 (s)	55.4 (CH_3)	3.92 (s)	55.52

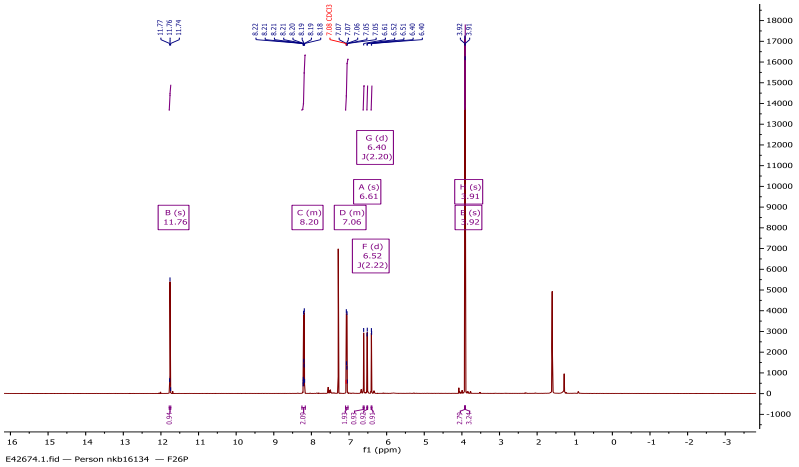

Figure 3-78: ^{1}H NMR (400 MHz) of 4',7-Dimethoxykaempferol in $CDCl_3$

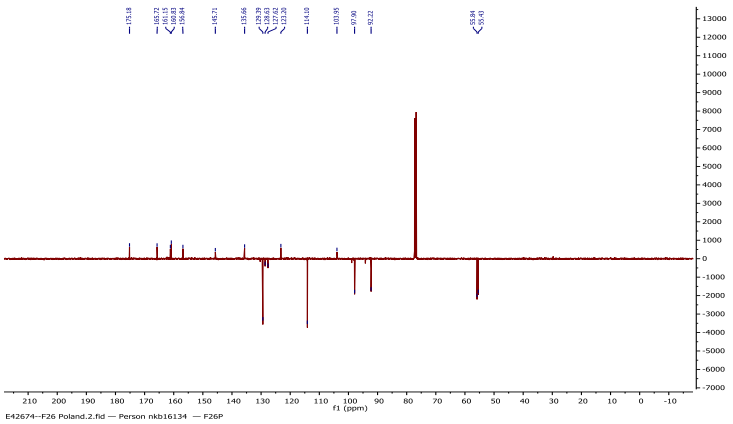

Figure 3-79: ^{13}C NMR (400 MHz) of 4',7-Dimethoxykaempferol in $CDCl_3$

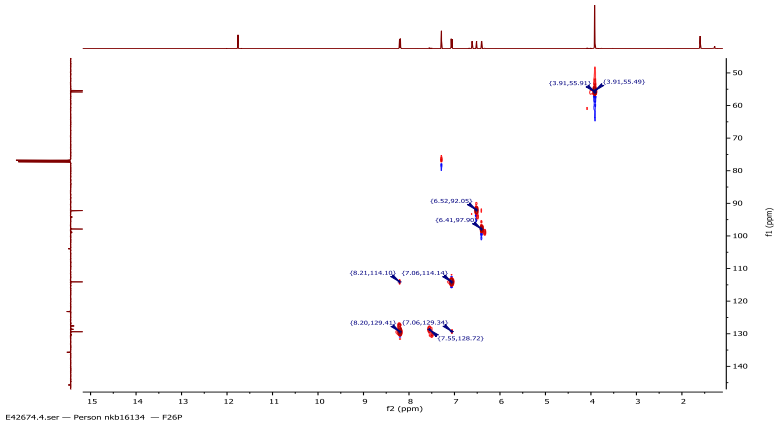

Figure 3-80: HSQC spectrum (400 MHz) of 4',7-Dimethoxykaempferol in $CDCl_3$

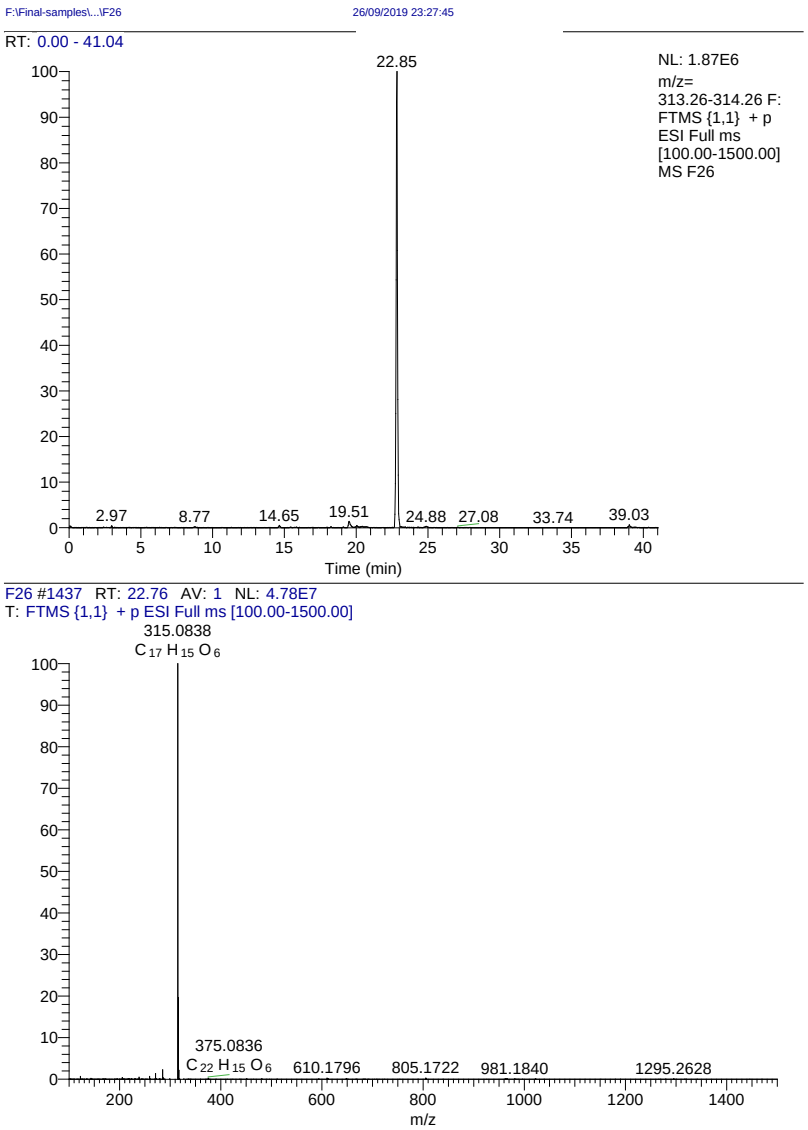

Figure 3-81: Extracted ion chromatogram and mass spectrum in positive ion mode for 4',7-Dimethoxykaempferol

3.1.13 Characterisation of fraction P20 as Naringenin 4',7-dimethyl ether (13)

The compound was obtained as a pale yellow solid following column chromatography and Sephadex column chromatography. The positive mode HRESI-MS spectrum of the compound gave a molecular ion $[M+H]^+$ at m/z 301.10443 (Calc for ($C_{17}H_{17}O_5$),

301. 1076) suggesting a molecular formula of $C_{17}H_{16}O_5$. The proton spectra Figure 3-83 were similar to that of P26 except for the presence of three aliphatic protons typical of a flavanone. The compound in its proton spectrum also showed signals for a deshielded and oxygenated methine doublet of doublets at δ_H 5.39 for H-2 and two other aliphatic protons at 2.81 and 3.11 ppm for H-3. Two meta coupled aromatic protons H-6 and H-8 appeared as doublets at δ 6.07 and 6.10 ppm. Four other aromatic proton signals for a disubstituted benzene ring were observed at δ 7.40 (H-2',6'), 6.98 (H-3', H-5'). Two sets of methoxy protons were observed at 3.83 and 3.86 ppm. The ^{13}C-NMR spectrum showed signals for 17 carbons including one carbonyl at δ_C 196.0 (C-4), four aromatic CH at 95.0 (C-6) and 94.2 (C-8), two aliphatic carbons at 78.9 (C-2) and 43.1 (C-3) and two methoxy carbon signals at 55.7 ppm (7-OCH_3) and 55.4 (4′-OCH_3). The rest of the carbons were for quarternary phenolic and non-phenolic aromatic carbons. Analysis of its 2D spectra identified the compound to be Naringenin-4,7-dimethyl ether, and the structure was confirmed using literature reports (Kim et al., 2007). The chemical shifts for the protons and carbon atoms are given in Table 3-37.

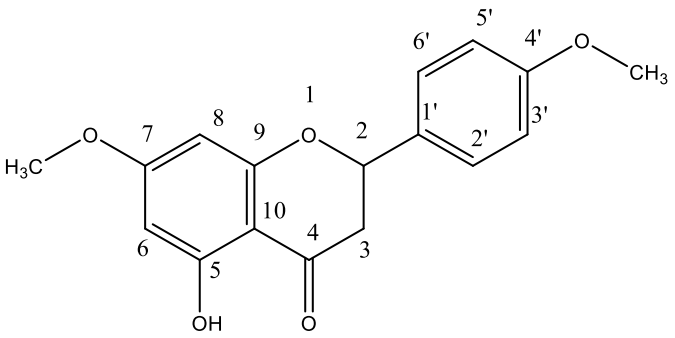

Figure 3-82: Chemical structure of Naringenin 4',7-dimethyl ether

Table 3-37: Chemical shifts for Naringenin 4',7-dimethyl ether

Position	**Naringenin 4',7-dimethyl ether**		Literature*	
	^{1}H δ ppm (mult, J in Hz)	^{13}C δ ppm, (mult)	^{1}H δ ppm, (mult, J in Hz)	^{13}C δ ppm, (mult)
1	-	-	-	-
2	5.39 (1H, dd, 13.0, 2.7)	78.9 (CH)	5.37 (1H, d, *J* = 11.7)	79.7
3a	3.11 (1H, dd, 17.2, 13.0)	43.1 (CH_2)	3.12 (dd, J = 17.1, 13.1 Hz, 1H),	43.2
3b	2.81(1H, d, 17.2, 3.0)		2.79(17.2,3.0 Hz,1H)	
4	-	196.0 (C)	-	197.3
5	-	164.0 (C)	-	164.3
6	6.07 (1H, 2.3)	95.0 (CH)	6.04 (1H, d, *J* = 2.2)	95.3

7	-	167.0 (C)	-	168.7
8	6.10 (1H, 2.3)	94.2 (CH)	6.07 (1H, d, *J* = 2.2)	94.4
9	-	163.0 (C)	-	163.9
10	-	103.2 (C)	-	103.5
1`	-	130.4 (C)	-	131.6
2`	7.40 (1H, d)	127.7 (CH)	7.39(1H, d *J* = 8.6 Hz)	128.7
3`	6.98 (1H, d)	114.2 (C)	6.96(1H, d *J* = 8.7 Hz)	114.5
4`	-	160.1 (C)	-	160.8
5`	6.98 (1H, d)	114.2 (CH)	6.96(1H, d *J* = 8.7 Hz)	114.5
6`	7.40 (1H, m)	119.9 (CH)	7.39(1H, d *J* = 8.6 Hz)	128.7
7-OCH_3	3.83 (3H, s)	55.7 (CH_3)	3.80 (s, 3H)	56.0
4'-OCH_3	3.86 (3H, s)	55.4 (CH_3)	3,89 (s, 3H)	55.4
5-OH	12.04 (s)	-	-	

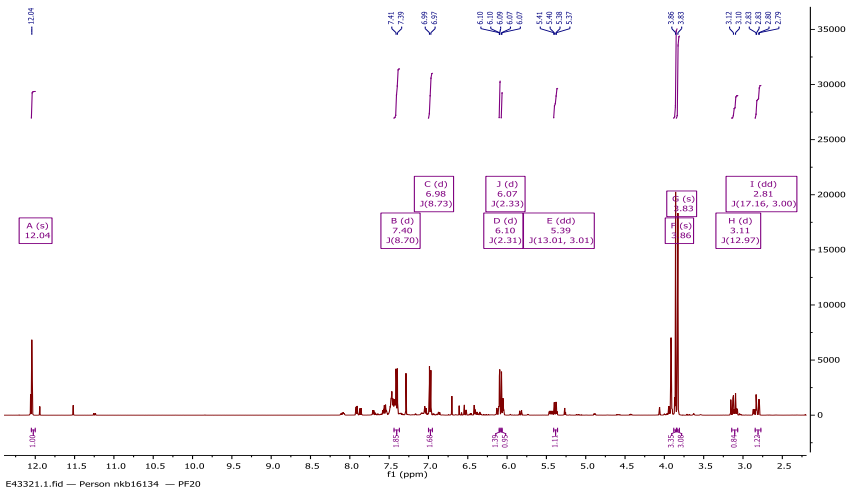

Figure 3-83: ^{1}H NMR (400 MHz) of Naringenin 4',7-dimethyl ether in $CDCl_3$

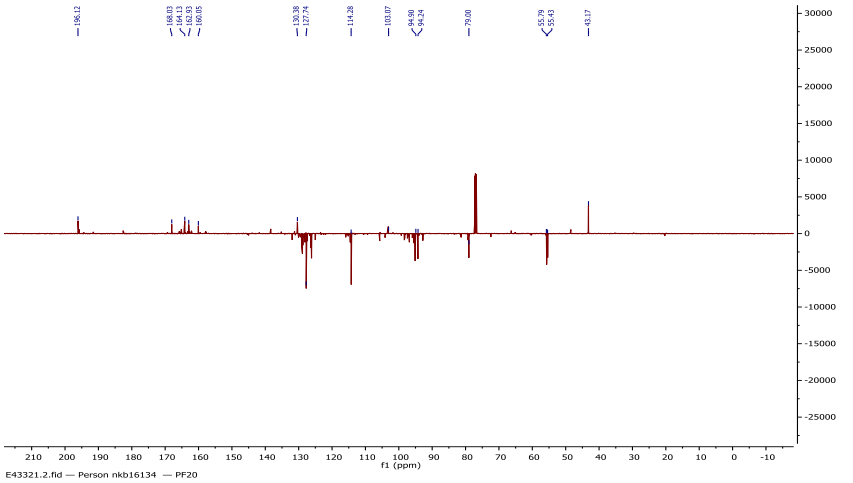

Figure 3-84: ^{13}C NMR (400 MHz) of Naringenin 4',7-dimethyl ether in $CDCl_3$

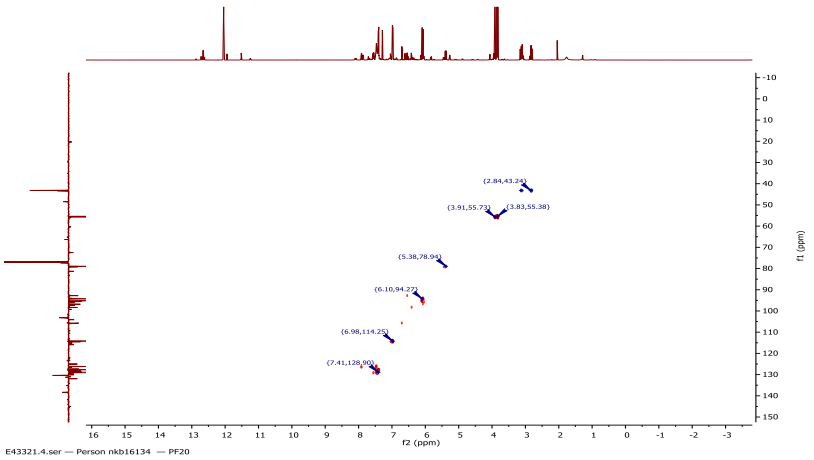

Figure 3-85: HSQC spectrum (400 MHz) of Naringenin 4',7-dimethyl ether in $CDCl_3$

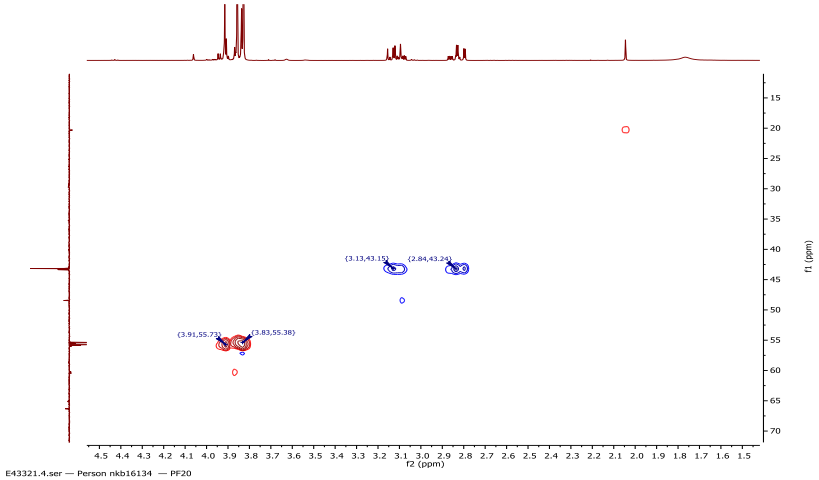

Figure 3-86: Selected HSQC spectrum expansion of Naringenin 4',7-dimethyl ether $CDCl_3$

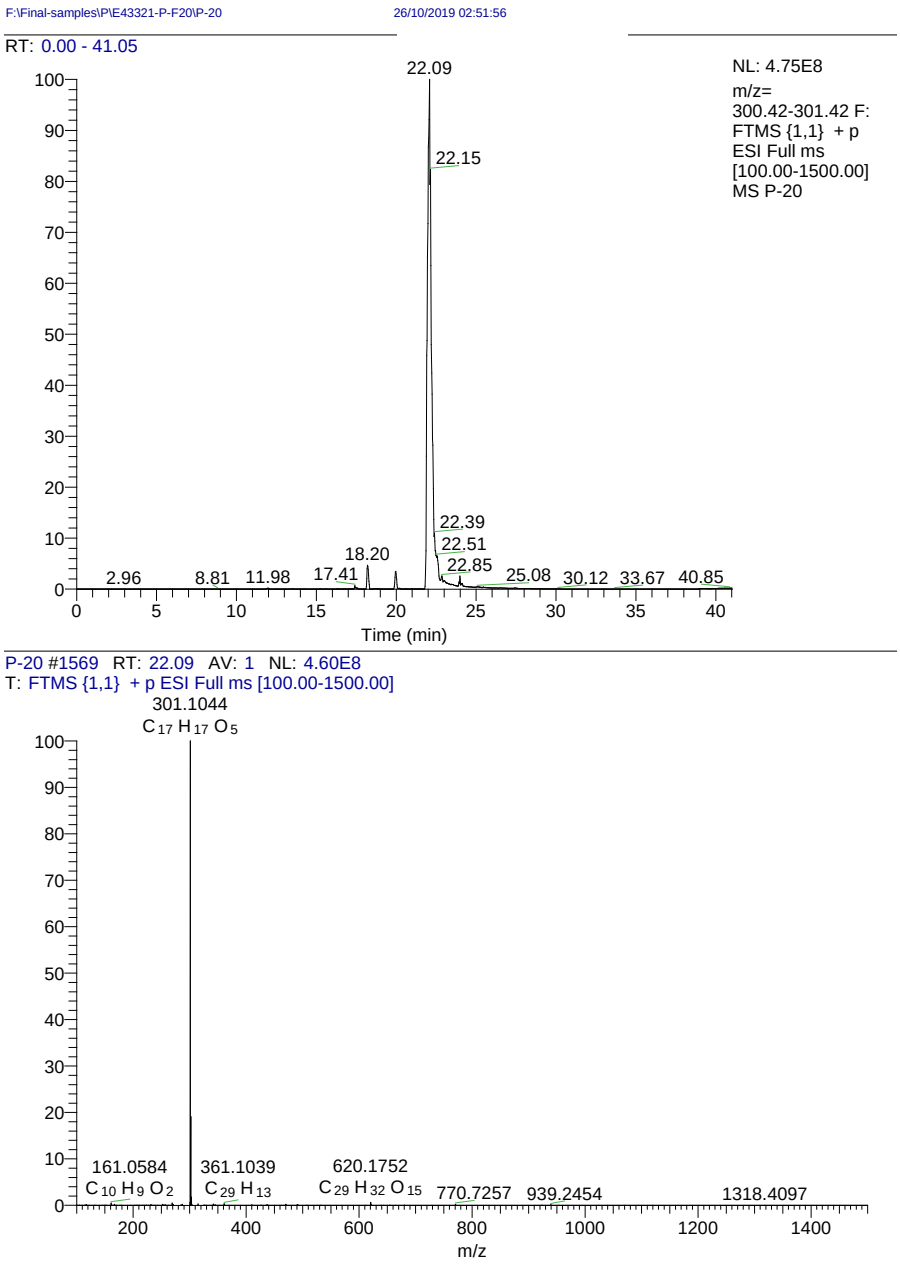

Figure 3-87: Extracted ion chromatogram and mass spectrum in positive ion mode for Naringenin 4',7-dimethyl ether

3.1.14 The biological activity of a Propolis sample from Poland

3.1.14.1 In-vitro Antitrypanosomal activity of Poland crude propolis sample and its isolated compounds against *T. brucei* (S427), B48 and *T. b. brucei* ISMR1

The EEP of the UK propolis sample and its three pure compounds isolated were tested against *T. brucei* (s427), *T. b. brucei* ISMR1 in comparison with Pentamidine as a drug control. Drug sensitivity was calculated, and the results, presented in Table 3-38, showed that the crude sample P and one of its isolated compounds Naringenin 4',7-dimethyl ether had significant activity against both strains of *T. brucei* with EC_{50} values of 4.45 and 5.25 µg/mL, respectively against *T. brucei* (s427) and 5.0 and 4.8 µg/mL, respectively against *T. brucei* ISMR1. The second isolated compound 4',7-Dimethoxykaempferol was the least effective against *T. brucei* (s427) and *T. b. brucei* ISMR1 at EC_{50} values 29.88 and 29.5 µg/mL, respectively.

Table 3-38: EC_{50} values(n=3) for anti-trypanosomal activity of the crude Poland sample and its isolated compounds against *T. brucei* (s427), *T. brucei* B4 and *T. b. brucei* ISMR1.

Exp code	**Pure compound**	**Types of Trypanosoma**									
		Tb S427WT		**B48**				**ISMR1**			
		AVR	**SEM**	**AVR**	**SEM**	**RF**	**t-test**	**AVR**	**SEM**	**RF**	**t-test**
P	crude	4.45	0.08	6.6	0.18	1.49	0.00002	5.0	0.30	1.13	0.068
P-F26	4',7-dimethoxykaempferol **(12)**	29.88(95.13 µM)	2.77	32.4(103.16 µM)	1.66	1.08	0.400	29.5 (94.6 µM)	3.06	0.99	0.926
P-F20	Naringenin 4',7-dimethyl	5.25(17.5 µM)	0.13	6.6(21.9 µM)	0.11	1.25	0.00012	4.8(16.0 µM)	0.10	0.92	0.030

ether**(13)**										
Pentamidine (µM)	0.00241	0.000430	0.57	0.473	0.05	195.89	0.00003	0.00017	21.8	0.000000053

3.1.15 In-vitro Cytotoxicity assay of Poland crude propolis extracts and some compounds isolated from it.

Toxic activity tests against human cell lines (THP cells) were carried out for the ethanolic extract of the Polish propolis sample and its pure compounds to evaluate their cytotoxicity and assesses EC_{50} values (µg/mL). The crude sample and its isolated compound 4',7-Dimethoxykaempferol showed moderate values against the THP cells with EC_{50} values 43.61 and 20,26 µg/mL, respectively. However, the second isolated compound Naringenin 4',7-dimethyl ether was the least cytotoxic to THP cells exhibiting EC_{50}> 100 µg/mL, as shown in Table 3-39.

Table 3-39: EC_{50} of Cytotoxicity of the crude sample from Poland and its pure compounds against THP cells.

Exp code	**Type of sample**	**EC_{50} (µg/mL)**
P	crude	43.61
P26	4',7-dimethoxykaempferol**(12)**	20.26 (64.50 µM)
P20	Naringenin 4',7-dimethyl ether**(13)**	>100

4 Chapter 4

4.1 Fractionation and Testing of Propolis samples from Saudi Arabia

4.1.1 Extraction of Saudi Arabian propolis

The samples of propolis from Saudi Arabia were extracted using the same protocol as used for the UK samples above (Section 3.1). The weights resulting from the extraction are presented in Table 4-1.

Table 4-1: The weight of Saudi propolis samples before and after extractions.

S/No	Sample Code	Origin Sample	Weight of resin (g)	Weight of ethanol extract (g)	% yield
1	SB	Baljurashi Saudi Arabia	35	19	54.2
2	T2	Alquoz Saudi Arabia	46	21	45.5

4.2 Chemical profiling and purification of sample code (SB) from Saudi Arabia

LC-MS profiling was carried for the ethanol extract of samples from Saudi Arabia, as shown in Table 4-2 and Figure 74). The LC-MS chromatogram of the crude extract showed mainly flavonoids, phenolic acids, esters, terpenoids and fatty acid compounds as judged from the elemental compositions of the peaks.

The EEP of the Saudi propolis sample (35g) was subjected to several methods of separation and purification to isolate its constituent compounds, mostly based on method **B,** according to Table 4-2. LC-MS and NMR analysis were carried out on SB-C-60-40, SBC-40-60 and SB-H20-E80, these fractions appeared rich in flavonoids and phenolic acids. Hence, from sub-fraction SB-C-60-40 (186 mg), yielding 25 sub-fractions. LC-MS and NMR analysis led to the identification of F8 as Lupeol **(15)**. The second fraction, SB-C-40-60 (467mg), yielded 30 sub-fractions which led to the isolation of two compounds as a mixture which were identified as Hesperetin-7-methyl ether **(14-a)** and Sakuranetin **(14-b).**

Table 4-2: The LC-MS profiling for ethanol Saudi propolis extract SB in negative and positive ion mode

Peak No	Rt (time)	[M-1]	[M+1]	Chemical Formula	RDB	δ (ppm)	Intensity
1	2.26	191.0564		$C_7H_{11}O_6$	2.5	1.563	3.28E7
2	6.05	581.1882		$C_{27}H_{33}O_{14}$	11.5	1.120	3.46E6
3	7.47	317.066		$C_{16}H_{13}O_7$	10.5	0.580	5.88E6
4	8.20	329.0668		$C_{17}H_{13}O_7$	11.5	0.463	5.98E6
5	9.00	287.0562		$C_{15}H_{11}O_6$	10.5	0.448	2.48E7
6	11.06	271.0613		$C_{15}H_{11}O_5$	10.5	0.639	3.48E7
7	11.30	301.0716		$C_{16}H_{13}O_6$	10.5	0.470	1.46E8
8	11.53	315.0515		$C_{16}H_{11}O_7$	11.5	1.727	5.33E7
9	15.74	285.0768		$C_{16}H_{13}O_5$	10.5	0.081	1.86E8
10	15.95	283.0613		$C_{16}H_{11}O_5$	11.5	0.612	8.35E7

11	16.33	313.0720		$C_{17}H_{13}O_6$	11.5	0.826	3.81E7
12	18.87	319.2281		$C_{20}H_{31}O_3$	5.5	0.769	2.54E7
13	21.55	271.2283		$C_{16}H_{31}O_3$	11.5	1.004	4.31E7
14	22.80	299.2018		$C_{20}H_{27}O_2$	7.5	0.724	1.13E8
15	28.32	301.2173		$C_{20}H_{29}O_2$	6.5	0.254	2.58E7
16	28.53	425.3723		$C_{30}H_{49}O$	6.5	-3.643	1.21E7
17	12.17		345.0965	$C_{18}H_{17}O_7$	10.5	-1.012	3.96E7
18	13.46		303.0858	$C_{16}H_{15}O_6$	9.5	-1.533	4.02E7
19	15.73		287.0913	$C_{16}H_{15}O_5$	9.5	-0.314	1.38E8
20	16.02		317.1	$C_{17}H_{17}O_6$	9.5	-0.582	2.02E8

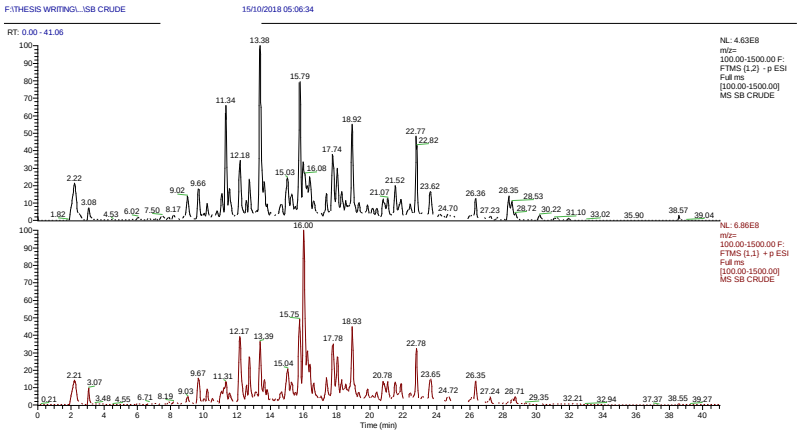

Figure 4-1: LC-MS chromatogram peaks of the ethanol extract of Saudi propolis (SB)

Table 4-3: Solvent system and fractions from column chromatography of SB

Fraction No SB	**Solvent system**	**Fraction obtained**	**Fractions obtained In vial 20ml**	**Fraction weight**	**Purified compound**	**Fraction weight mg**
1	Hexane 90% Ethyl acetate 10% 200ml	SB- H90-E10	F1-F20	47mg	-	-
2	Hexane 70% Ethyl acetate 30% 200ml	SB- H70-E30	F1-F20	123mg	-	-

3	Hexane 60% Ethyl acetate 40% 200ml	**SB-C-60-40**	F1-F25	186mg	Lupeol	11.0
4	Hexane 40% Ethyl acetate 60% 200ml	**SB-C-40-60**	F1-F30	467mg	Hesperetin-7-methyl ether **and** Sakuranetin	12.0
5	Hexane 30% Ethyl acetate 70% 150ml	**SB-C-30-70-**	F1-F25	210mg	-	-
6	Hexane 30% Ethyl acetate 70% 50ml	SB-H30-E70	F1-F20	32mg	-	-
7	Hexane 20% Ethyl acetate 80% 200ml	SB-H20-E80	F1-F20	115mg	-	-
8	Ethyl acetate 100% 200ml	SB-E100	F1-F20	72 mg	-	-
9	Ethyl acetate 70% Methanol 30% 200ml	SB-E30-M70	F1-F20	51mg	-	-

4.2.1 Characterisation of the major component of SB-C 40-60-F1CUP as Hesperetin-7-methyl ether (14 a)

The mixture of the compounds was obtained as Pale-yellow crystals from the ethanolic extract of propolis sample from Saudi Arabia by column chromatography. On TLC

with 10% MeOH, 40% EtOAc and 50% Hexane, it gave a yellow spot (R*f* = 0.64) after spraying with p-anisaldehyde-sulphuric acid reagent and heating. Two compounds were isolated as a mixture and due to their poor resolution separation of each compound was not performed.

The positive mode HRESI-MS spectrum of the major compound gave a molecular ion $[M+H]^+$ at m/z 317.1000, suggesting a formula $C_{17}H_{17}O_6$ (Calc 317.1025). Hence the molecular formula of the compound is $C_{17}H_{16}O_6$. The ^1H NMR spectrum Figure 4-3 of the compound similarly showed a chelated –OH proton signal at δ_H 12.04 (s) ppm and two meta coupled protons for the ring A in flavones; H-6 at δ_H 6.39 (1H, *J* = 2.3 Hz) and H-8 at 6.51 (1H, *J* = 2.3 Hz). It also showed three coupled aliphatic protons at δ_H 5.36 (1H, dd, *J* = 13.0, 2.7 Hz) and 3.11 (1H, dd, *J* = 17.2, 13.0 Hz) and 2.80 (1H, d, *J* = 17.2, 3.0 Hz) typical of a flavanone ring. Other signals were for three protons at 6.99 (1H, *J* = 2.0 Hz) and two overlapped signals at 6.95 (2H, m) ppm. There were also two methoxy group protons at 3.95 and 3.82 (each 3H, s) ppm. The ^{13}C spectrum Figure 4-4 showed a total of 17 carbon atoms composed of a carbonyl at δ_C 196.1, five aromatic CH, two aliphatic carbons at 79.3 (CH) and 43.4 (CH_2), two methoxy carbons, two quaternary aromatic and five phenolic carbon signals. Using correlations in its 2D spectra, the compound was identified as Hesperetin-7-methyl ether which was confirmed by literature reports (Yao and Qing, 2008). The chemical shifts for the protons and carbon atoms are given in Table 4-4.

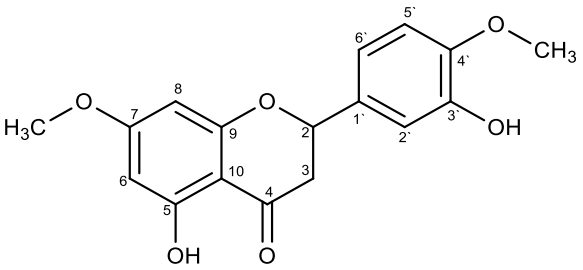

Figure 4-2: Chemical structure of Hesperetin-7-methyl ether

Table 4-4: ^{1}H and ^{13}C chemical shifts for Hesperetin-7-methyl ether in $CDCl_3$

Position	**Hesperetin-7-methyl ether**		Literature*	
	^{1}H δ ppm (mult, J in Hz)	^{13}C δ ppm, (mult)	^{1}H δ ppm, (mult, J in Hz)	^{13}C δ ppm, (mult)
1	-	-	-	-
2	5.36 (1H, dd, 13.0, 2.7)	79.3 (CH)	5.47 (1H, d, *J* = 12.7, 3.0 Hz)	79.0
3a	3.12 (1H, dd, 17.2, 13.0)	43.4 (CH_2)	3.20 (1H, d, *J* = 15.5, 12.6 Hz)	42.6
3b	2.80 (1H, d, 17.2, 3.0)		2.82(1H, dd, J=15.5,3.0 Hz	
4	-	196.1 (C)	-	197.0
5	-	164.2 (C)	-	163.8
6	6.10(1H,2.2)	94.5 (CH)	6.08 (1H, d, *J* = 2.2)	94.6
7	-	168.0 (C)	-	168.0
8	6.07(1H, 2.2)	95.4 (CH)	6.05(1H, d, *J* = 2.2)	93.7
9	-	163.0 (C)	-	163.1
10	-	103.4 (C)	-	102.9

1`	-	130.22(C)	-	131.8
2`	6.99 (1H, d, 2.0)	109.0 (CH)	7.05 (1H, d, J = 2.2 Hz)	111.3
3`	-	146.3 (C)		146.7
4`	-	146.5 (C)		147.8
5`	6.95 (1H, d)	114.6 (CH)	6.89 (1H, d, J = 8.0 Hz)	113.5
6`	6.95 (1H, d)	119.62 (CH)	6.93 (1H, dd J = 8.0, 2.2 Hz)	117.9
7-OCH_3	3.95 (3H, s)	56.0 (CH_3)	3.93 (3H, s)	55.3
4'-OCH_3	3.82 (3H, s)	55.7 (CH_3)	3.80 (3H, s)	55.4
5-OH	12.04 (s)	-	12.15 (1H, s)	-
3'-OH			-	

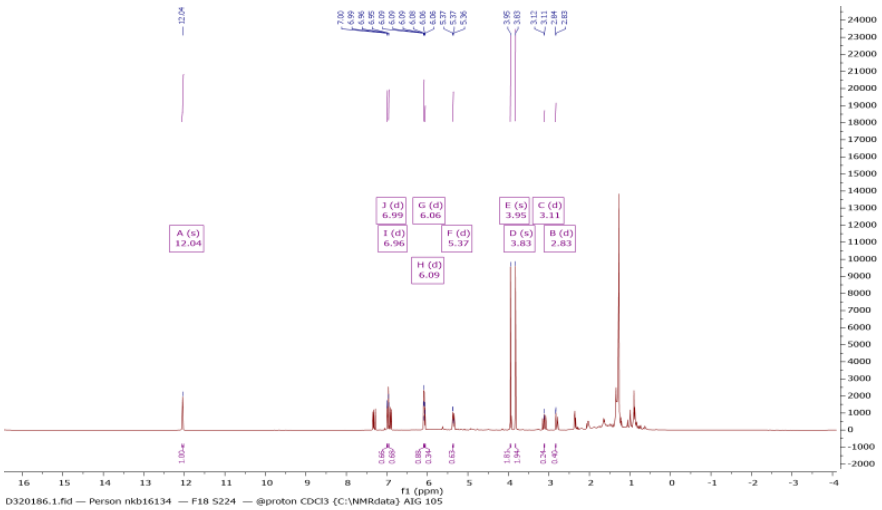

Figure 4-3: ^{1}H NMR (400 MHz) of Hesperetin-7-methyl ether in $CDCl_3$

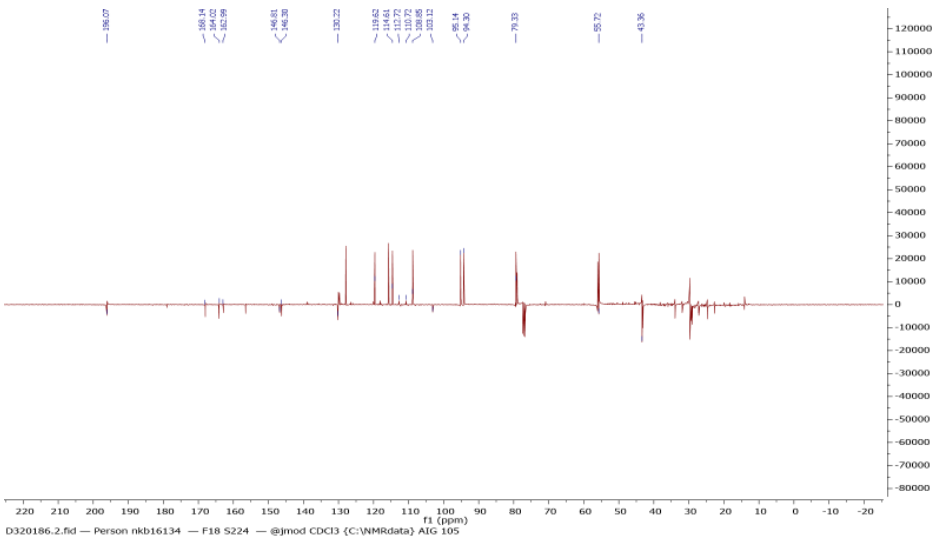

Figure 4-4: ^{13}C NMR (400 MHz) of Hesperetin-7-methyl ether in $CDCl_3$

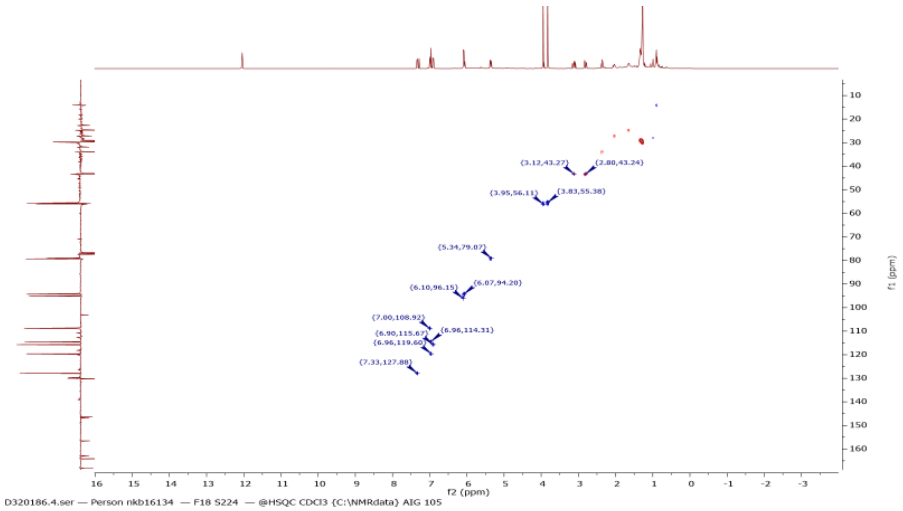

Figure 4-5: HSQC spectrum (400 MHz) of Hesperetin-7-methyl ether in $CDCl_3$

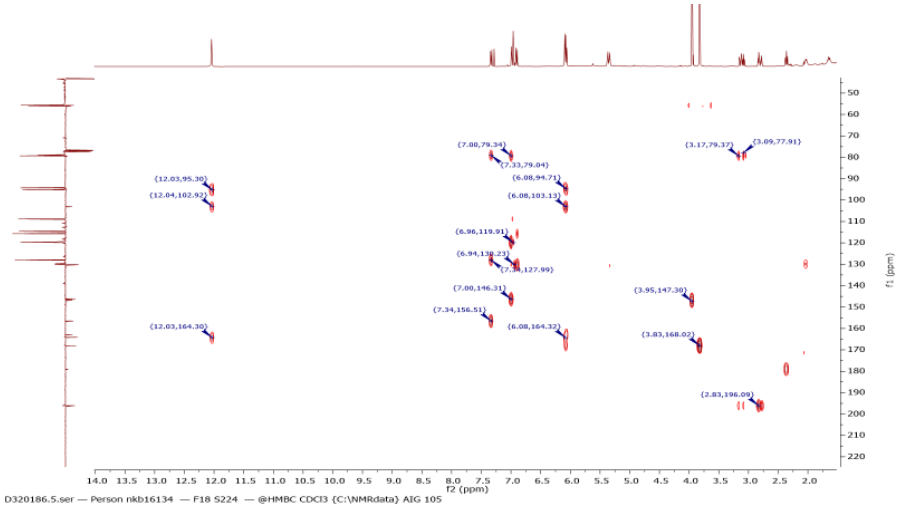

Figure 4-6: HMBC spectrum (400 MHz) of Hesperetin-7-methyl ether in $CDCl_3$

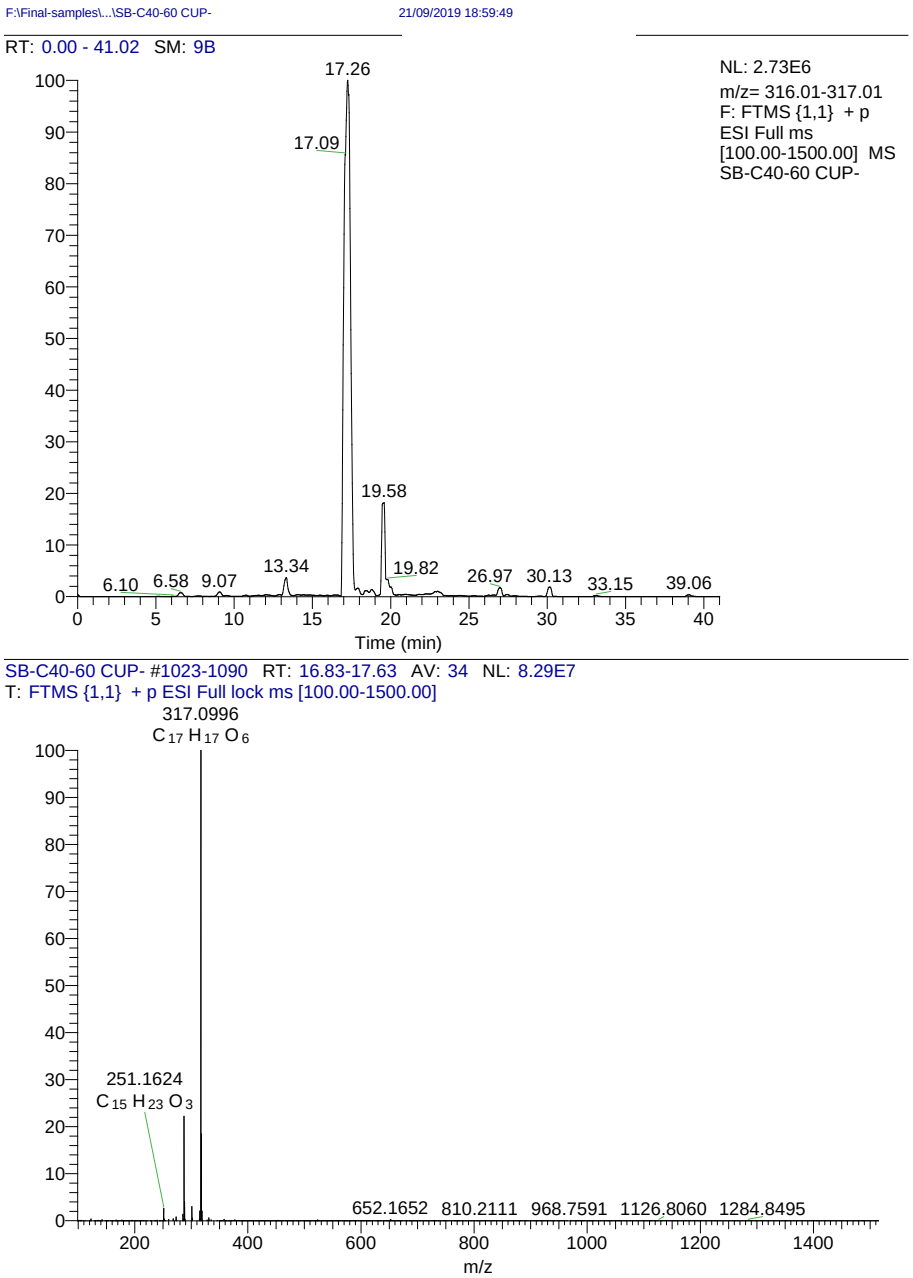

Figure 4-7: Extracted ion chromatogram and mass spectrum in positive ion mode for Hesperetin-7-methyl ether

4.2.2 Characterisation a minor component of SB-C H40-H60-F1CUP as Sakuranetin (14 b)

The minor compound gave a $[M-H]^-$ molecular ion at 287.0797 suggesting a formula $C_{16}H_{14}O_5$ (Calc 287.0763). Hence the molecular formula is $C_{16}H_{14}O_5$. It had identical proton and carbon spectral signals Figure 4-9 and Figure 4-10 to the major compound except for the AA'BB' para substitution on ring B with an –OH group at position C-4'. These doublets were observed at δ_H 6.90 (d, 2H, J = 8.6 Hz), δ_C 129.0 and 7.33 (d, 2H, J = 8.6 Hz), δ_C 115.7 ppm. The rest of the proton and carbon signals were overlapped, but on close examination, it was identified as Sakuranetin by comparison of its chemical shifts with literature reports (Jerz et al., 2005). Its proton and carbon chemical shifts are given in Table 4-5. Sakuranetin was isolated from propolis samples, which was collected in Western Australia (HURST, 1978).

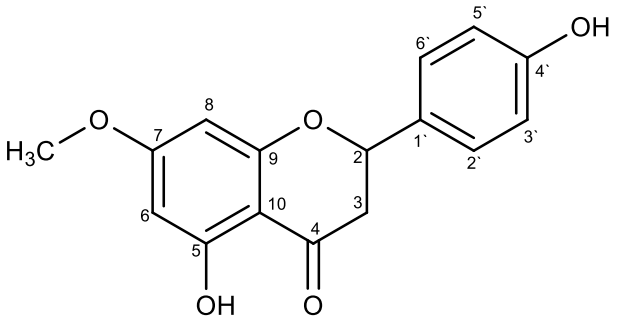

Figure 4-8: Chemical structure of Sakuranetin

Table 4-5: Chemical shifts for Sakuranetin

Position	**Sakuranetin**		Literature*	
	^{1}H δ ppm (mult, J in Hz)	^{13}C δ ppm, (mult)	^{1}H δ ppm, (mult, J in Hz)	^{13}C δ ppm, (mult)
1	-	-	-	-
2	5.34 (1H, d, 11.7)	79.0 (CH)	5.35 (1H, d, *J* = 11.7)	78.9
3a	3.09 (1H, dd, 17.2, 13.0)	43.2 (CH_2)	3.09(1H, dd, 17.0, 13.5)	43.2
3b	2.78 (1H, d, 13.2, 3.0)		2.79(1H, d, 13.5, 3.5)	
4	-	196.2 (C)	-	196.0
5	-	163.0 (C)	-	162.9
6	6.05 (1H, d, 2.2)	95.1(CH)	6.00 (1H, d, *J* = 2.2)	94.2
7	-	168.0 (C)	-	168.0
8	6.09 (1H, d, 2.2)	94.3 (CH)	6.04 (1H, d, *J* = 2.2)	95.1
9	-	162.9 (C)	-	164.1
10	-	103.1(C)	-	103.1
1`	-	130.2 (C)	-	130.7
2`	7.33 (1H, d, 8.6)	128.0 (CH)	7.35(1H, d)	128.0
3’	6.90 (1H, d, 8.6)	115.7 (CH)	6.89(1H, d)	115.7

4’		156.5 (C)		156.1
5’	6.90 (1H, d, 8.6)	115.7 (CH)	6.89(1H, d)	115.7
6`	7.33 (1H, d, 8.6)	128.0 (CH)	7.35(1H, d)	128.0
7-OCH_3	3.82 (3H, s)	55.7 (CH_3)	3.80(3H, s)	55.7
5-OH	12.02 (s)	-	12.03(1H, s)	-
4’-OH	-		5.02(1H, brs)	-

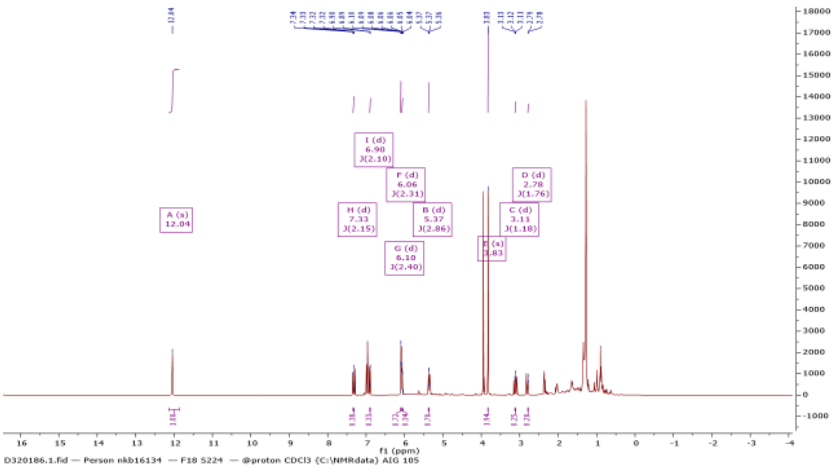

Figure 4-9: ^{1}H NMR (400 MHz) of Sakuranetin in $CDCl_3$

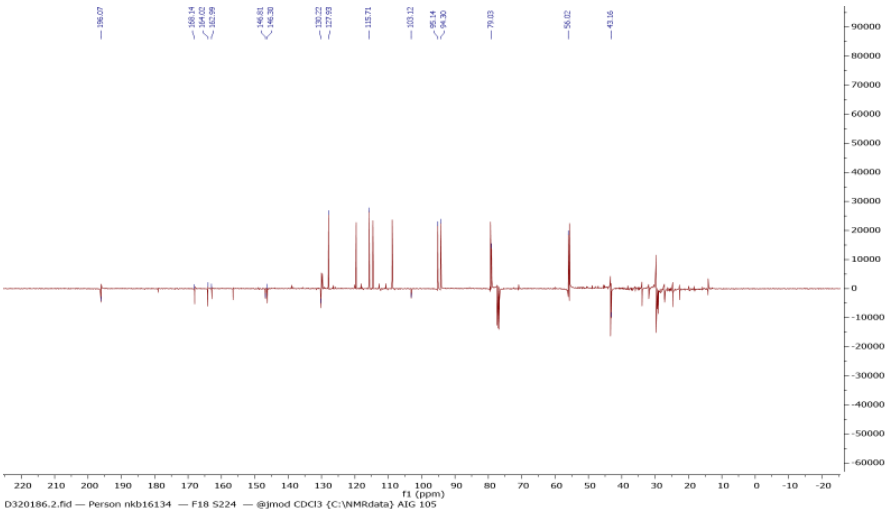

Figure 4-10: ^{13}C NMR (400 MHz) of Sakuranetin in $CDCl_3$

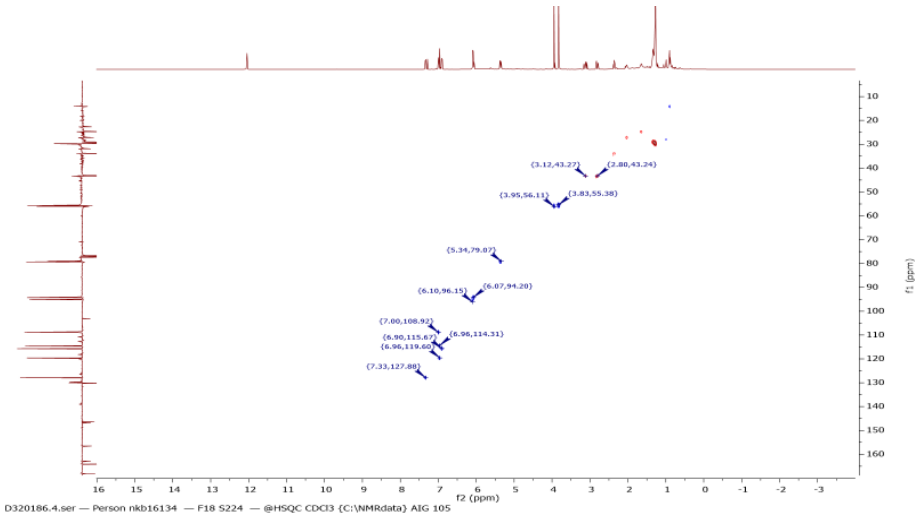

Figure 4-11: HSQC spectrum (400 MHz) of Sakuranetin in $CDCl_3$

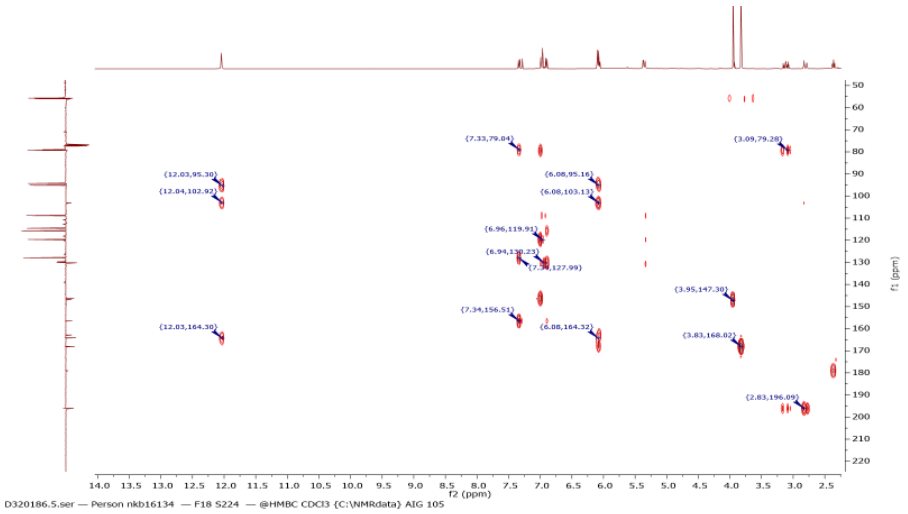

Figure 4-12: HMBC spectrum (400 MHz) of Sakuranetin in $CDCl_3$

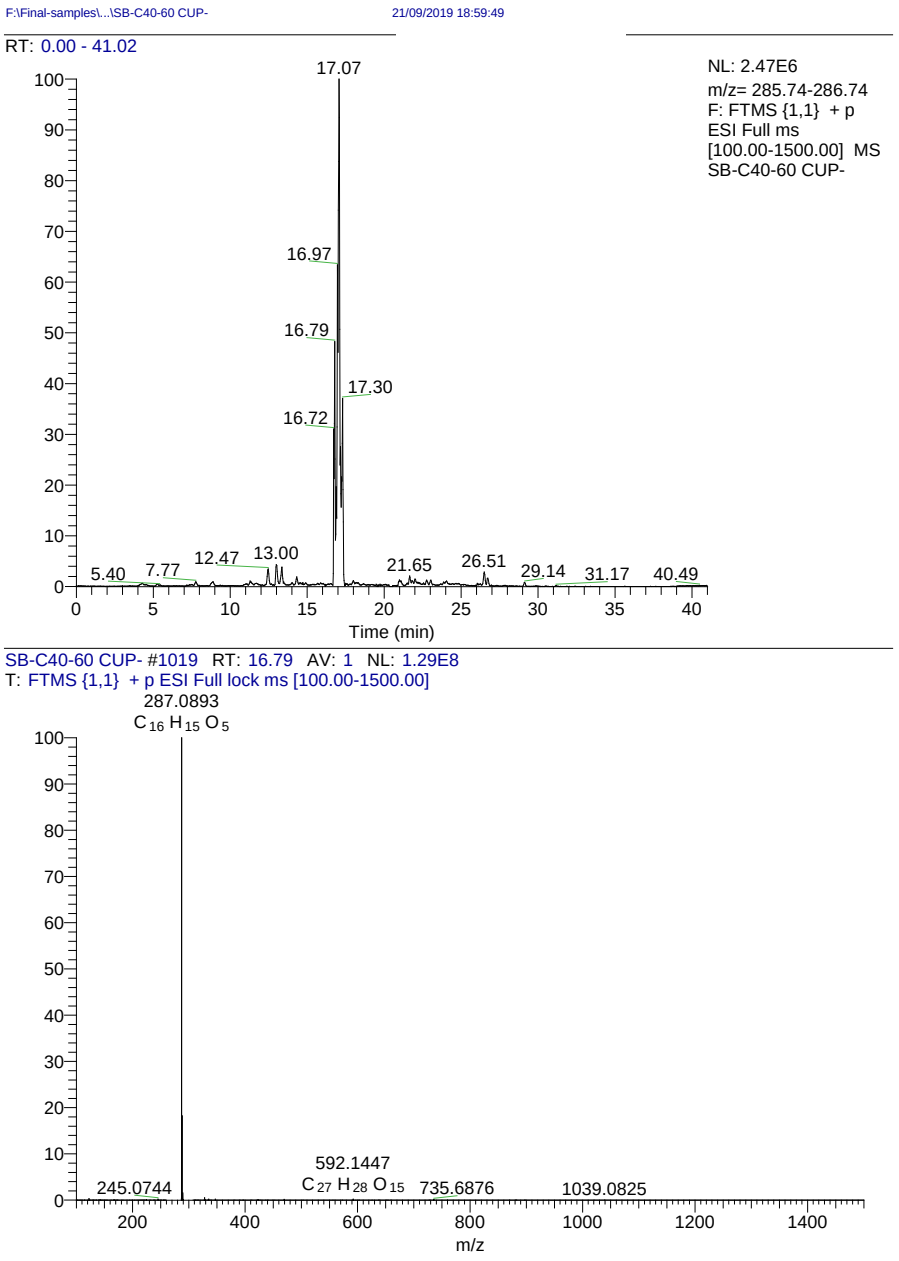

Figure 4-13: Extracted ion chromatogram and mass spectrum in positive ion mode for Sakuranetin ether

4.2.3 Characterisation of SB-H60-E40 as Lupeol (15)

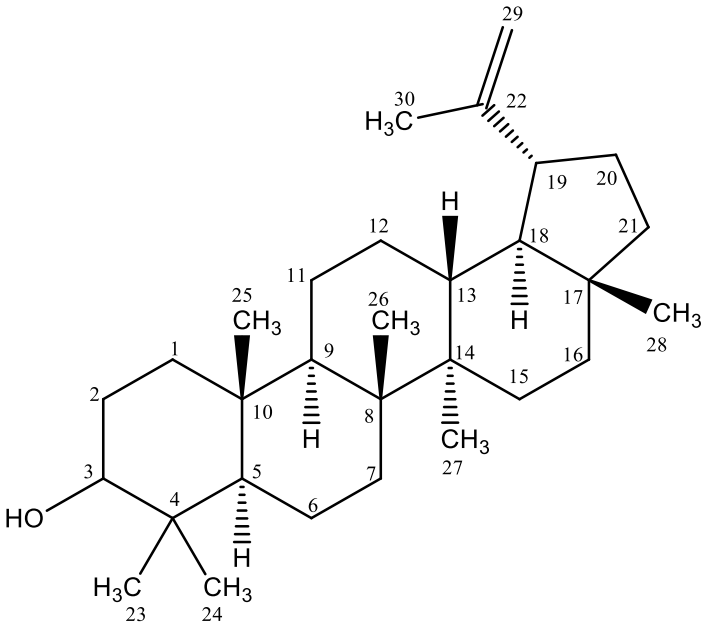

Figure 4-14: Chemical structure of Lupeol

The compound gave a purple spot characteristic of a terpenoid on spraying with Vanillin-sulfuric acid reagent and heating. The ^{1}H NMR spectrum Figure 4-15 gave two methylene protons at δ_H ppm 4.69 (d, J = 1.7 Hz) and 4.57, a methyl attached to a double bond at 1.69 ppm typical of the isopropylene side chain of a lupane triterpene. It also showed six other methyl groups between 0.77-1.04 ppm. Proton H-3 and H-19 were observed at 3.19 (dd, J = 11.2, 5.0 Hz) and 2.38 (ddd, J = 5.8, 11.0, 11.0 Hz) respectively. The ^{13}C NMR from the Dept-135 Figure 4-16 showed a total of 30 carbon atoms made up of seven methyl carbons, one oxygen-bearing carbon, one methylene carbon and one quaternary carbon attached to the methylene. No carbonyl carbon(s) were observed (confirmed by the absence of a carbonyl carbon in its ^{13}C NMR spectrum). Its proton and carbon chemical shifts are given in Table 4-6. The compound

was identified as lupeol, and the chemical shifts were in agreement with literature reports (Burns et al., 2000). Lupeol was previously isolated from red Brazilian propolis (Pereira et al., 2002).

Table 4-6: ^{1}H and ^{13}C NMR (400 MHz, CDCl3,) Data obtained for Lupeol

Position	Lupeol		Literature*	
	Proton (δ ppm)	Carbon (δ ppm)	Proton (δ ppm)	Carbon (δ ppm)
1	1.65, 0.89	38.94 (t)	1.67,0.90	38.72
2	1.58, 1.54	27.65 (t)	1.60,156	27.43
3	3.19	79.23 9 (d)	3.19	79.02
4	-	39.09 (s)	-	38.87
5	0.68	55.53 (d)	0.68	55.31
6	1.52, 1.37	18.55 (t)	1.51,1.39	18.33
7	1.40	34.52 (t)	1.39	34.29
8	-	41.07 (s)	-	40.84
9	1.27	50.68 (d)	1.27	50.35
10	-	37.40 (s)	-	37.18

11	1.44, 1.18	21.16 (t)	1.41,1.23	20.94
12	1.63, 1.04	25.38 (t)	1.67,1.07	25.16
13	1.65	38.29 (d)	1.66	38.07
14	-	43.06 (s)	-	42.85
15	1.69, 1.08	27.68 (t)	1.68,1.00	27.46
16	1.45, 1.21	35.81 (t)	1.47,137	35.60
17	-	43.23 (s)	-	43.01
18	1.55	48.54 (d)	1.36	48.32
19	2.38	48.21 (d)	2.38	48.00
20	-	151.20 (s)	-	150.98
21	1.96, 1.46	30.08 (t)	1.92,1.32	29.86
22	1.20, 1.34	40.23 (t)	1.19,138	40.02
23	0.95	28.21 (q)	0.97	28.00
24	0.77	15.59 (q)	0.76	15.38
25	0.83	16.34 (q)	0.83	16.13

26	1.04	16.20 (q)	1.03	15.99
27	0.98	14.78 (q)	0.94	14.56
28	0.80	18.23 (q)	0.78	18.02
29	4.69, 4.57	109.54 (t)	4.56,4.69	109.3
30	1.69	19.53 (q)	1.68	20.2

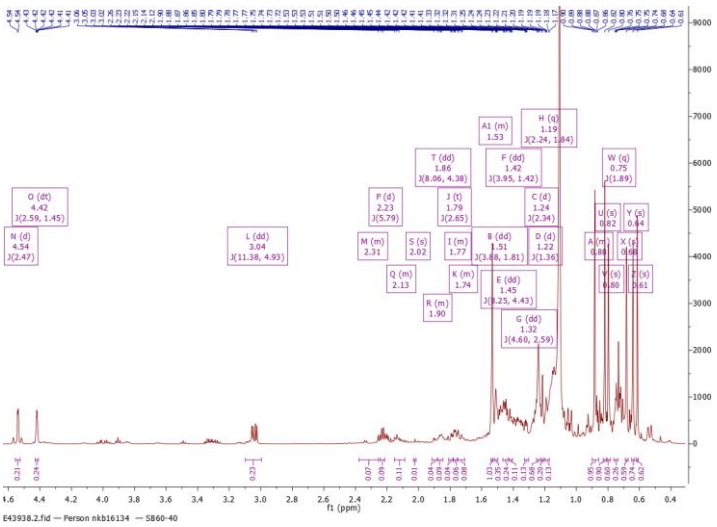

Figure 4-15: ^{1}H NMR (400 MHz) of Lupeol in $CDCl_3$

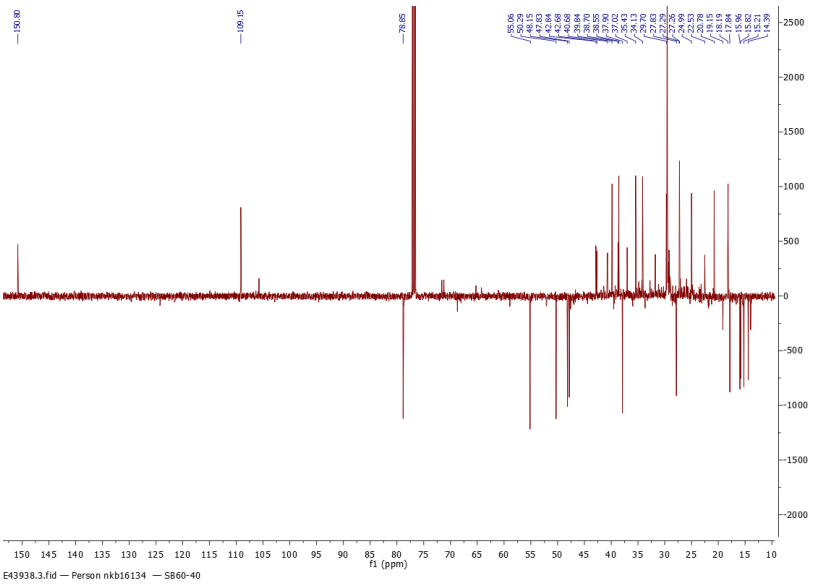

Figure 4-16: ^{13}C NMR (400 MHz) of Lupeol in $CDCl_3$

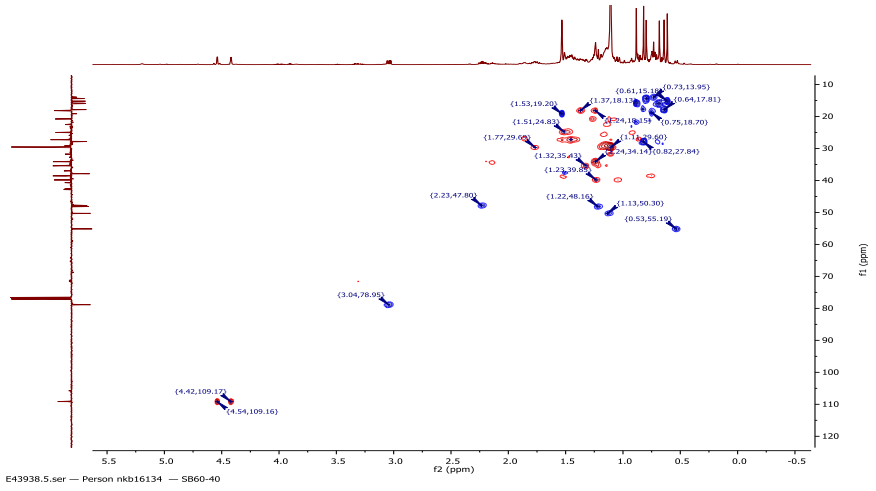

Figure 4-17: HSQC spectrum (400 MHz) of Lupeol in $CDCl_3$

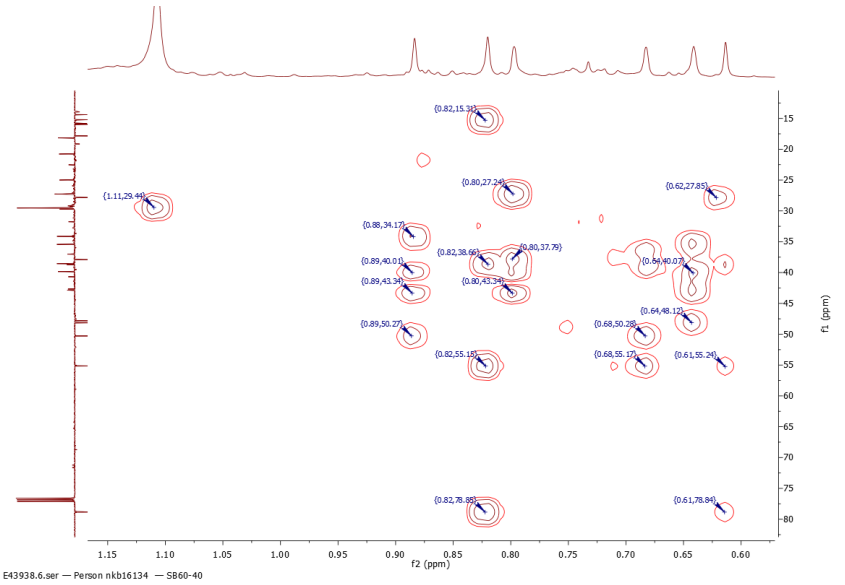

Figure 4-18: HMBC spectrum (400 MHz) of Lupeol in $CDCl_3$

4.3 The biological activity of a propolis sample from Saudi Arabia

4.3.1 In-vitro anti-trypanosomal activity of Saudi Arabia crude propolis extract and some of its pure compounds against *T. brucei* (S427) and *T. b. brucei* ISMR1

The EEP from the propolis sample from Saudi Arabia code (SB) and some of its pure compounds were tested against *T. brucei* (s427), B48 and *T. b. brucei* ISMR1, in comparison with pentamidine as a drug control and EC_{50} values, were calculated. The results showed that moderate activity against different *T. brucei* strains. The crude sample had moderate activity, as shown in Table 4-7. The isolated compound Lupeol had roughly the same value against *T. brucei* and *T. brucei* ISMR1 with EC_{50} values of 28.89 and 29.62 µg/mL, respectively. Also, two other isolated compounds Hesperetin-7-methyl ether and Sakuranetin, which were tested as a mixture, showed EC_{50} values of 100 > µg/mL.

Table 4-7: EC_{50} values(n=3) for Antitrypanosomal activity of crude Saudi Arabia sample (SB) and some of its pure compounds against *T. brucei* (s427), *T. brucei* B4 and *T. b. brucei* ISMR1.

Exp code	**Pure compound**	**Types of Trypanosoma**									
		Tb S427WT		**B48**				**ISMR1**			
		AVR	**SEM**	**AVR**	**SEM**	**RF**	**t-test**	**AVR**	**SEM**	**RF**	**t-test**
SB	**crude**	28.89	0.27	32.3	0.62	1.12	0.001	32.4	0.20	1.12	0.000020
SB CC40-60b	Hespereti n-7-methyl ether**(14a) and** Sakuraneti n**(14b)**	N/A	N/A	N/A	N/A	N/A	N/A	N/A	N/A	N/A	N/A
SB-C60-40	Lupeol**(15)**	29.62(69.46 µM)	0.18	31.7(74.34 µM)	0.31	1.07	0.0004	23.6(55.34 µM)	2.00	0.80	0.013
Pentamidine(µM)		0.00241	0.000430	0.57	0.473	0.05	195.89	0.000003	0.0017	21.8	<0.001

- N/A: Isolated compounds were inactive at 400 µg/mL

4.3.2 In vitro Cytotoxicity assay of crude propolis extract from Saudi Arabia (SB) and isolated compounds.

The ethanolic extract of propolis sample code (SB) from Saudi and its pure compounds isolated were tested for toxic activity against human cell line (THP cells) to evaluate their cytotoxicity and assess EC_{50} values(µg/mL) as Table 4-8. The result showed that although the crude sample had high cytotoxicity at 3.86 µg/mL, its isolated compounds had moderate values of cytotoxicity values at 38.5 and 62.12 µg/mL, respectively Table 4-8.

Table 4-8: EC_{50} of Cytotoxicity of Saudi Arabia crude sample and its pure compounds against THP cells.

Exp code	Type of sample	EC_{50} (µg/mL)
SB	crude	3.86
SB-C40-60	Hesperetin-7-methyl ether**(14a)and** Sakuranetin**(14b)**	38.5
SB-C60-40	Lupeol**(15)**	62.12(145.7 µM)

Sample code (T2) which was collected from Saudi Arabia was tested against *T. brucei* (s427) and *T. congolense* in comparison with pentamidine as a drug control and drug sensitivities were calculated the results as in Table 4-10 show that the crude sample T2 has high activity against *T. brucei* (s427) exhibiting an EC_{50} value at 7.56 µg/mL, while it had no activity against *T. congolense*. Toxic activity against the human cell line (THP cells) were carried out to evaluate their cytotoxicity and assesses EC_{50} values(µg/mL) and displayed high cytotoxicity at 9.38 µg/mL. This sample showed promising anti-trypanosomal activity, and from the elemental compositions shown in Table 4-9 combined with the RDB values, it contains diterpene acids which have been found both in Saudi and Libyan propolis samples(Siheri et al., 2014, Almutairi et al., 2014b). Unfortunately, however, there was not sufficient time to fractionate this sample further.

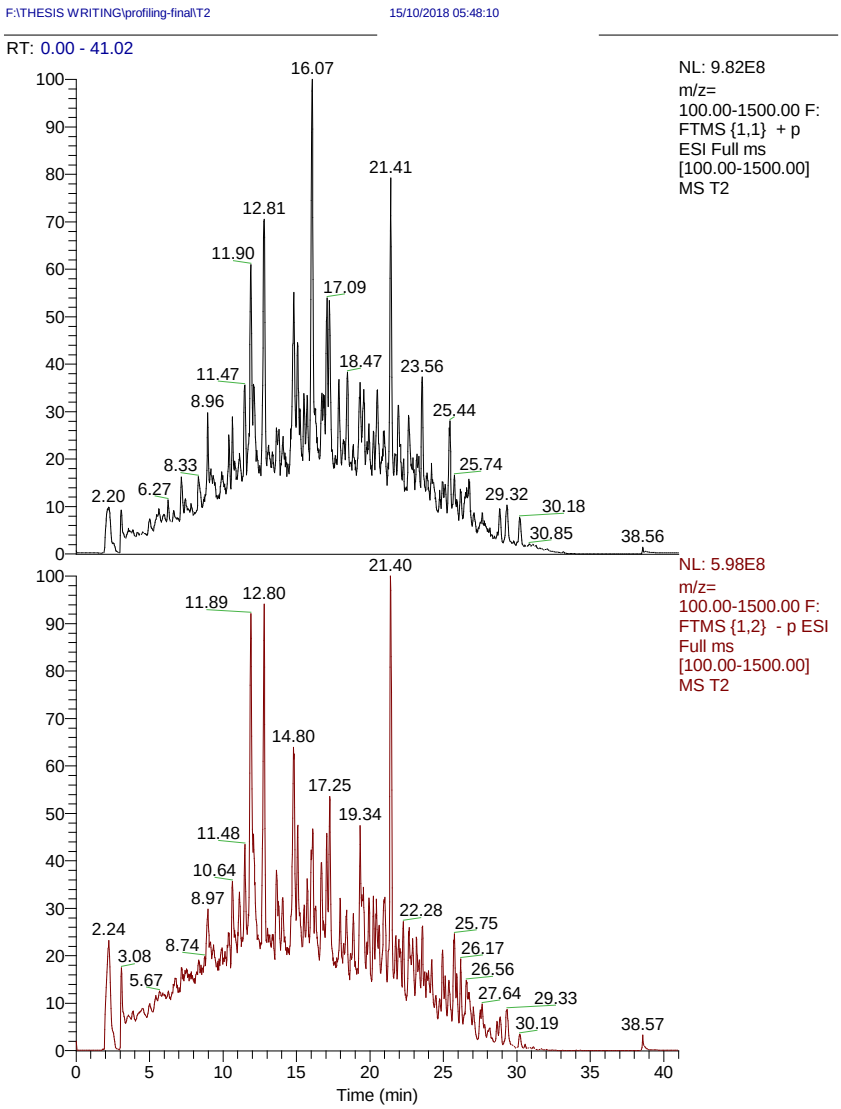

Figure 4-19: LC-MS chromatogram peaks of the EEP of T2

Table 4-9: The LC-MS profiling for EEP for Saudi propolis extract T2 in negative and positive ion mode.

Peak NoT2	Rt (time)	{M+1}	{M-1}	Chemical Formula	RDB	Delta (ppm)	intensity
1	3.02	163.03897		$C_9H_7O_3$	6.5	-0.056	3.09E6
2	7.17	285.2214		$C_{10}H_{11}O_4$	6.5	0.178	1.91E7
3	8.31	301.2164		$C_{20}H_{29}O_2$	6.5	0.193	9.36E6
4	8.94	303.2319		$C_{20}H_{31}O_2$	5.5	0.043	2.22E7
5	9.91	361.2352		$C_{22}H_{33}O_4$	6.5	-2.106	1.36E7
6	11.13	361.0920		$C_{18}H_{17}O_8$	10.5	0.216	2.30E7
7	11.43	299.2006		$C_{20}H_{27}O_2$	7.5	0.123	2.02E7
8	11.86	317.2112		$C_{20}H_{29}O_3$	6.5	0.089	8.54E7
9	13.58	345.0971		$C_{18}H_{17}O_7$	10.5	0.291	2.81E7
10	13.78	375.1077		$C_{19}H_{19}O_8$	10.5	0.256	8.65E7
11	17.90	389.1235		$C_{20}H_{21}O_8$	10.5	0.476	1.56E8
12	19.33	369.2791		$C_{25}H_{37}O_2$	7.5	0.333	4.96E7
13	19.55	419.1335		$C_{21}H_{23}O_9$	10.5	--.079	5.60E7
14	21.86	355.2994		$C_{25}H_{39}O$	6.5	-0.072	1.99E7
15	23.56	387.2893		$C_{25}H_{39}O_3$	6.5	-0.032	7.08E7
16	10.64		381.2288	$C_{21}H_{33}O_6$	5.5	1.464	4.13E7
17	11.91		333.2073	$C_{20}H_{29}O_4$	6.5	0.622	8.67E7
18	12.77		379.2127	$C_{21}H_{31}O_6$	6.5	0.417	1.19E8
19	13.68		313.0722	$C_{17}H_{13}O_6$	11.5	1.625	4.45E7
20	19.32		403.2857	$C_{25}H_{29}O_4$	6.5	0.885	8.64E7

Table 4-10: EC_{50} values for anti-trypanosomal activity of crude Saudi Arabia sample code(T2) against *T. brucei* (s427), T. and *T. congolense*. Cytotoxicity as well.

Exp code	Fraction	Tb S427WT		T. congolense		Cytotoxicity
		AVR	SEM	AVR	SEM	EC_{50} (µg/mL)
T2	crude	7.56	0.27	86.8	3.80	9.38
Pentamidine(µM)		0.0044	5.31E-04	0.81	0.04	-

5 Chapter 5

5.1 Discussion

The natural product called Propolis is collected by bees from plant sources to seal their hives to protect them from external contamination. The biological properties of propolis have captured the attention of researchers as a natural source of potential new drugs.

It is unlikely to be able to isolate pure compounds from propolis extracts with one analytical process due to the multiple constituents of the mixture; there are many aspects to be considered for isolation of compounds from natural extracts including stability, solubility (hydrophobicity or hydrophilicity), charge, molecular size and acid-base properties (Sak and practice, 2012) as a result, propolis samples, after initial fractionation, were subjected to further fractionation of similar fractions in polarity and molecular size. In this study, several flavonoids and phenolics were isolated by a range of chromatographic procedures, and their structures were characterised, the ethanolic extracts of European and Saudi propolis generated 15 known compounds.

In this work, twelve compounds two of them as amixture were isolated from four propolis samples from the UK, and two compounds from Polish propolis were characterised. In previous studies, most of these compounds were identified from two different geographical locations of Northern Italy where characterised flavonoids included Pinocembrin, Chrysin, Galangin, Pinobanskin-3-O-acetate, and Pinostrobin and several phenolic acids, Pinobanskin, Kaempferide, Apigenin (Pavlovic et al., 2020). Another study determined that the same classes of compounds are abundant in

new zealand propolis (Catchpole et al., 2015). The reason may be because, in temperate zones, bees collect propolis from different Poplar trees (Populus spp) with its chemical composition rich with flavonoids, aromatic acids and their esters (Bankova et al., 2000). This is supported by a study on ten propolis samples from Bulgaria, Italy, and Switzerland analysed by GC-MS, that found that most of the compounds were typical of poplar buds (Bankova et al., 2002). This data is in agreement with an earlier study for temperate poplar propolis from Turkey (Popova et al., 2005), suggesting that this might be the source of propolis samples in temperate zones.

Two other flavonoids as a mixture and one triterpenoid (Lupeol) were isolated from Saudi propolis extract; triterpenoid were previously reported to be the major compounds is Saudi propolis (Elnakady et al., 2017) and the most abundant categories in propolis of tropical origins as found in Brazilian red propolis (Trusheva et al., 2006).

Most of the compounds isolated had a flavonoid skeleton as shown in Figure **5-1**. The differences between the compounds were mostly in the saturation of the C-2 and C-3 bond (Structure F2) or unsaturation (Structure F1) in ring C. Those with a saturated ring C are known as flavanones. In contrast, those with unsaturated ring C are known as flavones. The next differences were in the substitution (-OH and $–OCH_3$) of ring B and the substitution of position C-7 with –OH or $–OCH_3$. Position C-3 in both structures could also be unsubstituted leading to three aliphatic protons in the flavanones (one deshielded and two shielded) and one aromatic or alkene proton singlet in the flavones or substituted by –OH in which case the H-3 proton singlet is absent in the flavones. Two deshielded aliphatic protons were observed in the 3-hydroxy

substituted flavanones or flavanonols. Since they all have the 5-OH which is usually H-bonded or chelated to the 4-C=O, the 5–OH proton appears between δ_H 11-13 ppm in the proton spectrum and the 4-C=O between δ_C 175 and 185 ppm in the flavones and between 190 and 200 ppm in the flavanones. Ring B can either be unsubstituted leading to a 5H set of multiplets or substituted at C-4′ leading to an AA′BB′ spin system or at C-3′ and C-4′ leading to an ABX substitution pattern. These structural features were easily confirmed using their 2D NMR correlations. Long-range correlations HMBC from the 5-OH usually identifies C-5, C-6 and C-10. Using the HSQC, proton H-6 is easily identified, and this proton is used to reveal C-8, H-8 (COSY) and C-7. Proton H-8 is used to identify C-9 and confirm C-7. This settles the chemical shifts for ring A. The presence of aliphatic protons implies ring C is saturated (Structure F2), which is confirmed by the high resonance of the C=O at C-4. Correlations from H-2 to aromatic ring B easily identifies C-2' and C-6' and subsequently H-2' and H-6'. Their multiplicity and integration determine if ring B is para or 4' substituted or 3' and 4'-disubstituted. Using the COSY spectrum, H-3' (if present) and H-5' are identified and their carbons too. For the flavones, an aromatic proton singlet indicates C-3 is unsubstituted, while the absence of the singlet indicates substitution usually by -OH. Correlations from this singlet identify C-1', C-10 and sometimes C-4, while correlations from H-2 when present identifies C-4 and confirms C-9. Finally, the chemical shifts are compared to literature reports, and a good agreement is used to confirm their structures.

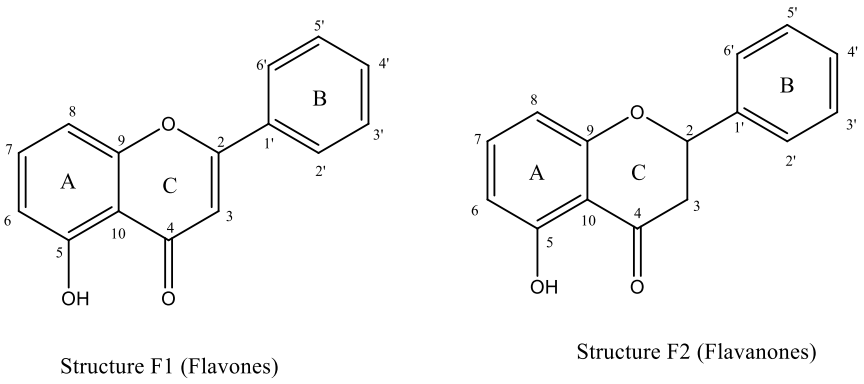

Figure 5-1: Flavonoid skeleton

The next class of compounds isolated were phenylpropanoids (Figure 5-2). These showed two trans coupled olefinic proton doublets between δ_H 6.00 and 7.50 ppm, (J = 16.0 Hz). Depending on the substitution of the aromatic ring; a C-4 substitution leads to an AA′BB′ spin system or substitution at C-3 and C-4 gives an ABX substitution while an unsubstituted phenyl ring leads to a 5H multiplet. Some of the compounds were esters with R in Figure 5-2 being a benzyl or phenethyl substituent. The carboxylic acid carbon was observed between δ_C 160 and 170 ppm. Similarly, a literature search for the spectra of identical compounds was used to confirm their structures.

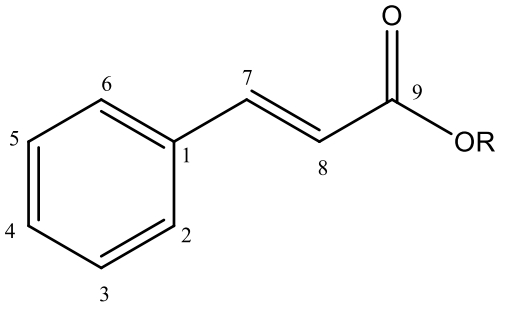

Figure 5-2: Phenylpropanoids

Several previous studies mentioned that propolis components isolated from various geographic locations are found to possess activity against bacteria and parasites (Dantas Silva et al., 2017, Burdock and toxicology, 1998, Almutairi et al., 2014a, Hashemi, 2016). Additionally, propolis showed high activity against *Leishmania donovani* and *Trypanosoma cruzi* (Aminimoghadamfarouj and Nematollahi, 2017, Alvarez-Suarez, 2017). It is worth noting that most drugs used to treat many diseases are toxic to healthy cells and have immune-suppressive side effects. Consequently, one of the essential aims of research in the biomedical sciences is to discover natural compounds that possess not only cytotoxic activity against various illnesses and pathogens but which also are non-toxic to healthy cells (Sak and practice, 2012).

Identification of high potency propolis samples with anti-protozoal and anti-microbial potency was of vital interest to this research to determine which had the highest biological activity, especially against *Trypanosoma* to lead us to attempt further fractionation for purification of those compounds that might be of responsible activity against *Trypanosoma*.

European and Saudi propolis samples were evaluated for antibacterial activity against *S. aureus*, *T.brucei* and two genetically modified strains, that are pentamidine resistant and cytotoxic activity against human cell line (THP cells) were identified.

European propolis including UK and Poland: Results of biological activity of samples from the UK against Trypanosoma which are presented in Table 3-29 were considered as having significant activity at EC_{50} ≤1.0 µg/mL, moderate activity with EC_{50} range 2.0-20µg/mL, and low activity with EC_{50} >25.0. Therefore, all ethanolic

extracts of propolis showed high activity except the sample S225, which revealed moderate activity at 14.04 µg/mL. Polish propolis shown in Table 3-38 exhibited high activity as well.

Focussing on the isolated compounds that have antiprotozoal activity against Trypanosoma brucie and two different genetically modified strains, that are pentamidine resistant, flavonoids and phenolics which were isolated from the UK propolis including (Pinobanksin 3-O-acetate (1), Kaempferol(3), 4'-Methoxykaempferol(5), Galangin(6), Chrysin(7), Apigenin(8), and Cinnamic acid (10) exhibited activity against T. brucei and two different genetically modified strains B48 and ISMR1 with EC_{50} <10 µg/mL. Additionally, Pinocembrin (4) and Pinostrobin(9) showed moderate activity with EC_{50} < 10-20 µg/mL. The most biologically active compound isolated was Apigenin(8) shown in Figure 3-45 with EC_{50} values of 2.74, 2.6 and 2.5 µg/mL for *T. brucei*, B48 and ISMR1, respectively. Apigenin is commonly available as a food supplement in high doses and thus has established low toxicity and could readily be taken in doses which would be toxic to Trypanosoma. No activity was observed for 7-Methoxychrysin (2). Although these compounds were previously isolated from propolis samples from different areas such as Poland, Italy, Jordon (Noudeh et al., 2010, Maciejewicz and technologies, 2001), this is the first study that has isolated and characterised constituents of the EEP samples from the UK and investigated the anti-trypanosomal activity. Propolis samples from Bulgaria which were evaluated for their activity against *Trypanosoma cruzi* as well as both acetone and ethanol extracts of the two samples showed strong inhibitory activity against *T.*

cruzi. The high activity similarity of those propolis samples could be due to the isolated compounds such as flavonoids in the UK which makes them similar to Bulgarian samples which contain a high level of flavonoids (Prytzyk et al., 2003). Regarding their cytotoxicity against human cell line (THP cells), the classification of the cytotoxic activity according to (Atjanasuppat et al., 2009) was divided into four groups based on EC_{50} values as follows: highly active (≤20µg/mL), moderately active (>20-100 µg/mL), weakly active (>100-1000µg/mL) and inactive extracts (>1000 µg/mL). Thus, four pure compounds Pinobanksin 3-O-acetate (1), Kaempferol(3), Galangin (6) and Chrysin (7) were shown to have a high level of cytotoxicity with values of EC_{50} <20 µg/mL, the rest of compounds had moderate activity except for Pinostrobin(9) which showed a weak cytotoxic activity of up to 100 µg/mL Table 3-32.

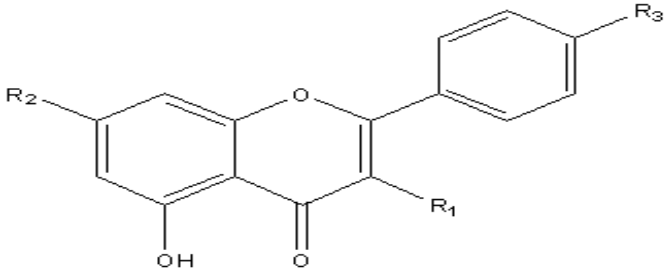

Isolated compound	type of flavonoid	R1	R2	R3
Pinobanksin 3-O-acetate (1)	flavone	$OCOCH_3$	OH	H
7-Methoxychrysin (2)	flavone	H	OCH_3	H
Kaempferol (3)	flavonol	OH	OH	OH
4'-Methoxykaempferol (5)	flavonol	OH	OH	OCH_3
Galangin (6)	flavonol	OH	OH	H
Chrysin (7)	flavone	H	OH	H
Apigenin (8)	flavone	H	OH	OH

Figure 5-3: Flavones/flavonols

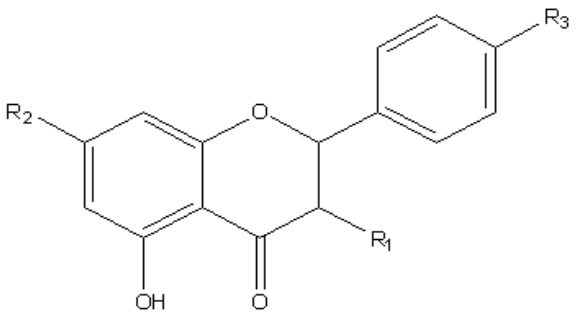

Isolated compound	type of flavonoid	R1	R2	R3
Pinocembrin (4)	flavonone	H	OH	H
Pinostrobin (9)	flavonone	H	OCH_3	H

Figure 5-4: Flavonone/flavononol

The study continued in more detail with the four active samples collected from different regions in the UK, using different chromatographic techniques to fractionate them in an attempt to isolate the components that might be responsible for the activity. Most compounds were identified as flavonoids and structurally elucidated by NMR and LC-MS. Within the classes of compounds isolated it appeared that the flavones as in Figure 5-3, which have a 2,3-double bond in the C ring and presence of hydroxyl group in the B ring such as Apigenin (8) were the more active anti-trypanosomal compounds. Thus, it is noticeable that Apigenin is a more active isomer of Galangin (6), so a hydroxyl group in the B ring gives higher activity than one in the C ring. Kaempferol (3), which has the same structure as Apigenin but has a 3-hydroxyl group in the C-ring, has less activity compared to Apigenin which led to the suggestion that the flavones are more active against Trypanosoma than flavonols. Additionally, Methyl kaempferol (5) is more active than Kaempferol, so methylation can increase activity, as is noticed in the flavanones by comparing the activity of Pinocembrin (4) and

Pinostrobin (9). The presence of a methoxy group is believed to be the cause of the increased activity of Pinostrobin over Pinocembrin, as observed in Figure 5-4.

A small variation in structure appeared to produce a noticeable difference in anti-trypanosomal activity. With flavanones being less active than flavones, this is evident by comparing the activity of Chrysin (7) and Pinocembrin (4) where Chrysin was more active and this could be attributed to the presence of a 2,3-double bond in the C ring.

There is a strong indication that the hydroxyl or methoxy group in the B ring could be contributing to the increased anti-trypanosomal activity. Regarding the influence of functional groups and the substitution effect of hydroxyl and methoxy groups, these conclusions generally agree with the study that evaluated the relationship between the structures of flavonoids and their activity against three typical influenza virus strains (Liu et al., 2008). Additionally, it may correspond to what was observed in a study of the anti-genotoxicity of flavonoids (Heo et al., 2001).

The two flavonoids identified from Polish propolis as 4’,7-Dimethoxykaempferol (12) and Naringenin 4',7-dimethyl ether (13) were tested against *Trypanosoma brucei* and two strains exhibiting pentamidine resistance. Although the crude sample had a high activity with an EC_{50} value of 4.5 µg/mL, one of these compounds (4’,7-Dimethoxykaempferol(12)) exhibited low activity with EC_{50} > 25 µg/mL, which suggests that the hydroxyl group at the 7 position may be important for activity when the activity is compared with that of 4'-Methoxyakaempferol. Naringenin 4',7-dimethyl ether(13) displayed a similar result to the crude sample, as shown in Table

3-38. When their cytotoxicity against human cell lines (THP cells) were evaluated, the crude sample and 4',7-Dimethoxykaempferol (12) had moderate activity (>20-100 µg/mL). However, Naringenin 4',7-dimethyl ether(13) showed weak cytotoxicity of up to 100 µg/mL, as shown in Table 3-39.

To my knowledge, there are limited studies about the biological activities against protozoa for samples of Saudi propolis. Hence, anti-trypanosomal activity and cytotoxicity were evaluated in this study for two Saudi propolis samples. Two ethanolic extracts of Saudi propolis were evaluated for anti-protozoal activity, and the results revealed that sample SB had a low activity with EC_{50} > 25 µg/mL, while T2 exhibited moderate activity with EC_{50} value at 7.9 µg/mL. Lupeol (15), which was isolated from sample SB had an activity equal to the crude sample. From the same sample, two flavonoids were isolated as a mixture of Hesperetin-7-methyl ether (14a) and Sakuranetin (14b), but they showed no activity against *T. brucie* and two different genetically modified strains, that are pentamidine resistant, Table 4-7. As for the cytotoxic activity, although the crude sample had strong activity against the human cell line (THP cells), its isolated compounds had moderate activity (>20-100 µg/mL).

6 Chapter 6

6.1 Conclusions and Further Work

A total of 15 compounds were isolated during this study; two of these were in a mixture. Summaries of the compounds isolated are shown in Table **6-1**. None of the compounds was novel although several had not been isolated from propolis before. All the isolated compounds and crude extracts from the propolis samples were tested for cytotoxicity as well as activity against different strains of *T.brucie*. None of the purified compounds was more active against *T.brucei* than crude extracts suggesting synergy between the different compounds within the extracts. At the beginning of this study, 35 samples of European propolis were tested for activity against *T.brucie*, *Leishmania mexicana* and *Crithidia fasiculata*. The results from this study were included in the published paper in appendix 1. In this preliminary screen of European samples modelling of the data suggested that Galangin and Methoxychrysin would be the most active individual compounds. Both of these compounds were isolated in the current study, and Galangin was one of the most active compounds isolated and tested. However, Methoxychrysin showed much lower activity. It might be that together these two compounds show some synergy.

With regard to future work, there are still many components within temperate propolis to isolate and although in this study, some of the major components have been isolated. Some of the minor components should be isolated and tested for antiprotozoal activity. The Saudi propolis sample exhibited very good activity in the crude extract, and it

would be interesting to isolate the active components from this sample. Overall, there is still a great deal to be understood regarding the significance of propolis to the bee, the variations in its constituents and elucidation of the structures and testing of the full range of components within propolis.

Table 6-1: Summary of isolated compounds in this study

S/N	Chemical name	Molecular formula	Molecular weight	Method (A/B)	Fraction code	Sample code	Sample origin
1	**3-Acetoxypinobanksin**	$C_{17}H_{13}O_6$	313.0728 (-ve)	A	C1-H40-E60-MPLC-F6	S224	UK
2	**7-Methoxychrysin**	$C_{16}H_{13}O_4$	269.0790(+ve)	A	C1H60-E40-MPLC-F3+4	S224	UK
3	**Kaempferol**	$C_{15}H_{10}O_6$	285.0403(-ve)	A	C3+4-H40-E60-M14-S7	S224	UK
				B	C1-40-60-S12	D6	UK
4	**Pinocembrin**	$C_{15}H_{11}O_4$	255.0665(-ve)	A	C H60-E40-mplc8-15-F4	S224	UK
				B	C3 H60-E40-F5	D6	UK
				B	C1-H60-E40-F5+6	D7	UK
5	**4'-Methoxykaempferol**	$C_{16}H_{13}O_6$	301.0701(+ve)	B	C6S-C-H40-E60-S9	S224	UK
				A	S224-C3+4-40-60-MPLC-15+16-F9	S224	UK
				A	S224-C1-40-60-MPLC-F7+8-F4	S224	UK
6	**Galangin**	$C_{15}H_9O_5$	269.450(-ve)	B	C6L-H40-E60-S8	S224	UK

				A	C3+4-40-60-MPLC-F19	S224	UK
				B	C3 H60-E40	D6	UK
				B	C2-H60-E40-S8	D7	UK
7	**Chrysin**	$C_{15}H_{11}O_4$	255.0632(+ve)	B	D7-C1-40-60-S17	D7	UK
				A	S224-C1-40-60-MPLC-F16	S224	UK
8	**Apigenin**	$C_{15}H_9O_5$	269.0458(-ve)	B	D6-C1-H40-E60-SE-F8	D6	UK
9	**Pinostrobin**	$C_{16}H_{15}O_4$	271,0939(+ve)	B	F1 VLC C60-40-C20-25	S224	UK
10	**Cinnamic acid**	$C_9H_9O_2$	149.0629(+ve)	B	F1 VLC C20-80-C30-33	S225	UK
11a	**Coumaric acid cinnamyl ester**	$C_{18}H_{16}O_3$	279.0998(-ve)	B	F1 VLC C1H40-E60-C10-12	S225	UK
11b	**Coumaric acid benzyl ester**	$C_{16}H_{15}O_3$	255.0995(+ve)	B	F1 VLC C1H40-E60-C10-12	S225	UK
12	**4',7-Dimethoxykaempferol**	$C_{17}H_{15}O_6$	315.0838(+ve)	B	P-F26	P	POLAND
13	**Naringenin 4',7-dimethyl ether**	$C_{17}H_{17}O_5$	301.1044(+ve)	B	P-F20	P	POLAND
14a	**Hesperetin-7-methy ether**	$C_{17}H_{17}O_6$	317.100(+ve)	B	SB-C 40-60-F1CUP	SB	SAUDI ARABIA
14b	**Sakuranetin**	$C_{16}H_{14}O_5$	285.0797 (-ve)	B	SB-C 40-60-F1CUP	SB	SAUDI ARABIA
15	**Lupeol**	$C_{30}H_{49}O$	425.3723(+ve)	B	SB-H60-E40	SB	SAUDI ARABIA

7 References

AL-ANI, I., ZIMMERMANN, S., REICHLING, J. & WINK, M. J. M. 2018. Antimicrobial activities of European propolis collected from various geographic origins alone and in combination with antibiotics. 5**,** 2.

ALDAY, E., NAVARRO-NAVARRO, M., GARIBAY-ESCOBAR, A., ROBLES-ZEPEDA, R., HERNANDEZ, J., VELAZQUEZ, C. J. B. & RESEARCH, B. C. A. I. 2016. Advances in pharmacological activities and chemical composition of propolis produced in Americas.

ALMUTAIRI, S., EAPEN, B., CHUNDI, S. M., AKHALIL, A., SIHERI, W., CLEMENTS, C., FEARNLEY, J., WATSON, D. G. & EDRADA-EBEL, R. J. P. L. 2014a. New anti-trypanosomal active prenylated compounds from African propolis. 10**,** 35-39.

ALMUTAIRI, S., EDRADA-EBEL, R., FEARNLEY, J., IGOLI, J. O., ALOTAIBI, W., CLEMENTS, C. J., GRAY, A. I. & WATSON, D. G. J. P. L. 2014b. Isolation of diterpenes and flavonoids from a new type of propolis from Saudi Arabia. 10**,** 160-163.

ALQARNI, A. M., FERRO, V. A., PARKINSON, J. A., DUFTON, M. J. & WATSON, D. G. J. V. 2018. Effect of melittin on metabolomic profile and cytokine production in PMA-differentiated THP-1 cells. 6**,** 72.

ALVAREZ-SUAREZ, J. M. 2017. *Bee products-chemical and biological properties*, Springer.

AMINIMOGHADAMFAROUJ, N. & NEMATOLLAHI, A. J. I. J. O. M. S. 2017. Propolis diterpenes as a remarkable bio-source for drug discovery development: a review. 18**,** 1290.

ANJUM, S. I., ULLAH, A., KHAN, K. A., ATTAULLAH, M., KHAN, H., ALI, H., BASHIR, M. A., TAHIR, M., ANSARI, M. J. & GHRAMH, H. A. J. S. J. O. B. S. 2019. Composition and functional properties of propolis (bee glue): A review. 26**,** 1695-1703.

ATJANASUPPAT, K., WONGKHAM, W., MEEPOWPAN, P., KITTAKOOP, P., SOBHON, P., BARTLETT, A. & WHITFIELD, P. J. J. J. O. E. 2009. In vitro screening for anthelmintic and antitumour activity of ethnomedicinal plants from Thailand. 123**,** 475-482.

BAIANU, I. & PRISECARU, V. 2011. NMR, NIR, and Infrared Spectroscopy of Carbohydrate–Protein Interactions and Glycoproteins. *NMR Spectroscopy of Polymers: Innovative Strategies for Complex Macromolecules.* ACS Publications.

BAKDASH, A., ALMOHAMMADI, O., TAHA, N. A., ABU-RUMMAN, A. & KUMAR, S. J. C. J. F. S. 2018. chemical composition of propolis from the Baha Region in Saudi Arabia. 36**,** 00-10.

BANKOVA, V., POPOV, S. & MAREKOV, N. J. J. O. N. P. 1983. A study on flavonoids of propolis. 46**,** 471-474.

BANKOVA, V., POPOVA, M., BOGDANOV, S. & SABATINI, A.-G. J. Z. F. N. C. 2002. Chemical composition of European propolis: expected and unexpected results. 57**,** 530-533.

BANKOVA, V. J. E.-B. C. & MEDICINE, A. 2005. Recent trends and important developments in propolis research. 2.

BANKOVA, V. J. J. O. E. 2005. Chemical diversity of propolis and the problem of standardization. 100**,** 114-117.

BANKOVA, V. S., DE CASTRO, S. L. & MARCUCCI, M. C. J. A. 2000. Propolis: recent advances in chemistry and plant origin. 31**,** 3-15.

BANSKOTA, A. H., TEZUKA, Y. & KADOTA, S. J. P. R. 2001. Recent progress in pharmacological research of propolis. 15**,** 561-571.

BARRETT, M. P., BOYKIN, D. W., BRUN, R. & TIDWELL, R. R. J. B. J. O. P. 2007. Human African trypanosomiasis: pharmacological re-engagement with a neglected disease. 152**,** 1155-1171.

BARRETT, M. P. & CROFT, S. L. J. B. M. B. 2012. Management of trypanosomiasis and leishmaniasis. 104**,** 175-196.

BERTELLI, D., PAPOTTI, G., BORTOLOTTI, L., MARCAZZAN, G. L. & PLESSI, M. J. P. A. 2012. 1H-NMR simultaneous identification of health-relevant compounds in Propolis extracts. 23**,** 260-266.

BETANCES-SALCEDO, E., REVILLA, I., VIVAR-QUINTANA, A. M. & GONZÁLEZ-MARTÍN, M. I. J. S. 2017. Flavonoid and antioxidant capacity of propolis prediction using near infrared spectroscopy. 17**,** 1647.

BOUTEILLE, B., OUKEM, O., BISSER, S., DUMAS, M. J. F. & PHARMACOLOGY, C. 2003. Treatment perspectives for human African trypanosomiasis. 17**,** 171-181.

BOYCE, G., SHOEB, M., KODALI, V., MEIGHAN, T., ROBERTS, J. R., ERDELY, A., KASHON, M. & ANTONINI, J. M. J. P. O. 2020. Using liquid chromatography mass spectrometry (LC-MS) to assess the effect of age, high-fat diet, and rat strain on the liver metabolome. 15**,** e0235338.

BREITMAIER, E. & SINNEMA, A. 1993. Structure elucidation by NMR in organic chemistry.

BRIDGES, D. J., GOULD, M. K., NERIMA, B., MÄSER, P., BURCHMORE, R. J. & DE KONING, H. P. J. M. P. 2007. Loss of the high-affinity pentamidine transporter is responsible for high levels of cross-resistance between arsenical and diamidine drugs in African trypanosomes. 71**,** 1098-1108.

BROWN, M., NOURSADEGHI, M., BOYLE, J. & DAVIDSON, R. J. B. J. O. D. 2005. Successful liposomal amphotericin B treatment of Leishmania braziliensis cutaneous leishmaniasis. 153**,** 203-205.

BURDOCK, G. J. F. & TOXICOLOGY, C. 1998. Review of the biological properties and toxicity of bee propolis (propolis). 36**,** 347-363.

BURNS, D., REYNOLDS, W. F., BUCHANAN, G., REESE, P. B. & ENRIQUEZ, R. G. J. M. R. I. C. 2000. Assignment of 1H and 13C spectra and investigation of hindered side-chain rotation in lupeol derivatives. 38**,** 488-493.

CASTALDO, S. & CAPASSO, F. J. F. 2002. Propolis, an old remedy used in modern medicine. 73**,** S1-S6.

CATCHPOLE, O., MITCHELL, K., BLOOR, S., DAVIS, P. & SUDDES, A. J. F. 2015. Antiproliferative activity of New Zealand propolis and phenolic compounds vs human colorectal adenocarcinoma cells. 106**,** 167-174.

CELIŃSKA-JANOWICZ, K., ZARĘBA, I., LAZAREK, U., TEUL, J., TOMCZYK, M., PAŁKA, J. & MILTYK, W. J. F. I. P. 2018. Constituents of propolis: Chrysin, caffeic acid, p-coumaric acid, and ferulic acid induce PRODH/POX-dependent apoptosis in human tongue squamous cell carcinoma cell (CAL-27). 9**,** 336.

CERONE, M., ULIASSI, E., PRATI, F., EBILOMA, G. U., LEMGRUBER, L., BERGAMINI, C., WATSON, D. G., DE AM FERREIRA, T., ROTH CARDOSO, G. S. H. & SOARES ROMEIRO, L. A. J. C. 2019. Discovery of Sustainable Drugs for Neglected Tropical Diseases: Cashew Nut Shell Liquid (CNSL)-Based Hybrids Target Mitochondrial Function and ATP Production in Trypanosoma brucei. 14**,** 621-635.

CONNELLY, J. C., CONNOR, S. C., MONTE, S., BAILEY, N. J., BORGEAUD, N., HOLMES, E., TROKE, J., NICHOLSON, J. K., GAVAGHAN, C. L. J. D. M. & DISPOSITION 2002. Application of directly coupled high performance liquid chromatography-NMR-mass spectometry and 1H NMR spectroscopic studies to the investigation of 2, 3-benzofuran metabolism in Sprague-Dawley rats. 30**,** 1357-1363.

DA SILVA, S. S., MIZOKAMI, S. S., FANTI, J. R., MIRANDA, M. M., KAWAKAMI, N. Y., TEIXEIRA, F. H., ARAÚJO, E. J., PANIS, C., WATANABE, M. A. & SFORCIN, J. M. J. P. R. 2016. Propolis reduces Leishmania amazonensis-induced inflammation in the liver of BALB/c mice. 115**,** 1557-1566.

DANTAS, A. P., SALOMÃO, K., BARBOSA, H. S. & DE CASTRO, S. L. J. M. D. I. O. C. 2006. The effect of Bulgarian propolis against Trypanosoma cruzi and during its interaction with host cells. 101**,** 207-211.

DANTAS SILVA, R. P., MACHADO, B. A. S., BARRETO, G. D. A., COSTA, S. S., ANDRADE, L. N., AMARAL, R. G., CARVALHO, A. A., PADILHA, F. F., BARBOSA, J. D. V. & UMSZA-GUEZ, M. A. J. P. O. 2017. Antioxidant, antimicrobial, antiparasitic, and cytotoxic properties of various Brazilian propolis extracts. 12**,** e0172585.

DARWISH, R. M., RA'ED, J., ZARGA, M. H. A. & NAZER, I. K. J. A. J. O. B. 2010. Antibacterial effect of Jordanian propolis and isolated flavonoids against human pathogenic bacteria. 9.

DAS, A. B., GOUD, V. V. & DAS, C. 2019. Phenolic compounds as functional ingredients in beverages. *Value-Added Ingredients and Enrichments of Beverages.* Elsevier.

DAVIDSON, R. N. 2005. Leishmaniasis. *Medicine,* 33**,** 43-46.

DE KONING, H. P., MACLEOD, A., BARRETT, M. P., COVER, B., JARVIS, S. M. J. M. & PARASITOLOGY, B. 2000. Further evidence for a link between melarsoprol resistance and P2 transporter function in African trypanosomes. 106**,** 181-185.

DUMAS, M.-E., CANLET, C., ANDRÉ, F., VERCAUTEREN, J. & PARIS, A. J. A. C. 2002. Metabonomic Assessment of Physiological Disruptions Using 1H− 13C HMBC-NMR Spectroscopy Combined with Pattern Recognition Procedures Performed on Filtered Variables. 74**,** 2261-2273.

DVOŘÁČKOVÁ, E., ŠNÓBLOVÁ, M. & HRDLIČKA, P. J. J. O. S. S. 2014. Carbohydrate analysis: From sample preparation to HPLC on different stationary phases coupled with evaporative light-scattering detection. 37**,** 323-337.

EL SOHAIMY, S., MASRY, S. J. A.-E. J. A. & SCI, E. 2014. Phenolic content, antioxidant and antimicrobial activities of Egyptian and Chinese propolis. 14**,** 1116-1124.

ELNAKADY, Y. A., RUSHDI, A. I., FRANKE, R., ABUTAHA, N., EBAID, H., BAABBAD, M., OMAR, M. O. & AL GHAMDI, A. A. J. S. R. 2017. Characteristics, chemical compositions and biological activities of propolis from Al-Bahah, Saudi Arabia. 7**,** 41453.

ELYASHBERG, M. J. T. T. I. A. C. 2015. Identification and structure elucidation by NMR spectroscopy. 69**,** 88-97.

FREITAS, S., SHINOHARA, L., SFORCIN, J. & GUIMARÃES, S. J. P. 2006. In vitro effects of propolis on Giardia duodenalis trophozoites. 13**,** 170-175.

FUNAKOSHI-TAGO, M., OKAMOTO, K., IZUMI, R., TAGO, K., YANAGISAWA, K., NARUKAWA, Y., KIUCHI, F., KASAHARA, T. & TAMURA, H. J. I. I. 2015. Anti-inflammatory activity of flavonoids in Nepalese propolis is attributed to inhibition of the IL-33 signaling pathway. 25**,** 189-198.

GHISALBERTI, E., JEFFERIES, P., LANTERI, R. & MATISONS, J. J. E. 1978. Constituents of propolis. 34**,** 157-158.
GOULD, M. K., VU, X. L., SEEBECK, T. & DE KONING, H. P. J. A. B. 2008. Propidium iodide-based methods for monitoring drug action in the kinetoplastidae: comparison with the Alamar Blue assay. 382**,** 87-93.
GRANADOS-PINEDA, J., URIBE-URIBE, N., GARCÍA-LÓPEZ, P., RAMOS-GODINEZ, M. D. P., RIVERO-CRUZ, J. F. & PÉREZ-ROJAS, J. M. J. M. 2018. Effect of pinocembrin isolated from Mexican brown propolis on diabetic nephropathy. 23**,** 852.
GUDIN, S., QUASHIE, N. B., CANDLISH, D., AL-SALABI, M. I., JARVIS, S. M., RANFORD-CARTWRIGHT, L. C. & DE KONING, H. P. J. E. P. 2006. Trypanosoma brucei: a survey of pyrimidine transport activities. 114**,** 118-125.
HASHEMI, J. M. J. E. J. A. S. 2016. Biological effect of bee propolis: a review. 8**,** 311-318.
HAUSEN, B., WOLLENWEBER, E., SENFF, H. & POST, B. J. C. D. 1987. Propolis allergy: (I). Origin, properties, usage and literature review. 17**,** 163-170.
HAVSTEEN, B. J. B. P. 1983. Flavonoids, a class of natural products of high pharmacological potency. 32**,** 1141-1148.
HELENO, S. A., MARTINS, A., QUEIROZ, M. J. R. & FERREIRA, I. C. J. F. C. 2015. Bioactivity of phenolic acids: Metabolites versus parent compounds: A review. 173**,** 501-513.
HEO, M. Y., SOHN, S. J. & AU, W. W. J. M. R. R. I. M. R. 2001. Anti-genotoxicity of galangin as a cancer chemopreventive agent candidate. 488**,** 135-150.
HERNÁNDEZ-RODRÍGUEZ, P., BAQUERO, L. P. & LARROTA, H. R. 2019. Flavonoids: Potential Therapeutic Agents by Their Antioxidant Capacity. *Bioactive Compounds.* Elsevier.
HIGASHI, K. & DE CASTRO, S. J. J. O. E. 1994. Propolis extracts are effective against Trypanosoma cruzi and have an impact on its interaction with host cells. 43**,** 149-155.
HUANG, S., ZHANG, C.-P., WANG, K., LI, G. Q. & HU, F.-L. J. M. 2014. Recent advances in the chemical composition of propolis. 19**,** 19610-19632.
HUANG, W.-Y., CAI, Y.-Z., ZHANG, Y. J. N. & CANCER 2009. Natural phenolic compounds from medicinal herbs and dietary plants: potential use for cancer prevention. 62**,** 1-20.
HURRELL, B. P., SCHUSTER, S., GRÜN, E., COUTAZ, M., WILLIAMS, R. A., HELD, W., MALISSEN, B., MALISSEN, M., YOUSEFI, S. & SIMON, H.-U. J. P. P. 2015. Rapid sequestration of Leishmania mexicana by neutrophils contributes to the development of chronic lesion. 11**,** e1004929.
HURST, P. J. R. A. I. P. 1978. REC0VERY 0F PRE-IMPLANTATI0N EMBRY0S IN MACACA MULATTA PR HURST, KATHRYN JEFFERIES, P. ECKSTEIN and AG WHEELER. 4**,** 185.
INASAKI, I. J. C. P. B. 2002. NII-Electronic Library Service. 43**,** 2091.
JERZ, G., ELNAKADY, Y. A., BRAUN, A., JÄCKEL, K., SASSE, F., AL GHAMDI, A. A., OMAR, M. O. & WINTERHALTER, P. J. J. O. C. A. 2014. Preparative mass-spectrometry profiling of bioactive metabolites in Saudi-Arabian propolis fractionated by high-speed countercurrent chromatography and off-line atmospheric pressure chemical ionization mass-spectrometry injection. 1347**,** 17-29.
JERZ, G., WAIBEL, R. & ACHENBACH, H. J. P. 2005. Cyclohexanoid protoflavanones from the stem-bark and roots of Ongokea gore. 66**,** 1698-1706.

KARUPPAGOUNDER, V., ARUMUGAM, S., THANDAVARAYAN, R. A., PITCHAIMANI, V., SREEDHAR, R., AFRIN, R., HARIMA, M., SUZUKI, H., SUZUKI, K. & NAKAMURA, M. J. I. I. 2015. Naringenin ameliorates daunorubicin induced nephrotoxicity by mitigating AT1R, ERK1/2-NFκB p65 mediated inflammation. 28**,** 154-159.

KASOTE, D., SULEMAN, T., CHEN, W., SANDASI, M., VILJOEN, A., VAN VUUREN, S. J. B. S. & ECOLOGY 2014. Chemical profiling and chemometric analysis of South African propolis. 55**,** 156-163.

KIM, C. H., KIM, M. Y., LEE, S.-W., JANG, K.-S. J. J. O. A. S. & TECHNOLOGY 2019. UPLC/FT-ICR MS-based high-resolution platform for determining the geographical origins of raw propolis samples. 10**,** 8.

KIM, J.-Y., PARK, K.-S., LEE, C.-W. & CHANG, Y.-H. J. B. O. T. K. C. S. 2007. Synthesis of a complete series of O-methyl analogues of naringenin and apigenin. 28**,** 2527-2530.

KOŒEVAR, N., GLAVAŒ, I. & KREFT, S. J. F. V. 2007. Flavonoidi. 58**,** 145.

KRZEK, J., KALETA, J., HUBICKA, U. & NIEDZWIEDZ, A. J. J. O. A. I. 2006. Reversed-phase high-performance liquid chromatography determination of selected phenolic acids in propolis concentrates in terms of standardization for drug manufacturing purposes. 89**,** 352-358.

KUMAR, S. & PANDEY, A. K. J. T. S. W. J. 2013. Chemistry and biological activities of flavonoids: an overview. 2013.

KUROPATNICKI, A. K., SZLISZKA, E., KROL, W. J. E.-B. C. & MEDICINE, A. 2013. Historical aspects of propolis research in modern times. 2013.

LEE, E.-J., MOON, B.-H., PARK, Y., HONG, S.-W., LEE, S.-H., LEE, Y.-G. & LIM, Y.-H. J. B. O. T. K. C. S. 2008. Effects of hydroxy and methoxy substituents on NMR data in flavonols. 29**,** 507-510.

LEE, I.-K., HAN, M.-S., KIM, D.-W., YUN, B.-S. J. B. & LETTERS, M. C. 2014. Phenylpropanoid acid esters from Korean propolis and their antioxidant activities. 24**,** 3503-3505.

LEGROS, D., OLLIVIER, G., GASTELLU-ETCHEGORRY, M., PAQUET, C., BURRI, C., JANNIN, J. & BÜSCHER, P. J. T. L. I. D. 2002. Treatment of human African trypanosomiasis—present situation and needs for research and development. 2**,** 437-440.

LI, F., AWALE, S., TEZUKA, Y., KADOTA, S. J. B. & CHEMISTRY, M. 2008. Cytotoxic constituents from Brazilian red propolis and their structure–activity relationship. 16**,** 5434-5440.

LIU, A.-L., WANG, H.-D., LEE, S. M., WANG, Y.-T., DU, G.-H. J. B. & CHEMISTRY, M. 2008. Structure–activity relationship of flavonoids as influenza virus neuraminidase inhibitors and their in vitro anti-viral activities. 16**,** 7141-7147.

LOTTI, C., CAMPO FERNANDEZ, M., PICCINELLI, A. L., CUESTA-RUBIO, O., MARQUEZ HERNANDEZ, I., RASTRELLI, L. J. J. O. A. & CHEMISTRY, F. 2010. Chemical constituents of red Mexican propolis. 58**,** 2209-2213.

MA, Z., WEI, X., FONTANILLA, C., NOELKER, C., DODEL, R., HAMPEL, H. & DU, Y. J. L. S. 2006. Caffeic acid phenethyl ester blocks free radical generation and 6-hydroxydopamine-induced neurotoxicity. 79**,** 1307-1311.

MACIEJEWICZ, W. J. J. O. L. C. & TECHNOLOGIES, R. 2001. Isolation of flavonoid aglycones from propolis by a column chromatography method and their identification by GC-MS and TLC methods. 24**,** 1171-1179.

MANDAL, S. M., CHAKRABORTY, D., DEY, S. J. P. S. & BEHAVIOR 2010. Phenolic acids act as signaling molecules in plant-microbe symbioses. 5**,** 359-368.

MARCUCCI, M. C., FERRERES, F., GARCıA-VIGUERA, C., BANKOVA, V., DE CASTRO, S., DANTAS, A., VALENTE, P. & PAULINO, N. J. J. O. E. 2001. Phenolic compounds from Brazilian propolis with pharmacological activities. 74**,** 105-112.
MARSTON, A. J. P. 2007. Role of advances in chromatographic techniques in phytochemistry. 68**,** 2786-2798.
MARTINOTTI, S., RANZATO, E. J. B. & TRAUMA 2015. Propolis: a new frontier for wound healing? 3**,** 9.
MELLIOU, E. & CHINOU, I. J. P. M. 2004. Chemical analysis and antimicrobial activity of Greek propolis. 70**,** 515-519.
MOLDOVEANU, S. & DAVID, V. J. E. I. M. H. S. E. 2013. Chapter 1-Basic Information about HPLC.
MOLDOVEANU, S. C. & DAVID, V. 2012. *Essentials in modern HPLC separations*, Newnes.
MONZOTE, L., CUESTA-RUBIO, O., CAMPO FERNANDEZ, M., MÁRQUEZ HERNANDEZ, I., FRAGA, J., PÉREZ, K., KERSTENS, M., MAES, L. & COS, P. J. M. D. I. O. C. 2012. In vitro antimicrobial assessment of Cuban propolis extracts. 107**,** 978-984.
NICULAE, M., LAURA, S., EMOKE, P., PAȘTIU, A. I., BALACI, I. M., MUSTE, S. & SPINU, M. J. N. B. H. A. C.-N. 2015. In vitro synergistic antimicrobial activity of Romanian propolis and antibiotics against Escherichia coli isolated from bovine mastitis. 43**,** 327-334.
NOUDEH, G. D., MOSHAFI, M. H., KAZAELI, P. & AKEF, F. J. A. J. O. B. 2010. Studies on bioemulsifier production by Bacillus licheniformis PTCC 1595. 9.
NUNES, D. D., MACHADO, B. A. S., BARRETO, G. D. A., SILVA, J. R., SILVA, D. F. D., ROCHA, J. L. C. D., BRANDÃO, H. N., BORGES, V. M. & GUEZ, M. A. U. 2018. Chemical characterization and biological activity of six different extracts of propolis through conventional methods and supercritical extraction.
NWEZE, N. E., OKORO, H. O., AL ROBAIAN, M., OMAR, R. M., TOR-ANYIIN, T. A., WATSON, D. G. & IGOLI, J. O. 2017. Effects of Nigerian red propolis in rats infected.
OLIVEIRA, A. P., FRANÇA, H., KUSTER, R., TEIXEIRA, L., ROCHA, L. J. J. O. V. A. & DISEASES, T. I. T. 2010. Chemical composition and antibacterial activity of Brazilian propolis essential oil. 16**,** 121-130.
OLIVEIRA, R. N., MCGUINNESS, G. B., RAMOS, M. E. T., KAJIYAMA, C. E. & THIRÉ, R. M. Properties of PVA Hydrogel Wound-Care Dressings Containing UK Propolis. Macromolecular Symposia, 2016. Wiley Online Library, 122-127.
OMAR, R. M., IGOLI, J., GRAY, A. I., EBILOMA, G. U., CLEMENTS, C., FEARNLEY, J., EDRADA EBEL, R. A., ZHANG, T., DE KONING, H. P. & WATSON, D. G. J. P. A. 2016. Chemical characterisation of Nigerian red propolis and its biological activity against Trypanosoma brucei. 27**,** 107-115.
OTA, C., UNTERKIRCHER, C., FANTINATO, V. & SHIMIZU, M. J. M. 2001. Antifungal activity of propolis on different species of Candida. 44**,** 375-378.
PAVLOVIC, R., BORGONOVO, G., LEONI, V., GIUPPONI, L., CECILIANI, G., SALA, S., BASSOLI, A. & GIORGI, A. J. M. 2020. Effectiveness of Different Analytical Methods for the Characterization of Propolis: A Case of Study in Northern Italy. 25**,** 504.
PEREIRA, A. S., NASCIMENTO, E. A. & DE AQUINO NETO, F. R. J. Z. F. N. C. 2002. Lupeol alkanoates in Brazilian propolis. 57**,** 721-726.
POBIEGA, K., GNIEWOSZ, M. & KRAŚNIEWSKA, K. J. Z. P. P. N. R. 2017. Antimicrobial and antiviral properties of different types of propolis. 589**,** 69-79.

POPOVA, M., GIANNOPOULOU, E., SKALICKA-WOŹNIAK, K., GRAIKOU, K., WIDELSKI, J., BANKOVA, V., KALOFONOS, H., SIVOLAPENKO, G., GAWEŁ-BĘBEN, K. & ANTOSIEWICZ, B. J. M. 2017. Characterization and biological evaluation of propolis from Poland. 22**,** 1159.

POPOVA, M., SILICI, S., KAFTANOGLU, O. & BANKOVA, V. J. P. 2005. Antibacterial activity of Turkish propolis and its qualitative and quantitative chemical composition. 12**,** 221-228.

POPOVA, M., TRUSHEVA, B., ANTONOVA, D., CUTAJAR, S., MIFSUD, D., FARRUGIA, C., TSVETKOVA, I., NAJDENSKI, H. & BANKOVA, V. J. F. C. 2011. The specific chemical profile of Mediterranean propolis from Malta. 126**,** 1431-1435.

POPOVA, M. P., GRAIKOU, K., CHINOU, I., BANKOVA, V. S. J. J. O. A. & CHEMISTRY, F. 2010. GC-MS profiling of diterpene compounds in Mediterranean propolis from Greece. 58**,** 3167-3176.

PRYTZYK, E., DANTAS, A. P., SALOMÃO, K., PEREIRA, A. S., BANKOVA, V. S., DE CASTRO, S. L. & NETO, F. R. A. J. J. O. E. 2003. Flavonoids and trypanocidal activity of Bulgarian propolis. 88**,** 189-193.

PRZYBYŁEK, I. & KARPIŃSKI, T. M. J. M. 2019. Antibacterial properties of propolis. 24**,** 2047.

PUJOL, M., PENA, C., PALLARES, R., AYATS, J., ARIZA, J., GUDIOL, F. J. E. J. O. C. M. & DISEASES, I. 1994. Risk factors for nosocomial bacteremia due to methicillin-resistantStaphylococcus aureus. 13**,** 96-102.

RAMAWAT, K. G. & MÉRILLON, J.-M. 2013. *Natural products: phytochemistry, botany and metabolism of alkaloids, phenolics and terpenes*, Springer.

RÄZ, B., ITEN, M., GRETHER-BÜHLER, Y., KAMINSKY, R. & BRUN, R. J. A. T. 1997. The Alamar Blue® assay to determine drug sensitivity of African trypanosomes (Tb rhodesiense and Tb gambiense) in vitro. 68**,** 139-147.

RIVERA-YAÑEZ, N., RODRIGUEZ-CANALES, M., NIETO-YAÑEZ, O., JIMENEZ-ESTRADA, M., IBARRA-BARAJAS, M., CANALES-MARTINEZ, M., RODRIGUEZ-MONROY, M. J. E.-B. C. & MEDICINE, A. 2018. Hypoglycaemic and antioxidant effects of propolis of Chihuahua in a model of experimental diabetes. 2018.

ROSANDY, A. R., DIN, L. B., YAACOB, W., YUSOFF, N. I., SAHIDIN, I., LATIP, J., NATAQAIN, S. & NOOR, N. M. J. M. J. A. S. 2013. Isolation and characterization of compounds from the stem bark of Uvaria rufa (Annonaceae). 17**,** 50-58.

RUFATTO, L., DOS SANTOS, D., MARINHO, F., HENRIQUES, J., ROESCH ELY, M. & MOURA, S. J. D. D. O. J. A. 2017. Red propolis: Chemical composition and pharmacological activity. Asian Pac J Trop Biomed [Internet]. 2017; 7 (7): 591–8. Available from: ttp. 9.

SAK, K. J. C. R. & PRACTICE 2012. Chemotherapy and dietary phytochemical agents. 2012.

SALAS, A. L., ALBERTO, M. R., ZAMPINI, I. C., CUELLO, A. S., MALDONADO, L., RÍOS, J. L., SCHMEDA-HIRSCHMANN, G. & ISLA, M. I. J. P. 2016. Biological activities of polyphenols-enriched propolis from Argentina arid regions. 23**,** 27-31.

SALITURO, G. M. & DUFRESNE, C. 1998. Isolation by low-pressure column chromatography. *Natural Products Isolation.* Springer.

SALOMAO, K., DE SOUZA, E., HENRIQUES-PONS, A., BARBOSA, H. & DE CASTRO, S. 2011. Brazilian green propolis: effects in vitro and in vivo on Trypanosoma cruzi. Evid Based Complement Altern Med.

SALOMAO, K., PEREIRA, P. R. S., CAMPOS, L. C., BORBA, C. M., CABELLO, P. H., MARCUCCI, M. C., DE CASTRO, S. L. J. E.-B. C. & MEDICINE, A. 2008. Brazilian propolis: correlation between chemical composition and antimicrobial activity. 5.

SAMPIETRO, D. A., VATTUONE, M. M. S. & VATTUONE, M. A. J. L. 2016. Immunomodulatory activity of Apis mellifera propolis from the North of Argentina. 70**,** 9-15.

SANTOS, V. R. 2012. *Propolis: alternative medicine for the treatment of oral microbial diseases*, chapter.

SARKER, S. D., LATIF, Z. & GRAY, A. I. 2005. Natural Product Isolation. *In:* SARKER, S. D., LATIF, Z. & GRAY, A. I. (eds.) *Natural Products Isolation.* Totowa, NJ: Humana Press.

SAWAYA, A. C. H. F., DA SILVA CUNHA, I. B. & MARCUCCI, M. C. J. C. C. J. 2011. Analytical methods applied to diverse types of Brazilian propolis. 5**,** 1-10.

SAWICKA, D., CAR, H., BORAWSKA, M. H. & NIKLIŃSKI, J. J. F. H. E. C. 2012. The anticancer activity of propolis. 50**,** 25-37.

SCHINOR, E., SALVADOR, M., ITO, I., DE ALBUQUERQUE, S. & DIAS, D. J. P. 2004. Trypanocidal and antimicrobial activities of Moquinia kingii. 11**,** 224-229.

SEEBECK, T. & MÄSER, P. 2009. Drug resistance in African trypanosomiasis. *Antimicrobial drug resistance.* Springer.

SEVEN, I., AKSU, T. & SEVEN, P. T. J. A.-A. J. O. A. S. 2010. The effects of propolis on biochemical parameters and activity of antioxidant enzymes in broilers exposed to lead-induced oxidative stress. 23**,** 1482-1489.

SFORCIN, J., FERNANDES JR, A., LOPES, C., BANKOVA, V. & FUNARI, S. J. J. O. E. 2000. Seasonal effect on Brazilian propolis antibacterial activity. 73**,** 243-249.

SFORCIN, J. J. J. O. E. 2007. Propolis and the immune system: a review. 113**,** 1-14.

SHEHU, A., ISMAIL, S., ROHIN, M. A. K., HARUN, A., AZIZ, A. A. & HAQUE, M. J. J. O. A. P. S. 2016. Antifungal properties of Malaysian Tualang honey and stingless bee propolis against Candida albicans and Cryptococcus neoformans. 6**,** 044-050.

SIHERI, W., EBILOMA, G. U., IGOLI, J. O., GRAY, A. I., BIDDAU, M., AKRACHALANONT, P., ALENEZI, S., ALWASHIH, M. A., EDRADA-EBEL, R. & MULLER, S. J. M. 2019. Isolation of a novel flavanonol and an alkylresorcinol with highly potent anti-trypanosomal activity from Libyan propolis. 24**,** 1041.

SIHERI, W., IGOLI, J. O., GRAY, A. I., NASCIEMENTO, T. G., ZHANG, T., FEARNLEY, J., CLEMENTS, C. J., CARTER, K. C., CARRUTHERS, J. & EDRADA-EBEL, R. J. P. R. 2014. The isolation of antiprotozoal compounds from Libyan propolis. 28**,** 1756-1760.

SIHERI, W., ZHANG, T., EBILOMA, G. U., BIDDAU, M., WOODS, N., HUSSAIN, M. Y., CLEMENTS, C. J., FEARNLEY, J., EBEL, R. E. & PAGET, T. J. P. O. 2016. Chemical and antimicrobial profiling of propolis from different regions within Libya. 11**,** e0155355.

SIMONE-FINSTROM, M. & SPIVAK, M. J. A. 2010. Propolis and bee health: the natural history and significance of resin use by honey bees. 41**,** 295-311.

SINGH, S. 2014. *Protective Role of Phyllanthus fraternus and Aegle marmelos against Cyclophosphamide-Induced pathophysiological changes in Liver, Kidney and Testis of Laboratory Mouse.* Banaras Hindu University.

SOSA-LÓPEZ, Á. A., CABRERA, M. G. & ÁLVAREZ, M. Y. J. J. O. T. S. A. B. 2017. Parámetros físicos y características organolépticas de propóleos provenientes de la Provincia de Misiones, Argentina. 5**,** 51-58.

STAR, A. E., RÖSLER, H., MABRY, T. J. & SMITH, D. M. J. P. 1975. Flavonoid and ceroptin pigments from frond exudates of Pityrogramma triangularis. 14**,** 2275-2278.
STEPANOVIC, S., ANTIC, N., DAKIC, I. J. V. A. A. O. P. & RES, A. D. M. M. Svabic vlahovic, 2003. 158**,** 353-357.
STEVERDING, D. J. P. & VECTORS 2008. The history of African trypanosomiasis. 1**,** 3.
STICH, A., BARRETT, M. P. & KRISHNA, S. J. T. I. P. 2003. Waking up to sleeping sickness. 19**,** 195-197.
STICHER, O. J. N. P. R. 2008. Natural product isolation. 25**,** 517-554.
STOYANOVA, R., BROWN, T. J. N. I. B. A. I. J. D. T. T. D. & VIVO, A. O. M. R. I. 2001. NMR spectral quantitation by principal component analysis. 14**,** 271-277.
TALZHANOV, N., SADYRBEKOV, D., SMAGULOVA, F., MUKANOV, R., RALDUGIN, V., SHAKIROV, M., TKACHEV, A., ATAZHANOVA, G., TULEUOV, B. & ADEKENOV, S. J. C. O. N. C. 2005. Components of Artemisia pontica. 41**,** 178-181.
TORRES-GUERRERO, E., QUINTANILLA-CEILLO, M., RUIZ-ESMENJAUD, J. & ARENAS, R. J. D. F1000Research 2017, 6, 750. 10**,** f1000research.
TRAN, V. H., DUKE, R. K., ABU-MELLAL, A. & DUKE, C. C. J. P. 2012. Propolis with high flavonoid content collected by honey bees from Acacia paradoxa. 81**,** 126-132.
TRUSHEVA, B., POPOVA, M., BANKOVA, V., SIMOVA, S., MARCUCCI, M. C., MIORIN, P. L., PASIN, F. D. R., TSVETKOVA, I. J. E.-B. C. & MEDICINE, A. 2006. Bioactive constituents of Brazilian red propolis. 3.
TRUSHEVA, B., POPOVA, M., BANKOVA, V., TSVETKOVA, I., NAYDENSKI, C. & SABATINI, A. J. R. I. E. 2003. A new type of European propolis, containing bioactive labdanes. 13**,** 3-8.
VALENZUELA-BARRA, G., CASTRO, C., FIGUEROA, C., BARRIGA, A., SILVA, X., DE LAS HERAS, B., HORTELANO, S. & DELPORTE, C. J. J. O. E. 2015. Anti-inflammatory activity and phenolic profile of propolis from two locations in Región Metropolitana de Santiago, Chile. 168**,** 37-44.
WANG, A. C. & BAX, A. J. J. O. B. N. 1993. Minimizing the effects of radio-frequency heating in multidimensional NMR experiments. 3**,** 715-720.
WANG, K., HU, L., JIN, X.-L., MA, Q.-X., MARCUCCI, M. C., NETTO, A. A. L., SAWAYA, A. C. H. F., HUANG, S., REN, W.-K. & CONLON, M. A. J. J. O. F. F. 2015. Polyphenol-rich propolis extracts from China and Brazil exert anti-inflammatory effects by modulating ubiquitination of TRAF6 during the activation of NF-κB. 19**,** 464-478.
WILDMAN, R. E. 2016. *Handbook of nutraceuticals and functional foods*, CRC press.
WOLLENWEBER, E. & BUCHMANN, S. L. J. Z. F. N. C. 1997. Feral honey bees in the Sonoran Desert: Propolis sources other than poplars (Populus spp.). 52**,** 530-535.
YANG, N., QIN, S., WANG, M., CHEN, B., YUAN, N., FANG, Y., YAO, S., JIAO, P., YU, Y. & ZHANG, Y. J. C. 2013. Pinocembrin, a major flavonoid in propolis, improves the biological functions of EPCs derived from rat bone marrow through the PI3K-eNOS-NO signaling pathway. 65**,** 541-551.
YAO, S. & QING, W. J. A. C. S. E. S. R. O. 2008. 5, 3'-Dihydroxy-7, 4'-dimethoxyflavanone from Artemisia sphaerocephala Kraschen. 64**,** o822-o822.

8 Appendix: 1 Papers Published

Published Paper

European propolis is highly active against trypanosomatids including *Crithidia fasciculata*

Abdullah Alotaibi[1], Godwin U. ebiloma[2], Roderick Williams[3], Samya Alenezi[1], Anne-Marie Donachie[2], Selome Guillaume[3], John o. igoli[1,4], James fearnley[5], Harry p. de Koning[2] & David G. Watson[1]

Extracts of 35 samples of European propolis were tested against wild type and resistant strains of the protozoal pathogens *Trypanosoma brucei, Trypanosoma congolense* and *Leishmania mexicana*. the extracts were also tested against *Crithidia fasciculata* a close relative of *Crithidia mellificae,* a parasite of bees. *Crithidia, Trypanosoma* and *Leishmania* are all members of the order Kinetoplastida. High levels of activity were obtained for all the samples with the levels of activity varying across the sample set. the highest levels of activity were found against *L. mexicana*. The propolis samples were profiled by using liquid chromatography with high resolution mass spectrometry (Lc-MS) and principal components analysis (pcA) of the data obtained indicated there was a wide variation in the composition of the propolis samples. orthogonal partial least squares (opLS) associated a butyrate ester of pinobanksin with high activity against *T. brucei* whereas in the case of *T. congolense* high activity was associated with methyl ethers of chrysin and pinobanksin. in the case of *C. fasciculata* highest activity was associated with methyl ethers of galangin and pinobanksin. opLS modelling of the activities against *L. mexicana* using the mass spectrometry produced a less successful model suggesting a wider range of active components.

Received: 22 February 2019. Accepted: 25 July 2019. Published online: 06 August 2019

[1]University of Strathclyde, Strathclyde Institute of Pharmacy and Biomedical Science, 161 Cathedral Street, Glasgow, G4 0RE, UK. [2]Institute of Infection, Immunity and Inflammation, College of Medical, Veterinary and Life Sciences, University of Glasgow, Glasgow, G12 8TA, UK. [3]IBEHR, School of Health and Life Science, University of the West of Scotland, High Street, Paisley, PA1 2BE, UK. [4]Department of Chemistry, University of Agriculture, PMB 2373

, Makurdi, Nigeria. [5]BeeVital, Whitby, North Yorkshire, YO22 5JR, UK. Correspondence and requests for materials should be addressed to D.G.W. (email: d.g.watson@strath.ac.uk)

Propolis is a resinous substance collected by bees, generally from plant buds. Its composition varies widely accord- ing to the vegetation surrounding the bee hive[1]. It is collected on the hindlegs of the bee and is removed with the help of other bees upon return to the hive and layered onto surfaces and used to fill any gaps within the hive, helping to maintain a sterile environment within the hive. In Northern Europe and other temperate regions such as Northern China and North America propolis is generally collected from the buds of poplar species[1,2], whereas in Southern Europe the predominant sources are various Cypress species and in tropical regions several different plant sources may be utilised[1,3]. Propolis almost always displays high activity against *Trypanosoma brucei* and other protozoa, particularly those from the order Kinetoplastida, and we have found this to be the case regardless of the region of origin. Antiprotozoal activity has been found in propolis from Libya, Nigeria, Cameroon, Saudi Arabia and Brazil[3–10]. Although propolis is also antibacterial this activity is often only moderate in most samples and absent in others; generally, the strongest antibacterial activity is found in tropical propolis samples[11,12]. It has recently become clear that protozoal infection in bees is widespread, this was originally thought to be caused by *Crithidia mellificae*, which has been found to be associated with a higher incidence of winter colony collapse in Belgian bee colonies[13], but it is now thought that the protozoal species *Lotmaria passim*[14,15] is the main infecting organism. It has been found that DNA from *L. passim* is the most abundant DNA from a pathogenic organ- ism within the DNA profile for the microbiome of Scottish

bees[16]. Recently, *L. passim* has also been found in Africanised bees from Argentina, Uruguay and Chile and in this report a heavy burden of infection was found to be associated with a higher incidence of Varroa mite infestation[17]. Thus far there is no evidence that bees ingest propolis but since the spread of the protozoal infection occurs via faeces, coating the surfaces in the hive with propolis that is active against trypanosomatids could prevent transmission[18]. It remains an unanswered question

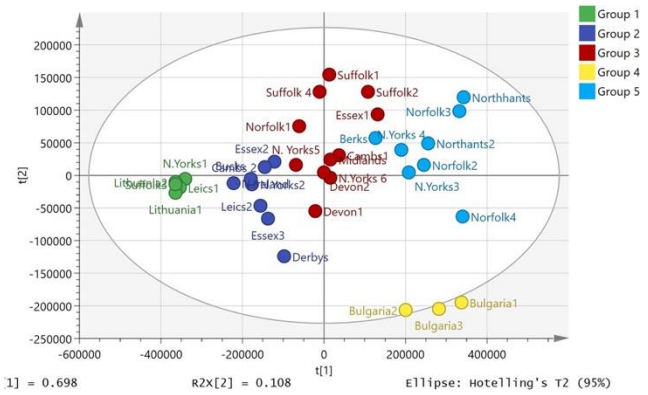

Figure1. PCA plot showing the variation of propolis composition across 35 European propolis samples (Pareto scaled based on 233 components).

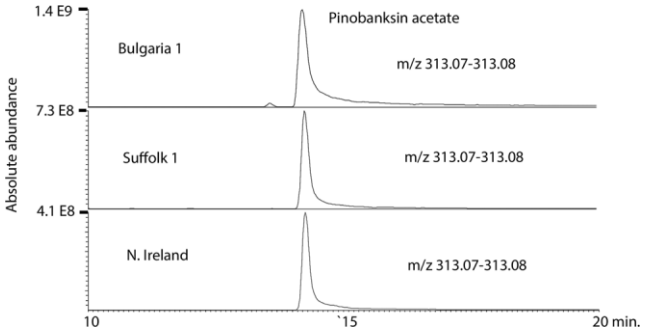

Figure2. Extracted ion trace showing variation in the levels of pinobanksin acetate across 3 European propolis samples.

just how important propolis is to the bee, and what its exact mechanism is in keeping down infections within the hive. European propolis has been extensively characterised and is composed of a complex mixture of >300 flavo- noids and cinnamic acid derivatives[19,20] and even though it has been worked on for many years there still remain components in it that have not been completely chemically or biologically characterised[20], especially with regards to their antimicrobial properties. In this paper we report the activity of 35 European propolis samples against *Trypanosoma brucei*, *Trypanosoma congolense*, *Leishmania mexicana* and *Crithidia fasciculata*.

Results

Figure 1 shows the spread of the compositions of the propolis samples in a PCA model. We have previously characterised most of the major components in propolis from the UK by using accurate mass measurement with LC-MS^n[20]. Although the samples have broadly similar compositions, there are some quite marked varia- tions in individual components. For instance, Fig. 2 shows extracted ion chromatograms for a major component, pinobanksin acetate, across three samples from different positions in the PCA plot. Pinobanksin acetate is most abundant in the Bulgarian samples, which contain ~3.5-fold more of the compound than a sample from Northern Ireland. In contrast, Fig. 3 shows extracted ion traces for a component putatively identified as trimethyl dihydro- kaempferol, which is abundant in the Northern Ireland sample but only present at low levels in the Bulgarian sample. Table 1 shows the results obtained in testing the 35 samples of European propolis against *Trypanosoma brucei, Trypanosoma congolense* and the multidrug resistant strain *Trypanosoma brucei B48*. Of these, 4 sam- ples displayed high activity, i.e. EC_{50} values <5 µg/mL, and 21 displayed intermediate activity between 5 and 10 µg/mL for the standard drug-sensitive strain Lister 427WT. The propolis samples from Norfolk displayed the highest activity, followed by the adjoining county of Suffolk and nearby Northamptonshire. The EC_{50} values for the multidrug resistant stain B48 were within ~1.5-fold of the control (Resistance Index (RI) 0.63–1.56; average 0.83 ± 0.04) although the RI for pentamidine was 222 ($P < 0.001$, Student's unpaired t-test; Table 1).

OPLS was used to model the activity of the different propolis samples against *T. brucei* B48 in relation to their composition. It was possible to produce a model for 33 of the samples based on 5 components, including a butyl ester of pinobanksin, which produced a reasonable fit of predicted against observed activity shown in Fig. 4 (the corresponding loadings plot is shown in Fig. S1). The highest activity was associated with a

butyl ester of pinobanksin and a propionyl ester of pinobanksin. Table S1 includes MS^n data used to further characterise the compounds associated with high activity. It can be seen from the extracted ion trace shown in Fig. 5 that the highest activity sample from Norfolk contains about 4 times the concentration of pinobanksin butyrate present in the lowest activity sample from Leicestershire. The wild type strain of *T. brucei* 427 gave similar results. Figure S2

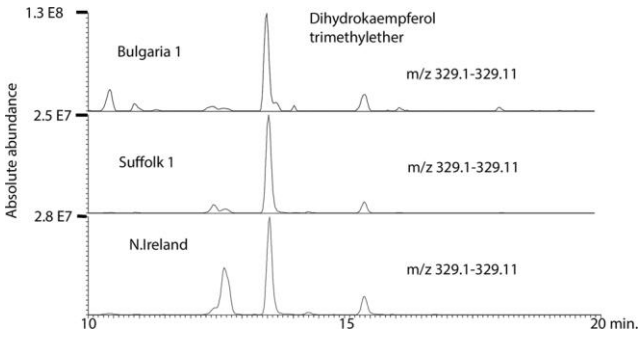

Figure 3. Extracted ion trace showing variation in trimethyl dihydrokaempferol across 3 European propolis samples.

Propolis sample	*T. brucei*				*T. congolense*
	427WT EC_{50}	**B48 EC_{50}**	**R.I.**	**P value**	**IL3000 EC_{50}**
Suffolk 4, UK	7.42 ± 0.37	5.7 ± 0.17	0.77	0.013	8.46 ± 1.47
Bulgaria 1	5.20 ± 0.18	3.6 ± 0.52	0.69	0.043	3.69 ± 0.79
Suffolk 2, UK	6.69 ± 0.36	7.7 ± 1.1	1.15	0.423	5.66 ± 1.55
North Yorkshire 1, UK	13.5 ± 0.61	11.0 ± 0.70	0.82	0.058	18.9 ± 1.1
Northamptonshire 1, UK	4.49 ± 0.22	3.0 ± 0.20	0.67	0.007	5.69 ± 1.10
Essex 1, UK	5.97 ± 0.17	4.6 ± 0.26	0.77	0.013	4.40 ± 0.47
Essex 2, UK	14.0 ± 0.13	10.6 ± 1.6	0.75	0.102	17.3 ± 2.4
Norfolk 1, UK	5.23 ± 0.49	3.3 ± 0.31	0.63	0.029	3.08 ± 0.90
Devon 1, UK	8.57 ± 0.26	10.8 ± 1.2	1.26	0.144	11.4 ± 1.8
Leicestershire 1, UK	13.7 ± 1.18	11.6 ± 2.3	0.85	0.448	15.3 ± 3.0
Leicestershire 2, UK	17.8 ± 2.16	22.1 ± 1.4	1.24	0.169	27.6 ± 5.3
Derbyshire, UK	11.8 ± 0.57	9.5 ± 1.49	0.81	0.228	26.4 ± 4.5
Lithuania 1	18.4 ± 1.30	22.1 ± 0.24	1.20	0.049	30.9 ± 2.8
Lithuania 2	16.1 ± 0.93	25.0 ± 1.0	1.56	0.003	23.4 ± 1.4
Suffolk 1, UK	6.82 ± 0.87	4.5 ± 0.23	0.66	0.058	5.12 ± 0.68
Suffolk 3, UK	4.37 ± 0.18	2.9 ± 0.15	0.66	0.003	3.26 ± 1.03
Bulgaria 2	5.80 ± 0.36	4.1 ± 0.41	0.71	0.036	2.06 ± 1.12
Bulgaria 3	6.28 ± 0.69	5.3 ± 0.14	0.84	0.249	1.96 ± 1.01
Cambridgeshire 1, UK	9.79 ± 0.37	8.2 ± 0.32	0.84	0.034	5.65 ± 1.95
Norfolk 2, UK	6.18 ± 0.27	4.2 ± 0.41	0.68	0.015	2.13 ± 0.38
Northamptonshire 2, UK	5.24 ± 0.42	3.4 ± 0.39	0.65	0.030	4.83 ± 1.67
Cambridgeshire 2, UK	12.7 ± 0.09	10.3 ± 1.22	0.81	0.116	7.78 ± 2.15
North Yorkshire 2, UK	18.5 ± 0.48	14.9 ± 0.31	0.81	0.003	16.5 ± 3.1
Northern Ireland, UK	6.30 ± 0.33	6.7 ± 0.34	1.06	0.476	15.2 ± 4.2
North Yorkshire 3, UK	6.97 ± 0.60	5.4 ± 0.72	0.77	0.174	4.90 ± 1.53
North Yorkshire 4, UK	6.79 ± 0.45	4.7 ± 0.31	0.69	0.019	4.99 ± 2.06
North Yorkshire 5, UK	10.0 ± 0.06	9.0 ± 1.3	0.90	0.477	7.41 ± 1.25
North Yorkshire 6, UK	8.75 ± 0.34	7.3 ± 0.41	0.83	0.055	13.6 ± 3.1
Essex 3, UK	6.86 ± 0.71	5.4 ± 0.18	0.79	0.122	35.7 ± 6.5
Berkshire, UK	6.23 ± 0.12	4.2 ± 0.30	0.67	0.003	4.07 ± 1.10
Midlands, UK	5.28 ± 0.51	4.7 ± 0.31	0.89	0.395	6.12 ± 1.82
Devon 2, UK	8.68 ± 0.43	5.6 ± 0.23	0.65	0.003	7.52 ± 1.62
Buckinghamshire, UK	17.4 ± 0.96	13.1 ± 1.5	0.75	0.071	28.4 ± 6.0
Norfolk 3, UK	3.67 ± 0.30	2.5 ± 0.14	0.68	0.028	3.47 ± 0.92
Norfolk 4, UK	4.19 ± 0.21	2.9 ± 0.04	0.69	0.004	3.60 ± 0.99
Pentamidine (μM)	0.0027 ± 3.90E-04	0.6 ± 0.01	222	<0.0001	N.D.
Diminazene (μM)	N.D.	N.D.			0.37 ± 0.12

Table 1. The activity (μg/mL) of 35 European propolis samples against the standard drug-sensitive *T. brucei* 427WT and multi-drug resistant strain *T. brucei* B48, and *T. congolense*. Effective Concentration 50% (EC_{50}) values (μg/mL) are given as averages and SEM of 3 independent experiments for *T. brucei* and 3–4 experiments for *T. congolense*. P value is based on a Student's unpaired t-test, comparing *T. brucei* WT and B48. R. I. is the resistance index, being the ratio of the EC_{50} values for *T. brucei* WT and B48. N.D., not determined.

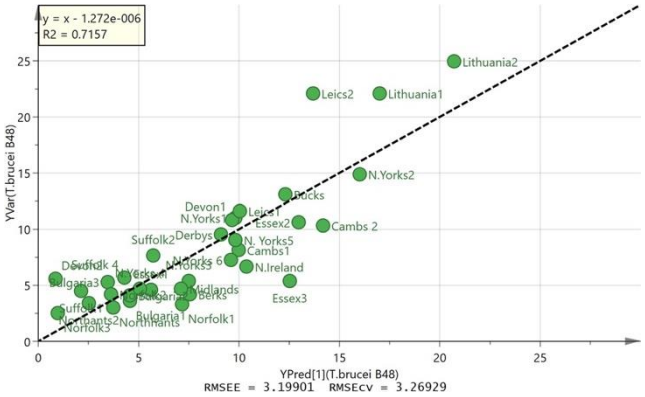

Figure 4. OPLS plot of observed against predicted activity against *T. brucei* B48 for 33 propolis samples based on five components.

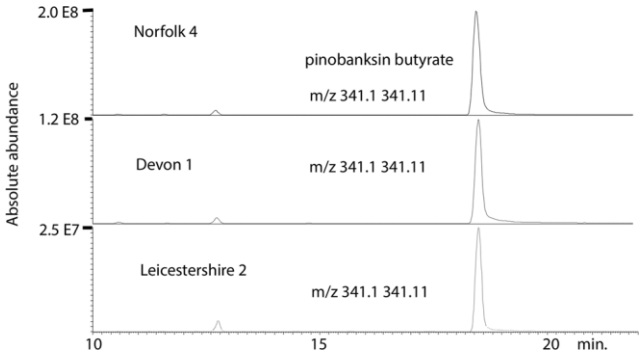

Figure 5. Extracted ion traces pinobanksin butyrate in samples with high, moderate and low activity against *T. brucei*.

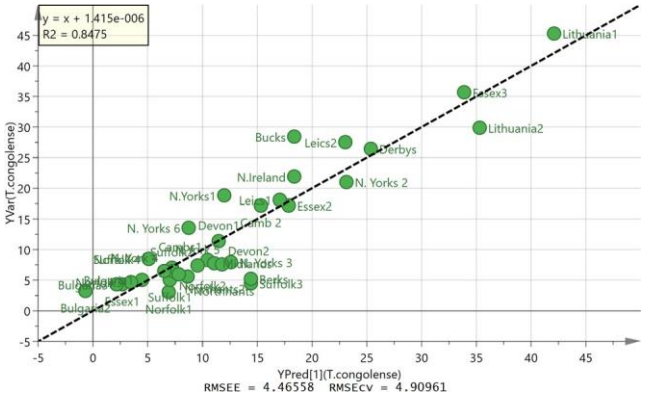

Figure 6. OPLS plot of observed against predicted activity against *T. congolense* for 35 propolis samples based on seven components.

shows an OPLS plot of predicted against measured activity with the corresponding loadings plot shown in Fig. S3. The highest activity is again associated with a butyl ester of pinobanksin and two propionyl esters of pinobanksin. The same propolis samples were also tested against the veterinary trypanosome species *T. congolense* (Table 1) with very similar results, as the average of the ratio of EC_{50} (Tbb427WT)/EC_{50}(*T. congolense*) was 1.21 ± 0.11. Interestingly, the two Bulgarian samples were ~3-fold more active against *T. congolense*

than against either of the *T. brucei* clones, as was one sample from Norfolk, UK. Figure 6 shows the OPLS plot obtained for the activ- ity against *T. congolense*. The correlation between composition and activity was based on seven components. Figure S4 shows the corresponding loadings plot. There was a stronger fit for this plot than for the activity against *T. brucei* B48 and all 35 samples could be included in the model. Most active components against *T. congolense* are

Propolis	*C. fasciculate* EC_{50} AVG ± SEM	Ratio EC_{50}(Tbb)/ EC_{50}(Cf)	P value
Suffolk 4, UK	6.41 ± 0.22	1.16	0.0798
Bulgaria 1	3.78 ± 0.65	1.37	0.1048
Suffolk 2, UK	2.80 ± 0.47	2.39	0.0029
North Yorkshire 1, UK	8.56 ± 1.19	1.57	0.0215
Northamptonshire 1, UK	3.54 ± 0.20	1.27	0.0324
Essex 1, UK	2.72 ± 0.23	2.20	0.0004
Essex 2, UK	13.4 ± 0.94	1.05	0.5182
Norfolk 1, UK	3.05 ± 0.48	1.71	0.0340
Devon 1, UK	8.11 ± 1.43	1.06	0.7664
Leicestershire 1, UK	9.58 ± 0.25	1.43	0.0269
Leicestershire 2, UK	23.8 ± 1.85	0.75	0.1030
Derbyshire, UK	5.64 ± 0.68	2.09	0.0022
Lithuania 1	5.92 ± 0.03	3.10	0.0007
Lithuania 2	10.1 ± 1.56	1.59	0.0310
Suffolk 1, UK	9.46 ± 1.03	0.72	0.1213
Suffolk 3, UK	7.94 ± 0.70	0.55	0.0077
Bulgaria 2	6.11 ± 0.66	0.95	0.6931
Bulgaria 3	5.55 ± 0.57	1.13	0.4633
Cambridgeshire 1, UK	8.44 ± 0.69	1.16	0.1597
Norfolk 2, UK	5.64 ± 0.93	1.10	0.6068
Northamptonshire 2, UK	4.62 ± 0.56	1.13	0.4258
Cambridgeshire 2, UK	22.7 ± 1.06	0.56	0.0007
North Yorkshire 2, UK	13.7 ± 1.15	1.35	0.0187
Northern Ireland, UK	11.6 ± 0.77	0.54	0.0032
North Yorkshire 3, UK	5.04 ± 0.71	1.38	0.1062
North Yorkshire 4, UK	2.95 ± 0.25	2.30	0.0018
North Yorkshire 5, UK	7.46 ± 1.00	1.34	0.0647
North Yorkshire 6, UK	3.98 ± 0.15	2.20	0.0002
Essex 3, UK	14.0 ± 0.99	0.49	0.0043
Berkshire, UK	5.56 ± 0.70	1.12	0.4015
Midlands, UK	3.27 ± 0.54	1.62	0.0540
Devon 2, UK	2.58 ± 0.43	3.36	0.0006
Buckinghamshire, UK	21.4 ± 1.34	0.81	0.0716
Norfolk 3, UK	4.34 ± 0.35	0.84	0.2208
Norfolk 4, UK	4.21 ± 0.49	1.00	0.9715
PAO[a] (μM)	5.35 ± 4.72	5.44	5.17

Table2. EC_{50} values (μg/mL) for European propolis against *C. fasciculata* (n=3). [a]PAO=phenylarsine oxide.

different from the most active against *T. brucei* and thus the OPLS plot highlights, galangin, an isomer of kaemp- ferol, and a methylether of chrysin as the most active components (Table S1).

Table 2 shows the data obtained from testing propolis against *C. fasciculata* which is a closer relative to the trypanosomatids that infect bees than *T. brucei* is. A wide range of activities were obtained. In many cases the samples were less active against *C. fasciculata* than against *T. brucei*. The OPLS model did not give as strong a correlation with the components in the sample as for *T. congolense* (Fig. 7) although it was possible to reduce the

number of variables supporting the plot to thus giving a better indication of which components might be associ- ated with high activity. The corresponding loadings plot is shown in Fig. S5. Galangin methyl ether is associated with high activity and this can be seen in Fig. 8 where one of the most active samples from Essex has about four times the amount of this component in comparison to a sample from Leicestershire.

Table 3 shows the activity obtained for 25 of the propolis samples against *L. mexicana*. The activity of the propolis samples against *L. mexicana* was higher than that obtained against *T. brucei*, with average EC_{50} values below 1 µg/mL for 52% of samples, and all EC_{50} values were under 5 µg/mL. The highest activity was obtained for one of the Bulgarian samples, at 0.35 ± 0.03 µg/mL. In most cases activity was equal or superior against the miltefosine APC12-resistant cell line, giving an average Resistance Index of 0.74 ± 0.09, but it was not possible to fit a strong an OPLS model for the data obtained for *L. mexicana* as for the *T. brucei* data, probably because the range of activities obtained across the samples is lower than for *T. brucei* and the number of samples tested was smaller. The activities obtained against *Leishmania* were an order of magnitude higher than those obtained for *C. fasciculata* and *T. brucei*, as shown in Fig. 9.

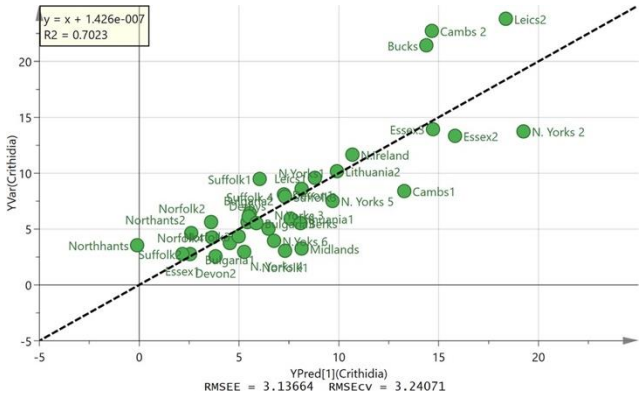

Figure 7. OPLS model of predicted against observed activity for propolis against *C. fasciculata* based on 4 components.

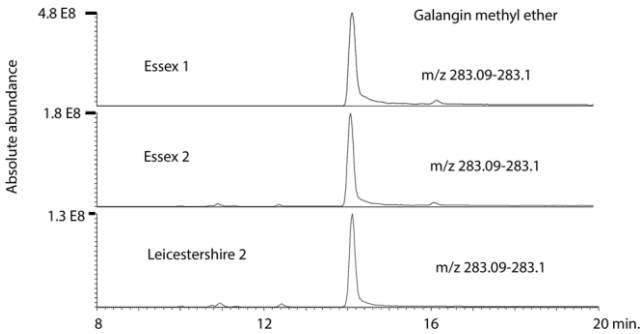

Figure 8. Extracted ion traces for galangin methyl ether in samples with high, moderate and low activity against *C. fasciculata*.

Discussion

The importance of propolis to bees is not entirely clear, in so far as some strains of bee do not collect much of it. However, experimental work has been carried out in order to establish the role of propolis in protecting the hive against infection[21–29]. There is evidence that bees that collect greater amounts of propolis are healthier and produce more viable broods than bees which are selected for reduced propolis collection[21]. Bees that collected propolis were found to exhibit superior hygienic behaviour in comparison with those that collected less[22]. It was found that a parasite challenge encouraged bees to collect more propolis and that the propolis envelop improved the immunity of colonies against infection[23–27]. As in the current study, regional variations in the antimicrobial properties of propolis have been found to exist[28]. Several acyl esters of flavonoids were recently isolated from temperate propolis and were fully characterised by spectroscopic methods. The isolated compounds were tested against honey bee pathogens *Paenibacillus larvae*

(American foulbrood) and *Ascosphaera apis* (chalkbrood). The most active compound against *A. apis* was pinobanksin 3-butyrate while the most active compound against *Paenibacillus larvae* was pinobanksin 3-octanoate[29]. The OPLS model for activity against *T. brucei* reflects this with two butyrate esters of pinobanksin being associated with the highest activity samples. In the current case the EC_{50} values against *T. brucei* in µg/mL terms are similar to those obtained for purified pinobanksin butyrate tested against *A. apis*. Interestingly the most active acyl flavonoid tested against *Paenibacillus larvae* was different from the most active against *A. apis* and this would seem to be the same in the current case, particularly for *C. fasciculata*, where the most active components were a methyl ether of galangin, a methyl ether of pinobanksin and pinobanksin. Thus propolis would appear to have broad spectrum activity with individual components in the mixture having activity against different organisms. Figure 9 shows a good overall correlation between the effects of the various samples against each of the kinetoplastid species. Especially between *T. brucei* and *T. con- golense* the correlation is very close, which is important as African animal trypanosomiasis is caused by multiple *Trypanosoma* species including *T. congolense*, *T. b. brucei* and, in Eastern Africa, *T. b. rhodesiense*[30] and the dis- ease has now spread far beyond Africa for *T. vivax* and *T. evansi*[31]. Even more important is that the correlation between the drug-resistant and the sensitive strains was very good, with activity against the resistant strains on average better than against the parental strains. This is in line with previous observations that cross-resistance with current drugs will not be a problem for propolis-derived phytochemicals[3,6], although it cannot be denied that resistance to any new, propolis-derived compound is likely to arise at some point unless a suitable combination therapy can be devised[32].

The consistent high levels of activity obtained for propolis extracts against protozoa coupled with the prev- alence of protozoal DNA amongst the DNA of pathogenic species in the metagenome[16] of the bee suggests that

Propolis ID	*L. mexicana* wild type (µg/mL)	*L. mexicana* C12Rx (µg/mL)	Resistance Index	ttest
Suffolk 4, UK	1.04 ± 0.19	0.81 ± 0.15	0.78	0.40
Bulgaria 1	0.35 ± 0.03	0.29 ± 0.04	0.85	0.33
Suffolk 2, UK	0.85 ± 0.14	0.45 ± 0.03	0.53	0.048
North Yorkshire 1, UK	0.90 ± 0.17	0.94 ± 0.15	0.96	0.87
Northamptonshire 1, UK	0.59 ± 0.05	0.28 ± 0.08	0.48	0.029
Essex 1, UK	0.62 ± 0.07	0.37 ± 0.07	0.60	0.073
Essex 2, UK	0.89 ± 0.10	0.42 ± 0.09	0.47	0.027
Norfolk 1, UK	1.94 ± 0.44	0.61 ± 0.003	0.31	0.027
Devon 1, UK	4.97 ± 0.23	0.95 ± 0.16	0.25	0.00014
Leicestershire 1, UK	5.67 ± 0.43	1.33 ± 0.09	0.23	0.00058
Leicestershire 2, UK	4.71 ± 0.33	1.06 ± 0.02	0.23	0.00041
Derbyshire, UK	1.23 ± 0.08	0.50 ± 0.17	0.41	0.016
Lithuania 1	1.51 ± 0.06	1.35 ± 0.02	0.89	0.064
Lithuania 2	0.65 ± 0.12	1.55 ± 0.01	2.38	0.0018
Suffolk 1, UK	0.67 ± 0.05	0.79 ± 0.09	1.17	0.32
Suffolk 3 UK	1.02 ± 0.18	0.50 ± 0.04	0.49	0.048
Bulgaria 2	1.13 ± 0.17	0.69 ± 0.22	0.61	0.19
Bulgaria 3	1.17 ± 0.18	0.78 ± 0.11	0.67	0.14
Cambridgeshire 1, UK	2.38 ± 0.40	1.53 ± 0.21	0.64	0.13
Norfolk 2, UK	0.93 ± 0.06	0.60 ± 0.05	0.65	0.020
Northamptonshire 2, UK	0.65 ± 0.05	0.49 ± 0.002	0.78	0.018
North Yorkshire 2	2.68 ± 0.15	1.36 ± 0.08	0.51	0.003
Northern Ireland	0.61 ± 0.05	0.78 ± 0.17	1.27	0.17
North Yorkshire 4, UK	0.72 ± 0.22	0.67 ± 0.06	0.94	0.75
North Yorkshire 5, UK	0.42 ± 0.12	0.58 ± 0.07	1.38	0.12
Miltefosine APC 12	0.1 ± 0.03	67.0 ± 12.6	670	<0.001
Miltefosine APC 16	2.0 ± 0.20	56 ± 9.7	28	<0.001

Table 3. The activity (µg/mL) of propolis against wild type and miltefosine-APC12 resistant *L. mexicana* (C12Rx). All EC_{50} values are given as average ± SEM (n=3). Statistical difference between EC_{50} values of the same sample against two strains was analysed using Student's unpaired t-test.

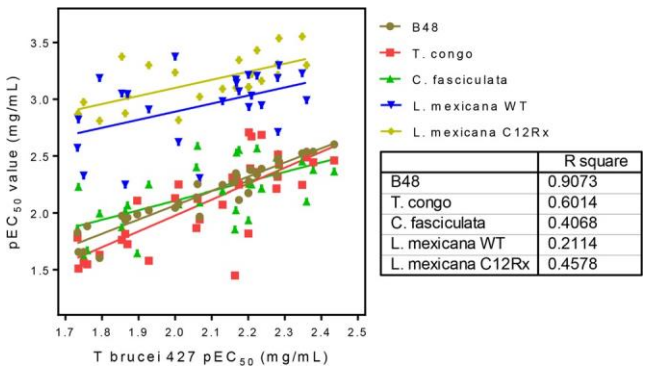

Figure 9. Correlation between the EC_{50} values of propolis samples against *T. brucei* 427WT and the other parasite strains and species.

these organisms may exert a greater pressure than may be currently appreciated on bee health. There remains much to understand about the role of propolis in bee health and also with regard to its potential in treating human infections, and the broad anti-kinetoplastid activity of propolis components reported here gives ample scope for further investigations.

Materials and Methods

chemicals and materials. Absolute ethanol, HPLC grade acetonitrile, methanol, formic acid, water and Acrodisc syringe filters were obtained from Fisher Scientific (Loughborough, UK). 36 raw propolis samples were collected from different areas of the UK and Europe following a request by Mr James Fearnley for people to sub- mit samples for testing. Miltefosine analogues APC12 and APC16 were obtained from Anatrace (Ohio, USA).

extraction of propolis samples. A sample of each propolis sample (500 mg) was extracted with 10 ml of ethanol by sonication for 1 h. The solvent was evaporated under a stream of nitrogen and the extracts were weighed and then redissolved in 5 ml of ethanol and then aliquoted into volumes containing 10 mg which were then blown to dryness under a stream of nitrogen.

Lc-MS conditions. LC-MS was carried out by using an Accela pump connected to an Orbitrap Exactive mass spectrometer operated in positive/negative switching mode. The sheath gas and auxiliary gas were set at 50 and 17 arbitrary units, respectively. The needle voltage was 4.5 kV in positive mode and 4.0 kV in negative mode. The heated capillary temperature was 320 °C. The HPLC was fitted with an ACE C18 column 150 × 4.6 mm, 3 µM particle size (Hichrom, Reading, UK). Solvent A was 0.1% formic acid in water and solvent B was 0.1% formic acid in acetonitrile. The flow rate was 0.3 ml/min and the solvent gradient was as follows: 0 min 30% B, 30 min 100% B, 40 min 100% B, 41 min 30% B, 50 min 30% B. The files were processed by using m/z Mine 20.1 and then the masses were searched against an in-house database. The extracted data was then processed by using Simca P

14.1 (Umetrics, Umea, Sweden). To produce PCA and OPLS models[33,34]. MS^n experiments for characterisation of the activity marker compounds were carried out on an LTQ Orbitrap with a collision energy of 35 V and used the chromatographic and mass spectrometry conditions given above.

Strains and cultures. Bloodstream forms of *T. b. brucei* were grown in standard HMI-9 medium with 10% fetal bovine serum at 37 °C/5% CO_2, in vented culture flasks, exactly as described)[35]. The standard laboratory strain Lister 427WT[36] was used as drug sensitive standard and the multi-drug resistant clone B48[37] was used to assess the potential for cross-resistance with the diamidine and melaminophenyl arsenical classes of trypano- cides. *T. congolense* strain IL3000 (Savannah-type) was cultured as described previously in Minimal

Essential Medium (MEM) base with 10% goat serum, supplemented with 14 µL/L β-mercaptoethanol, glutamine and antibiotics as described[38].

Transgenic *Leishmania mexicana* promastigotes (5×10^6 cells.ml) of strain MYNC/BZ/62/M379 expressing the firefly luciferase gene and sensitive to the miltefosine APC12 with 12 alkyl carbon chain called APC12[39] were designated WT; a related strain, C12Rx, resistant to 80 µg/mL APC12, was selected under controlled conditions by a stepwise progressive increase of APC12 (Fig. S6), with surviving stationary phase cells at each dose, used to inoculate subsequent cultures. Cells able to grow in the presence of the drug were cloned under drug pressure by limiting dilution to 1 cell/mL in 20 ml of growth medium and plated out into 96-well plates. Both were cultured in complete Modified Eagle's Medium (M199 supplemented with 10% (v/v) heat-inactivated foetal calf serum) at 25 °C. The transgenic line cultures were further supplemented with Hygromycin B in order to retain the luciferase gene.

A standard wild-type *C. fasciculata* (strain HS6, a kind gift from Professor Terry K. Smith, University of St-Andrews, UK) was grown at 27 °C in axenic serum-free defined media containing yeast extract (5 mg/mL), tryptone (4 mg/mL), sucrose (15 mg/mL), triethanolamine (4.4 mg/mL) and Tween 80 (0.5%) and supplemented with 10 µg/mL of haemin, exactly as described by Kipandula *et al.*[40].

Testing against *T. brucei*, *T. congolense* and *C. fasciculata*. The extracts were tested against *T. brucei* as described previously[3,6], using our standard Alamar blue (resazurin) method in white opaque 96 well plates (Greiner Bio-One, Frickenhausen, Germany), with 23 doubling dilutions and a no-drug control for each sample, using 2×10^4 *T. brucei* or 5×10^4 *T. congolense* per well and incubating 48 h with test compound prior to the addition of resazurin sodium salt (Sigma) and a further incubation of 24 h. The method is based on live but not cells metabolizing blue, non-fluorescent resazurin to pink, fluorescent resorufin, with fluorescence intensity being proportional to cell numbers[41]. Stock solutions of each compound or mixture

prepared in DMSO for each concentration so that there was a constant percentage of DMSO per well (1% v/v).

Testing against *C. fasciculata* involved a very similar procedure, using 5×10^3 cells/well and incubations of 48 h and 24 h (27 °C, 5% CO_2) before and after the addition of resazurin, respectively. Cell densities were deter- mined using a haemocytometer after adding 1% v/v glycerol to the culture sample to immobilize the parasites. Cell density was then adjusted to 5×10^4 cells/mL with fresh medium, of which 100 µL was added to each well of a pre-prepared 96-well plate with the doubling dilution of test compound/sample.

Fluorescence was determined using a FLUOstar Optima (BMG Labtech, Durham, NC, USA) plate reader (λ_{ex} = 544 nm; λ_{em} = 590 nm) and the output was plotted to a sigmoid curve with variable slope (Prism 5.0, GraphPad software) to obtain 50% effective concentrations (EC_{50} values).

testing against *L. mexicana*. A miltefosine APC12-resistant *L. mexicana* was strain was selected as shown in Fig. S6. Both cell lines were screened with propolis samples at a starting concentration of 0.125 mg/mL, doubly diluted eleven times across a 96 well plate in triplicate and incubated for 72 h at 25 °C. Wells with no propolis added were used in control experiments. After, luciferin solution (1 µg/mL) was added and the light emitted was measured using a luminometer (Biotek Synergy HT) at a wavelength of 440/40 nm. Viability was taken to be pro- portional to light emitted from for each drug-treated well, and was expressed as a faction of emission from the 'no drug' control. IC_{50} values were determined using Prism 5.0, GraphPad software.

Data Availability

The datasets generated during and/or analysed during the current study are available from the corresponding author on reasonable request.

References

1. Bankova, V., Popova, M. & Trusheva, B. The phytochemistry of the honeybee. *Phytochemistry* **155**, 1–11 (2018).
2. Wilson, M. B., Spivak, M., Hegeman, A. D., Rendahl, A. & Cohen, J. D. Metabolomics Reveals the Origins of Antimicrobial Plant Resins Collected by Honey Bees. *PloS one* **8**, e77512 (2013).
3. Omar, R. M. *et al*. Chemical characterisation of Nigerian red propolis and its biological activity against *Trypanosoma brucei*. *Phytochemical Analysis* **27**, 107–115 (2016).
4. Siheri, W. *et al*. Chemical and antimicrobial profiling of propolis from different regions within Libya. *PLoS One* **11**, e0155355 (2016).
5. Siheri, W. *et al*. The isolation of antiprotozoal compounds from Libyan propolis. *Phytotherapy research* **28**, 1756–1760 (2014).
6. Omar, R. *et al*. The chemical Characterisation of Nigerian propolis samples and their activity against *Trypanosoma brucei*. *Scientific reports* **7**, 923 (2017).
7. Nweze, N. E. *et al*. Effects of Nigerian red propolis in rats infected with *Trypanosoma brucei brucei*. *Comparative Clinical Pathology* **26**, 1129–1133 (2017).
8. Almutairi, S. *et al*. New anti-trypanosomal active prenylated compounds from African propolis. *Phytochemistry Letters* **10**, 35–39 (2014).
9. Almutairi, S. *et al*. Isolation of diterpenes and flavonoids from a new type of propolis from Saudi Arabia. *Phytochemistry letters* **10**, 160–163 (2014).
10. Do Nascimento, T. G. *et al*. Polymeric Nanoparticles of Brazilian red propolis extract: preparation, Characterisation, antioxidant and leishmanicidal activity. *Nanoscale research letters* **11**, 301 (2016).
11. Seidel, V., Peyfoon, E., Watson, D. G. & Fearnley, J. Comparative study of the antibacterial activity of propolis from different geographical and climatic zones. *Phytotherapy Research* **22**, 1256–1263 (2008).
12. Raghukumar, R., Vali, L., Watson, D., Fearnley, J. & Seidel, V. Antimethicillin-resistant Staphylococcus aureus (MRSA) activity of 'pacific propolis' and isolated prenylflavanones. *Phytotherapy research* **24**, 1181–1187 (2010).
13. Ravoet, J. *et al*. Comprehensive bee pathogen screening in Belgium reveals Crithidia mellificae as a new contributory factor to winter mortality. *PLoS One* **8**, e72443 (2013).
14. Schwarz, R. S. *et al*. Characterisation of two species of trypanosomatidae from the honey bee *Apis mellifera*: *Crithidia mellificae* Langridge and McGhee, and *Lotmaria passim* n. gen., n. sp. *Journal of Eukaryotic Microbiology* **62**, 567–583 (2015).
15. Ravoet, J. *et al*. Differential diagnosis of the honey bee trypanosomatids *Crithidia mellificae* and *Lotmaria passim*. *Journal of invertebrate pathology* **130**, 21–27 (2015).
16. Regan, T. *et al*. Characterisation of the British honey bee metagenome. *Nature. Communications* **9**, 4995 (2018).
17. Castelli, L. *et al*. Detection of *Lotmaria passim* in Africanized and European honey bees from Uruguay, Argentina and Chile. *Journal of invertebrate pathology* **160**, 95–97 (2018).
18. Ruiz-Gonzalez, M. X. & Brown, M. J. Honey bee and bumblebee trypanosomatids: specificity and potential for transmission. *Ecological Entomology* **31**, 616–622 (2006).
19. De Groot, A. C., Popova, M. P. & Bankova, V. S. An update on the constituents of poplar-type propolis. *Wapserveen, The Netherlands: Acdegroot publishing*, ISBN 978-90-813233-0-7 (2014).
20. Saleh, K., Zhang, T., Fearnley, J. & Watson, D. G. A comparison of the constituents of propolis from different regions of the United Kingdom by liquid chromatography-high resolution mass spectrometry using a metabolomics approach. *Current Metabolomics* **3**, 42–53 (2015).
21. Simone-Finstrom, M. & Spivak, M. Propolis and bee health: the natural history and significance of resin use by honey bees. *Apidologie* **41**, 295–311 (2010).
22. Nicodemo, D., Malheiros, E. B., De Jong, D. & Couto, R. H. N. Increased brood viability and longer lifespan of honeybees selected for propolis production. *Apidologie* **45**, 269–275 (2014).
23. Nicodemo, D., De Jong, D., Couto, R. H. N. & Malheiros, B. Honey bee lines selected for high propolis production also have superior hygienic behavior and increased honey and pollen stores. *Genetics and Molecular Research* **12**, 6931–6938 (2013).
24. Simone-Finstrom, M. D. & Spivak, M. Increased resin collection after parasite challenge: a case of self-medication in honey bees? *PloS one* **7**, e34601 (2012).
25. Simone-Finstrom, M., Borba, R., Wilson, M. & Spivak, M. Propolis counteracts some threats to honey bee health. *Insects* **8**, 46 (2017).
26. Borba, R. S., Klyczek, K. K., Mogen, K. L. & Spivak, M. Seasonal benefits of a natural propolis envelope to honey bee immunity and colony health. *Journal of Experimental Biology*, jeb. 127324 (2015).
27. Borba, R. S. & Spivak, M. Propolis envelope in *Apis mellifera* colonies supports honey bees against the pathogen, *Paenibacillus larvae*. *Scientific Reports* **7**, 11429 (2017).
28. Wilson, M., Brinkman, D., Spivak, M., Gardner, G. & Cohen, J. D. Regional variation in composition and antimicrobial activity of US propolis against *Paenibacillus larvae* and *Ascosphaera apis*. *Journal of invertebrate pathology* **124**, 44–50 (2015).
29. Wilson, M. B. *et al*. 3-Acyl dihydroflavonols from poplar resins collected by honey bees are active against the bee pathogens *Paenibacillus larvae* and *Ascosphaera apis*. *Phytochemistry* **138**, 83–92 (2017).
30. Giordani, F., Morrison, L. J., Rowan, T. G., De Koning, H. P. & Barrett, M. P. The animal trypanosomiases and their chemotherapy: a review. *Parasitology* **143**, 1862–1889 (2016).
31. Aregawi, W. G., Agga, G. E., Abdi, R. D. & Büscher, P. Systematic review and meta-analysis on the global distribution, host range, and prevalence of Trypanosoma evansi. *Parasites & Vectors* **12**, 67 (2019).
32. de Koning, H. P. Drug resistance in protozoan parasites. *Emerging Topics in Life Sciences* **1**, 627–632 (2017).
33. Eriksson, L., Byrne, T., Johansson, E., Trygg, J. & Vikstrom, C. *In Multi- and Megavariate Data Analysis: Basic Principles and Application* Ch. 503, 455–456 (MKS Umetrics AB, 2013).
34. Eriksson, L., Trygg, J. & Wold, S. CV-ANOVA for significance testing of PLS and OPLS (R) models. *J Chemometr* **22**, 594–600, https://doi.org/10.1002/cem.1187 (2008).
35. Gudin, S. *et al*. *Trypanosoma brucei*: a survey of pyrimidine transport activities. *Experimental parasitology* **114**, 118–125 (2006).
36. de Koning, H. P., MacLeod, A., Barrett, M. P., Cover, B. & Jarvis, S. M. Further evidence for a link between melarsoprol resistance and P2 transporter function in African trypanosomes. *Molecular and biochemical parasitology* **106**, 181–185 (2000).
37. Bridges, D. J. *et al*. Loss of the high affinity pentamidine transporter is responsible for high levels of cross-resistance between arsenical and diamidine drugs in African trypanosomes. *Molecular pharmacology* **71**, 1098–1108 (2007).
38. Cerone, M. *et al*. Discovery of sustainable drugs for neglected tropical diseases: cashew nut shell liquid (CNSL)-based hybrids target mitochondrial function and ATP production in *Trypanosoma brucei*. *ChemMedChem* **14**, https://doi.org/10.1002/cmdc.201800790 (2019).
39. Hurrell, B. P. *et al*. Rapid sequestration of *Leishmania mexicana* by neutrophils contributes to the development of chronic lesion. *PLoS pathogens* **11**, e1004929 (2015).
40. Kipandula, W., Young, S. A., MacNeill, S. A. & Smith, T. K. Screening of the MMV and GSK open access chemical boxes using a viability assay developed against the kinetoplastid Crithidia fasciculata. *Molecular and biochemical parasitology* **222**, 61–69 (2018).
41. Gould, M. K., Vu, X. L., Seebeck, T. & de Koning, H. P. Propidium iodide-based methods for monitoring drug action in the kinetoplastidae: comparison with the Alamar Blue assay. *Analytical biochemistry* **382**, 87–93 (2008).

Acknowledgements

GUE was supported by a studentship from the Nigerian Tertiary Education Trust Fund. AA was supported by a Saudi Government studentship.

Author contributions

A.A., S.A., A.M.D., S.G., G.U.E., D.G.W. and R.W. carried out the experimental work and data processing and interpretation. W.S., D.G.W., J.O.I., H.P.d.K. and J.F. contributed to the authorship of the manuscript. J.F. collected the propolis samples.

Additional information

Supplementary information accompanies this paper at https://doi.org/10.1038/s41598-019-47840-y.

Competing Interests: The authors declare no competing interests.

Publisher's note: Springer Nature remains neutral with regard to jurisdictional claims in published maps and institutional affiliations.

European propolis is highly active against trypanosomatids including *Crithidia fasciculata*

Abdullah Alotaibi[1], Godwin U. Ebiloma[2], Roderick Williams[3], Sameah Alenezi[1], Anne-Marie Donachie[2], Selome Guillaume[3], John O. Igoli[1,4], James Fearnley[5], Harry P. de Koning[2] and David G. Watson[1*].

1. University of Strathclyde, Strathclyde Institute of Pharmacy and Biomedical Science, 161 Cathedral Street, Glasgow, G4 0RE, UK.
2. Institute of Infection, Immunity and Inflammation, College of Medical, Veterinary and Life Sciences, University of Glasgow, Glasgow G12 8TA, UK
3. IBEHR, School of Health and Life Science, University of the West of Scotland, High Street, Paisley PA1 2BE
4. Department of Chemistry, University of Agriculture, PMB 2373, Makurdi, Nigeria
5. BeeVital, Whitby, North Yorkshire, YO22 5JR, UK.

*Corresponding author

d.g.watson@strath.ac.uk

+441415482651

Supplementary Information

Figure S1 Loadings plot corresponding to figure 4 for an OPLS model of propolis activity against *T.brucei* B48.

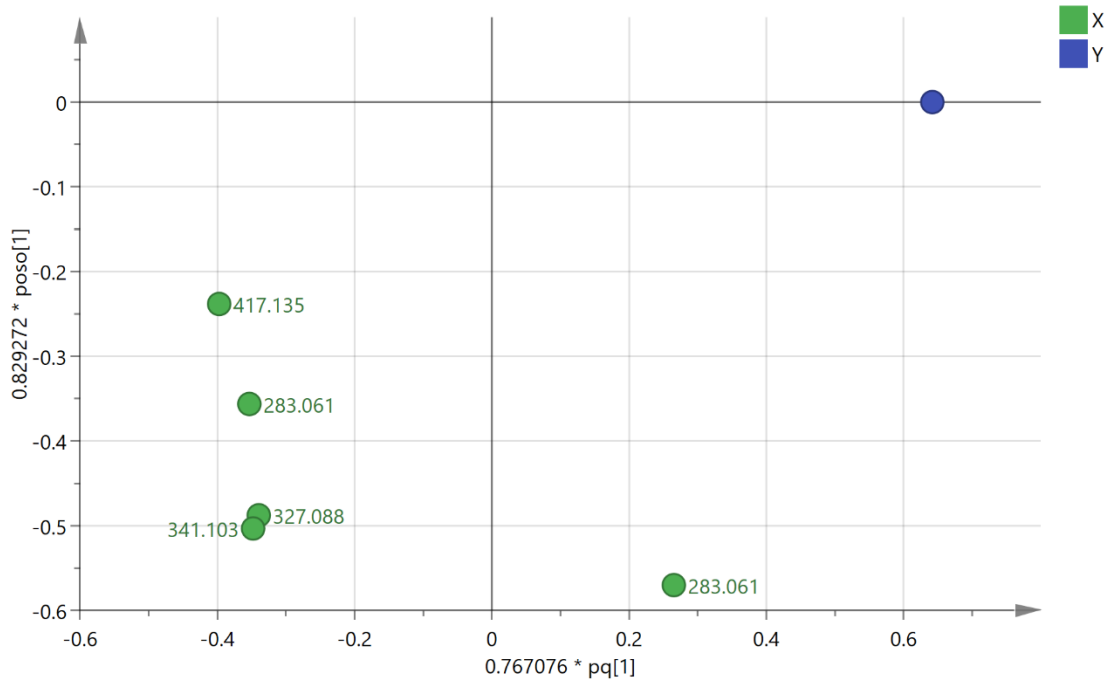

Figure S2 OPLS model for observed against predicted activity of 33 propolis against *T. brucei* 427 WT based on 7 components.

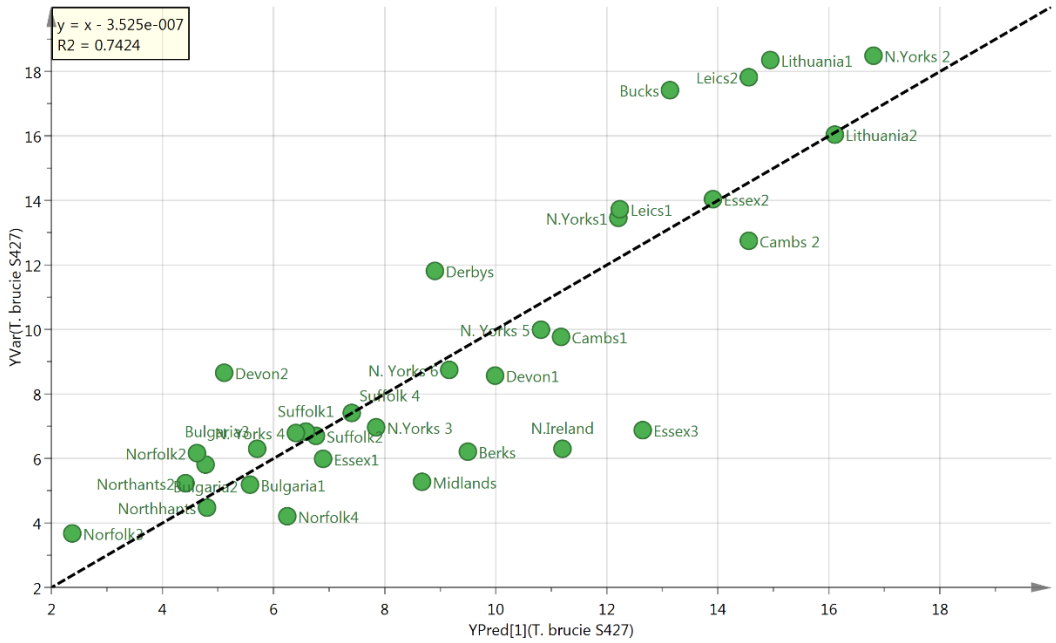

Figure S3 The loadings plot corresponding to figure S2 which shows a plot of predicted against observed activity for 33 propolis samples against *T. brucei* 247 WT.

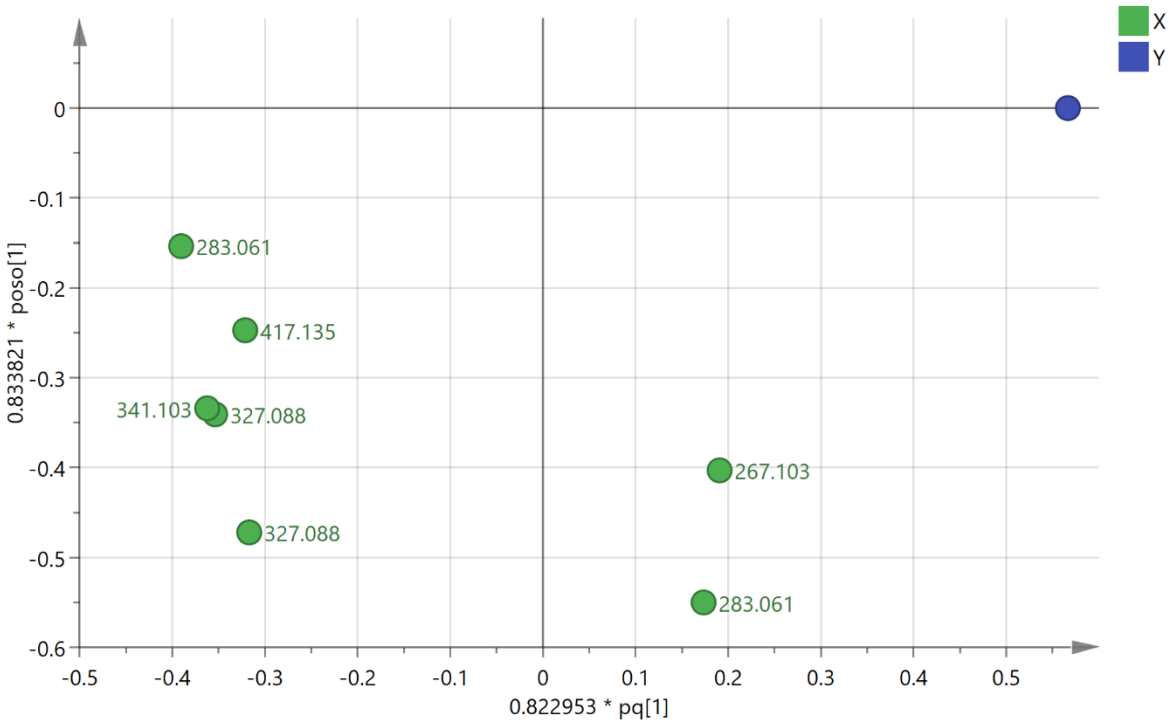

Figure S4 The loadings plot corresponding to figure 6 which shows a plot of predicted against observed activity of 35 propolis samples against *T. congolense*.

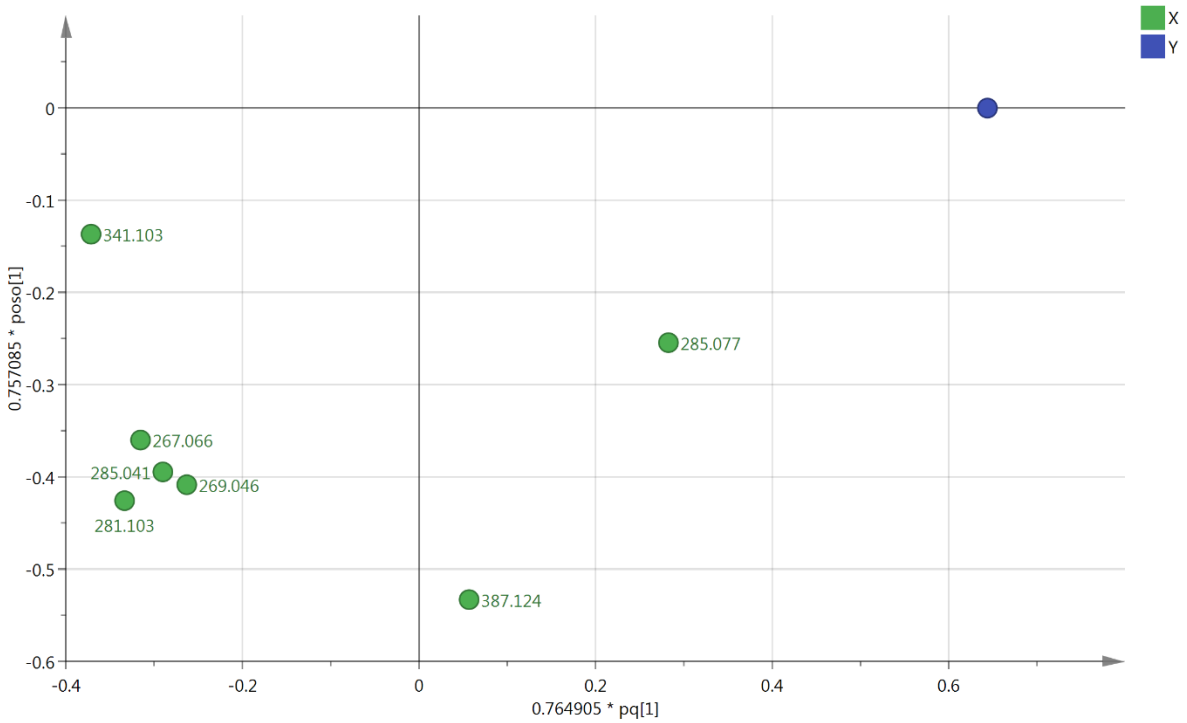

Figure S5 Loadings plot corresponding to figure 7 which shows a plot of predicted against observed activity of 35 propolis samples against *C. fasciculata*.

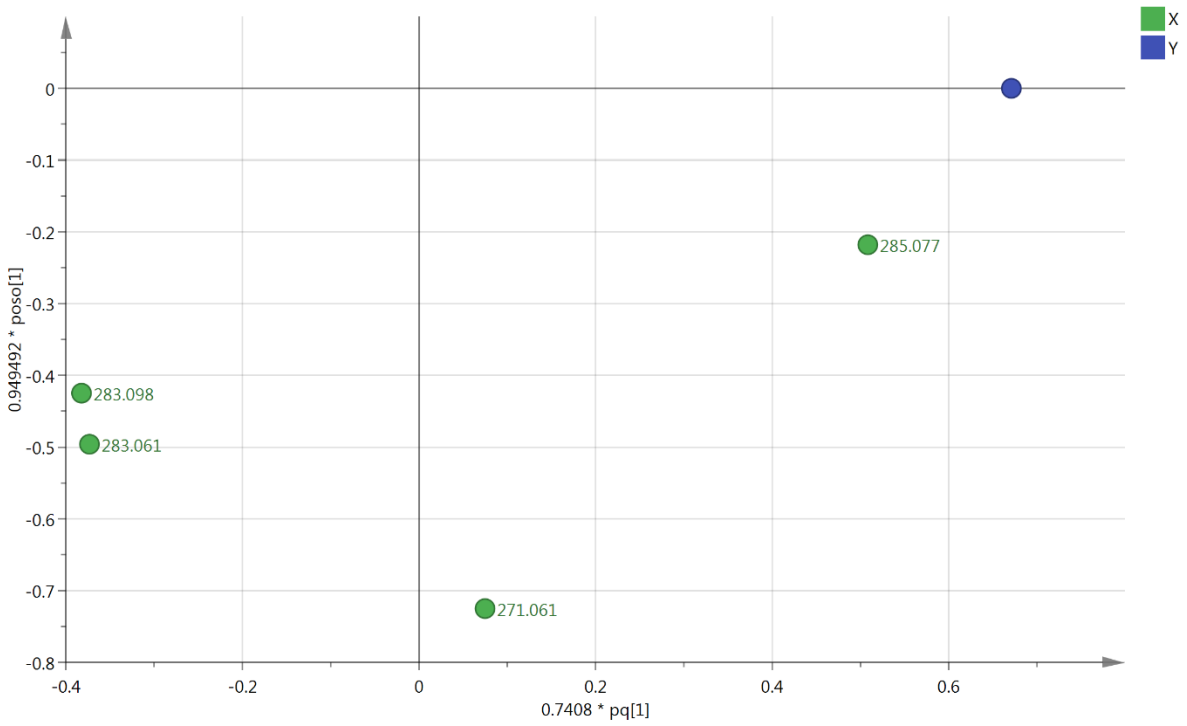

Figures S6 Selection of APC12-resistance in *L. mexicana* promastigotes.

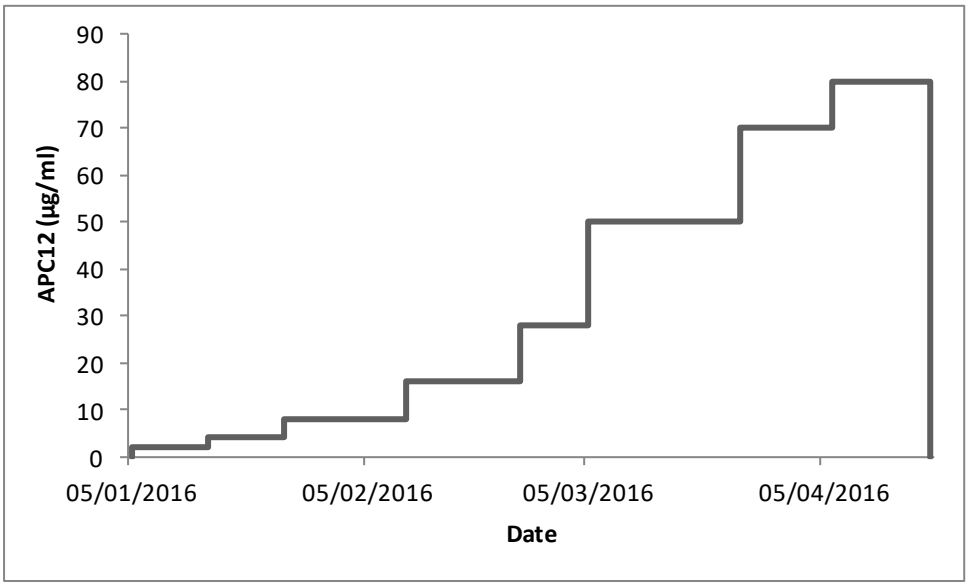

L. mexicana promastigotes designated C12Rx were selected under controlled conditions over 8 passages (150 days) in increasing concentrations of miltefosine analogue APC12. Adaptation continued until the population was resistant to 80 µg/mL, APC12 in the medium, beyond which death ensued. The IC_{50} of C12Rx was 67.0 µg/mL and 56.0 µg/mL for APC12 and APC16 (miltefosine) while for *L. mexicana* WT to the same drugs, they were 0.1 µg/mL and 2.0 µg/mL (resistance index 670 and 28 for APC12 and APC16 respectively).

Table S1 MS^n data for the active compounds observed in OPLS plots of predicted and observed activity obtained with a collision energy of 35V.

Tentative id	m/z	Rt min	[M-H]$^-$ Composition	Fragments (relative intensity, elemental composition)
			***T. brucei* B48**	
Dimethyl kaempferol phenethyl ether	417.135	17.4	$C_{25}H_{21}O_6$	402.1098(95, $C_{24}H_{18}O_6$), 387.086 (15, $C_{23}H_{15}O_6$) 375.123 (3 $C_{23}H_{19}O_5$) 298.0478 (100, $C_{16}H_{10}O_6$) MS^3 (298.0478) 270.053(100, $C_{15}H_{10}O_5$)
Galangin methyl ether	283.061	15.4	$C_{16}H_{11}O_5$	268.038 (100, $C_{15}H_8O_5$), 255.030 (65, $C_{14}H_7O_5$) MS^3 (268.038) 239.035 (100, $C_{14}H_7O_4$), 213.0399 (15.3, $C_{13}H_7O_3$)
Galangin methyl ether	283.061	14.4	$C_{16}H_{11}O_5$	268.038 (100, $C_{15}H_8O_5$)
Pinobanksin butyrate	341.103	18.5	$C_{19}H_{17}O_6$	MS^2 253.050 (100, $C_{15}H_9O_4$) MS^3 (253.050) 209.0605 (100, $C_{14}H_9O_2$) 181.0657 (6.8, $C_{13}H_9O$)
Pinobanksin propionate	327.088	16.5	$C_{18}H_{15}O_6$	MS^2 253.051 (100, $C_{15}H_9O_4$)
Pinobanskin propionate	327.088	10.7	$C_{18}H_{15}O_6$	MS^2 253.051 (100, $C_{15}H_9O_4$)
			***T. brucei* 247 WT**	
Pinobanksin butyrate	341.103	18.5	$C_{19}H_{17}O_6$	MS^2 253.050 (100, $C_{15}H_9O_4$) MS^3 (253.050) 209.0605 (100, $C_{14}H_9O_2$) 181.0657 (6.8, $C_{13}H_9O$)
Methyl ether of dihydrokaempferol	301.072	9.3	$C_{16}H_{13}O_6$	273.077 (100, $C_{15}H_{13}O_5$) 257.046 (6.7, $C_{14}H_9O_5$)
Coumaric acid phenyl propenyl ester	279.103	18.5	$C_{18}H_{15}O_3$	235.1123 (100, $C_{17}H_{15}O$), 194.0814 (95, $C_{14}H_{11}O$) 162.0319 (15.8, $C_9H_6O_3$)
Pinobanksin methyl ether	285.077	15.5	$C_{16}H_{13}O_5$	270.053 (100, $C_{15}H_{10}O_5$), 243.066 (100, $C_{14}H_{11}O_4$) 164.011 (42, $C_8H_4O_4$)
			C. fasciculata	
Pinobanksin methyl ether	285.077	15.5	$C_{16}H_{13}O_5$	270.053 (100, $C_{15}H_{10}O_5$), 243.066 (100, $C_{14}H_{11}O_4$) 164.011 (42, $C_8H_4O_4$)
Galangin methyl ether	283.061	15.4	$C_{16}H_{11}O_5$	268.038 (100, $C_{15}H_8O_5$), 255.030 (65, $C_{14}H_7O_5$) MS^3 (268.038) 239.035 (100, $C_{14}H_7O_4$), 213.0399 (15, $C_{13}H_7O_3$)
Octyl ester of caffeic acid	283.098	17.1	$C_{17}H_{15}O_4$	179.035 (100, $C_9H_7O_4$) 135.045 (20, $C_8H_7O_2$)
Pinobanksin	271.061	9.3	$C_{15}H_{11}O_5$	253.050 (100, $C_{15}H_9O_4$) 225.055 (21, $C_{14}H_9O_3$) 197.061 (16, $C_{13}H_9O_2$) 151.004(6.4, $C_7H_3O_4$)
			T. congolense	
Pentenoyl ester of caffeic acid	281.103	3.4	$C_{14}H_{17}O_6$	179.035 (78, $C_9H_7O_4$) 135.045 (100, $C_8H_7O_2$)
‡Kaempferol isomer	285.041	6.5	$C_{15}H_9O_6$	241.0504 (100, $C_{14}H_9O_4$) 151.0036 (12.1%, $C_7H_3O_4$)
Methyl ether of chrysin	267.066	7.9	$C_{16}H_{11}O_4$	252.042 (100, $C_{15}H_8O_4$), 224.047 ($C_{14}H_8O_3$) 14.2
Pinobanksin methyl ether	285.077	15.5	$C_{16}H_{13}O_5$	270.053 (100, $C_{15}H_{10}O_5$), 243.066 (100, $C_{14}H_{11}O_4$) 164.011 (42, $C_8H_4O_4$)
*Galangin	269.046	8.8	$C_{15}H_9O_5$	MS^2 225.056 (100, $C_{14}H_9O_3$) 201.056 (23 $C_{12}H_9O_3$) 149.024 (26, $C_8H_5O_3$)
Unknown flavonoid	387.124	18.4	$C_{24}H_{19}O_5$	MS^2 359.129 (14.4, $C_{23}H_{19}O_4$,), 343.134 (6.5, $C_{23}H_{19}O_3$), 281.082 (49.3, $C_{17}H_{13}O_4$), 267.066 (100, $C_{16}H_{11}O_4$)

*Retention time and fragmentation pattern corresponding to that of a standard. ‡ Elutes earlier than the standard.